THE ROLE OF INFLAMMATORY MEDIATORS IN HYPERTENSIVE REMODELING OF CEREBRAL ARTERIES: FOCUS ON PERIVASCULAR MACROPHAGES, MATRIX METALLOPROTEINASES AND TUMOR NECROSIS FACTOR - α.

By

Paulo Wagner Pires

A DISSERTATION

Submitted to
Michigan State University
in partial fulfillment of the requirements
for the degree of

Pharmacology and Toxicology – Doctor of Philosophy

2013

ABSTRACT

THE ROLE OF INFLAMMATORY MEDIATORS IN HYPERTENSIVE REMODELING OF CEREBRAL ARTERIES: FOCUS ON PERIVASCULAR MACROPHAGES, MATRIX METALLOPROTEINASES AND TUMOR NECROSIS FACTOR - α.

By

Paulo Wagner Pires

Inflammation is linked to the pathophysiology of hypertension, and high blood pressure is a major risk factor for ischemic stroke occurrences. Hypertension has detrimental effects on the cerebral vasculature that might account for the increased stroke risk. We showed that chronic hypertension leads to narrowing of the lumen (inward remodeling) in the middle cerebral artery (MCA), which is linked to larger infarcts after MCA occlusion. Hypertension also causes impairment in endothelium-dependent dilation of cerebral arteries. This can reduce collateral perfusion, thus worsening stroke outcome. The mechanisms underlying hypertensive inward remodeling and endothelium dysfunction of cerebral arteries are still poorly understood. It is possible that vascular inflammation is involved in cerebrovascular remodeling and dysfunction.

There is accumulation of perivascular macrophages in cerebral arteries and arterioles of hypertensive animals. It is possible that perivascular macrophages are involved in hypertensive remodeling and dysfunction. In fact, these inflammatory cells release mediators that are known to alter vascular function, such as matrix metalloproteinases (MMPs) and tumor necrosis factor (TNF)-α. MMPs are zinc-dependent endopeptidases that degrade elements of the extracellular matrix. These enzymes were shown to be involved in

remodeling of the thoracic aorta, although their role in hypertension-induced changes in the cerebral vasculature is unknown. TNF-α is a proinflammatory cytokine known to induce vascular smooth muscle cells proliferation and to impair endothelium-dependent dilation of arteries in the periphery.

Therefore, the present dissertation describes the studies aimed at understanding the role of proinflammatory mediators in hypertensive remodeling and dysfunction of the middle cerebral artery (MCA) in rats. The working hypothesis is that perivascular macrophages are associated with MCA remodeling and endothelium dysfunction in stroke-prone spontaneously hypertensive rats, through a mechanism dependent on MMPs and TNF-α. We tested this hypothesis by depleting macrophages with liposome-encapsulated clodronate (Aim 1, Chapter 2), inhibition of MMPs with doxycycline (Aim 2, Chapter 3) and TNF-α inhibition with etanercept (Aim 3, Chapter 3).

DEDICATION

This work is dedicated to my wife Juliana. You are my life companion, my best friend, and the most wonderful woman I know. You are my safe harbor and the reason why I wake up in the morning.

To my parents, Paulino and Rosabel, and my brother Caio. Your efforts and hard work made this possible. We are a true family, loving and caring, even at this long a distance.

ACKNOWLEDGEMENTS

I could not have achieved any victories without the help, support and friendship of all those that crossed my path throughout these years. I will always be in debt to you all.

First and foremost, I am thankful to my mentor Dr. Anne Dorrance. You believed in me when no one else did, and you rekindled my passion for science. Your support, understanding, mentorship, patience and knowledge were invaluable for my training. Everything I achieved during my graduate career, I owe it to you. And you will always a source of inspiration to me.

I also want to thank Dr. William Jackson, who has been a co-mentor to me throughout my years as a graduate student. Our talks intellectually challenged me in ways I never imagined possible, and you always made me think “outside the box”. Thank you for your patience and help in our collaborations, and for all the knowledge you shared with me.

I sincerely appreciate my Ph.D. guidance committee members Dr. Gregory Fink, Dr. Stephanie Watts, Dr. David Kreulen and Dr. Iris Jaffe. You kept me on track and gave valuable input into my work. This dissertation would not exist if not for you, for the time you dedicated to help me and for all the insightful comments regarding my data.

The Ph.D. experience would not have been complete without my great friends, Jonathon, Natasha, Emily, Angelica and JT. Thank you for your friendship and for all the

talks, laughter, foolishness and moments we shared. I will always remember those moments fondly, and they will be with me forever.

The cozy, “family-like” atmosphere of the Dorrance lab is the work of its past and present members. You are, and always will be, my extended family and my scientific network. We work hard and we have fun being scientists. A special mention goes to my former “mentee” Saavia Girgla, who helped me immensely and patiently endured as I learned how to mentor a student. I would also like to thank Nusrat Matin, Kaye Long, George Neros, Curt Rogers, Naiomy Rios and Stephanie DeBolle for all the fun moments we had.

A special thanks goes to the faculty of the Department of Pharmacology and Toxicology at MSU. You inspired me to follow an academic career, and I learned much from you. You shaped my career, and I hope to work with you in the future.

I want to thank the administrative personnel in the department, who helped me deal with the many problems throughout these years. Your help, dedication and hard work are appreciated.

Finally, I want to acknowledge all the rats used in these studies. The road to a better understanding of human diseases is today a little shorter thanks to you.

TABLE OF CONTENTS

LIST OF TABLES

LIST OF FIGURES

KEY TO ABBREVIATIONS

5-HT: 5-hydroxytriptamine

α-SMA: α-smooth muscle actin

ACEi: angiotensin-converting enzyme inhibitor

Ach: acetylcholine

ADP: adenosine diphosphate

AT1R: angiotensin II type 1 receptor

AT2R: angiotensin II type 2 receptor

BK: bradykinin

BP: blood pressure

CBV: cerebral arteries (MCA, posterior and anterior communicating, posterior and anterior cerebral, and basilar arteries)

cGMP: cyclic guanine monophosphate

CLOD: liposome-encapsulated clodronate

CRP: C-reactive protein

CSA: cross-sectional area

DOCA: deoxycosticosterone-acetate

Dox: doxycycline

ECM: extracellular matrix

EDHF: endothelium-derived hyperpolarizing factor

eNOS: endothelial nitric oxide synthase

ETN: etanercept

FCM: flow cytometry

HMG-CoA: 3-hydroxy-3-methylglutaryl-coenzyme A

ICAM: intercellular adhesion molecule

IF: immunofluorescence

IL: interleukin

IK_{Ca}: intermediate conductance, Ca^{+2}-activated K^{+} channels

L-NAME: N-nitro-L-arginine methyl ester

MCA: middle cerebral artery

MCAO: middle cerebral artery occlusion

MCP: monocyte chemotactic protein

mCSF: macrophage colony stimulating factor

mmHg: millimeters of mercury

MMP: matrix metalloproteinases

MR: mineralocorticoid receptor

MRA: mesenteric resistance arteries

NADPH-oxidase: nicotinamide adenine dinucleotide phosphate-oxidase

NF-κB: nuclear factor kappa-light-chain-enhancer of activated B cells

NO: nitric oxide

PBS: phosphate-buffered saline

PBS lipo: liposome-encapsulated PBS

PSS: physiological saline solution

qRT-PCR: quantitative real-time polymerase chain reaction

RAAS: renin-angiotensin-aldosterone system

SHR: spontaneously hypertensive rats

SHRSP: stroke-prone spontaneously hypertensive rats

SK_{Ca}: small conductance, Ca^{+2}-activated K^{+} channels

SNP: sodium nitroprusside

TIMP: tissue inhibitor of MMP

t-PA: tissue-type plasminogen activator

TNF-α: tumor necrosis factor-α

TTC: 2,3,5-triphenyltetrazolium chloride

WKY: Wistar-Kyoto rats

CHAPTER 1

The Cerebral Vasculature in Health and Chronic Hypertension: Focus on Vascular Inflammation and Matrix Metalloproteinases.

1. Overview

The brain is one of the most highly perfused organs in the body. It accounts for approximately 2% of the body weight of a healthy human, yet it receives 15 to 20% of the cardiac output. The brain has a high metabolic activity and neurons have a limited ability to store energy and oxygen, thus relying on the circulation to provide nutrients to maintain their homeostasis. Total blood flow to the brain is fairly constant even during conditions when blood flow to other organs changes, such as during exercise [1]. Acute interruptions in cerebral perfusion, either global as observed during cardiac arrest or focal as observed during ischemic stroke, can have devastating long-term effects on brain function [2].

The cerebral circulation has many anatomical and physiological specializations that allow it to properly maintain cerebral perfusion. Pathological conditions, particularly hypertension, cause maladaptive alterations in cerebral arteries, which increase an individual's risk of having a stroke, and worsen the outcome of ischemia. This chapter will summarize the main characteristics of the cerebral circulation, followed by a discussion of the effects of hypertension on this highly specialized vascular bed.

1.1 – Anatomy of the cerebral circulation

1.1.1 – Extracranial arteries and circle of Willis

Blood flow to the brain is supplied by 2 pairs of large extracranial arteries: the right and left internal carotid arteries and the right and left vertebral arteries. The internal

carotid arteries branch from the common carotid arteries and provide approximately 80% of the total blood flow to the cerebrum; the vertebral arteries run along the spinal cord and fuse at the base of the brainstem into the basilar artery. They provide approximately 20% of the total cerebral perfusion. At the base of the cerebrum, the basilar artery fuses with the *circle of Willis*, which is a complete anastomotic ring. The circle of Willis is formed by the posterior communicating arteries, posterior cerebral arteries, internal carotids, anterior cerebral arteries and the anterior communicating artery (Figure 1.1). The circle of Willis provides collateral blood flow when one of the major extracranial or intracranial arteries becomes occluded, minimizing ischemic damage.

1.1.2 – Intracranial arteries

Branching from the circle of Willis at the base of the cerebrum are three major intracranial arteries: the posterior, middle and anterior cerebral arteries. They run along the surface of the brain and perfuse distinct regions of the cerebral cortex. The posterior cerebral artery and its branches supply blood to parts of the hippocampus and parts of the anterior and posterior temporal cortex and the calcarine and portions of the parieto-occipital cortex [3]. These regions are mainly associated with memory, visual and olfactory sensory information processing. The middle cerebral artery and its branches supply the largest area of the brain: 5 regions of the temporal lobe (polar, anterior, middle, posterior, occipital), angular, anterior and posterior parietal, central, precentral, prefrontal and orbitofrontal cortex. These regions are involved in motor control and synchronization, hearing, speech, writing, understanding, insight, mood and judgment

[4]. Lastly, the anterior cerebral artery and its branches supply a smaller territory, including the innermost regions of the superior and inferior parietal cortex, the paracentral cortex, the internal portion of the perifrontal cortex, the pericallosal region, and the internal portion of the frontopolar and orbitopolar cortex. These regions are involved in motor control of the legs, motor synchronization, memory, insight, mood, judgment and emotion [5].

1.1.3 – Pial arteries

Branches of the large intracranial arteries and the circle of Willis on the surface of the brain form the pial circulation. Pial arteries continue to branch into smaller arteries and arterioles, providing some cerebrovascular resistance. One striking characteristic of the pial circulation is the high number of anastomoses present in these arteries [6]. Anastomoses are reconnection between two arteries downstream of their branching point from the main feed artery. These anastomoses connect the posterior to the middle circulation, as well as the middle to the anterior circulation (Figure 1.2), and they provide important collateral blood flow when a small surface artery is occluded [7]. In fact, occlusion of one small pial artery/ arteriole causes only a small reduction in blood flow that disappears downstream from the first branch of the occluded artery [8].

1.1.4 – Penetrating arteries and arterioles

Penetrating arteries and arterioles branch from pial arteries and dive into the underlying parenchyma in an almost 90^{o} angle (Figure 1.3). At their proximal regions (closest to the originating artery) they are located within the Virchow-Robin space and

are bathed in cerebrospinal fluid. These arterioles have few branches and anastomoses and are considered bottlenecks connecting the pial circulation to the deeper parenchymal microcirculation [9]. They provide blood flow to discrete regions of the brain, and controlled alterations in their diameter are sufficient to cause focal increases in blood flow to match local neuronal demand [10]. Occlusion of a single penetrating arteriole leads to a cylindrical microinfarction that can lead to cognitive impairment [11]. As the penetrating arterioles dive further into the parenchyma they are surrounded by astrocytic end-feet and some scarce neuron axonal endings [12].

1.1.5 – Parenchymal capillaries

The brain has a high capillary density, particularly in the grey matter, and approximately 90% of all capillaries are continuously perfused [13]. Capillary endothelial cells are encased by a basal lamina, and then are surrounded by pericytes, which are cells with contractile properties that regulate capillary lumen and perfusion rate [14]. The ratio of endothelial cells to pericytes in brain capillaries is higher than most vascular beds (ranging between 1:3 to 1:5 in the brain, compared to 1:100 in capillaries from striated muscle) [15], further highlighting the importance of local control of blood flow. Astrocytic end-feet surround the entire structure, and adjacent neurons have synapses with these astrocytes, generating an integrated functional unit called the *neurovascular unit* (Figure 1.4). The neurovascular unit has received much attention in the recent years as a possible therapeutic target for ischemic stroke [16] and Alzheimer's disease [17].

Endothelial cells from cerebral capillaries have a high density of tight junctions, leading to the formation of a barrier that prevents diffusion of most substances dissolved in the plasma into the cerebral parenchyma and shields the brain from possibly harmful substances [18]. This selectively permeable endothelium is the first structure of the *blood-brain-barrier*, a physical and biochemical barrier important to maintain cerebral homeostasis, which also comprises pericytes, astrocytes and microglia [18]. It is important to note that the intracranial arteries, pial arteries and penetrating arterioles also have blood-brain-barrier properties [19].

1.1.6 – Veins

Drainage of the blood from the cerebrum is performed by two valveless venous systems: the superficial cortical veins and the deep veins [7]. The first system is located in the surface of the brain and drains the cortex and the subcortical white matter. The deep veins drain the most internal portions of the cerebrum, including the third and lateral ventricles and the deep white and grey matter surrounding these regions. The veins then anastomose and empty into the sinuses and the jugular vein.

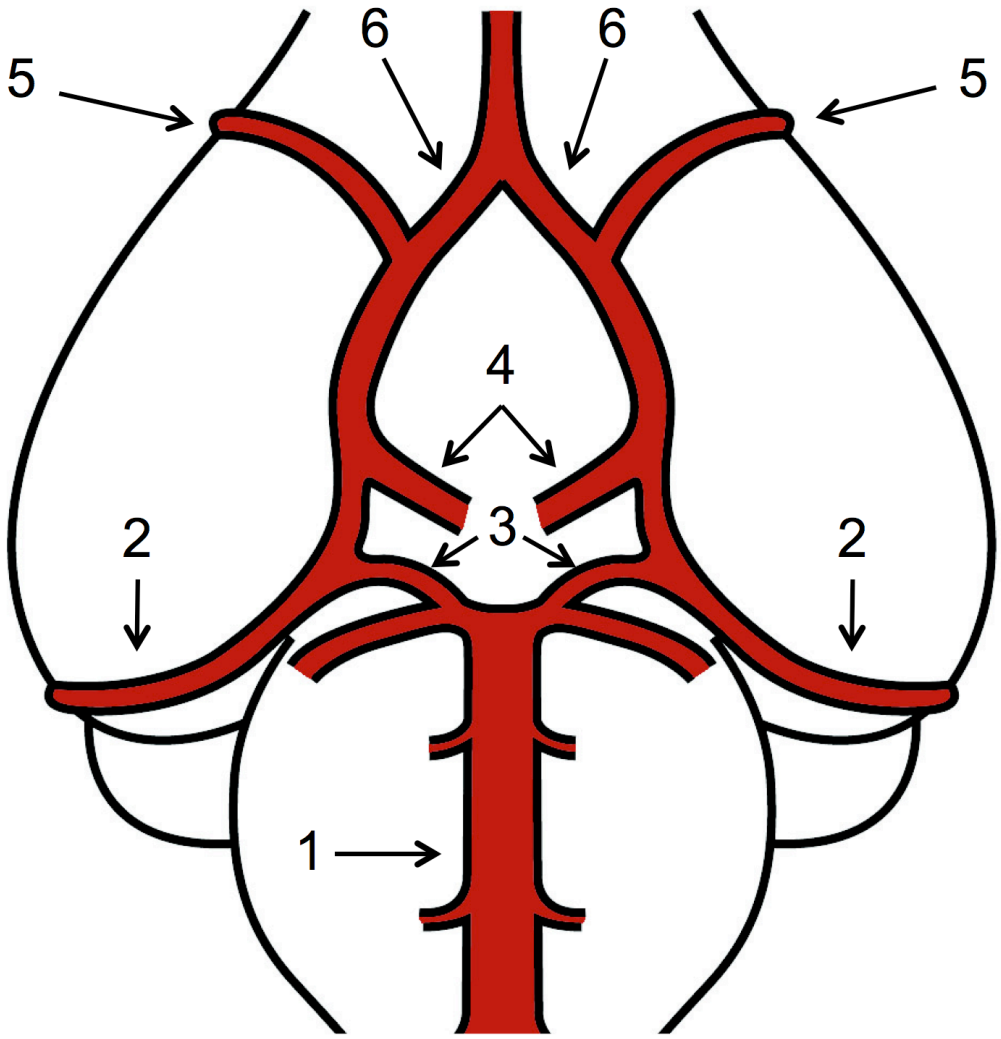

Figure 1.1 – The circle of Willis in rats. 1: basilar artery; 2: posterior cerebral arteries; 3: posterior communicating arteries; 4: internal carotid arteries; 5: middle cerebral arteries; 6: anterior cerebral arteries. Figure courtesy of Daniel Bollman. For interpretation of the references to color in this and all other figures, the reader is referred to the electronic version of the dissertation.

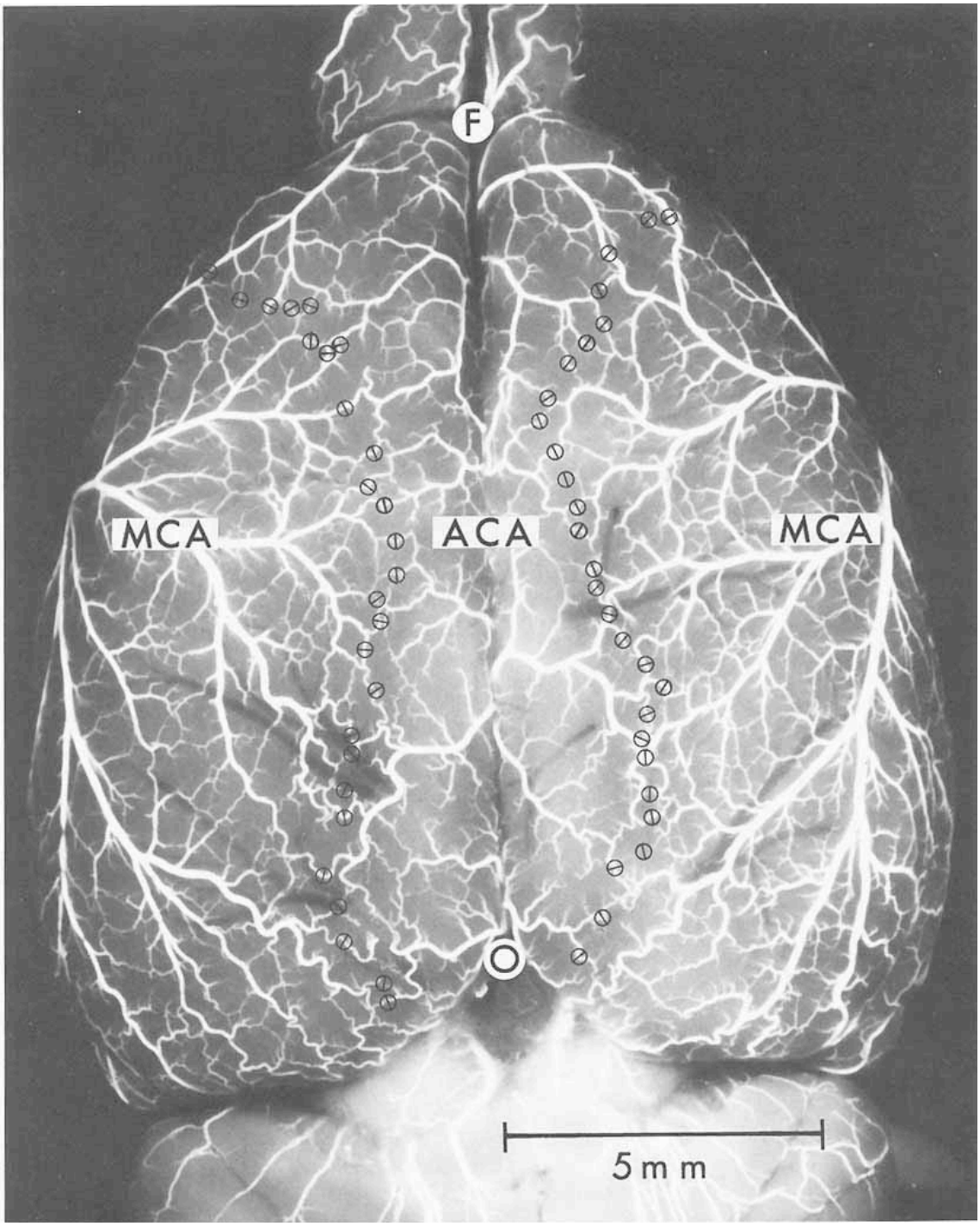

Figure 1.2: Rat pial circulation. The image highlights the high density of anastomoses present in the pial arteries and arterioles. The circles show the locations of interarterial anastomoses between branches of the anterior cerebral artery (ACA) and MCA. From [6], with permission.

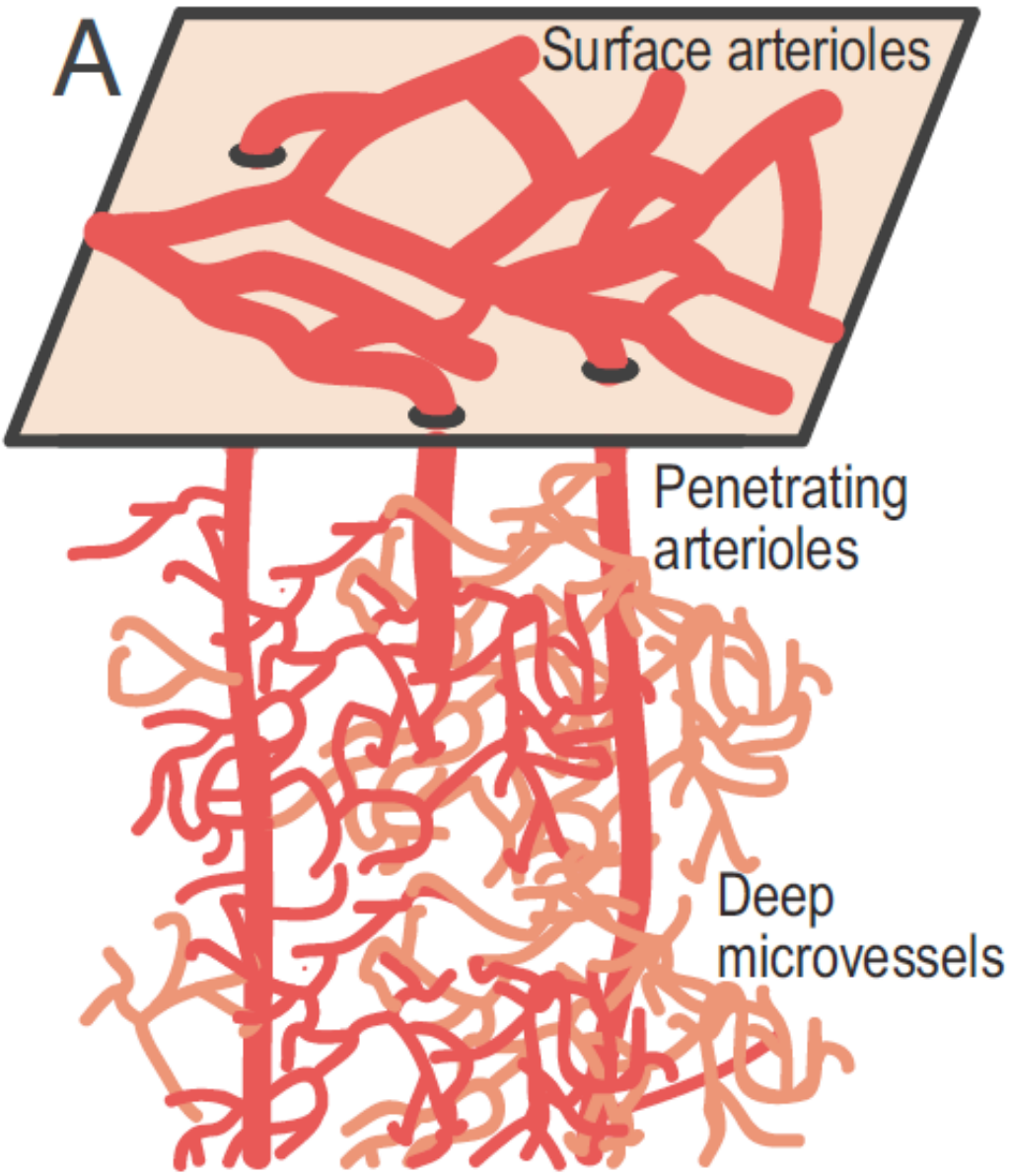

Figure 1.3: Schematic of penetrating arterioles. Surface (pial) arteries and arterioles form a highly interconnected vascular complex that branches perpendicular to the surface of the brain generating penetrating arterioles. These arterioles dive into the brain parenchyma and connect the surface circulation to the deep cerebral microcirculation. Penetrating arterioles have few anastomoses and branches. From [9], with permission.

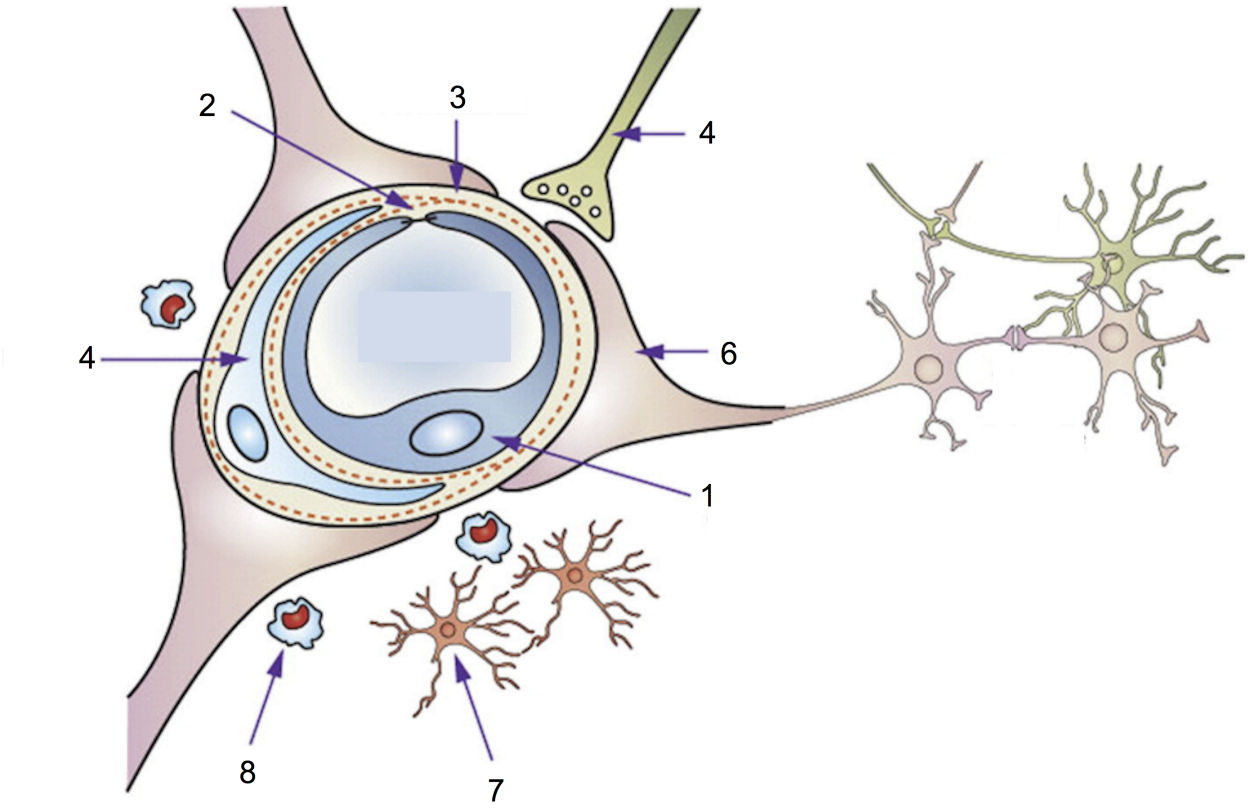

Figure 1.4: The neurovascular unit. Cerebral capillary endothelial cells (1), connected to each other by tight junctions (2), are encased by the basal lamina (3), astrocytic end-feet (4) and contractile cells called pericytes (5). Astrocytes communicate with subcortical and cortical neurons (6), as well as microglia, and regulate local perfusion through the artery to match metabolic demands of the surrounding neurons. Also, the tight junctions between endothelial cells and astrocytic end-feet form the physical and biochemical barrier that maintains cerebral homeostasis, the blood-brain-barrier. Also note the presence of perivascular macrophages (7). Adapted from [20], reproduced with permission.

1.2 – Physiology of cerebral arteries

Maintenance of a constant blood flow and the ability to match regional perfusion to neuronal demand is a direct consequence of *cerebrovascular autoregulation* and the endothelial control of vascular tone. Autoregulation is possible because of the myogenic reactivity of cerebral arteries, which is an intrinsic property of vascular smooth muscle cells to constrict in face of increases in intraluminal pressure. Myogenic reactivity is tightly regulated by the endothelium, showing that the two aforementioned processes are ultimately linked. This section will briefly review the mechanisms associated with myogenic tone generation, autoregulation and endothelial control of cerebrovascular tone.

1.1.1 – Cerebrovascular autoregulation, myogenic reactivity and resistance

Total cerebral perfusion is maintained constant even when arterial pressure fluctuates. This is a consequence of the ability of cerebral arteries to rapidly respond to intraluminal pressure by changing their diameter, a process known as autoregulation. According to Pouiselle's law (flow = $(8 \times \eta \times L)/r^4$, where η is the blood's viscosity, L is the length of the vessel and *r* is vessel's radius) the major determinant of perfusion through an artery is its diameter. Because acute alterations in blood viscosity and arterial length are rare and flow is related to eh fourth power of the artery radius, even small changes in diameter can have a significant impact in blood flow. In healthy humans the cerebral autoregulatory range is between blood pressures of 50 and 150mmHg [21]; pressures below the lower limit of the autoregulation curve can cause hypoperfusion and ischemia, and pressures above the upper limit can cause increases

in blood flow and vasogenic edema (Figure 1.5). At its most basic level, autoregulation is a consequence of the myogenic reactivity observed in cerebral arteries [22].

Myogenic reactivity is the ability of an artery to change its tone in response to alterations in wall stress while maintaining blood flow constant [23]. Intracranial arteries respond to increases in pressure by increasing tone, this reduces their lumen diameter and the blood flow through the artery (Figure 5) [24]. The tone generated is thought to be myogenic in nature, which is an intrinsic property of arteries to maintain contractile activity in the smooth muscle cells [22]. The contractility is, in turn, a response of smooth muscle cells to stretch, although the extent and duration of the response is controlled by the endothelium [25, 26].

Another striking hemodynamic characteristic of the cerebral circulation is the fact that large intracranial arteries (diameter >150μm) carry almost 50% of the total cerebrovascular resistance [27]. This is in contrast with peripheral vascular beds, where almost the totality of vascular resistance occurs in small arteries and arterioles with a diameter <100μm [28]. The high cerebrovascular resistance in large arteries is thought to be important for local control of blood flow, coupling of perfusion with metabolic demand and, to relieve microvascular pressure when systemic pressure increases acutely [7].

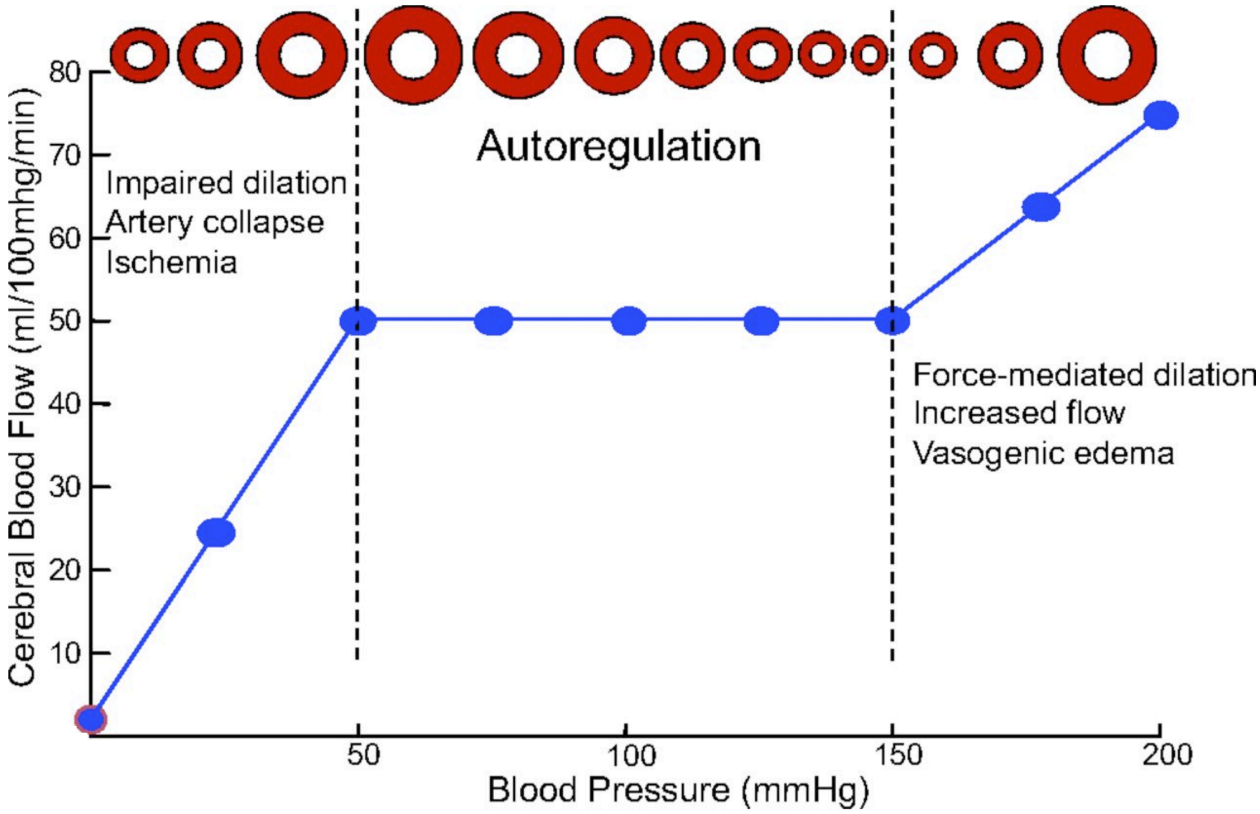

Figure 1.5: Relationship between cerebrovascular autoregulation and diameter of large cerebral arteries. Cerebral perfusion is maintained relatively constant at the interval between 50 and 150mmHg due to the myogenic reactivity of cerebral arteries, observed as a reduction in their lumen diameter. Intraluminal pressure values below 50mmHg can cause arterial collapse, hypoxia and ischemia, whereas intraluminal pressures above 150mmHg lead to force mediated dilation and vasogenic edema. From [22], originally modified from [29] with permission.

1.2.2 – Endothelium control of cerebral vascular function

The endothelium plays a central role in the regulation of vascular tone through the release of many signaling molecules that regulate smooth muscle contractility and, consequently, cerebral blood flow. The cerebral endothelium is thought to

counterbalance vascular tone by the production of signaling molecules that cause smooth muscle relaxation, including nitric oxide (NO), prostaglandin I_2 and endothelium-derived hyperpolarizing factor (EDHF).

1.2.2.1 – Nitric oxide

NO is the most studied vasodilator in the cerebral vasculature and it is an important regulator of basal myogenic tone in cerebral arteries [30]. NO is produced by the enzyme NO synthase (NOS), which converts L-arginine to NO and L-citrulline in the presence of the co-factor tetrahydrobiopterin [31]. There are three major isoforms of NOS: endothelial NOS (eNOS), neuronal NOS (nNOS), and inducible NOS (iNOS) [32]. In the cerebral vasculature, eNOS is the most important producer of NO and regulator of vascular tone, although there is evidence suggesting that NO produced from nitrergic neurons (containing nNOS) also plays a role [33]. Independently of its source, NO diffuses to smooth muscle cells and binds to an iron-containing heme moiety in the soluble guanylate cyclase. This exposes the catalytic site of the enzyme, leading to production of cyclic guanine monophosphate (cGMP) [34], which activates protein kinase G, leading to opening of potassium channels, cell hyperpolarization and relaxation [35, 36].

NO-mediated dilation is observed in all branches of the cerebrovascular tree, although the initial stimulus might differ. Large intracranial arteries and pial arteries receive extrinsic parasympathetic cholinergic innervation [12, 37]. Although parasympathetic cholinergic innervation is present in large arteries, this innervation does not seem to play a role in the physiological control of cerebral perfusion, but is

important in pathological situations, such as migraines [38]. Penetrating arterioles are intrinsically innervated by subcortical cholinergic neurons [12]. The muscarinic acetylcholine receptors M_3 and M_5 are present in endothelial cells of cerebral microvessels [39]. Receptor activation causes a small increase in intracellular calcium, which activates the Ca^{+2}/calmodulin-dependent protein kinase, leading to eNOS phosphorylation and NO production. Intrinsic cholinergic innervation is important for local control of cerebral perfusion and, consequently, functional hyperemia [40].

Purinergic receptors are also present in the endothelium of cerebral arteries, particularly the P_2Y_1 and the P_2Y_2 subtypes, and they both elicit dilation. The main agonist for the P_2Y_1 is ADP and, upon activation, this receptor elicits dilation predominantly through NO production [41]. Interestingly, branches of the MCA and penetrating arterioles do not dilate when exposed to ADP, suggesting that the P_2Y_1 may not be present in these segments [42]. The main agonists for the P_2Y_2 receptor are ATP and UDP, and activation of this receptor leads to dilation through a mechanism that is mediated by both NO and EDHF [41]. The P_2Y_2 receptor is present ubiquitously throughout the cerebrovascular tree, although its dilatory mechanism differs among different branches. In the MCA, P_2Y_2 dilation has a large NO component, whereas it shifts towards EDHF in branches of the MCA and penetrating arterioles [42]. The role of these receptors in physiological maintenance of cerebral blood flow remains unclear, although they seem to play a role in modulating astrocytic regulation of local perfusion [43].

1.2.2.2 – Endothelium-derived hyperpolarizing factor

EDHF is a dilatory mechanism dependent on activation of K^+ channels in the endothelium and subsequent hyperpolarization of smooth muscle cells [44]. EDHF dilations are present even after inhibition of NOS and cyclooxygenases and can cause maximal dilation of cerebral arteries in these conditions [41]. Even though the molecular identity of EDHF is still under debate, the dilatory process is dependent on small- and intermediate-conductance, Ca^{+2}-activated K^+ channels (SK_{Ca} and IK_{Ca}, respectively), expressed in endothelial cells [45]. In the MCA, IK_{Ca} seems to be the major channel involved in EDHF-mediated dilation [46]. Opening of these channels causes endothelial cell hyperpolarization, which is transferred to adjacent smooth muscle cells through low-resistance gap junctions present in myoendothelial junctions [47]. Some chemical mediators thought to be EDHF include epoxygenase metabolites of arachidonic acid [48] and hydrogen sulfide [49].

The role of EDHF in the physiological maintenance of cerebral blood flow is controversial. Although EDHF is important in agonist-induced dilations of large cerebral arteries [41], it does not seem to play a role regulation of basal tone, since inhibition of IK_{Ca} and SK_{Ca} does not change myogenic tone in the MCA [50]. On the other hand, penetrating arterioles are more sensitive to disturbances in EDHF. As mentioned previously, dilation of penetrating arterioles mediated by purinergic receptors occurs almost exclusively by an EDHF-mediated pathway [42]. Further, inhibition of IK_{Ca} and SK_{Ca} increases basal myogenic tone in penetrating arterioles [50]. Thus it is possible

that one of the mechanisms through which astrocytes control regional perfusion is by activation of EDHF pathways. In fact, astrocytes express the enzymatic machinery necessary to produce epoxygenase metabolites of arachidonic acid, which are thought to cause endothelium-dependent hyperpolarization [51]. However, it is unknown if arachidonic acid metabolites lead to dilation of penetrating arterioles through action on the endothelium or by directly hyperpolarizing smooth muscle cells [51].

1.3 – Hypertension and the cerebral vasculature

The chronic increase in arterial pressure observed during hypertension leads to alterations in the structure and function of cerebral arteries. The effects of chronic hypertension in cerebral arteries have recently been reviewed [22], and this section will summarize some of the changes relevant for the studies presented here.

1.3.1 – Hypertension-induced structural changes in the vasculature

One of the hallmarks of hypertension is increased vascular resistance, which can be caused by an increase in the contractility of the arteries or by structural changes resulting in an artery with a reduced diameter. It is becoming increasingly clear that changes in arterial structure may be the most important factor for the increased vascular resistance [52]. Alterations in the arterial structure are commonly referred to as *vascular remodeling* [53], and they are thought to be consequence of an initial response of the arterial wall to normalize tangential wall stress [54]. However, with time, it becomes maladaptive and can impair blood flow regulation, leading to a reduction in perfusion and end-organ damage [55].

The first quantitative evidence for hypertensive remodeling came from a study published in 1956, where Folkow measured vascular resistance in the forearm of patients after ischemia-induced maximal vascular relaxation and observed that resistance was higher in those with essential hypertension, suggesting a narrowing in the arterial lumen [56]. The invention of the small artery myograph by Mulvany and Halpern in 1976 allowed the assessment of structural, mechanical and functional properties of small arteries *ex vivo* [57]. Early studies using this system showed that the "narrowed lumen" hypothesis was indeed correct for subcutaneous small arteries, both in humans with essential hypertension [58] and in rodent models of high blood pressure [59]. Narrowing of the lumen in chronic hypertension, a phenomena named *inward remodeling*, occurs in many different vascular beds, including the mesenteric arcade [60] and coronary arteries [61]. Importantly, recent epidemiological studies show that remodeling is an independent factor that increases the risk for cardiovascular events [55, 62].

Most studies suggest that the narrowed lumen of peripheral arteries observed in chronic hypertension is due to rearrangement of wall elements instead of increase in smooth muscle mass [63]. This is referred to as *eutrophic inward remodeling*, which results in an increase in the wall-to-lumen ratio of the artery without an increase in the media cross-sectional area [53]. However, in some specific vascular beds, particularly the cerebral vasculature, there is a remarkable increase in media thickness. This wall hypertrophy, referred to as *wall growth* or *hypertrophic remodeling* [64], can be caused by an increase in the number of smooth muscle cells (hyperplasia) or simply an increase in the their volume (hypertrophy).

1.3.2 – Hypertensive remodeling of the cerebral vasculature

The first studies of the effects of chronic hypertension in the cerebral vasculature were performed in the early 1980's using pressurized basilar arteries in the Mulvany-Halpern myograph. This study showed that basilar arteries from spontaneously hypertensive rats (SHR), a genetic model of essential hypertension, have smaller lumen diameters when compared to normotensive Wistar-Kyoto (WKY) rats [65]. A similar finding was reported for pressurized basilar artery [66] and pial arterioles from stroke-prone spontaneously hypertensive rats (SHRSP) observed through a cranial window [67]. Interestingly, inward remodeling of cerebral arteries does not seem to occur in every model of hypertension. Pial arteries from rats with renal hypertension (uninephrectomy and clipping of the remaining renal artery) did not show narrowing of the lumen [68]. In this study there was no difference in systolic blood pressure between renal hypertensive rats and SHR, suggesting that blood pressure might not be the sole mechanism governing inward remodeling.

Hypertensive remodeling of the MCA has been extensively studied using many different models of hypertension. As with other segments of the cerebrovascular tree, the MCA undergoes inward remodeling, as shown in the SHRSP [69, 70], in obesity-induced hypertension [71, 72] and mineralocorticoid receptor-dependent hypertension [73, 74]. Moreover, studies from our laboratory show that, in the SHRSP, there is a dramatic thickening of the MCA wall, together with narrowing of the lumen [70, 75] (Figure 1.6). Wall thickening could be a consequence of two major processes in the MCA: 1) accumulation of extracellular matrix elements, mainly collagen and elastin and 2) smooth muscle cells hypertrophy/ hyperplasia. Our findings suggest that the second

mechanism is most likely responsible for wall thickening in the MCA of SHRSP. Support for this hypothesis comes from the finding that we do not observe changes in mechanical properties of the MCA, such as distensibility and stiffness, between SHRSP and normotensive WKY rats [70]. If there was accumulation of collagen or elastin, distensibility and stiffness would change. Thus, an alteration in smooth muscle mass is the likely explanation, although if that is caused by hypertrophy or hyperplasia is still unknown.

Organization of the smooth muscle cells in the wall of cerebral arteries is also altered in hypertensive rats. In normotensive rats, smooth muscle cells are organized concentrically and their longer axis forms a 90° angle with the direction of blood flow. However, smooth muscle cells in some regions of the basilar artery from SHRSP are rearranged in such a way that they are no longer at a 90° angle [76, 77]. These discrete regions of the vascular wall were associated with areas where the adventitia was thinner, and could represent regions where the artery is prone aneurism formation of or wall rupture. Moreover, the rearrangement of smooth muscle cells does not appear to be a general consequence of hypertension, but rather a genetic trait in SHRSP. L-NAME hypertensive rats did not have identifiable changes in the orientation of smooth muscle cells from the medial layer, even though remodeling of the basilar artery was present [78]. This suggests that the rearrangement might be genetically induced in the SHRSP, thus contributing to the “stroke-prone” phenotype observed in these rats.

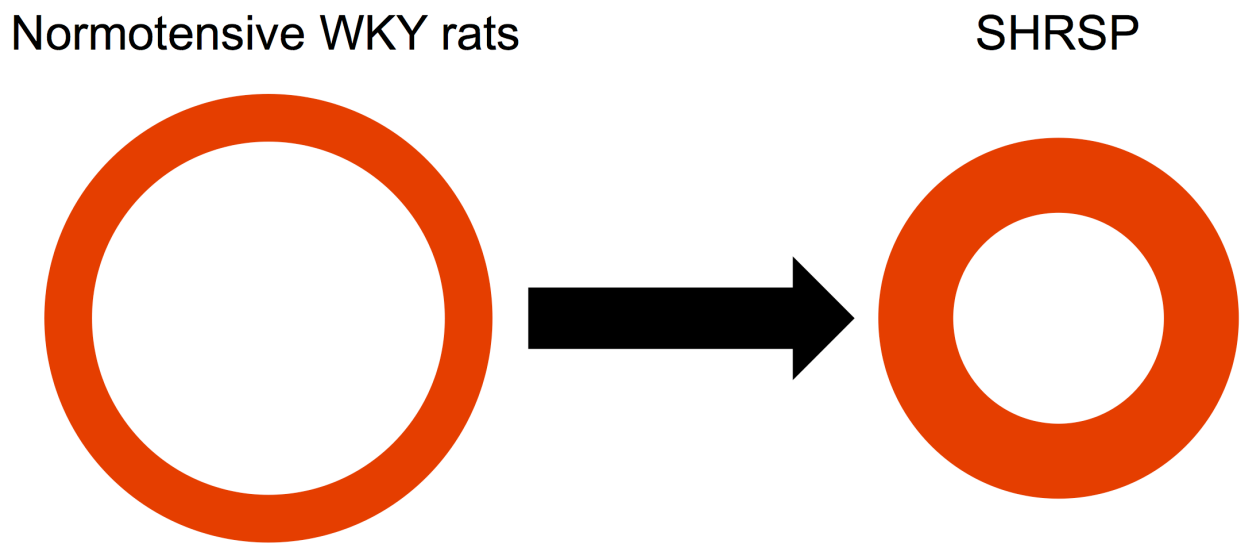

Figure 1.6: Schematic diagram of the inward hypertrophic remodeling in the MCA from SHRSP. Chronic hypertension leads to reduction in the MCA diameter, narrowing of the MCA's lumen (inward remodeling), and wall hypertrophy, observed here as an increase in the wall thickness.

1.3.3 – Mechanisms underlying hypertensive cerebral vascular remodeling

Two major mechanisms are involved in hypertensive vascular remodeling: increased circumferential wall stress and neurohumoral factors, and the evidence suggests that they are independent, at least to some extent. The first evidence of a blood pressure-independent component modulating hypertensive remodeling of cerebral arteries came from Baumbach and Hadju, who showed that pial arteries from rats with renal hypertension did not undergo inward remodeling [68]. In the recent years, many studies have shown that pharmacological interventions modulating humoral vasoactive factors prevent, and even reverse, hypertensive cerebral artery remodeling, without any significant effects on systemic pressure. Many of these studies have

focused on members of the renin-angiotensin-aldosterone system, particularly on angiotensin II (AngII) and aldosterone.

Treatment of SHR with the angiotensin-converting enzyme inhibitor (ACEi) cilazapril caused a reduction in the wall-to-lumen ratio of the MCA and pial arteries (diameter between 100 and 300μm), although blood pressure was also reduced in this study [79]. A similar finding was reported for pial arterioles from SHRSP treated with cilazapril [80] or perindopril [81]. The effects of perindopril were compared to anti-hypertensive treatment that does not target the RAAS directly. The increase in lumen diameter observed in SHRSP treated with perindopril was more pronounced than in rats treated with propranolol, although both drugs caused a similar drop in systemic blood pressure [81]. This suggested that blood pressure lowering alone was not sufficient to reduce remodeling and, perhaps, inhibition of circulating factors, such as AngII, is more effective. In fact, treatment of SHR with low-dose telmisartan (0.3mg/kg/day), an angiotensin II type 1 receptor (AT1R) antagonist, attenuated inward remodeling of the MCA to the same extent as high-dose telmisartan (3mg/kg/day), without the blood pressure lowering effect observed at the high-dose [82].

Studies in SHRSP treated with the mineralocorticoid receptor (MR) antagonist spironolactone further the evidence of a blood pressure independent component of remodeling. Our laboratory showed that treatment of SHRSP with spironolactone during the development phase of hypertension greatly attenuated MCA inward remodeling without affecting blood pressure [69]. When SHRSP with established hypertension were treated with spironolactone, we observed a reversal of the MCA remodeling, again without effects on blood pressure [83]. It has been long appreciated that MR antagonists

have little blood pressure lowering effects when given alone, although they can greatly reduce morbidity and mortality from cardiovascular accidents [84, 85]. In the SHRSP, spironolactone treatment reduced the damage after MCA occlusion, a model of ischemic stroke [69], and reduced the mortality from cerebral hemorrhages after salt-loading [86].

Similar to AngII and aldosterone blockade, other pathways are linked to cerebrovascular remodeling independently of the blood pressure. Quenching of superoxide with tempol in SHRSP attenuates MCA inward remodeling [87]. It is important to note that both AngII and aldosterone are linked to increased vascular oxidative stress [88, 89]. Therefore, it is possible that some of the effects described above for AT1R and MR antagonists are linked to reduced vascular reactive oxygen species. Moreover, activation of the peroxisome proliferation-activator receptor γ prevents remodeling of the posterior cerebral artery in L-NAME hypertensive rats [90]. The ability to prevent or reverse cerebral artery remodeling without lowering blood pressure is particularly important for the present dissertation, because blood pressure was not reduced in the studies all studies described here.

1.3.4 – Hypertension, cerebral autoregulation and myogenic reactivity

Hypertensive subjects do not show an alteration in resting cerebral blood flow, suggesting that cerebrovascular resistance is increased to counteract the high perfusion pressure [10]. In fact, during chronic hypertension, there is a shift of the autoregulatory curve to the right [21] (Figure 1.7). In SHRs, the autoregulatory range of the posterior cerebral artery ranges from 65 to 190mmHg, opposed to the range of 45 to 150mmHg

observed in WKY rats [91]. This shift in the autoregulatory curve is a consequence of increased myogenic tone generation by smooth muscle cells [92]. Remodeling of large intracranial arteries is another contributor to the shift in autoregulation due to increased cerebrovascular resistance caused by narrowing of the lumen. However, the shift in the lower end of the autoregulatory curve can increase the brain's susceptibility to ischemic damage. In the event of an occlusion, intraluminal pressure in downstream arteries may fall below the lower limit of the autoregulatory curve. In this situation, collateral blood flow becomes dependent on the passive diameter of the artery, which is narrowed in chronic hypertension.

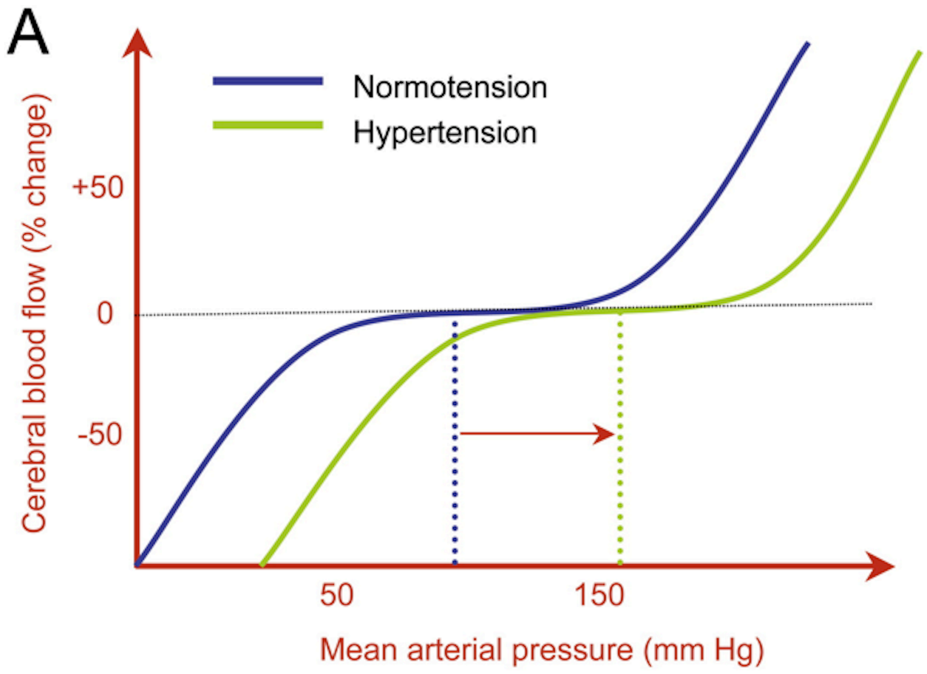

Figure 1.7: Autoregulation in chronic hypertension. Note the shift of the curve to the right in individuals with chronic hypertension (right, green curve). The dotted lines show the mean arterial pressure corresponding to the middle of the autoregulatory curve in normotensive (blue, left line) and hypertensive (right, blue line) patients. From [10], with permission.

1.3.5 – Hypertension and endothelial function

Impaired endothelium-dependent dilation is a hallmark of hypertension that has been described in the peripheral circulation and cerebral arteries. Pial arteries and arterioles from SHRSP show reduced dilatory responses to acetylcholine, serotonin and bradykinin when compared to WKY rats [93, 94]. Studies using adenosine, an endothelium-independent dilator, suggest that this difference is mediated by the endothelium and not by the smooth muscle cell's ability to hyperpolarize [94]. Furthermore, these studies suggest that the impaired vasodilation is a result of a deficiency in NO production by the endothelium, because exposure to NO donors elicited a smilar dilation in SHRSP and WKY rats [94]. Two mechanisms could account for the reduced NO bioavailability: 1) reduced NO production by NOS and 2) NO degradation by superoxide.

Incubation of pial arterioles with the calcium ionophore A23187, a receptor-independent activator of NOS, elicits a strong dilatory response in WKY rats, which is attenuated in SHRSP [93]. This suggests that the first hypothesis is correct. Reduced NOS activity could a direct consequence of uncoupling, which occurs in SHR [95]. When NOS is uncoupled, it produces superoxide instead of NO, thus reducing NO levels in endothelial cells. Additionally, cerebral microvessels from SHR have reduced eNOS expression when compared to WKY rats, which could further blunt NO production [96]. Finally, it is also possible that during chronic hypertension there is less eNOS phosphorylation in cerebral arteries, suggesting lower eNOS activation. Treatment of SHR with cilostazol, a phosphodiesterase-3 inhibitor, increases the expression of

phosphorylated eNOS and increases post-ischemic cerebral blood flow in SHR, suggesting that eNOS phosphorylation might be reduced in this model [97].

NO bioavailability can also be reduced by excessive production of superoxide. NO readily reacts with superoxide and generates peroxynitrite, thus reducing NO availability [98]. Importantly, superoxide production is increased in the vasculature of hypertensive subjects [99]. Under physiological circumstances, superoxide is dismutated into hydrogen peroxide by superoxide dismutase. Surprisingly, expression of different superoxide dismutase isoforms is increased in cerebral arteries from hypertensive rats [100]. This could be an attempt to reduce superoxide levels, or to sustain elevated levels of hydrogen peroxide, a known dilator of cerebral arteries [101]. It is possible that overproduction of hydrogen peroxide acts as a compensatory vasodilatory mechanism to counteract the chronic reduction in NO levels.

Little is known about the effects of hypertension on EDHF-mediated dilation. Although no direct studies have been performed in cerebral arteries, data from other vascular beds suggest that EDHF could be impaired in the hypertensive cerebral vasculature. EDHF-dependent dilation is reduced in mesenteric arteries from SHRSP despite an increase in the expression of IK_{Ca} [102]. In the renal artery, EDHF dilation is prominent in young SHR, but it is almost abolished as the rat ages and hypertension becomes established [103]. Impaired EDHF-mediated dilation of cerebral arteries could have a dramatic effect in the outcome of cerebral ischemia, since EDHF is an important dilatory mechanism after MCA occlusion [104].

1.3.6 – Hypertension and ischemic stroke

Ischemic stroke is a major cause of adult disability and mortality in developed countries [105]. Currently, only one pharmacological therapy is FDA-approved for treatment of ischemic stroke: tissue-type plasminogen activator (t-PA). Although efficacious, t-PA has a narrow therapeutic window, which limits its use. As a result, less than 5% of patients diagnosed with ischemic stroke are eligible for t-PA therapy. The narrow therapeutic window for t-PA is linked to its adverse affects, such as intracerebral hemorrhage, which can be fatal, and systemic bleeding [106]. Much effort in the recent years has been given to find small molecules that improve neuronal survival, with very little translational success due to the heterogeneity in the pathophysiology of ischemic stroke [107]. Therefore, primary prevention through modification and management of risk factors is still the best option for patients at risk of stroke [108].

Hypertension is a major modifiable risk factor for ischemic stroke occurrences. Anti-hypertensive therapies, including β-blockers, ACEi and AT1R antagonists, effectively reduce the risk of having an ischemic stroke (reviewed in [108]). However, there is evidence suggesting that blood pressure alone is not the only factor involved in ischemic stroke risk. A clinical trial comparing AT1R antagonists and β-blockers reported that the former was more efficacious in reducing ischemic stroke, even though both therapies caused a similar reduction is systemic blood pressure [109]. Almost 40% of hypertensive patients taking anti-hypertensive therapy do not have their blood pressure under control leaving them at risk [105]. The ONTARGET trial showed treatment of hypertensive patients with the AT1R antagonist telmisartan caused a reduction in ischemic stroke occurrences similar to that observed with the ACEi ramipril,

even though telmisartan had no effect on blood pressure, whereas ramipril did [110]. The ONTARGET trial suggests that there is a blood pressure-independent component for ischemic stroke risk, which is possibly improvement in cerebral vascular structure and function. These two aspects of the pathophysiology of ischemic stroke have been studied in rodent models of hypertension.

An important determinant of ischemic cerebral damage relies on the ability of the collateral circulation to compensate for the blocked artery. The first evidence that the collateral circulation might be impaired in hypertensive rats came from a study performed by Coyle and Jokelainen in 1983 [111]. The authors compared the outcome of MCA occlusion between mildly hypertensive young SHRSP (5-6 weeks of age) and age-matched normotensive WKY rats. The authors observed that SHRSP had bigger infarcts than WKY rats, which could not be solely explained by blood pressure. Thus, they speculated that the difference in infarct was due to a genetically determined inability of the collateral circulation to overcome the MCA occlusion, leading to impaired perfusion and bigger infarcts. This hypothesis was proven correct in a later study, where cerebral perfusion pre- and post-ischemia was measured using microspheres [112]. Although no differences were observed in pre-ischemic blood flow, the study demonstrated that SHRSP had lower post-ischemic perfusion than WKY rats, even after maximal dilation of cerebral arteries [112]. Further, the impairment in collateralization in SHRSP persists up to one month after MCA occlusion, whereas in WKY rats blood flow to the territory of the occluded artery is restored [113]. It is important to note that the collateral exist in SHRSP, they are just not providing proper perfusion. Possible

mechanisms of impaired collateral perfusion are reduced endothelium-dependent dilation and narrowing of the arterial lumen.

Endothelium-dependent dilation of cerebral arteries relies on two major pathways, NO and EDHF, as mentioned previously. During occlusion of a large intracranial artery, such as the MCA, the arteries on the circle of Willis are the most important collateral network to overcome the blockage [114]. Endothelium-dependent vasodilatory mechanisms in these proximal arteries rely mainly in nitric oxide generation [42], thus this pathway may be linked to the size of ischemic damage in the brain. Infusion of L-arginine, the substrate for NO production, increased post-ischemic cerebral blood flow in the MCA territory in SHR [115]. It also reduced infarct size [116] and promoted functional brain recovery as measured by electrocorticogram [117]. Mice deficient for eNOS had larger infarcts after MCA occlusion, which was linked to a reduction in perfusion of the MCA territory [118]. Further support for the role of NO-dependent dilation in the outcome of cerebral ischemia comes from studies with anti-hypertensive drugs. The ACEi imidapril reduced infarct size after laser-induced thrombosis in SHRSP, an effect that was lost when rats were concomitantly treated with the eNOS inhibitor L-NAME [119]. The HMG-CoA reductase inhibitor simvastatin also reduced infarct size following transient MCA occlusion, a model of ischemia/reperfusion injury, in mice. This was linked to increased post-ischemic cerebral blood flow and eNOS activity and expression [120]. Similar findings have been recently demonstrated for the antiplatelet drug cilostazol, a phosphodiesterase-3 inhibitor. Treatment of SHR with cilostazol at doses that do not inhibit platelet aggregation significantly reduced infarct size and improved cerebral blood flow [121]. This may be a consequence of

increased expression of phosphorylated, active eNOS [97]. Importantly, the findings for cilostazol have clinical significance, since the Cilostazol Stroke Prevention Study showed that patients treated with this drug were protected against secondary ischemic stroke occurences; this effect of cilostazol was independent from its antiplatelet activity [122].

Narrowing of the lumen as consequence of inward remodeling in cerebral arteries also has a profound impact in the outcome of cerebral ischemia. After cerebral ischemia/reperfusion injury, myogenic tone is reduced in the MCA [123, 124], thus it is possible that the major determinant of the MCA diameter in this circumstance is its passive structure. As mentioned above, SHRSP have larger infarcts than normotensive WKY rats when ischemic stroke is induced experimentally [111, 113]. Similarly, Wistar rats made hypertensive by treatment with deoxycosticosterone-acetate (DOCA) had larger cerebral infarcts than placebo-treated controls, an effect linked to inward remodeling of the MCA in this model [73]. In the past decade, many studies showed a link between inward remodeling of the cerebral arteries and ischemic damage. They showed that improving MCA structure reduced infarct size, mostly through blood pressure independent effects. Inhibition of the AT1R with candesartan increased the diameter of the MCA in SHR, resulting in reduced infarct after MCA occlusion [96]. Further, when SHRSP were treated with spironolactone, there was attenuation in the inward remodeling of the MCA [69], together with a reduction in cerebral ischemic damage, without changing systemic blood pressure [125]. The link between MCA remodeling and infarct size was also observed in a rodent model of diet-induced

obesity-associated hypertension. The obese and hypertensive rats showed inward hypertrophic remodeling of the MCA and larger infarcts after MCA occlusion [72].

In conclusion, treatments aimed at improving cerebral artery function and structure may be a useful therapy for hypertensive patients that do not respond to antihypertensive drugs and are at high-risk for ischemic stroke occurrences. Thus, a better understanding of the mechanisms underlying hypertensive remodeling and dysfunction of the MCA is warranted in order to provide new targets for therapy. One possible mechanism that has gathered attention in the recent years is the role of vascular inflammation.

1.3.7 – The stroke-prone spontaneously hypertensive rat

The SHRSP strain is a widely used genetic model of essential hypertension and cerebrovascular disease. SHRSP were initially isolated through inbreeding of SHR and selection for a stroke phenotype [126]. These rats are normotensive at 4 weeks of age [127], but their blood pressure starts rising exponentially after the 6th week of age, until reaching a plateau at approximately 20 weeks of age (Figure 1.8) [128]. Blood pressure in SHRSP can reach 220mmHg in adult males and cerebrovascular lesions can be observed in 80% of rats older than 30 weeks of age [129]. Salt-loading accelerates the development of hypertension and incidence of lethal cerebral hemorrhages in this model.

The pathophysiology of hypertension in SHRSP and development of end-organ damage is similar to that observed in hypertensive humans. SHRSP have an overactive renin-angiotensin system [130], upregulation of the endothelin-1 system [131] and

increased sympathetic nerve activity [132]. Further, SHRSP develop hypertensive end-organ damage in a similar manner to humans with malignant hypertension. As SHRSP age, they develop kidney damage, observed as glomerular necrosis, arteriolar fibrinosis and necrosis, uremia and proteinuria [133]. Myocardial infarctions, myocardial fibrosis and arteriolar stenosis or even occlusions are found in the heart [133]. Similar renal and cardiac lesions are seen in humans with malignant hypertension.

SHRSP have extensive cerebrovascular damage, loss of blood-brain-barrier integrity and parenchymal damage. Cerebral vascular damage is observed as arteriolar fibrinoid necrosis [133], loss of smooth muscle cells in the wall of penetrating arterioles and presence of intraluminal fibrin-rich thrombi [134]. Accumulation of erythrocytes in capillaries of SHRSP occurs in approximately 60% of animals at 12 weeks of age [135]. As the hypertension progresses and the SHRSP ages, there is extravasation of erythrocytes into the parenchyma (microbleeds), microthrombosis and small lacunar infarctions in virtually every rat [136]. These lacunar infarcts are similar to those found in human brains. The current hypothesis is that lacunar infarcts observed in SHRSP are caused by blood-brain-barrier breakdown and endothelial damage, that leads to the occlusion of small arterioles [137]. Small lacunar infarcts in SHRSP are frequently observed in the white matter [134], and may underlie cognitive impairments observed in this model [138]. Although spontaneous large cerebral infarcts are rarely observed in SHRSP, experimental MCA occlusion results in a larger cerebral infarction in these rats than in normotensive WKY rats, as discussed previously.

In conclusion, SHRSP are a relevant model of malignant hypertension, particularly for studies of cerebral small vessel disease and ischemic stroke. Recently, it

has been emphasized the importance of studying strokes with co-morbidities in an attempt to better model the clinical situation [139]. In this scenario, SHRSP are a useful model to evaluate hypertensive cerebral vascular damage and its consequences.

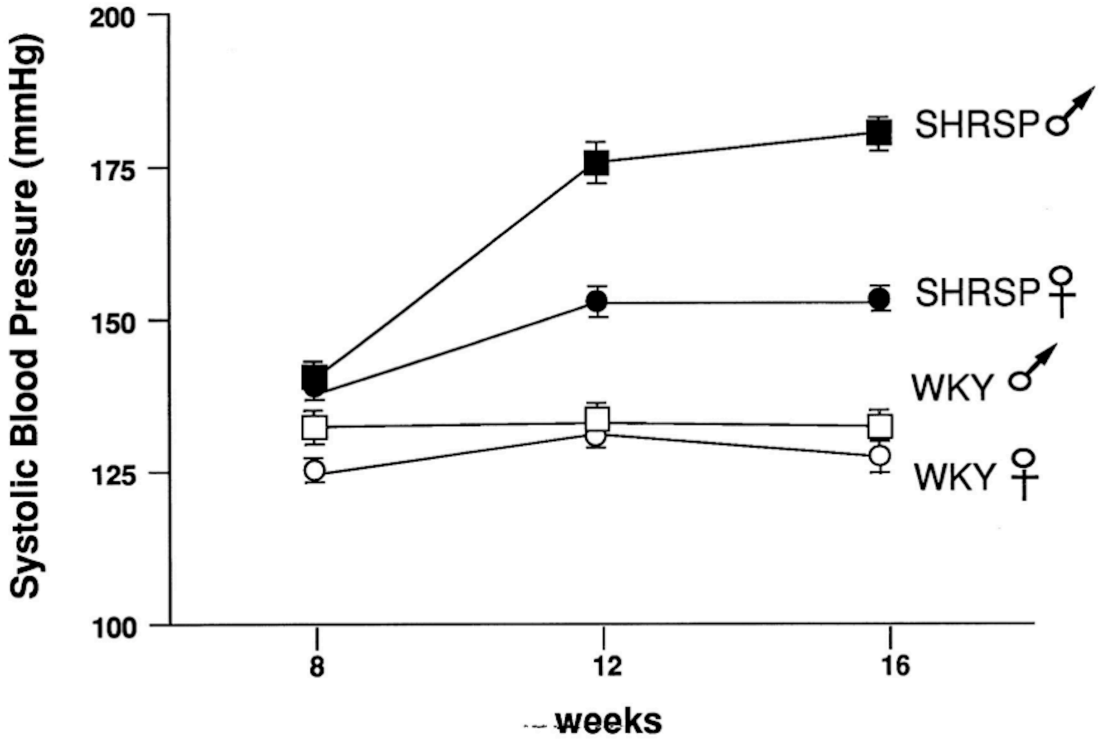

Figure 1.8: Temporal blood pressure increases in SHRSP. Systolic blood pressure increases exponentially in male SHRSP (black filled squares) between 6 and 12 weeks of age, reaching a plateau after the age of 16-20 weeks. Blood pressure in female SHRSP (black-filled circles), although higher than female normotensive WKY rats, does not reach the same levels as males. Blood pressure in WKY rats is not different between males and females (open squares and circles, respectively). Reproduced with permission from [128].

1.4 – Vascular inflammation

Chronic hypertension causes a systemic low-grade, chronic inflammatory response, as well as a more pronounced and localized inflammation in the vasculature. In the recent years, much focus has been placed on the role played by inflammatory mediators in the pathophysiology of hypertension, and a link between vascular inflammation and high blood pressure has emerged. This link provided the rationale for the overarching hypothesis of this dissertation, which is that inflammation is a causative agent in hypertensive remodeling and dysfunction of cerebral arteries.

1.4.1 – Inflammation and the pathophysiology of hypertension

The initial evidence that inflammation might be linked to the development of hypertension came from epidemiological studies in the early 2000s. A cross-sectional study found that increased systolic blood pressure was positively correlated to circulating levels of the inflammatory markers soluble intercellular adhesion molecule (ICAM)-1 and interleukin (IL)-6 [140]. Similarly, plasma levels of C-reactive protein (CRP) were increased in newly diagnosed, untreated hypertensive patients when compared to levels found in normotensive individuals [141]. In another epidemiological study with a cohort of more than 20,000 patients followed for 7.8 years, it was shown that plasma levels of high-sensitive CRP successfully predicted the development of hypertension, even in patients with an initial low blood pressure [142]. It is possible that inflammation increases the likelihood of developing hypertension through structural and functional changes in the vasculature that increase total peripheral resistance. The current literature supports this possibility.

Many vasoactive hormones that play a role in hypertension also lead to vascular inflammation. AngII induces activation of NF-κB in vascular smooth muscle cells [143, 144]. NF-κB is a major regulator of the expression of proinflammatory cytokines. AT1R antagonism prevented the upregulation of mRNA for proinflammatory cytokines, including tumor necrosis factor (TNF)-α, in a mouse model of neointimal hyperplasia and *in vivo* smooth muscle cell proliferation [145]. Interestingly, some circulating proinflammatory mediators, including CRP [146] and IL-6 [147], induce expression of the AT1R in cultured smooth muscle cells. This gives rise to a feedforward loop that could potentiate vascular inflammation and damage. AngII also induced NF-κB-mediated expression of adhesion molecules in cultured endothelial cells [148]. Aldosterone induces expression of ICAM-1 in cultured human coronary endothelial cells through activation of the mineralocorticoid receptor, leading to an increase in leukocyte adhesion to endothelial cells [149]. This fact could have in vivo implications for leukocyte infiltration into the vessel wall, and these cells may be mediators of hypertensive vascular remodeling and dysfunction.

1.4.2 – Perivascular macrophages

Leukocyte adhesion and infiltration into tissues is an important step of the inflammatory response. This process is dependent on the expression of adhesion molecules in both the leukocytes and endothelial cells, as well as presence of chemotactic factors. Hypertensive patients have increased circulating levels of soluble ICAM-1 and monocyte chemotactic protein (MCP)-1 [150]. In addition, circulating levels of preactivated monocytes, precursors of tissue macrophages, are increased in patients

with essential hypertension [151]. Taken together, these observations present the possibility that there is increased leukocyte recruitment and, most likely, accumulation in the vasculature. In fact, accumulation of perivascular macrophages was reported in the aorta, mesenteric, intramyocardial arteries and cerebral microvessels of hypertensive rats [152, 153]. Importantly, macrophages release many mediators known to lead to vascular dysfunction and remodeling.

Phagocytes, such as macrophages, express high levels of NADPH-oxidase, a major source of reactive oxygen species [154]. Particularly, they express the NOX2 isoform, which is inducible and releases a burst of superoxide upon activation [155]. The immediate consequence of this, as explained previously, is reduction in NO levels [156] and, consequently, endothelial dysfunction. Additionally, superoxide is a mediator of MCA remodeling in SHRSP [87]. Evidence that perivascular macrophages are involved in vascular remodeling was provided by studies using homozygous osteopetrotic mice (Op/Op), a mouse strain deficient in macrophage-colony stimulating factor. Implantation of DOCA pellets in wild-type (+/+) and heterozygous (Op/+) mice caused hypertension, endothelial dysfunction, vascular oxidative stress and remodeling of mesenteric arteries. In contrast, mesenteric arteries from the homozygous Op/Op mice did not exhibit remodeling, had improved endothelial function and lower superoxide levels [157]. Similar findings were reported when Op/Op mice were infused with AngII [158]. A final observation made in these studies was that hypertensive wild-type mice showed higher levels of NF-κB activation in the aorta and mesenteric arteries than Op/Op littermates. As mentioned earlier, NF-κB is a major transcription factor

involved in expression of proinflammatory cytokines, such as TNF-α, and matrix metalloproteinases [159]. These two macromolecules will be discussed in detail below.

One major problem in elucidating the role of perivascular macrophages in hypertensive vascular remodeling has been to separate the effects of lowering blood pressure. In both studies mentioned above, Op/Op mice showed only a modest increase in blood pressure than wild-type littermates, thus it could be argued that the protective effects observed were consequence of a lower arterial pressure. Treatment of SHR with the AT1R antagonist candesartan reduced the number of perivascular macrophages in the cerebral microvasculature, but it also reduced blood pressure in these rats [160]. The only evidence that perivascular macrophages may be involved in remodeling of the cerebral vasculature independently of systemic pressure comes from a study in which SHRSP were treated with pioglitazone. In this study, pioglitazone reduced the number of perivascular macrophages in the cerebral microvasculature of SHRSP and improved MCA structure [153]. However, a causative link between macrophages and structure of the MCA was not explored in the study.

A valuable pharmacological tool to study the role of macrophages in disease processes is liposome-encapsulated clodronate (CLOD). Clodronate (dichloromethylene - biphosphonate) is a highly polar bisphosphonate drug used for the treatment of osteolytic diseases. It has a short half-life when freely circulating in the plasma and does not cross biological membranes due to its polarity and hydrophylicity [161]. The main therapeutic use of bisphosphonates is to prevent bone reabsorption, because these drugs accumulate in the bone and are internalized by osteoclasts, where their intracellular concentration rise to toxic levels, leading to apoptosis [162]. This

physicochemical characteristic of clodronate makes it an interesting drug to be administered via liposomes, conferring some selectivity for targets. The membrane composition and size of the liposome can be manipulated such as the final product has a selectivity for cells with high phagocytic activity, including macrophages (Figure 8). The most commonly used formulation was developed by Dr. Nico vanRooijen, and consists of multilamellar liposomes rich in phosphatidylcholine and cholesterol [163]. Once the clodronate-containing liposome is engulfed by macrophages through endocytosis, it fuses with lysosomes containing phospholipases, which then disrupt the liposomal membrane, releasing clodronate. This event is called cell-trapping, because free clodronate does not cross the plasma membrane and accumulates in the cytoplasm, reaching concentrations that lead to apoptosis [164] (Figure 1.8). The usefulness of CLOD for vascular research is highlighted by a few studies. The neointimal hyperplasia that occurs after balloon injury in the carotid artery of both rabbits and rats is reduced by acute macrophage depletion with CLOD [165]. Chronic macrophage depletion with CLOD also prevented flow-induced outward remodeling of the common carotid artery in rats [166]. However, no studies have assessed the role of perivascular macrophages in hypertensive inward remodeling of the cerebral vasculature.

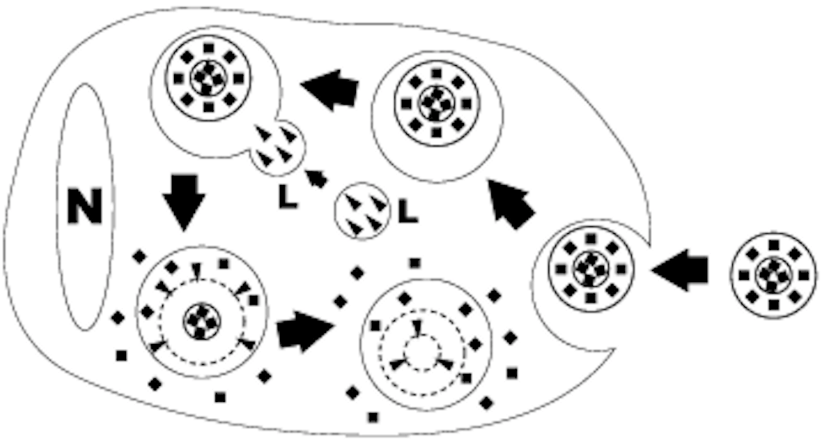

Figure 1.9: Liposome-encapsulated clodronate and the "macrophage suicide" technique. Clodronate liposomes are internalized by macrophages through endocytosis and fuse with lysosomes (L) in the cytoplasm. Lysossomal phospholipases disrupt the membrane of the liposome, and free clodronate is released, accumulating in the cytoplasm to a toxic concentration, leading to cell death. (N): macrophage nucleus. From [163], with permission.

1.4.3 – Tumor necrosis factor-alpha

The involvement of TNF-α in the development of hypertension has been elucidated in the recent years. Patients with rheumatoid arthritis undergoing anti-TNF-α therapy showed a modest reduction in systolic and diastolic blood pressures [167]. This mild anti-hypertensive effect could be a consequence of improved endothelial function observed after prolonged TNF-α inhibition [168]. In rats with angiotensin II-salt dependent hypertension, etanercept (ETN) treatment delayed the development of hypertension, although blood pressure was similar between groups at the end of the study [169]. Deletion of the TNF-α gene in mice prevented the rise in mean arterial

pressure after angiotensin II infusion, and this effect was lost after administration of exogenous TNF-α [170]. In addition to its effects on blood pressure, TNF-α is also involved in hypertensive organ damage. Inhibition of TNF-α with ETN prevented renal damage in rats with angiotensin II-salt hypertension [169]. A similar effect was observed in DOCA-salt hypertensive rats [171].

TNF-α may be the link between perivascular macrophages and vascular remodeling. Increased levels of this cytokine are observed in flow-induced remodeling of mesenteric arteries in rats even before any structural changes are observed [172]. The increase in TNF-α was associated with higher expression of macrophage markers [172]. TNF-α activates many intracellular pathways that can culminate in remodeling. Vascular smooth muscle cell proliferation and migration were increased after *in vitro* incubation with TNF-α [173, 174]. Further, TNF-α also induces expression of matrix metalloproteinases (MMPs) by vascular smooth muscle cells [175] and collagen deposition in the rodent heart [176]. Interestingly, the proliferative responses and production of MMPs induced by TNF-α were more pronounced in vascular smooth muscle cells isolated from SHR than in those from normotensive WKY rats [175]. TNF-α also induces expression of ICAM-1 in endothelial cells [177], which could potentially increase leukocyte infiltration to the vessel wall, generating a feed-forward loop of vascular inflammation. It remains to be determined if TNF-α plays a role in the hypertensive remodeling of the cerebral vasculature.

Vascular function, including myogenic tone generation and endothelium-dependent dilation, can also be affected by TNF-α. Although the role of TNF-α in regulation of cerebral vascular function under physiological condition is unknown, a

recent study suggests that this cytokine is important during pathological conditions. Myogenic tone of the posterior cerebral artery is increased in a rodent model of heart failure, which compromises cerebral perfusion [178]. The increase in myogenic tone seems to be dependent on TNF-α, since ETN treatment reduces myogenic tone generation [178]. Similarly, TNF-α potentiates hemolysis-induced vasoconstriction of basilar arteries and ETN alleviates cerebral vasospasm induced by subarachnoid hemorrhages [179]. How TNF-α affects myogenic tone of cerebral arteries in chronic hypertension is unknown.

As mentioned previously, an important regulator of cerebral myogenic tone is endothelium-derived NO, and TNF-α interferes with NO production and bioavailability. *In vitro*, TNF-α reduces eNOS expression by reducing promoter activity [180], destabilization of the eNOS mRNA [181, 182] and reduced levels of the protein [183]. Further, this cytokine reduces eNOS production of NO after *in vitro* stimulation of endothelial cells by vasodilators, such as bradykinin [183]. Taken together, these data suggests that TNF-α might mediate endothelial dysfunction. In fact, coronary arteries from obese rats treated with TNF-α show a blunted response to acetylcholine, which is recovered by ETN treatment [184]. The reduced NO bioavailability could be a consequence of increased superoxide production by NADPH-oxidase. *In vitro* incubation of human aortic smooth muscle cells with TNF-α caused an upregulation of Nox-1 and Nox-4, together with an increased in superoxide production [185]. Although still undetermined, it is possible that TNF-α is a mediator of hypertensive endothelial dysfunction of cerebral arteries.

1.4.4 – Matrix metalloproteinases

Rearrangement of arterial wall elements observed in chronic hypertension is largely dependent on the activity of enzymes that degrade extracellular components, the matrix metalloproteinases. These enzymes are a family of zinc-dependent peptidases that share sequence homology and degrade the many different components of the extracellular matrix. All members of the MMP family share some domain homology with MMP-1: a pro-domain, which contains a cysteine switch motif (important for enzyme activation) and a zinc-binding domain in the catalytic site with a conserved sequence rich in histidine [186]. MMP family members are categorized into subfamilies according to their substrate specificity (Figure 1.9). Collagenases degrade fibrillar interstitial collagen, such as collagens type I, II and III; MMP-1, -8 and -13 are members of this subfamily. The gelatinases MMP-2 and MMP-9 degrade cleaved collagen and elements of the basement membrane, including non-fibrillar collagen IV and laminin. Macrophage metalloelastase, or MMP-12, is mainly involved in cleavage of elastin fibers. The membrane-type MMPs, particularly MMP-14, degrade fibrillar collagen and activate other MMPs.

MMP expression and activity is regulated at many levels, including transcriptional and post-translational mechanisms. Most MMPs have a low-level constitutive expression and are important for normal tissue physiology. However, during pathological conditions, their expression increases. Proinflammatory cytokines are important stimulators of MMP expression [187], and the promoter region of the MMP-1, -3 and -9 genes have a NF-κB binding sequence [188]. In fact, in human aortic smooth muscle cells, TNF-α induced the expression of MMP-9 through activation of NF-κB,

which binds directly to its *cis*-element in the promoter region of the MMP-9 gene [189]. Although transcriptional regulation is important for MMP expression, these enzymes are synthesized in a zymogen form and require post-translational activation. Activation of the MMP pro-form occurs upon cleavage of the hemopexin domain, which can be performed by non-specific proteases or by other MMPs. As an example, activation of pro-MMP-2 requires the hemopexin domain to be cleaved by membrane-type MMPs [190]. Finally, a third level of regulation of MMP activity is dependent on the expression of the tissue inhibitor of MMPs (TIMPs), which bind to active MMPs in a 1:1 stoichiometry [191]. TIMPs are wedge-shaped small peptides that inhibit MMPs by binding to the active site in a manner similar to their substrate [192]. Interestingly, activation of MMP-2 by the membrane-type MMP requires prior formation of a complex between pro-MMP-2 and TIMP-2, which in turn binds to the membrane-type MMP and leads to cleavage and activation of MMP-2 [193].

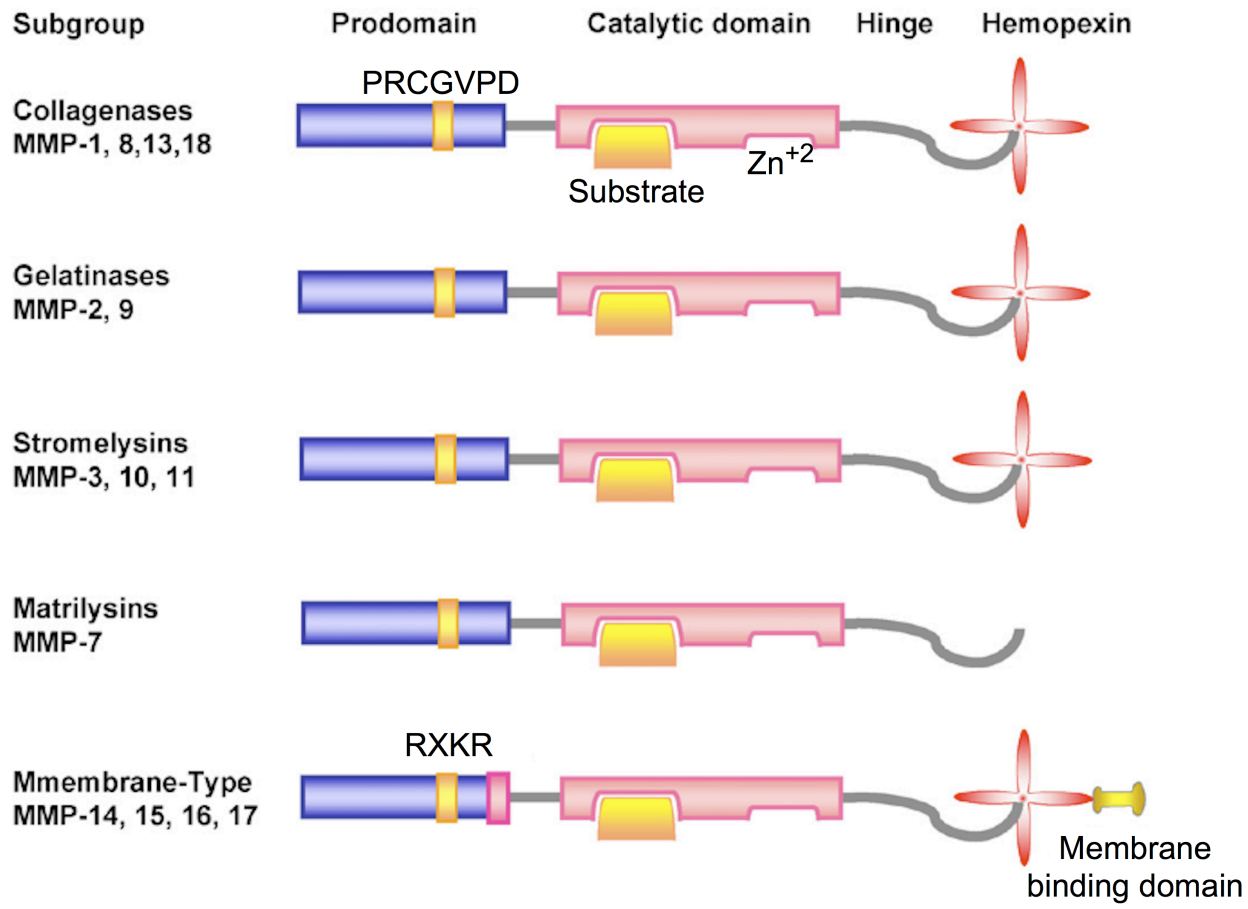

Figure 1.10: Structure of matrix metalloproteinases. The prodomain contains a cysteine switch (PRCGVPD) that is important for activation of the zymogen. Upon activation, the MMP detaches from the hemopexin domain and is free to bind to its substrate in the active site. Only the membrane-type MMPs have a membrane binding domain. From [186], with permission.

In the cardiovascular field, most studies have focused on the activity and expression of the gelatinases MMP-2 and MMP-9. Serum levels of MMP-2 and MMP-9 are elevated in patients with isolated systolic hypertension and correlate with arterial stiffening and aortic pulse wave velocity [194]. Further, MMP-9 levels are elevated in the early stages of essential hypertension in humans [195], and this enzyme is a predictor

of cardiovascular risk in patients with coronary artery disease [196]. Increased MMP-2 and MMP-9 activity and expression has also been observed in rodent models of hypertension. Protein expression and gelatinolytic activity of both MMP-2 and MMP-9 were increased in the thoracic aorta from DOCA-salt hypertensive rats, a model that shows hypertrophic remodeling of the thoracic aorta [197]. Similar findings were reported for the thoracic aorta from L-NAME and 2-kidneys-1-clip hypertensive rats [198, 199], and in carotid arteries from angiotensin II-salt hypertensive mice [200]. Although the role of gelatinases in hypertensive remodeling of conduit arteries is well described, little is known about the role these enzymes play in remodeling of resistance arteries. One study reports that, in the L-NAME hypertensive rat, expression and activity of MMP-2 is increased in mesenteric resistance arteries, which undergo eutrophic remodeling [198].

Given the importance of MMPs for hypertensive vascular remodeling, inhibition of these enzymes might prevent, or at least ameliorate, the deleterious effects of high blood pressure in arteries. Tetracycline antibiotics, particularly doxycycline (Dox), are potent broad-spectrum inhibitors of MMPs. Dox inhibits MMPs at lower concentrations than those required for antimicrobial activity [201], suggesting that MMP inhibition is independent of its antibiotic mechanism of action. In fact, Dox inhibits MMPs by directly binding to the zinc domain, thus altering their interaction with substrates and, consequently, their enzymatic activity [202]. Dox also reduced MMP gene transcription [203]. Combined, the effects of Dox on MMP expression and activity can be protective against hypertensive vascular remodeling. In support of this hypothesis, Dox completely prevented the hypertrophic remodeling of the thoracic aorta in the 2-kidneys-1-clip

hypertensive rat [204], and partially prevented the increase in media-to-lumen ratio of the thoracic aorta in L-NAME hypertensive rats [198].

Vascular function can also be altered by MMPs, since these enzymes are involved in processing of vasoconstrictors and NO bioavailability. Recent evidence suggests that MMP activity leads to vasoconstriction and may impair endothelium-dependent vasodilation [205]. MMP-2 is involved in cleavage of the big endothelin-1 peptide in rat mesenteric arteries, yielding two small peptides with vasoconstrictor activity, one of them endothelin-1 [206]. In addition, MMPs cleave the vasodilator calcitonin gene-related peptide into smaller peptides that show a 20-fold lower dilatory capability [207]. Similarly, MMP-2 cleaves adrenomedullin into many different smaller peptides, some of them without vasodilatory activity and one with possible vasoconstrictor activity [208]. Aortic rings from 2-kidneys-1-clip hypertensive rats showed impaired endothelium-dependent dilation to acetylcholine, which was reversed by Dox treatment [204]. This effect is likely a consequence of the increased NO bioavailability observed in the study, which could in turn be caused by a decrease in superoxide generation after Dox treatment [209]. Improved response to acetylcholine was also reported in mesenteric arteries of normotensive MMP-9 knockout mice [210].

Activity of MMP-2 and -9 in the arterial wall can be triggered by both hemodynamic and humoral stimuli. MMP-2 expression is increased in carotid arteries following balloon injury, and is potentiated by low flow conditions [211]. Increased transmural pressure induced the expression and activity of gelatinases in *ex vivo* carotid arteries [212], suggesting that wall stress might be involved in the regulation of MMP expression and activity. AngII stimulates *in vitro* expression and release of MMP-1 and -

9 from human vascular smooth muscle cells, but not MMP-2 [213]. The stimulation is dependent on NF-κB activation by the AT1R, since the expression of MMP-1 is blunted when AT1R antagonists are present, as well as by knockdown of NF-κB [213]. Angiotensin II also acted synergistically with increased transmural tension to induce MMP-2 expression in the thoracic aorta of transgenic mice [214], suggesting an interplay between hemodynamic effects and humoral stimulus. Another link between AT1R and MMP expression is through activation of NADPH-oxidase, a known target of the AT1R [215]. Reactive oxygen species, especially peroxynitrite, can also cause MMP-2 activation by altering the chemical structure of the cysteine switch in the active site, by causing intramolecular cleavage of the propeptide [190]. Mechanical stretch induces MMP-2 mRNA and protein expression in cultured aortic smooth muscle cells isolated from mice, through a mechanism dependent on the NADPH oxidase subunit p47*phox* [216]. Aldosterone stimulates MMP-2 and MMP-9 activity in cultured cardiac myocytes via NADPH oxidase generation of reactive oxygen species [217]. MMP-2 mRNA expression was also increased in the aorta of aldosterone-hypertensive rats, as well as the mRNA for p47*phox* [218]. It is important to note that both AT1R antagonists and mineralocorticoid receptors antagonists prevent hypertensive remodeling of the MCA [69, 82]. Although not evaluated in these studies, it is possible that one of the downstream mediators responsible for the AT1R and mineralocorticoid receptor dependent remodeling are MMPs.

Inflammatory mediators, including inflammatory cells and proinflammatory cytokines, also stimulate MMP expression and activity in the vasculature. Incubation of human vascular smooth muscle cells with TNF-α causes secretion of MMP-1, -2 and -3

in vitro [213]. TNF-α also induces MMP-2 activity in cultured cardiac fibroblasts isolated from adult rats [219]. Further, TNF-α stimulates activation of pro-MMP-2 in human skin by increasing expression of the membrane-type MMP-1 via the NF-κB pathway [220]. Macrophages derived from human circulating monocytes also express MMP-2 in culture [221]. Macrophage-derived foam cells are a major source of MMPs in atherosclerotic lesions, and the activity of these enzymes determines plaque stability [222]. In particular, MMP-12 is exclusively expressed by macrophages and its activity is important to allow macrophage infiltration through the wall of arteries and arterioles that possess an elastic lamina. Thus, it is possible that perivascular macrophages also modulate vascular remodeling both by releasing MMPs and by releasing proinflammatory cytokines, especially TNF-α, which will in turn stimulate MMP release from vascular smooth muscle cells.

1.5 – Scope of this project

Based on the gaps in the literature and the rationale provided in the introduction, the central hypothesis of this research project was that perivascular macrophages play a causative role in hypertensive remodeling of both the cerebral and peripheral resistance vasculature through a mechanism dependent on MMPs and TNF-α (Figure 1.11). This hypothesis was tested by the following experimental protocols:

1.5.1 – Removal of perivascular macrophages with CLOD

As mentioned previously, CLOD is a powerful tool to deplete circulating phagocytic cells, including monocytes/macrophages. This study predicted that chronic

macrophage depletion would reduce the number of perivascular macrophages in the MCA of SHRSP. This would improve the passive structure and endothelium-dependent dilation of the MCA and reduce TNF-α and MMPs expression in cerebral arteries from the circle of Willis. MRA passive structure was assessed to determine if the MCA response to CLOD was specific or a generalized improvement in resistance arteries.

1.5.2 – MMP inhibition with Dox

The tetracycline antibiotic Dox is a potent broad-spectrum MMPs inhibitor, which prevents hypertrophy of the thoracic aorta in renal hypertensive rats [204]. The hypothesis for this study was that MMPs inhibition with Dox would attenuate hypertensive remodeling and dysfunction of the MCA, resulting in improved cerebral perfusion and reduced brain damage after MCA occlusion. In addition, this study was designed to investigate if Dox would prevent inward hypertrophic remodeling of the peripheral vasculature, particularly the mesenteric arcade.

1.5.3 - TNF-α inhibition with ETN

Tumor necrosis factor-α is a proinflammatory cytokine released mainly by macrophages that is implicated in vascular remodeling and dysfunction. The hypothesis for this study was that chronic ETN treatment would attenuate hypertensive remodeling of the MCA, leading to improved cerebral blood flow and reduced ischemic damage after MCA occlusion. This study also aimed at assessing the role of TNF-α in hypertensive remodeling of the mesenteric resistance vasculature.

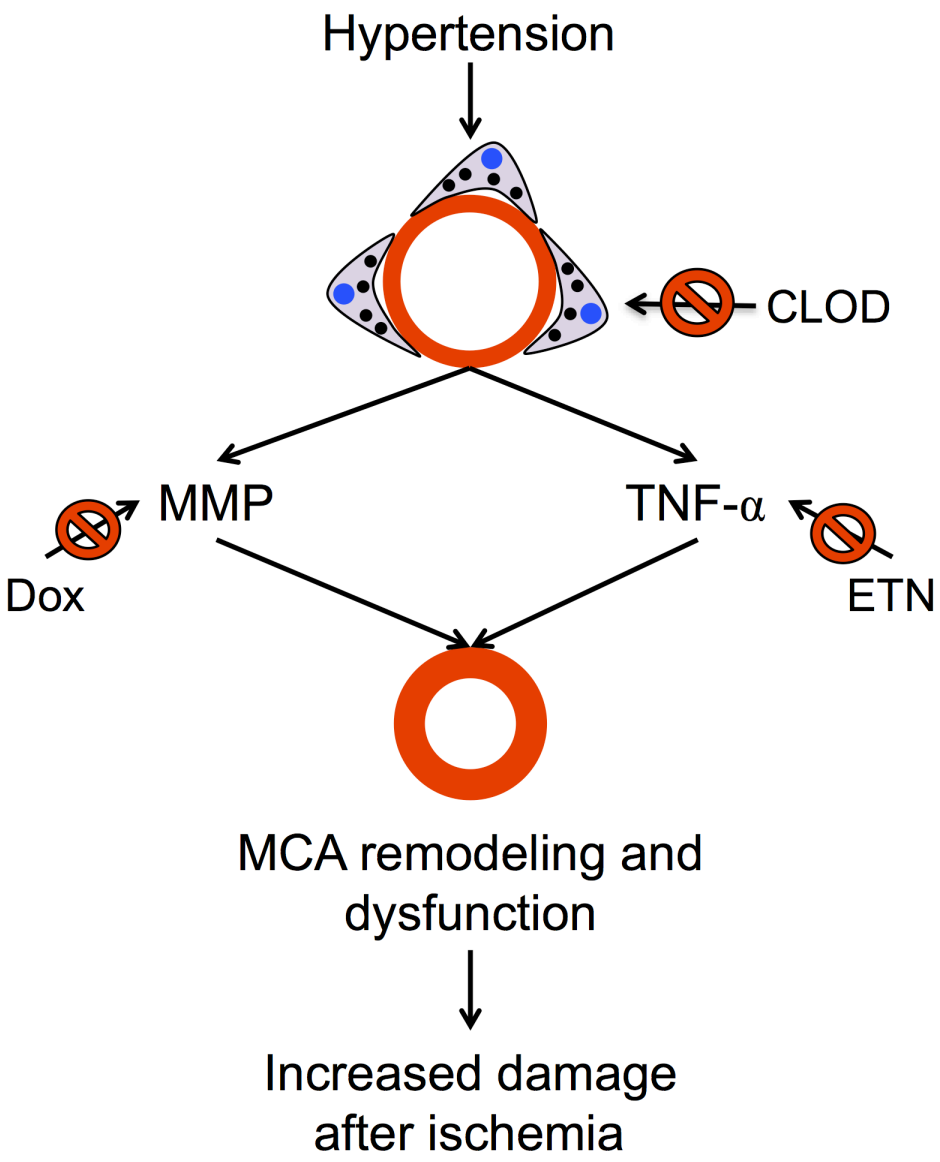

Figure 1.11: Overarching hypothesis of the present project. Hypertension increases the number of perivascular macrophages, which leads to MCA remodeling and dysfunction through release of MMP and TNF-α in the arterial wall. MCA remodeling and dysfunction will increase infarct size after cerebral ischemia. This hypothesis was tested by macrophage depletion with CLOD (Aim 1), MMP inhibition with Dox (Aim 2) and TNF-α inhibition with ETN (Aim 3).

APPENDICES

Appendix A: License Agreement for Figure 1.2

JOHN WILEY AND SONS LICENSE TERMS AND CONDITIONS

Aug 07, 2013

This is a License Agreement between Paulo W Pires ("You") and John Wiley and Sons ("John Wiley and Sons") provided by Copyright Clearance Center ("CCC"). The license consists of your order details, the terms and conditions provided by John Wiley and Sons, and the payment terms and conditions.

All payments must be made in full to CCC. For payment instructions, please see information listed at the bottom of this form.

License Number	3203810398436
License date	Aug 07, 2013
Licensed content publisher	John Wiley and Sons
Licensed content publication	The Anatomical Record: Advances in Integrative Anatomy and Evolutionary Biology
Licensed content title	Dorsal cerebral arterial

	collaterals of the rat
Licensed copyright line	Copyright © 1982 Wiley-Liss, Inc.
Licensed content author	Peter Coyle,Pentti T. Jokelainen
Licensed content date	Jan 26, 2005
Start page	397
End page	404
Type of use	Dissertation/Thesis
Requestor type	University/Academic
Format	Print and electronic
Portion	Figure/table
Number of figures/tables	1
Original Wiley figure/table number(s)	FIGURE 3
Will you be translating?	No
Total	0.00 USD

TERMS AND CONDITIONS

copies prepared before may be distributed thereafter). The Materials shall not be used in any other manner or for any other purpose. Permission is granted subject to an appropriate acknowledgement given to the author, title of the material/book/journal and the publisher. You shall also duplicate the copyright notice that appears in the Wiley publication in your use of the Material. Permission is also granted on the understanding that nowhere in the text is a previously published source acknowledged for all or part of this Material. Any third party material is expressly excluded from this permission.

3. With respect to the Materials, all rights are reserved. Except as expressly granted by the terms of the license, no part of the Materials may be copied, modified, adapted (except for minor reformatting required by the new Publication), translated, reproduced, transferred or distributed, in any form or by any means, and no derivative works may be made based on the Materials without the prior permission of the respective copyright owner. You may not alter, remove or suppress in any manner any copyright, trademark or other notices displayed by the Materials. You may not license, rent, sell, loan, lease, pledge, offer as security, transfer or assign the Materials, or any of the rights granted to you hereunder to any other person.

4. The Materials and all of the intellectual property rights therein shall at all times remain the exclusive property of John Wiley & Sons Inc or one of its related companies (WILEY) or their respective licensors, and your interest therein is only that of having possession of and the right to reproduce the Materials pursuant to

Section 2 herein during the continuance of this Agreement. You agree that you own no right, title or interest in or to the Materials or any of the intellectual property rights therein. You shall have no rights hereunder other than the license as provided for above in Section 2. No right, license or interest to any trademark, trade name, service mark or other branding ("Marks") of WILEY or its licensors is granted hereunder, and you agree that you shall not assert any such right, license or interest with respect thereto.

5. NEITHER WILEY NOR ITS LICENSORS MAKES ANY WARRANTY OR REPRESENTATION OF ANY KIND TO YOU OR ANY THIRD PARTY, EXPRESS, IMPLIED OR STATUTORY, WITH RESPECT TO THE MATERIALS OR THE ACCURACY OF ANY INFORMATION CONTAINED IN THE MATERIALS, INCLUDING, WITHOUT LIMITATION, ANY IMPLIED WARRANTY OF MERCHANTABILITY, ACCURACY, SATISFACTORY QUALITY, FITNESS FOR A PARTICULAR PURPOSE, USABILITY, INTEGRATION OR NON-INFRINGEMENT AND ALL SUCH WARRANTIES ARE HEREBY EXCLUDED BY WILEY AND ITS LICENSORS AND WAIVED BY YOU.

6. WILEY shall have the right to terminate this Agreement immediately upon breach of this Agreement by you.

7. You shall indemnify, defend and hold harmless WILEY, its Licensors and their respective directors, officers, agents and employees, from and against any actual or threatened claims, demands, causes of action or proceedings arising

from any breach of this Agreement by you.

8. IN NO EVENT SHALL WILEY OR ITS LICENSORS BE LIABLE TO YOU OR ANY OTHER PARTY OR ANY OTHER PERSON OR ENTITY FOR ANY SPECIAL, CONSEQUENTIAL, INCIDENTAL, INDIRECT, EXEMPLARY OR PUNITIVE DAMAGES, HOWEVER CAUSED, ARISING OUT OF OR IN CONNECTION WITH THE DOWNLOADING, PROVISIONING, VIEWING OR USE OF THE MATERIALS REGARDLESS OF THE FORM OF ACTION, WHETHER FOR BREACH OF CONTRACT, BREACH OF WARRANTY, TORT, NEGLIGENCE, INFRINGEMENT OR OTHERWISE (INCLUDING, WITHOUT LIMITATION, DAMAGES BASED ON LOSS OF PROFITS, DATA, FILES, USE, BUSINESS OPPORTUNITY OR CLAIMS OF THIRD PARTIES), AND WHETHER OR NOT THE PARTY HAS BEEN ADVISED OF THE POSSIBILITY OF SUCH DAMAGES. THIS LIMITATION SHALL APPLY NOTWITHSTANDING ANY FAILURE OF ESSENTIAL PURPOSE OF ANY LIMITED REMEDY PROVIDED HEREIN.

9. Should any provision of this Agreement be held by a court of competent jurisdiction to be illegal, invalid, or unenforceable, that provision shall be deemed amended to achieve as nearly as possible the same economic effect as the original provision, and the legality, validity and enforceability of the remaining provisions of this Agreement shall not be affected or impaired thereby.

10. The failure of either party to enforce any term or condition of this Agreement

shall not constitute a waiver of either party's right to enforce each and every term and condition of this Agreement. No breach under this agreement shall be deemed waived or excused by either party unless such waiver or consent is in writing signed by the party granting such waiver or consent. The waiver by or consent of a party to a breach of any provision of this Agreement shall not operate or be construed as a waiver of or consent to any other or subsequent breach by such other party.

11. This Agreement may not be assigned (including by operation of law or otherwise) by you without WILEY's prior written consent.

12. Any fee required for this permission shall be non-refundable after thirty (30) days from receipt

13. These terms and conditions together with CCC's Billing and Payment terms and conditions (which are incorporated herein) form the entire agreement between you and WILEY concerning this licensing transaction and (in the absence of fraud) supersedes all prior agreements and representations of the parties, oral or written. This Agreement may not be amended except in writing signed by both parties. This Agreement shall be binding upon and inure to the benefit of the parties' successors, legal representatives, and authorized assigns.

14. In the event of any conflict between your obligations established by these terms and conditions and those established by CCC's Billing and Payment terms

and conditions, these terms and conditions shall prevail.

15. WILEY expressly reserves all rights not specifically granted in the combination of (i) the license details provided by you and accepted in the course of this licensing transaction, (ii) these terms and conditions and (iii) CCC's Billing and Payment terms and conditions.

16. This Agreement will be void if the Type of Use, Format, Circulation, or Requestor Type was misrepresented during the licensing process.

17. This Agreement shall be governed by and construed in accordance with the laws of the State of New York, USA, without regards to such state's conflict of law rules. Any legal action, suit or proceeding arising out of or relating to these Terms and Conditions or the breach thereof shall be instituted in a court of competent jurisdiction in New York County in the State of New York in the United States of America and each party hereby consents and submits to the personal jurisdiction of such court, waives any objection to venue in such court and consents to service of process by registered or certified mail, return receipt requested, at the last known address of such party.

Wiley Open Access Terms and Conditions

Wiley publishes Open Access articles in both its Wiley Open Access Journals program [http://www.wileyopenaccess.com/view/index.html] and as Online Open articles in its subscription journals. The majority of Wiley Open Access Journals

sites.

Conditions applicable to all Wiley Open Access articles:

• The authors' moral rights must not be compromised. These rights include the right of "paternity" (also known as "attribution" - the right for the author to be identified as such) and "integrity" (the right for the author not to have the work altered in such a way that the author's reputation or integrity may be damaged).
• Where content in the article is identified as belonging to a third party, it is the obligation of the user to ensure that any reuse complies with the copyright policies of the owner of that content.
• If article content is copied, downloaded or otherwise reused for research and other purposes as permitted, a link to the appropriate bibliographic citation (authors, journal, article title, volume, issue, page numbers, DOI and the link to the definitive published version on Wiley Online Library) should be maintained. Copyright notices and disclaimers must not be deleted.
◦ Creative Commons licenses are copyright licenses and do not confer any other rights, including but not limited to trademark or patent rights.
•
• Any translations, for which a prior translation agreement with Wiley has not been agreed, must prominently display the statement: "This is an unofficial translation of an article that appeared in a Wiley publication. The publisher has not endorsed this translation."

• **Conditions applicable to non-commercial licenses (CC BY-NC and CC BY-NC-ND)** For non-commercial and non-promotional purposes individual non-commercial users may access, download, copy, display and redistribute to colleagues Wiley Open Access articles. In addition, articles adopting the CC BY-NC may be adapted, translated, and text- and data-mined subject to the conditions above. **Use by commercial "for-profit" organizations** Use of non-commercial Wiley Open Access articles for commercial, promotional, or marketing purposes requires further explicit permission from Wiley and will be subject to a fee. Commercial purposes include:

◦ Copying or downloading of articles, or linking to such articles for further redistribution, sale or licensing;

◦ Copying, downloading or posting by a site or service that incorporates advertising with such content;

◦ The inclusion or incorporation of article content in other works or services (other than normal quotations with an appropriate citation) that is then available for sale or licensing, for a fee (for example, a compilation produced for marketing purposes, inclusion in a sales pack)

◦ Use of article content (other than normal quotations with appropriate citation) by for-profit organizations for promotional purposes

◦ Linking to article content in e-mails redistributed for promotional, marketing or educational purposes;

◦ Use for the purposes of monetary reward by means of sale, resale,

license, loan, transfer or other form of commercial exploitation such as marketing products

◦ Print reprints of Wiley Open Access articles can be purchased from: corporatesales@wiley.com

◦ The modification or adaptation for any purpose of an article referencing the CC BY-NC-ND License requires consent which can be requested from RightsLink@wiley.com .

◦

◦ Other Terms and Conditions:

◦

◦ BY CLICKING ON THE "I AGREE..." BOX, YOU ACKNOWLEDGE THAT YOU HAVE READ AND FULLY UNDERSTAND EACH OF THE SECTIONS OF AND PROVISIONS SET FORTH IN THIS AGREEMENT AND THAT YOU ARE IN AGREEMENT WITH AND ARE WILLING TO ACCEPT ALL OF YOUR OBLIGATIONS AS SET FORTH IN THIS AGREEMENT.

◦ **v1.8**

If you would like to pay for this license now, please remit this license along with your payment made payable to "COPYRIGHT CLEARANCE CENTER" otherwise you will be invoiced within 48 hours of the license date. Payment should be in the form of a check or money order referencing your account number and this invoice number RLNK501085497. Once you receive your invoice for this order, you may pay your invoice by credit card. Please

follow instructions provided at that time. Make Payment To: Copyright Clearance Center Dept 001 P.O. Box 843006 Boston, MA 02284-3006 For suggestions or comments regarding this order, contact RightsLink Customer Support: customercare@copyright.com or +1-877-622-5543 (toll free in the US) or +1-978-646-2777.

Gratis licenses (referencing $0 in the Total field) are free. Please retain this printable license for your reference. No payment is required.

Appendix B: License Agreement for Figure 1.4

ELSEVIER LICENSE TERMS AND CONDITIONS

Aug 19, 2013

This is a License Agreement between Paulo W Pires ("You") and Elsevier ("Elsevier") provided by Copyright Clearance Center ("CCC"). The license consists of your order details, the terms and conditions provided by Elsevier, and the payment terms and conditions.

All payments must be made in full to CCC. For payment instructions, please see information listed at the bottom of this form.

Supplier	Elsevier Limited The Boulevard,Langford Lane Kidlington,Oxford,OX5 1GB,UK
Registered Company Number	1982084
Customer name	Paulo W Pires
Customer address	1355 Bogue Street EAST LANSING, MI 48824

License number	3212521281783
License date	Aug 19, 2013
Licensed content publisher	Elsevier
Licensed content publication	Advanced Drug Delivery Reviews
Licensed content title	Modern methods for delivery of drugs across the blood–brain barrier
Licensed content author	Yan Chen,Lihong Liu
Licensed content date	15 May 2012
Licensed content volume number	64
Licensed content issue number	7
Number of pages	26
Start Page	640

End Page	665
Type of Use	reuse in a thesis/dissertation
Intended publisher of new work	other
Portion	figures/tables/illustrations
Number of figures/tables/illustrations	1
Format	both print and electronic
Are you the author of this Elsevier article?	No
Will you be translating?	No
Order reference number	
Title of your thesis/dissertation	The role of inflammatory mediators in hypertensive remodeling of cerebral arteries
Expected completion date	Sep 2013

Estimated size (number of pages)	200
Elsevier VAT number	GB 494 6272 12
Permissions price	0.00 USD
VAT/Local Sales Tax	0.0 USD / 0.0 GBP
Total	0.00 USD

Terms and Conditions

INTRODUCTION

1. The publisher for this copyrighted material is Elsevier. By clicking "accept" in connection with completing this licensing transaction, you agree that the following terms and conditions apply to this transaction (along with the Billing and Payment terms and conditions established by Copyright Clearance Center, Inc. ("CCC"), at the time that you opened your Rightslink account and that are available at any time at http://myaccount.copyright.com).

GENERAL TERMS

2. Elsevier hereby grants you permission to reproduce the aforementioned material subject to the terms and conditions indicated.

3. Acknowledgement: If any part of the material to be used (for example, figures) has appeared in our publication with credit or acknowledgement to another source, permission must also be sought from that source. If such permission is not obtained then that material may not be included in your publication/copies. Suitable acknowledgement to the source must be made, either as a footnote or in a reference list at the end of your publication, as follows:

“Reprinted from Publication title, Vol /edition number, Author(s), Title of article / title of chapter, Pages No., Copyright (Year), with permission from Elsevier [OR APPLICABLE SOCIETY COPYRIGHT OWNER].” Also Lancet special credit - “Reprinted from The Lancet, Vol. number, Author(s), Title of article, Pages No., Copyright (Year), with permission from Elsevier.”

4. Reproduction of this material is confined to the purpose and/or media for which permission is hereby given.

5. Altering/Modifying Material: Not Permitted. However figures and illustrations may be altered/adapted minimally to serve your work. Any other abbreviations, additions, deletions and/or any other alterations shall be made only with prior written authorization of Elsevier Ltd. (Please contact Elsevier at permissions@elsevier.com)

6. If the permission fee for the requested use of our material is waived in this instance, please be advised that your future requests for Elsevier materials

may attract a fee.

7. Reservation of Rights: Publisher reserves all rights not specifically granted in the combination of (i) the license details provided by you and accepted in the course of this licensing transaction, (ii) these terms and conditions and (iii) CCC's Billing and Payment terms and conditions.

8. License Contingent Upon Payment: While you may exercise the rights licensed immediately upon issuance of the license at the end of the licensing process for the transaction, provided that you have disclosed complete and accurate details of your proposed use, no license is finally effective unless and until full payment is received from you (either by publisher or by CCC) as provided in CCC's Billing and Payment terms and conditions. If full payment is not received on a timely basis, then any license preliminarily granted shall be deemed automatically revoked and shall be void as if never granted. Further, in the event that you breach any of these terms and conditions or any of CCC's Billing and Payment terms and conditions, the license is automatically revoked and shall be void as if never granted. Use of materials as described in a revoked license, as well as any use of the materials beyond the scope of an unrevoked license, may constitute copyright infringement and publisher reserves the right to take any and all action to protect its copyright in the materials.

9. Warranties: Publisher makes no representations or warranties with respect

to the licensed material.

10. Indemnity: You hereby indemnify and agree to hold harmless publisher and CCC, and their respective officers, directors, employees and agents, from and against any and all claims arising out of your use of the licensed material other than as specifically authorized pursuant to this license.

11. No Transfer of License: This license is personal to you and may not be sublicensed, assigned, or transferred by you to any other person without publisher's written permission.

12. No Amendment Except in Writing: This license may not be amended except in a writing signed by both parties (or, in the case of publisher, by CCC on publisher's behalf).

13. Objection to Contrary Terms: Publisher hereby objects to any terms contained in any purchase order, acknowledgment, check endorsement or other writing prepared by you, which terms are inconsistent with these terms and conditions or CCC's Billing and Payment terms and conditions. These terms and conditions, together with CCC's Billing and Payment terms and conditions (which are incorporated herein), comprise the entire agreement between you and publisher (and CCC) concerning this licensing transaction. In the event of any conflict between your obligations established by these terms and conditions and those established by CCC's Billing and Payment terms and

conditions, these terms and conditions shall control.

14. Revocation: Elsevier or Copyright Clearance Center may deny the permissions described in this License at their sole discretion, for any reason or no reason, with a full refund payable to you. Notice of such denial will be made using the contact information provided by you. Failure to receive such notice will not alter or invalidate the denial. In no event will Elsevier or Copyright Clearance Center be responsible or liable for any costs, expenses or damage incurred by you as a result of a denial of your permission request, other than a refund of the amount(s) paid by you to Elsevier and/or Copyright Clearance Center for denied permissions.

LIMITED LICENSE

The following terms and conditions apply only to specific license types:

15. **Translation**: This permission is granted for non-exclusive world **English** rights only unless your license was granted for translation rights. If you licensed translation rights you may only translate this content into the languages you requested. A professional translator must perform all translations and reproduce the content word for word preserving the integrity of the article. If this license is to re-use 1 or 2 figures then permission is granted for non-exclusive world rights in all languages.

16. **Website**: The following terms and conditions apply to electronic reserve

and author websites: **Electronic reserve**: If licensed material is to be posted to website, the web site is to be password-protected and made available only to bona fide students registered on a relevant course if: This license was made in connection with a course, This permission is granted for 1 year only. You may obtain a license for future website posting, All content posted to the web site must maintain the copyright information line on the bottom of each image, A hyper-text must be included to the Homepage of the journal from which you are licensing at http://www.sciencedirect.com/science/journal/xxxxx or the Elsevier homepage for books at http://www.elsevier.com , and Central Storage: This license does not include permission for a scanned version of the material to be stored in a central repository such as that provided by Heron/XanEdu.

17. **Author website** for journals with the following additional clauses:

All content posted to the web site must maintain the copyright information line on the bottom of each image, and the permission granted is limited to the personal version of your paper. You are not allowed to download and post the published electronic version of your article (whether PDF or HTML, proof or final version), nor may you scan the printed edition to create an electronic version. A hyper-text must be included to the Homepage of the journal from which you are licensing at http://www.sciencedirect.com/science/journal/xxxxx . As part of our normal production process, you will receive an e-mail notice when your article appears on Elsevier's online service ScienceDirect (www.sciencedirect.com). That e-mail will include the article's Digital Object

Identifier (DOI). This number provides the electronic link to the published article and should be included in the posting of your personal version. We ask that you wait until you receive this e-mail and have the DOI to do any posting.

Central Storage: This license does not include permission for a scanned version of the material to be stored in a central repository such as that provided by Heron/XanEdu.

18. **Author website** for books with the following additional clauses: Authors are permitted to place a brief summary of their work online only. A hyper-text must be included to the Elsevier homepage at http://www.elsevier.com . All content posted to the web site must maintain the copyright information line on the bottom of each image. You are not allowed to download and post the published electronic version of your chapter, nor may you scan the printed edition to create an electronic version.

Central Storage: This license does not include permission for a scanned version of the material to be stored in a central repository such as that provided by Heron/XanEdu.

19. **Website** (regular and for author): A hyper-text must be included to the Homepage of the journal from which you are licensing at http://www.sciencedirect.com/science/journal/xxxxx. or for books to the Elsevier homepage at http://www.elsevier.com

20. **Thesis/Dissertation**: If your license is for use in a thesis/dissertation your thesis may be submitted to your institution in either print or electronic form. Should your thesis be published commercially, please reapply for permission. These requirements include permission for the Library and Archives of Canada to supply single copies, on demand, of the complete thesis and include permission for UMI to supply single copies, on demand, of the complete thesis. Should your thesis be published commercially, please reapply for permission.

21. **Other Conditions**:

v1.6

If you would like to pay for this license now, please remit this license along with your payment made payable to "COPYRIGHT CLEARANCE CENTER" otherwise you will be invoiced within 48 hours of the license date. Payment should be in the form of a check or money order referencing your account number and this invoice number RLNK501093236. Once you receive your invoice for this order, you may pay your invoice by credit card. Please follow instructions provided at that time. Make Payment To: Copyright Clearance Center Dept 001 P.O. Box 843006 Boston, MA 02284-3006 For suggestions or comments regarding this order, contact RightsLink Customer Support: customercare@copyright.com or +1-877-622-5543 (toll free in the US) or +1-978-646-2777.

Gratis licenses (referencing $0 in the Total field) are free. Please retain this printable license for your reference. No payment is required.

Appendix C: License Agreement for Figure 1.7

ELSEVIER LICENSE TERMS AND CONDITIONS

Aug 19, 2013

This is a License Agreement between Paulo W Pires ("You") and Elsevier ("Elsevier") provided by Copyright Clearance Center ("CCC"). The license consists of your order details, the terms and conditions provided by Elsevier, and the payment terms and conditions.

All payments must be made in full to CCC. For payment instructions, please see information listed at the bottom of this form.

Supplier	Elsevier Limited The Boulevard,Langford Lane Kidlington,Oxford,OX5 1GB,UK
Registered Company Number	1982084
Customer name	Paulo W Pires
Customer address	1355 Bogue Street

	EAST LANSING, MI 48824
License number	3212521481443
License date	Aug 19, 2013
Licensed content publisher	Elsevier
Licensed content publication	Cell Metabolism
Licensed content title	Hypertension and Cerebrovascular Dysfunction
Licensed content author	Costantino Iadecola,Robin L. Davisson
Licensed content date	4 June 2008
Licensed content volume number	7
Licensed content issue number	6

Number of pages	9
Start Page	476
End Page	484
Type of Use	reuse in a thesis/dissertation
Intended publisher of new work	other
Portion	figures/tables/illustrations
Number of figures/tables/illustrations	1
Format	both print and electronic
Are you the author of this Elsevier article?	No
Will you be translating?	No
Order reference number	

Title of your thesis/dissertation	The role of inflammatory mediators in hypertensive remodeling of cerebral arteries
Expected completion date	Sep 2013
Estimated size (number of pages)	200
Elsevier VAT number	GB 494 6272 12
Permissions price	0.00 USD
VAT/Local Sales Tax	0.0 USD / 0.0 GBP
Total	0.00 USD

Terms and Conditions

INTRODUCTION

1. The publisher for this copyrighted material is Elsevier. By clicking "accept" in connection with completing this licensing transaction, you agree that the following terms and conditions apply to this transaction (along with the Billing and Payment terms and conditions established by Copyright Clearance Center, Inc. ("CCC"), at the time that you opened your Rightslink account and that are

available at any time at http://myaccount.copyright.com).

GENERAL TERMS

2. Elsevier hereby grants you permission to reproduce the aforementioned material subject to the terms and conditions indicated.

3. Acknowledgement: If any part of the material to be used (for example, figures) has appeared in our publication with credit or acknowledgement to another source, permission must also be sought from that source. If such permission is not obtained then that material may not be included in your publication/copies. Suitable acknowledgement to the source must be made, either as a footnote or in a reference list at the end of your publication, as follows:

"Reprinted from Publication title, Vol /edition number, Author(s), Title of article / title of chapter, Pages No., Copyright (Year), with permission from Elsevier [OR APPLICABLE SOCIETY COPYRIGHT OWNER]." Also Lancet special credit - "Reprinted from The Lancet, Vol. number, Author(s), Title of article, Pages No., Copyright (Year), with permission from Elsevier."

4. Reproduction of this material is confined to the purpose and/or media for which permission is hereby given.

5. Altering/Modifying Material: Not Permitted. However figures and illustrations may be altered/adapted minimally to serve your work. Any other abbreviations,

additions, deletions and/or any other alterations shall be made only with prior written authorization of Elsevier Ltd. (Please contact Elsevier at permissions@elsevier.com)

6. If the permission fee for the requested use of our material is waived in this instance, please be advised that your future requests for Elsevier materials may attract a fee.

7. Reservation of Rights: Publisher reserves all rights not specifically granted in the combination of (i) the license details provided by you and accepted in the course of this licensing transaction, (ii) these terms and conditions and (iii) CCC's Billing and Payment terms and conditions.

8. License Contingent Upon Payment: While you may exercise the rights licensed immediately upon issuance of the license at the end of the licensing process for the transaction, provided that you have disclosed complete and accurate details of your proposed use, no license is finally effective unless and until full payment is received from you (either by publisher or by CCC) as provided in CCC's Billing and Payment terms and conditions. If full payment is not received on a timely basis, then any license preliminarily granted shall be deemed automatically revoked and shall be void as if never granted. Further, in the event that you breach any of these terms and conditions or any of CCC's Billing and Payment terms and conditions, the license is automatically revoked and shall be void as if never granted. Use of materials as described in a

revoked license, as well as any use of the materials beyond the scope of an unrevoked license, may constitute copyright infringement and publisher reserves the right to take any and all action to protect its copyright in the materials.

9. Warranties: Publisher makes no representations or warranties with respect to the licensed material.

10. Indemnity: You hereby indemnify and agree to hold harmless publisher and CCC, and their respective officers, directors, employees and agents, from and against any and all claims arising out of your use of the licensed material other than as specifically authorized pursuant to this license.

11. No Transfer of License: This license is personal to you and may not be sublicensed, assigned, or transferred by you to any other person without publisher's written permission.

12. No Amendment Except in Writing: This license may not be amended except in a writing signed by both parties (or, in the case of publisher, by CCC on publisher's behalf).

13. Objection to Contrary Terms: Publisher hereby objects to any terms contained in any purchase order, acknowledgment, check endorsement or other writing prepared by you, which terms are inconsistent with these terms and conditions or CCC's Billing and Payment terms and conditions. These

terms and conditions, together with CCC's Billing and Payment terms and conditions (which are incorporated herein), comprise the entire agreement between you and publisher (and CCC) concerning this licensing transaction. In the event of any conflict between your obligations established by these terms and conditions and those established by CCC's Billing and Payment terms and conditions, these terms and conditions shall control.

14. Revocation: Elsevier or Copyright Clearance Center may deny the permissions described in this License at their sole discretion, for any reason or no reason, with a full refund payable to you. Notice of such denial will be made using the contact information provided by you. Failure to receive such notice will not alter or invalidate the denial. In no event will Elsevier or Copyright Clearance Center be responsible or liable for any costs, expenses or damage incurred by you as a result of a denial of your permission request, other than a refund of the amount(s) paid by you to Elsevier and/or Copyright Clearance Center for denied permissions.

LIMITED LICENSE

The following terms and conditions apply only to specific license types:

15. **Translation**: This permission is granted for non-exclusive world **English** rights only unless your license was granted for translation rights. If you licensed translation rights you may only translate this content into the languages you requested. A professional translator must perform all translations and

reproduce the content word for word preserving the integrity of the article. If this license is to re-use 1 or 2 figures then permission is granted for non-exclusive world rights in all languages.

16. **Website**: The following terms and conditions apply to electronic reserve and author websites: **Electronic reserve**: If licensed material is to be posted to website, the web site is to be password-protected and made available only to bona fide students registered on a relevant course if: This license was made in connection with a course, This permission is granted for 1 year only. You may obtain a license for future website posting, All content posted to the web site must maintain the copyright information line on the bottom of each image, A hyper-text must be included to the Homepage of the journal from which you are licensing at http://www.sciencedirect.com/science/journal/xxxxx or the Elsevier homepage for books at http://www.elsevier.com , and Central Storage: This license does not include permission for a scanned version of the material to be stored in a central repository such as that provided by Heron/XanEdu.

17. **Author website** for journals with the following additional clauses:

All content posted to the web site must maintain the copyright information line on the bottom of each image, and the permission granted is limited to the personal version of your paper. You are not allowed to download and post the published electronic version of your article (whether PDF or HTML, proof or final version), nor may you scan the printed edition to create an electronic

version. A hyper-text must be included to the Homepage of the journal from which you are licensing at http://www.sciencedirect.com/science/journal/xxxxx . As part of our normal production process, you will receive an e-mail notice when your article appears on Elsevier's online service ScienceDirect (www.sciencedirect.com). That e-mail will include the article's Digital Object Identifier (DOI). This number provides the electronic link to the published article and should be included in the posting of your personal version. We ask that you wait until you receive this e-mail and have the DOI to do any posting.

Central Storage: This license does not include permission for a scanned version of the material to be stored in a central repository such as that provided by Heron/XanEdu.

18. **Author website** for books with the following additional clauses: Authors are permitted to place a brief summary of their work online only. A hyper-text must be included to the Elsevier homepage at http://www.elsevier.com . All content posted to the web site must maintain the copyright information line on the bottom of each image. You are not allowed to download and post the published electronic version of your chapter, nor may you scan the printed edition to create an electronic version.

Central Storage: This license does not include permission for a scanned version of the material to be stored in a central repository such as that provided by Heron/XanEdu.

19. **Website** (regular and for author): A hyper-text must be included to the Homepage of the journal from which you are licensing at http://www.sciencedirect.com/science/journal/xxxxx. or for books to the Elsevier homepage at http://www.elsevier.com

20. **Thesis/Dissertation**: If your license is for use in a thesis/dissertation your thesis may be submitted to your institution in either print or electronic form. Should your thesis be published commercially, please reapply for permission. These requirements include permission for the Library and Archives of Canada to supply single copies, on demand, of the complete thesis and include permission for UMI to supply single copies, on demand, of the complete thesis. Should your thesis be published commercially, please reapply for permission.

21. **Other Conditions**:

v1.6

If you would like to pay for this license now, please remit this license along with your payment made payable to "COPYRIGHT CLEARANCE CENTER" otherwise you will be invoiced within 48 hours of the license date. Payment should be in the form of a check or money order referencing your account number and this invoice number RLNK501093246. Once you receive your invoice for this order, you may pay your invoice by credit card. Please follow instructions provided at that time. Make Payment To: Copyright Clearance Center Dept 001 P.O.

Box 843006 Boston, MA 02284-3006 For suggestions or comments regarding this order, contact RightsLink Customer Support: customercare@copyright.com or +1-877-622-5543 (toll free in the US) or +1-978-646-2777.

Gratis licenses (referencing $0 in the Total field) are free. Please retain this printable license for your reference. No payment is required.

Appendix D: License Agreement for Figure 1.8

WOLTERS KLUWER HEALTH LICENSE TERMS AND CONDITIONS

Aug 19, 2013

This is a License Agreement between Paulo W Pires ("You") and Wolters Kluwer Health ("Wolters Kluwer Health") provided by Copyright Clearance Center ("CCC"). The license consists of your order details, the terms and conditions provided by Wolters Kluwer Health, and the payment terms and conditions.

All payments must be made in full to CCC. For payment instructions, please see information listed at the bottom of this form.

License Number	3212530142525
License date	Aug 19, 2013
Licensed content publisher	Wolters Kluwer Health
Licensed	Hypertension

content publication	
Licensed content title	Blood Pressure in Genetically Hypertensive Rats: Influence of the Y Chromosome
Licensed content author	Anne O. Davidson, Nicholas Schork, Bryon C. Jaques, Andrew W. Kelman, Roger G. Sutcliffe, John L. Reid, Anna F. Dominiczak
Licensed content date	Sep 1, 1995
Volume Number	26
Issue Number	3
Type of Use	Dissertation/Thesis
Requestor type	Individual
Author of this Wolters Kluwer	No

article	
Title of your thesis / dissertation	The role of inflammatory mediators in hypertensive remodeling of cerebral arteries
Expected completion date	Sep 2013
Estimated size(pages)	200
Billing Type	Invoice
Billing address	1355 Bogue Street Room B340 Life Sciences EAST LANSING, MI 48824 United States
Total	0.00 USD

Terms and Conditions

Terms and Conditions

- A credit line will be prominently placed and include: for books - the author(s), title of book, editor, copyright holder, year of publication; For journals - the author(s), title of article, title of journal, volume number, issue number and inclusive pages.
- The requestor warrants that the material shall not be used in any manner which may be considered derogatory to the title, content, or authors of the material, or to Wolters Kluwer.
- Permission is granted for a one time use only within 12 months from the date of this invoice. Rights herein do not apply to future reproductions, editions, revisions, or other derivative works. Once the 12-month term has expired, permission to renew must be submitted in writing.
- Permission granted is non-exclusive, and is valid throughout the world in the English language and the languages specified in your original request.
- Wolters Kluwer cannot supply the requestor with the original artwork or a "clean copy."
- The requestor agrees to secure written permission from the author (for book material only).
- Permission is valid if the borrowed material is original to a Wolters Kluwer imprint (Lippincott-Raven Publishers, Williams & Wilkins, Lea & Febiger, Harwal, Igaku-Shoin, Rapid Science, Little Brown & Company, Harper & Row Medical, American Journal of Nursing Co, and Urban & Schwarzenberg - English Language).

- If you opt not to use the material requested above, please notify Rightslink within 90 days of the original invoice date.
- Please note that articles in the ahead-of-print stage of publication can be cited and the content may be re-used by including the date of access and the unique DOI number. Any final changes in manuscripts will be made at the time of print publication and will be reflected in the final electronic version of the issue.?Disclaimer: Articles appearing in the Published Ahead-of-Print section have been peer-reviewed and accepted for publication in the relevant journal and posted online before print publication. Articles appearing as publish ahead-of-print may contain statements, opinions, and information that have errors in facts, figures, or interpretation. Accordingly, Lippincott Williams & Wilkins, the editors and authors and their respective employees are not responsible or liable for the use of any such inaccurate or misleading data, opinion or information contained in the articles in this section.
- 1This permission does not apply to images that are credited to publications other than Wolters Kluwer journals. For images credited to non-Wolters Kluwer journal publications, you will need to obtain permission from the journal referenced in the figure or table legend or credit line before making any use of the image(s) or table(s).
- In case of **Disease Colon Rectum, Plastic Reconstructive Surgery, The Green Journal, Critical Care Medicine, Pediatric Critical Care Medicine, the American Heart Publications, the American Academy**

of Neurology the following guideline applies: no drug brand/trade name or logo can be included in the same page as the material re-used

- When requesting a permission to translate a full text article, Wolters Kluwer/Lippincott Williams & Wilkins requests to receive the pdf of the translated document
- “Adaptations of single figures do not require Wolters Kluwer **further** approval if the permission has been granted previously. However, the adaptation should be credited as follows:?Adapted with permission from Lippincott Williams and Wilkins/Wolters Kluwer Health: [JOURNAL NAME] (reference citation), copyright (year of publication)”
- **Please note that modification of text within figures or full-text articles is strictly forbidden.**
- The following statement needs to be added when reprinting the material in Open Access journals only: 'promotional and commercial use of the material in print, digital or mobile device format is prohibited without the permission from the publisher Lippincott Williams & Wilkins. Please contact journalpermissions@lww.com for further information”.
- Other Terms and Conditions:
-

v1.8

If you would like to pay for this license now, please remit this license along with your payment made payable to "COPYRIGHT CLEARANCE

CENTER" otherwise you will be invoiced within 48 hours of the license date. Payment should be in the form of a check or money order referencing your account number and this invoice number RLNK501093252. Once you receive your invoice for this order, you may pay your invoice by credit card. Please follow instructions provided at that time. Make Payment To: Copyright Clearance Center Dept 001 P.O. Box 843006 Boston, MA 02284-3006 For suggestions or comments regarding this order, contact RightsLink Customer Support: customercare@copyright.com or +1-877-622-5543 (toll free in the US) or +1-978-646-2777.

Gratis licenses (referencing $0 in the Total field) are free. Please retain this printable license for your reference. No payment is required.

Appendix E: License Agreement for Figure 1.9

ELSEVIER LICENSE TERMS AND CONDITIONS

Aug 19, 2013

This is a License Agreement between Paulo W Pires ("You") and Elsevier ("Elsevier") provided by Copyright Clearance Center ("CCC"). The license consists of your order details, the terms and conditions provided by Elsevier, and the payment terms and conditions.

All payments must be made in full to CCC. For payment instructions, please see information listed at the bottom of this form.

Supplier	Elsevier Limited The Boulevard,Langford Lane Kidlington,Oxford,OX5 1GB,UK
Registered Company Number	1982084
Customer name	Paulo W Pires
Customer address	1355 Bogue Street

	EAST LANSING, MI 48824
License number	3212531013493
License date	Aug 19, 2013
Licensed content publisher	Elsevier
Licensed content publication	Journal of Immunological Methods
Licensed content title	Liposome mediated depletion of macrophages: mechanism of action, preparation of liposomes and applications
Licensed content author	Nico Van Rooijen,Annemarie Sanders
Licensed content date	14 September 1994
Licensed content volume number	174
Licensed content issue number	1–2

Number of pages	11
Start Page	83
End Page	93
Type of Use	reuse in a thesis/dissertation
Intended publisher of new work	other
Portion	figures/tables/illustrations
Number of figures/tables/illustrations	1
Format	both print and electronic
Are you the author of this Elsevier article?	No
Will you be translating?	No
Order reference number	

Title of your thesis/dissertation	The role of inflammatory mediators in hypertensive remodeling of cerebral arteries
Expected completion date	Sep 2013
Estimated size (number of pages)	200
Elsevier VAT number	GB 494 6272 12
Permissions price	0.00 USD
VAT/Local Sales Tax	0.0 USD / 0.0 GBP
Total	0.00 USD

Terms and Conditions

INTRODUCTION

1. The publisher for this copyrighted material is Elsevier. By clicking "accept" in connection with completing this licensing transaction, you agree that the following terms and conditions apply to this transaction (along with the Billing

and Payment terms and conditions established by Copyright Clearance Center, Inc. ("CCC"), at the time that you opened your Rightslink account and that are available at any time at http://myaccount.copyright.com).

GENERAL TERMS

2. Elsevier hereby grants you permission to reproduce the aforementioned material subject to the terms and conditions indicated.

3. Acknowledgement: If any part of the material to be used (for example, figures) has appeared in our publication with credit or acknowledgement to another source, permission must also be sought from that source. If such permission is not obtained then that material may not be included in your publication/copies. Suitable acknowledgement to the source must be made, either as a footnote or in a reference list at the end of your publication, as follows:

“Reprinted from Publication title, Vol /edition number, Author(s), Title of article / title of chapter, Pages No., Copyright (Year), with permission from Elsevier [OR APPLICABLE SOCIETY COPYRIGHT OWNER].” Also Lancet special credit - “Reprinted from The Lancet, Vol. number, Author(s), Title of article, Pages No., Copyright (Year), with permission from Elsevier.”

4. Reproduction of this material is confined to the purpose and/or media for which permission is hereby given.

5. Altering/Modifying Material: Not Permitted. However figures and illustrations may be altered/adapted minimally to serve your work. Any other abbreviations, additions, deletions and/or any other alterations shall be made only with prior written authorization of Elsevier Ltd. (Please contact Elsevier at permissions@elsevier.com)

6. If the permission fee for the requested use of our material is waived in this instance, please be advised that your future requests for Elsevier materials may attract a fee.

7. Reservation of Rights: Publisher reserves all rights not specifically granted in the combination of (i) the license details provided by you and accepted in the course of this licensing transaction, (ii) these terms and conditions and (iii) CCC's Billing and Payment terms and conditions.

8. License Contingent Upon Payment: While you may exercise the rights licensed immediately upon issuance of the license at the end of the licensing process for the transaction, provided that you have disclosed complete and accurate details of your proposed use, no license is finally effective unless and until full payment is received from you (either by publisher or by CCC) as provided in CCC's Billing and Payment terms and conditions. If full payment is not received on a timely basis, then any license preliminarily granted shall be deemed automatically revoked and shall be void as if never granted. Further, in the event that you breach any of these terms and conditions or any of CCC's

Billing and Payment terms and conditions, the license is automatically revoked and shall be void as if never granted. Use of materials as described in a revoked license, as well as any use of the materials beyond the scope of an unrevoked license, may constitute copyright infringement and publisher reserves the right to take any and all action to protect its copyright in the materials.

9. Warranties: Publisher makes no representations or warranties with respect to the licensed material.

10. Indemnity: You hereby indemnify and agree to hold harmless publisher and CCC, and their respective officers, directors, employees and agents, from and against any and all claims arising out of your use of the licensed material other than as specifically authorized pursuant to this license.

11. No Transfer of License: This license is personal to you and may not be sublicensed, assigned, or transferred by you to any other person without publisher's written permission.

12. No Amendment Except in Writing: This license may not be amended except in a writing signed by both parties (or, in the case of publisher, by CCC on publisher's behalf).

13. Objection to Contrary Terms: Publisher hereby objects to any terms contained in any purchase order, acknowledgment, check endorsement or

other writing prepared by you, which terms are inconsistent with these terms and conditions or CCC's Billing and Payment terms and conditions. These terms and conditions, together with CCC's Billing and Payment terms and conditions (which are incorporated herein), comprise the entire agreement between you and publisher (and CCC) concerning this licensing transaction. In the event of any conflict between your obligations established by these terms and conditions and those established by CCC's Billing and Payment terms and conditions, these terms and conditions shall control.

14. Revocation: Elsevier or Copyright Clearance Center may deny the permissions described in this License at their sole discretion, for any reason or no reason, with a full refund payable to you. Notice of such denial will be made using the contact information provided by you. Failure to receive such notice will not alter or invalidate the denial. In no event will Elsevier or Copyright Clearance Center be responsible or liable for any costs, expenses or damage incurred by you as a result of a denial of your permission request, other than a refund of the amount(s) paid by you to Elsevier and/or Copyright Clearance Center for denied permissions.

LIMITED LICENSE

The following terms and conditions apply only to specific license types:

15. **Translation**: This permission is granted for non-exclusive world **English** rights only unless your license was granted for translation rights. If you licensed

translation rights you may only translate this content into the languages you requested. A professional translator must perform all translations and reproduce the content word for word preserving the integrity of the article. If this license is to re-use 1 or 2 figures then permission is granted for non-exclusive world rights in all languages.

16. **Website**: The following terms and conditions apply to electronic reserve and author websites: **Electronic reserve**: If licensed material is to be posted to website, the web site is to be password-protected and made available only to bona fide students registered on a relevant course if: This license was made in connection with a course, This permission is granted for 1 year only. You may obtain a license for future website posting, All content posted to the web site must maintain the copyright information line on the bottom of each image, A hyper-text must be included to the Homepage of the journal from which you are licensing at http://www.sciencedirect.com/science/journal/xxxxx or the Elsevier homepage for books at http://www.elsevier.com , and Central Storage: This license does not include permission for a scanned version of the material to be stored in a central repository such as that provided by Heron/XanEdu.

17. **Author website** for journals with the following additional clauses:

All content posted to the web site must maintain the copyright information line on the bottom of each image, and the permission granted is limited to the personal version of your paper. You are not allowed to download and post the

published electronic version of your article (whether PDF or HTML, proof or final version), nor may you scan the printed edition to create an electronic version. A hyper-text must be included to the Homepage of the journal from which you are licensing at http://www.sciencedirect.com/science/journal/xxxxx . As part of our normal production process, you will receive an e-mail notice when your article appears on Elsevier's online service ScienceDirect (www.sciencedirect.com). That e-mail will include the article's Digital Object Identifier (DOI). This number provides the electronic link to the published article and should be included in the posting of your personal version. We ask that you wait until you receive this e-mail and have the DOI to do any posting.

Central Storage: This license does not include permission for a scanned version of the material to be stored in a central repository such as that provided by Heron/XanEdu.

18. **Author website** for books with the following additional clauses: Authors are permitted to place a brief summary of their work online only. A hyper-text must be included to the Elsevier homepage at http://www.elsevier.com . All content posted to the web site must maintain the copyright information line on the bottom of each image. You are not allowed to download and post the published electronic version of your chapter, nor may you scan the printed edition to create an electronic version.

Central Storage: This license does not include permission for a scanned

version of the material to be stored in a central repository such as that provided by Heron/XanEdu.

19. **Website** (regular and for author): A hyper-text must be included to the Homepage of the journal from which you are licensing at http://www.sciencedirect.com/science/journal/xxxxx. or for books to the Elsevier homepage at http://www.elsevier.com

20. **Thesis/Dissertation**: If your license is for use in a thesis/dissertation your thesis may be submitted to your institution in either print or electronic form. Should your thesis be published commercially, please reapply for permission. These requirements include permission for the Library and Archives of Canada to supply single copies, on demand, of the complete thesis and include permission for UMI to supply single copies, on demand, of the complete thesis. Should your thesis be published commercially, please reapply for permission.

21. **Other Conditions**:

v1.6

If you would like to pay for this license now, please remit this license along with your payment made payable to "COPYRIGHT CLEARANCE CENTER" otherwise you will be invoiced within 48 hours of the license date. Payment should be in the form of a check or money order referencing your account number and this invoice number

RLNK501093264. Once you receive your invoice for this order, you may pay your invoice by credit card. Please follow instructions provided at that time. Make Payment To: Copyright Clearance Center Dept 001 P.O. Box 843006 Boston, MA 02284-3006 For suggestions or comments regarding this order, contact RightsLink Customer Support: customercare@copyright.com or +1-877-622-5543 (toll free in the US) or +1-978-646-2777.

Gratis licenses (referencing $0 in the Total field) are free. Please retain this printable license for your reference. No payment is required.

Appendix F: License Agreement for Figure 1.10

ELSEVIER LICENSE TERMS AND CONDITIONS

Aug 19, 2013

This is a License Agreement between Paulo W Pires ("You") and Elsevier ("Elsevier") provided by Copyright Clearance Center ("CCC"). The license consists of your order details, the terms and conditions provided by Elsevier, and the payment terms and conditions.

All payments must be made in full to CCC. For payment instructions, please see information listed at the bottom of this form.

Supplier	Elsevier Limited The Boulevard,Langford Lane Kidlington,Oxford,OX5 1GB,UK
Registered Company Number	1982084
Customer name	Paulo W Pires
Customer	1355 Bogue Street

address	EAST LANSING, MI 48824
License number	3212531127743
License date	Aug 19, 2013
Licensed content publisher	Elsevier
Licensed content publication	Biochemical Pharmacology
Licensed content title	Matrix metalloproteinases and their inhibitors in vascular remodeling and vascular disease
Licensed content author	Joseph D. Raffetto,Raouf A. Khalil
Licensed content date	15 January 2008
Licensed content volume number	75

Licensed content issue number	2
Number of pages	14
Start Page	346
End Page	359
Type of Use	reuse in a thesis/dissertation
Intended publisher of new work	other
Portion	figures/tables/illustrations
Number of figures/tables/illustrations	1
Format	both print and electronic
Are you the author of this Elsevier article?	No
Will you be	No

translating?

Order reference number	
Title of your thesis/dissertation	The role of inflammatory mediators in hypertensive remodeling of cerebral arteries
Expected completion date	Sep 2013
Estimated size (number of pages)	200
Elsevier VAT number	GB 494 6272 12
Permissions price	0.00 USD
VAT/Local Sales Tax	0.0 USD / 0.0 GBP
Total	0.00 USD

Terms and Conditions

INTRODUCTION

1. The publisher for this copyrighted material is Elsevier. By clicking "accept" in connection with completing this licensing transaction, you agree that the following terms and conditions apply to this transaction (along with the Billing and Payment terms and conditions established by Copyright Clearance Center, Inc. ("CCC"), at the time that you opened your Rightslink account and that are available at any time at http://myaccount.copyright.com).

GENERAL TERMS

2. Elsevier hereby grants you permission to reproduce the aforementioned material subject to the terms and conditions indicated.

3. Acknowledgement: If any part of the material to be used (for example, figures) has appeared in our publication with credit or acknowledgement to another source, permission must also be sought from that source. If such permission is not obtained then that material may not be included in your publication/copies. Suitable acknowledgement to the source must be made, either as a footnote or in a reference list at the end of your publication, as follows:

“Reprinted from Publication title, Vol /edition number, Author(s), Title of article / title of chapter, Pages No., Copyright (Year), with permission from Elsevier [OR APPLICABLE SOCIETY COPYRIGHT OWNER].” Also Lancet special credit - “Reprinted from The Lancet, Vol. number, Author(s), Title of article, Pages No.,

Copyright (Year), with permission from Elsevier."

4. Reproduction of this material is confined to the purpose and/or media for which permission is hereby given.

5. Altering/Modifying Material: Not Permitted. However figures and illustrations may be altered/adapted minimally to serve your work. Any other abbreviations, additions, deletions and/or any other alterations shall be made only with prior written authorization of Elsevier Ltd. (Please contact Elsevier at permissions@elsevier.com)

6. If the permission fee for the requested use of our material is waived in this instance, please be advised that your future requests for Elsevier materials may attract a fee.

7. Reservation of Rights: Publisher reserves all rights not specifically granted in the combination of (i) the license details provided by you and accepted in the course of this licensing transaction, (ii) these terms and conditions and (iii) CCC's Billing and Payment terms and conditions.

8. License Contingent Upon Payment: While you may exercise the rights licensed immediately upon issuance of the license at the end of the licensing process for the transaction, provided that you have disclosed complete and accurate details of your proposed use, no license is finally effective unless and until full payment is received from you (either by publisher or by CCC) as

provided in CCC's Billing and Payment terms and conditions. If full payment is not received on a timely basis, then any license preliminarily granted shall be deemed automatically revoked and shall be void as if never granted. Further, in the event that you breach any of these terms and conditions or any of CCC's Billing and Payment terms and conditions, the license is automatically revoked and shall be void as if never granted. Use of materials as described in a revoked license, as well as any use of the materials beyond the scope of an unrevoked license, may constitute copyright infringement and publisher reserves the right to take any and all action to protect its copyright in the materials.

9. Warranties: Publisher makes no representations or warranties with respect to the licensed material.

10. Indemnity: You hereby indemnify and agree to hold harmless publisher and CCC, and their respective officers, directors, employees and agents, from and against any and all claims arising out of your use of the licensed material other than as specifically authorized pursuant to this license.

11. No Transfer of License: This license is personal to you and may not be sublicensed, assigned, or transferred by you to any other person without publisher's written permission.

12. No Amendment Except in Writing: This license may not be amended except in a writing signed by both parties (or, in the case of publisher, by CCC

on publisher's behalf).

13. Objection to Contrary Terms: Publisher hereby objects to any terms contained in any purchase order, acknowledgment, check endorsement or other writing prepared by you, which terms are inconsistent with these terms and conditions or CCC's Billing and Payment terms and conditions. These terms and conditions, together with CCC's Billing and Payment terms and conditions (which are incorporated herein), comprise the entire agreement between you and publisher (and CCC) concerning this licensing transaction. In the event of any conflict between your obligations established by these terms and conditions and those established by CCC's Billing and Payment terms and conditions, these terms and conditions shall control.

14. Revocation: Elsevier or Copyright Clearance Center may deny the permissions described in this License at their sole discretion, for any reason or no reason, with a full refund payable to you. Notice of such denial will be made using the contact information provided by you. Failure to receive such notice will not alter or invalidate the denial. In no event will Elsevier or Copyright Clearance Center be responsible or liable for any costs, expenses or damage incurred by you as a result of a denial of your permission request, other than a refund of the amount(s) paid by you to Elsevier and/or Copyright Clearance Center for denied permissions.

LIMITED LICENSE

The following terms and conditions apply only to specific license types:

15. **Translation**: This permission is granted for non-exclusive world **English** rights only unless your license was granted for translation rights. If you licensed translation rights you may only translate this content into the languages you requested. A professional translator must perform all translations and reproduce the content word for word preserving the integrity of the article. If this license is to re-use 1 or 2 figures then permission is granted for non-exclusive world rights in all languages.

16. **Website**: The following terms and conditions apply to electronic reserve and author websites: **Electronic reserve**: If licensed material is to be posted to website, the web site is to be password-protected and made available only to bona fide students registered on a relevant course if: This license was made in connection with a course, This permission is granted for 1 year only. You may obtain a license for future website posting, All content posted to the web site must maintain the copyright information line on the bottom of each image, A hyper-text must be included to the Homepage of the journal from which you are licensing at http://www.sciencedirect.com/science/journal/xxxxx or the Elsevier homepage for books at http://www.elsevier.com , and Central Storage: This license does not include permission for a scanned version of the material to be stored in a central repository such as that provided by Heron/XanEdu.

17. **Author website** for journals with the following additional clauses:

All content posted to the web site must maintain the copyright information line on the bottom of each image, and the permission granted is limited to the personal version of your paper. You are not allowed to download and post the published electronic version of your article (whether PDF or HTML, proof or final version), nor may you scan the printed edition to create an electronic version. A hyper-text must be included to the Homepage of the journal from which you are licensing at http://www.sciencedirect.com/science/journal/xxxxx . As part of our normal production process, you will receive an e-mail notice when your article appears on Elsevier's online service ScienceDirect (www.sciencedirect.com). That e-mail will include the article's Digital Object Identifier (DOI). This number provides the electronic link to the published article and should be included in the posting of your personal version. We ask that you wait until you receive this e-mail and have the DOI to do any posting.

Central Storage: This license does not include permission for a scanned version of the material to be stored in a central repository such as that provided by Heron/XanEdu.

18. **Author website** for books with the following additional clauses: Authors are permitted to place a brief summary of their work online only. A hyper-text must be included to the Elsevier homepage at http://www.elsevier.com . All content posted to the web site must maintain the copyright information line on the bottom of each image. You are not allowed to download and post the published electronic version of your chapter, nor may you scan the printed

edition to create an electronic version.

Central Storage: This license does not include permission for a scanned version of the material to be stored in a central repository such as that provided by Heron/XanEdu.

19. **Website** (regular and for author): A hyper-text must be included to the Homepage of the journal from which you are licensing at http://www.sciencedirect.com/science/journal/xxxxx. or for books to the Elsevier homepage at http://www.elsevier.com

20. **Thesis/Dissertation**: If your license is for use in a thesis/dissertation your thesis may be submitted to your institution in either print or electronic form. Should your thesis be published commercially, please reapply for permission. These requirements include permission for the Library and Archives of Canada to supply single copies, on demand, of the complete thesis and include permission for UMI to supply single copies, on demand, of the complete thesis. Should your thesis be published commercially, please reapply for permission.

21. **Other Conditions**:

v1.6

If you would like to pay for this license now, please remit this license along with your payment made payable to "COPYRIGHT CLEARANCE CENTER" otherwise you will be invoiced within 48 hours of the license

date. Payment should be in the form of a check or money order referencing your account number and this invoice number RLNK501093269. Once you receive your invoice for this order, you may pay your invoice by credit card. Please follow instructions provided at that time. Make Payment To: Copyright Clearance Center Dept 001 P.O. Box 843006 Boston, MA 02284-3006 For suggestions or comments regarding this order, contact RightsLink Customer Support: customercare@copyright.com or +1-877-622-5543 (toll free in the US) or +1-978-646-2777.

Gratis licenses (referencing $0 in the Total field) are free. Please retain this printable license for your reference. No payment is required.

REFERENCES

REFERENCES

1. Vander, A.J.S.J.H.L., D. S., *Human physiology: the mechanisms of body function*. 5th edition ed1990, USA: McGraw-Hill Publishing Company.

2. Madl, C. and M. Holzer, *Brain function after resuscitation from cardiac arrest.* Curr Opin Crit Care, 2004. **10**(3): p. 213-7.

3. Hayman, L.A., S.A. Berman, and V.C. Hinck, *Correlation of CT cerebral vascular territories with function: II. Posterior cerebral artery.* AJR Am J Roentgenol, 1981. **137**(1): p. 13-9.

4. Berman, S.A., L.A. Hayman, and V.C. Hinck, *Correlation of CT cerebral vascular territories with function: 3. Middle cerebral artery.* AJR Am J Roentgenol, 1984. **142**(5): p. 1035-40.

5. Berman, S.A., L.A. Hayman, and V.C. Hinck, *Correlation of CT cerebral vascular territories with function: I. Anterior cerebral artery.* AJR Am J Roentgenol, 1980. **135**(2): p. 253-7.

6. Coyle, P. and P.T. Jokelainen, *Dorsal cerebral arterial collaterals of the rat.* Anat Rec, 1982. **203**(3): p. 397-404.

7. Cipolla, M.J., in *The Cerebral Circulation*2009: San Rafael (CA).

8. Schaffer, C.B., et al., *Two-photon imaging of cortical surface microvessels reveals a robust redistribution in blood flow after vascular occlusion.* PLoS Biol, 2006. **4**(2): p. e22.

9. Nishimura, N., et al., *Penetrating arterioles are a bottleneck in the perfusion of neocortex.* Proc Natl Acad Sci U S A, 2007. **104**(1): p. 365-70.

10. Iadecola, C. and R.L. Davisson, *Hypertension and cerebrovascular dysfunction.* Cell Metab, 2008. **7**(6): p. 476-84.

11. Shih, A.Y., et al., *The smallest stroke: occlusion of one penetrating vessel leads to infarction and a cognitive deficit.* Nat Neurosci, 2013. **16**(1): p. 55-63.

12. Hamel, E., *Perivascular nerves and the regulation of cerebrovascular tone.* J Appl Physiol, 2006. **100**(3): p. 1059-64.

13. Gobel, U., H. Theilen, and W. Kuschinsky, *Congruence of total and perfused capillary network in rat brains.* Circ Res, 1990. **66**(2): p. 271-81.

14. Sa-Pereira, I., D. Brites, and M.A. Brito, *Neurovascular unit: a focus on pericytes.* Mol Neurobiol, 2012. **45**(2): p. 327-47.

15. Dalkara, T., Y. Gursoy-Ozdemir, and M. Yemisci, *Brain microvascular pericytes in health and disease.* Acta Neuropathol, 2011. **122**(1): p. 1-9.

16. Dirnagl, U., *Pathobiology of injury after stroke: the neurovascular unit and beyond.* Ann N Y Acad Sci, 2012. **1268**: p. 21-5.

17. Stanimirovic, D.B. and A. Friedman, *Pathophysiology of the neurovascular unit: disease cause or consequence?* J Cereb Blood Flow Metab, 2012. **32**(7): p. 1207-21.

18. Abbott, N.J., et al., *Structure and function of the blood-brain barrier.* Neurobiol Dis, 2010. **37**(1): p. 13-25.

19. Zlokovic, B.V., *The blood-brain barrier in health and chronic neurodegenerative disorders.* Neuron, 2008. **57**(2): p. 178-201.

20. Chen, Y. and L. Liu, *Modern methods for delivery of drugs across the blood-brain barrier.* Adv Drug Deliv Rev, 2012. **64**(7): p. 640-65.

21. Paulson, O.B., S. Strandgaard, and L. Edvinsson, *Cerebral autoregulation.* Cerebrovasc Brain Metab Rev, 1990. **2**(2): p. 161-92.

22. Pires, P.W., et al., *The effects of hypertension on the cerebral circulation.* Am J Physiol Heart Circ Physiol, 2013. **304**(12): p. H1598-614.

23. Bayliss, W.M., *On the local reactions of the arterial wall to changes of internal pressure.* J Physiol, 1902. **28**(3): p. 220-31.

24. Osol, G., et al., *Myogenic tone, reactivity, and forced dilatation: a three-phase model of in vitro arterial myogenic behavior.* Am J Physiol Heart Circ Physiol, 2002. **283**(6): p. H2260-7.

25. Cipolla, M.J., J.M. Porter, and G. Osol, *High glucose concentrations dilate cerebral arteries and diminish myogenic tone through an endothelial mechanism.* Stroke, 1997. **28**(2): p. 405-10; discussion 410-1.

26. Geary, G.G., D.N. Krause, and S.P. Duckles, *Estrogen reduces mouse cerebral artery tone through endothelial NOS- and cyclooxygenase-dependent mechanisms.* Am J Physiol Heart Circ Physiol, 2000. **279**(2): p. H511-9.

27. Faraci, F.M. and D.D. Heistad, *Regulation of large cerebral arteries and cerebral microvascular pressure.* Circ Res, 1990. **66**(1): p. 8-17.

28. Johnson, P.C., *The myogenic response*. Handbook of Physiology. The Cardiovascular System. Vascular Smooth Muscle. Vol. II. 1981, Bethesda, MD: The American Physiological Society.

29. Mangat, H.S., *Severe traumatic brain injury.* Continuum (Minneap Minn), 2012. **18**(3): p. 532-46.

30. Faraci, F.M. and J.E. Brian, Jr., *Nitric oxide and the cerebral circulation.* Stroke, 1994. **25**(3): p. 692-703.

31. Moncada, S., R.M. Palmer, and E.A. Higgs, *Nitric oxide: physiology, pathophysiology, and pharmacology.* Pharmacol Rev, 1991. **43**(2): p. 109-42.

32. Knowles, R.G. and S. Moncada, *Nitric oxide synthases in mammals.* Biochem J, 1994. **298 (Pt 2)**: p. 249-58.

33. Tong, X.K. and E. Hamel, *Basal forebrain nitric oxide synthase (NOS)-containing neurons project to microvessels and NOS neurons in the rat neocortex: cellular basis for cortical blood flow regulation.* Eur J Neurosci, 2000. **12**(8): p. 2769-80.

34. Ignarro, L.J., *Nitric oxide as a unique signaling molecule in the vascular system: a historical overview.* J Physiol Pharmacol, 2002. **53**(4 Pt 1): p. 503-14.

35. Robertson, B.E., et al., *cGMP-dependent protein kinase activates Ca-activated K channels in cerebral artery smooth muscle cells.* Am J Physiol, 1993. **265**(1 Pt 1): p. C299-303.

36. Faraci, F.M. and C.G. Sobey, *Role of soluble guanylate cyclase in dilator responses of the cerebral microcirculation.* Brain Res, 1999. **821**(2): p. 368-73.

37. Suzuki, N., J.E. Hardebo, and C. Owman, *Origins and pathways of choline acetyltransferase-positive parasympathetic nerve fibers to cerebral vessels in rat.* J Cereb Blood Flow Metab, 1990. **10**(3): p. 399-408.

38. Goadsby, P.J.E., L., *Neurovascular control of the cerebral circulation*. 2nd edition ed. Cerebral Blood Flow and Metabolism, ed. L.K. Edvinsson, D.N.2002, Philadelphia, PA: Lippincott Williams & Wilkins.

39. Garcia-Villalon, A.L., et al., *Heterogeneity of muscarinic receptor subtypes in cerebral blood vessels.* J Pharmacol Exp Ther, 1991. **258**(1): p. 304-10.

40. Yamada, M., et al., *Cholinergic dilation of cerebral blood vessels is abolished in M(5) muscarinic acetylcholine receptor knockout mice.* Proc Natl Acad Sci U S A, 2001. **98**(24): p. 14096-101.

41. You, J., et al., *Endothelial-mediated dilations of rat middle cerebral arteries by ATP and ADP.* Am J Physiol, 1997. **273**(3 Pt 2): p. H1472-7.

42. You, J., et al., *Functional heterogeneity of endothelial P2 purinoceptors in the cerebrovascular tree of the rat.* Am J Physiol, 1999. **277**(3 Pt 2): p. H893-900.

43. Koehler, R.C., R.J. Roman, and D.R. Harder, *Astrocytes and the regulation of cerebral blood flow.* Trends Neurosci, 2009. **32**(3): p. 160-9.

44. Golding, E.M., et al., *Endothelium-derived hyperpolarizing factor in the brain: a new regulator of cerebral blood flow?* Stroke, 2002. **33**(3): p. 661-3.

45. Stankevicius, E., et al., *Opening of small and intermediate calcium-activated potassium channels induces relaxation mainly mediated by nitric-oxide release in large arteries and endothelium-derived hyperpolarizing factor in small arteries from rat.* J Pharmacol Exp Ther, 2011. **339**(3): p. 842-50.

46. Marrelli, S.P., M.S. Eckmann, and M.S. Hunte, *Role of endothelial intermediate conductance KCa channels in cerebral EDHF-mediated dilations.* Am J Physiol Heart Circ Physiol, 2003. **285**(4): p. H1590-9.

47. Triggle, C.R., et al., *The endothelium: influencing vascular smooth muscle in many ways.* Can J Physiol Pharmacol, 2012. **90**(6): p. 713-38.

48. Ellinsworth, D.C., et al., *Endothelial control of vasodilation: integration of myoendothelial microdomain signalling and modulation by epoxyeicosatrienoic acids.* Pflugers Arch, 2013.

49. Mustafa, A.K., et al., *Hydrogen sulfide as endothelium-derived hyperpolarizing factor sulfhydrates potassium channels.* Circ Res, 2011. **109**(11): p. 1259-68.

50. Cipolla, M.J., et al., *SKCa and IKCa Channels, myogenic tone, and vasodilator responses in middle cerebral arteries and parenchymal arterioles: effect of ischemia and reperfusion.* Stroke, 2009. **40**(4): p. 1451-7.

51. Harder, D.R., et al., *Functional hyperemia in the brain: hypothesis for astrocyte-derived vasodilator metabolites.* Stroke, 1998. **29**(1): p. 229-34.

52. Mulvany, M.J., *Small artery remodelling in hypertension.* Basic Clin Pharmacol Toxicol, 2012. **110**(1): p. 49-55.

53. Mulvany, M.J., *Vascular remodelling of resistance vessels: can we define this?* Cardiovasc Res, 1999. **41**(1): p. 9-13.

54. Hayashi, K. and T. Naiki, *Adaptation and remodeling of vascular wall; biomechanical response to hypertension.* J Mech Behav Biomed Mater, 2009. **2**(1): p. 3-19.

55. Mathiassen, O.N., et al., *Small artery structure is an independent predictor of cardiovascular events in essential hypertension.* J Hypertens, 2007. **25**(5): p. 1021-6.

56. Folkow, B., *Structural, myogenic, humoral and nervous factors controlling peripheral resistance.* 1st edition ed. Hypotensive drugs., ed. M. Haringtон1956, London: Pergamon.

57. Mulvany, M.J. and W. Halpern, *Mechanical properties of vascular smooth muscle cells in situ.* Nature, 1976. **260**(5552): p. 617-9.

58. Aalkjaer, C., et al., *Evidence for increased media thickness, increased neuronal amine uptake, and depressed excitation--contraction coupling in isolated resistance vessels from essential hypertensives.* Circ Res, 1987. **61**(2): p. 181-6.

59. Mulvany, M.J., O.K. Hansen, and C. Aalkjaer, *Direct evidence that the greater contractility of resistance vessels in spontaneously hypertensive rats is associated with a narrowed lumen, a thickened media, and an increased number of smooth muscle cell layers.* Circ Res, 1978. **43**(6): p. 854-64.

60. Deng, L.Y. and E.L. Schiffrin, *Effects of endothelin-1 and vasopressin on resistance arteries of spontaneously hypertensive rats.* Am J Hypertens, 1992. **5**(11): p. 817-22.

61. Jalil, J.E., et al., *Coronary vascular remodeling and myocardial fibrosis in the rat with renovascular hypertension. Response to captopril.* Am J Hypertens, 1991. **4**(1 Pt 1): p. 51-5.

62. Izzard, A.S., et al., *Small artery structure and hypertension: adaptive changes and target organ damage.* J Hypertens, 2005. **23**(2): p. 247-50.

63. Mulvany, M.J., et al., *Vascular remodeling.* Hypertension, 1996. **28**(3): p. 505-6.

64. Heagerty, A.M., et al., *Small artery structure in hypertension. Dual processes of remodeling and growth.* Hypertension, 1993. **21**(4): p. 391-7.

65. Winquist, R.J. and D.F. Bohr, *Structural and functional changes in cerebral arteries from spontaneously hypertensive rats.* Hypertension, 1983. **5**(3): p. 292-7.

66. Toda, N., H. Okunishi, and M. Miyazaki, *Length-passive tension relationships in cerebral and peripheral arteries isolated from spontaneously hypertensive and normotensive rats.* Jpn Circ J, 1982. **46**(10): p. 1088-94.

67. Baumbach, G.L. and D.D. Heistad, *Remodeling of cerebral arterioles in chronic hypertension.* Hypertension, 1989. **13**(6 Pt 2): p. 968-72.

68. Baumbach, G.L. and M.A. Hajdu, *Mechanics and composition of cerebral arterioles in renal and spontaneously hypertensive rats.* Hypertension, 1993. **21**(6 Pt 1): p. 816-26.

69. Rigsby, C.S., D.M. Pollock, and A.M. Dorrance, *Spironolactone improves structure and increases tone in the cerebral vasculature of male spontaneously hypertensive stroke-prone rats.* Microvasc Res, 2007. **73**(3): p. 198-205.

70. Pires, P.W., et al., *Doxycycline, a matrix metalloprotease inhibitor, reduces vascular remodeling and damage after cerebral ischemia in stroke-prone spontaneously hypertensive rats.* Am J Physiol Heart Circ Physiol, 2011. **301**(1): p. H87-97.

71. Osmond, J.M., et al., *Obesity increases blood pressure, cerebral vascular remodeling, and severity of stroke in the Zucker rat.* Hypertension, 2009. **53**(2): p. 381-6.

72. Deutsch, C., et al., *Diet-induced obesity causes cerebral vessel remodeling and increases the damage caused by ischemic stroke.* Microvasc Res, 2009. **78**(1): p. 100-6.

73. Dorrance, A.M., N.C. Rupp, and E.F. Nogueira, *Mineralocorticoid receptor activation causes cerebral vessel remodeling and exacerbates the damage caused by cerebral ischemia.* Hypertension, 2006. **47**(3): p. 590-5.

74. Osmond, J.M. and A.M. Dorrance, *11beta-hydroxysteroid dehydrogenase type II inhibition causes cerebrovascular remodeling and increases infarct size after cerebral ischemia.* Endocrinology, 2009. **150**(2): p. 713-9.

75. Pires, P.W., et al., *Improvement in Middle Cerebral Artery Structure and Endothelial Function in Stroke-Prone Spontaneously Hypertensive Rats after Macrophage Depletion.* Microcirculation, 2013.

76. Arribas, S.M., et al., *Functional reduction and associated cellular rearrangement in SHRSP rat basilar arteries are affected by salt load and calcium antagonist treatment.* J Cereb Blood Flow Metab, 1999. **19**(5): p. 517-27.

77. Arribas, S.M., et al., *Confocal microscopic characterization of a lesion in a cerebral vessel of the stroke-prone spontaneously hypertensive rat.* Stroke, 1996. **27**(6): p. 1118-22; discussion 1122-3.

78. Arribas, S.M., et al., *Cellular changes induced by chronic nitric oxide inhibition in intact rat basilar arteries revealed by confocal microscopy.* J Hypertens, 1997. **15**(12 Pt 2): p. 1685-93.

79. Clozel, J.P., H. Kuhn, and F. Hefti, *Effects of cilazapril on the cerebral circulation in spontaneously hypertensive rats.* Hypertension, 1989. **14**(6): p. 645-51.

80. Hajdu, M.A., D.D. Heistad, and G.L. Baumbach, *Effects of antihypertensive therapy on mechanics of cerebral arterioles in rats.* Hypertension, 1991. **17**(3): p. 308-16.

81. Chillon, J.M. and G.L. Baumbach, *Effects of an angiotensin-converting enzyme inhibitor and a beta-blocker on cerebral arterioles in rats.* Hypertension, 1999. **33**(3): p. 856-61.

82. Kumai, Y., et al., *Protective effects of angiotensin II type 1 receptor blocker on cerebral circulation independent of blood pressure.* Exp Neurol, 2008. **210**(2): p. 441-8.

83. Rigsby, C.S., et al., *Effects of Spironolactone on Cerebral Vessel Structure in Rats With Sustained Hypertension.* Am J Hypertens, 2011.

84. Pitt, B., et al., *The effect of spironolactone on morbidity and mortality in patients with severe heart failure. Randomized Aldactone Evaluation Study Investigators.* N Engl J Med, 1999. **341**(10): p. 709-17.

85. Pitt, B., et al., *Eplerenone, a selective aldosterone blocker, in patients with left ventricular dysfunction after myocardial infarction.* N Engl J Med, 2003. **348**(14): p. 1309-21.

86. Rocha, R., et al., *Mineralocorticoid blockade reduces vascular injury in stroke-prone hypertensive rats.* Hypertension, 1998. **31**(1 Pt 2): p. 451-8.

87. Pires, P.W., et al., *Tempol, a superoxide dismutase mimetic, prevents cerebral vessel remodeling in hypertensive rats.* Microvasc Res, 2010. **80**(3): p. 445-52.

88. De Silva, T.M. and F.M. Faraci, *Effects of angiotensin II on the cerebral circulation: role of oxidative stress.* Front Physiol, 2012. **3**: p. 484.

89. Newfell, B.G., et al., *Aldosterone regulates vascular gene transcription via oxidative stress-dependent and -independent pathways.* Arterioscler Thromb Vasc Biol, 2011. **31**(8): p. 1871-80.

90. Cipolla, M.J., et al., *PPAR{gamma} activation prevents hypertensive remodeling of cerebral arteries and improves vascular function in female rats.* Stroke, 2010. **41**(6): p. 1266-70.

91. Osol, G. and W. Halpern, *Myogenic properties of cerebral blood vessels from normotensive and hypertensive rats.* Am J Physiol, 1985. **249**(5 Pt 2): p. H914-21.

92. Brayden, J.E., et al., *Transient receptor potential (TRP) channels, vascular tone and autoregulation of cerebral blood flow.* Clin Exp Pharmacol Physiol, 2008. **35**(9): p. 1116-20.

93. Yang, S.T., et al., *Endothelium-dependent responses of cerebral blood vessels during chronic hypertension.* Hypertension, 1991. **17**(5): p. 612-8.

94. Mayhan, W.G., F.M. Faraci, and D.D. Heistad, *Impairment of endothelium-dependent responses of cerebral arterioles in chronic hypertension.* Am J Physiol, 1987. **253**(6 Pt 2): p. H1435-40.

95. Bhatt, S.R., M.F. Lokhandwala, and A.A. Banday, *Resveratrol prevents endothelial nitric oxide synthase uncoupling and attenuates development of hypertension in spontaneously hypertensive rats.* Eur J Pharmacol, 2011. **667**(1-3): p. 258-64.

96. Yamakawa, H., et al., *Normalization of endothelial and inducible nitric oxide synthase expression in brain microvessels of spontaneously hypertensive rats by angiotensin II AT1 receptor inhibition.* J Cereb Blood Flow Metab, 2003. **23**(3): p. 371-80.

97. Oyama, N., et al., *Cilostazol, not aspirin, reduces ischemic brain injury via endothelial protection in spontaneously hypertensive rats.* Stroke, 2011. **42**(9): p. 2571-7.

98. Paravicini, T.M. and C.G. Sobey, *Cerebral vascular effects of reactive oxygen species: recent evidence for a role of NADPH-oxidase.* Clin Exp Pharmacol Physiol, 2003. **30**(11): p. 855-9.

99. Touyz, R.M. and A.M. Briones, *Reactive oxygen species and vascular biology: implications in human hypertension.* Hypertens Res, 2011. **34**(1): p. 5-14.

100. Miller, A.A., et al., *NADPH oxidase activity and function are profoundly greater in cerebral versus systemic arteries.* Circ Res, 2005. **97**(10): p. 1055-62.

101. Sobey, C.G., D.D. Heistad, and F.M. Faraci, *Mechanisms of bradykinin-induced cerebral vasodilatation in rats. Evidence that reactive oxygen species activate K+ channels.* Stroke, 1997. **28**(11): p. 2290-4; discussion 2295.

102. Giachini, F.R., et al., *Upregulation of intermediate calcium-activated potassium channels counterbalance the impaired endothelium-dependent vasodilation in stroke-prone spontaneously hypertensive rats.* Transl Res, 2009. **154**(4): p. 183-93.

103. Bussemaker, E., et al., *Aged spontaneously hypertensive rats exhibit a selective loss of EDHF-mediated relaxation in the renal artery.* Hypertension, 2003. **42**(4): p. 562-8.

104. Marrelli, S.P., et al., *P2 purinoceptor-mediated dilations in the rat middle cerebral artery after ischemia-reperfusion.* Am J Physiol, 1999. **276**(1 Pt 2): p. H33-41.

105. Go, A.S., et al., *Heart disease and stroke statistics--2013 update: a report from the American Heart Association.* Circulation, 2013. **127**(1): p. e6-e245.

106. Clark, W.M., et al., *Recombinant tissue-type plasminogen activator (Alteplase) for ischemic stroke 3 to 5 hours after symptom onset. The ATLANTIS Study: a randomized controlled trial. Alteplase Thrombolysis for Acute Noninterventional Therapy in Ischemic Stroke.* Jama, 1999. **282**(21): p. 2019-26.

107. Muir, K.W., *Heterogeneity of stroke pathophysiology and neuroprotective clinical trial design.* Stroke, 2002. **33**(6): p. 1545-50.

108. Goldstein, L.B., et al., *Primary prevention of ischemic stroke: a guideline from the American Heart Association/American Stroke Association Stroke Council: cosponsored by the Atherosclerotic Peripheral Vascular Disease Interdisciplinary Working Group; Cardiovascular Nursing Council; Clinical Cardiology Council; Nutrition, Physical Activity, and Metabolism Council; and the Quality of Care and Outcomes Research Interdisciplinary Working Group: the American Academy of Neurology affirms the value of this guideline.* Stroke, 2006. **37**(6): p. 1583-633.

109. Lindholm, L.H., et al., *Cardiovascular morbidity and mortality in patients with diabetes in the Losartan Intervention For Endpoint reduction in hypertension study (LIFE): a randomised trial against atenolol.* Lancet, 2002. **359**(9311): p. 1004-10.

110. Fitchett, D., *Results of the ONTARGET and TRANSCEND studies: an update and discussion.* Vasc Health Risk Manag, 2009. **5**(1): p. 21-9.

111. Coyle, P. and P.T. Jokelainen, *Differential outcome to middle cerebral artery occlusion in spontaneously hypertensive stroke-prone rats (SHRSP) and Wistar Kyoto (WKY) rats.* Stroke, 1983. **14**(4): p. 605-11.

112. Coyle, P. and D.D. Heistad, *Blood flow through cerebral collateral vessels in hypertensive and normotensive rats.* Hypertension, 1986. **8**(6 Pt 2): p. II67-71.

113. Coyle, P. and D.D. Heistad, *Blood flow through cerebral collateral vessels one month after middle cerebral artery occlusion.* Stroke, 1987. **18**(2): p. 407-11.

114. Liebeskind, D.S., *Collateral circulation.* Stroke, 2003. **34**(9): p. 2279-84.

115. Morikawa, E., S. Rosenblatt, and M.A. Moskowitz, *L-arginine dilates rat pial arterioles by nitric oxide-dependent mechanisms and increases blood flow during focal cerebral ischaemia.* Br J Pharmacol, 1992. **107**(4): p. 905-7.

116. Morikawa, E., Z. Huang, and M.A. Moskowitz, *L-arginine decreases infarct size caused by middle cerebral arterial occlusion in SHR.* Am J Physiol, 1992. **263**(5 Pt 2): p. H1632-5.

117. Dalkara, T., et al., *Blood flow-dependent functional recovery in a rat model of focal cerebral ischemia.* Am J Physiol, 1994. **267**(2 Pt 2): p. H678-83.

118. Huang, Z., et al., *Enlarged infarcts in endothelial nitric oxide synthase knockout mice are attenuated by nitro-L-arginine.* J Cereb Blood Flow Metab, 1996. **16**(5): p. 981-7.

119. Sasaki, Y., et al., *Protective effects of imidapril on He-Ne laser-induced thrombosis in cerebral blood vessels of stroke-prone spontaneously hypertensive rats.* Thromb Haemost, 2000. **83**(5): p. 722-7.

120. Endres, M., et al., *Stroke protection by 3-hydroxy-3-methylglutaryl (HMG)-CoA reductase inhibitors mediated by endothelial nitric oxide synthase.* Proc Natl Acad Sci U S A, 1998. **95**(15): p. 8880-5.

121. Ito, H., et al., *Cilostazol, a phosphodiesterase inhibitor, attenuates photothrombotic focal ischemic brain injury in hypertensive rats.* J Cereb Blood Flow Metab, 2010. **30**(2): p. 343-51.

122. Shinohara, Y., et al., *Cilostazol for prevention of secondary stroke (CSPS 2): an aspirin-controlled, double-blind, randomised non-inferiority trial.* Lancet Neurol, 2010. **9**(10): p. 959-68.

123. Cipolla, M.J., et al., *Reperfusion decreases myogenic reactivity and alters middle cerebral artery function after focal cerebral ischemia in rats.* Stroke, 1997. **28**(1): p. 176-80.

124. Cipolla, M.J., et al., *Threshold duration of ischemia for myogenic tone in middle cerebral arteries: effect on vascular smooth muscle actin.* Stroke, 2001. **32**(7): p. 1658-64.

125. Dorrance, A.M., et al., *Spironolactone reduces cerebral infarct size and EGF-receptor mRNA in stroke-prone rats.* Am J Physiol Regul Integr Comp Physiol, 2001. **281**(3): p. R944-50.

126. Okamoto, K., et al., *Pathogenesis and prevention of stroke in spontaneously hypertensive rats.* Clin Sci Mol Med Suppl, 1975. **2**: p. 161s-163s.

127. Yamori, Y., et al., *Pathogenetic similarity of strokes in stroke-prone spontaneously hypertensive rats and humans.* Stroke, 1976. **7**(1): p. 46-53.

128. Davidson, A.O., et al., *Blood pressure in genetically hypertensive rats. Influence of the Y chromosome.* Hypertension, 1995. **26**(3): p. 452-9.

129. Tagami, M., et al., *Ultrastructural characteristics of occluded perforating arteries in stroke-prone spontaneously hypertensive rats.* Stroke, 1987. **18**(4): p. 733-40.

130. Obata, J., et al., *Increased gene expression of components of the renin-angiotensin system in glomeruli of genetically hypertensive rats.* J Hypertens, 2000. **18**(9): p. 1247-55.

131. Savage, P. and A.Y. Jeng, *Upregulation of endothelin-1 binding in tissues of salt-loaded stroke-prone spontaneously hypertensive rats.* Can J Physiol Pharmacol, 2002. **80**(5): p. 470-4.

132. Kishi, T., et al., *Increased reactive oxygen species in rostral ventrolateral medulla contribute to neural mechanisms of hypertension in stroke-prone spontaneously hypertensive rats.* Circulation, 2004. **109**(19): p. 2357-62.

133. Ogata, J., et al., *Stroke-prone spontaneously hypertensive rats as an experimental model of malignant hypertension. A pathological study.* Virchows Arch A Pathol Anat Histol, 1982. **394**(3): p. 185-94.

134. Fredriksson, K., et al., *Cerebrovascular lesions in stroke-prone spontaneously hypertensive rats.* Acta Neuropathol, 1985. **68**(4): p. 284-94.

135. Schreiber, S., et al., *The pathologic cascade of cerebrovascular lesions in SHRSP: is erythrocyte accumulation an early phase?* J Cereb Blood Flow Metab, 2012. **32**(2): p. 278-90.

136. Schreiber, S., et al., *Kidney pathology precedes and predicts the pathological cascade of cerebrovascular lesions in stroke prone rats.* PLoS ONE, 2011. **6**(10): p. e26287.

137. Schreiber, S., et al., *Blood brain barrier breakdown as the starting point of cerebral small vessel disease? - New insights from a rat model.* Exp Transl Stroke Med, 2013. **5**(1): p. 4.

138. Kimura, S., et al., *Pathogenesis of vascular dementia in stroke-prone spontaneously hypertensive rats.* Toxicology, 2000. **153**(1-3): p. 167-78.

139. Kahle, M.P. and G.J. Bix, *Successfully Climbing the "STAIRs": Surmounting Failed Translation of Experimental Ischemic Stroke Treatments.* Stroke Res Treat, 2012. **2012**: p. 374098.

140. Chae, C.U., et al., *Blood pressure and inflammation in apparently healthy men.* Hypertension, 2001. **38**(3): p. 399-403.

141. Schillaci, G., et al., *Increased C-reactive protein concentrations in never-treated hypertension: the role of systolic and pulse pressures.* J Hypertens, 2003. **21**(10): p. 1841-6.

142. Sesso, H.D., et al., *C-reactive protein and the risk of developing hypertension.* Jama, 2003. **290**(22): p. 2945-51.

143. Ruiz-Ortega, M., et al., *Angiotensin II activates nuclear transcription factor kappaB through AT(1) and AT(2) in vascular smooth muscle cells: molecular mechanisms.* Circ Res, 2000. **86**(12): p. 1266-72.

144. Kranzhofer, R., et al., *Angiotensin induces inflammatory activation of human vascular smooth muscle cells.* Arterioscler Thromb Vasc Biol, 1999. **19**(7): p. 1623-9.

145. Wu, L., et al., *Roles of angiotensin II type 2 receptor stimulation associated with selective angiotensin II type 1 receptor blockade with valsartan in the improvement of inflammation-induced vascular injury.* Circulation, 2001. **104**(22): p. 2716-21.

146. Wang, C.H., et al., *C-reactive protein upregulates angiotensin type 1 receptors in vascular smooth muscle.* Circulation, 2003. **107**(13): p. 1783-90.

147. Wassmann, S., et al., *Interleukin-6 induces oxidative stress and endothelial dysfunction by overexpression of the angiotensin II type 1 receptor.* Circ Res, 2004. **94**(4): p. 534-41.

148. Pueyo, M.E., et al., *Angiotensin II stimulates endothelial vascular cell adhesion molecule-1 via nuclear factor-kappaB activation induced by intracellular oxidative stress.* Arterioscler Thromb Vasc Biol, 2000. **20**(3): p. 645-51.

149. Caprio, M., et al., *Functional mineralocorticoid receptors in human vascular endothelial cells regulate intercellular adhesion molecule-1 expression and promote leukocyte adhesion.* Circ Res, 2008. **102**(11): p. 1359-67.

150. Madej, A., et al., *Plasma concentrations of adhesion molecules and chemokines in patients with essential hypertension.* Pharmacol Rep, 2005. **57**(6): p. 878-81.

151. Dorffel, Y., et al., *Preactivated peripheral blood monocytes in patients with essential hypertension.* Hypertension, 1999. **34**(1): p. 113-7.

152. Pu, Q., et al., *Effects of combined AT1 receptor antagonist/NEP inhibitor on vascular remodeling and cardiac fibrosis in SHRSP.* J Hypertens, 2008. **26**(2): p. 322-33.

153. Nakamura, T., et al., *Pioglitazone exerts protective effects against stroke in stroke-prone spontaneously hypertensive rats, independently of blood pressure.* Stroke, 2007. **38**(11): p. 3016-22.

154. Touyz, R.M., *Reactive oxygen species and angiotensin II signaling in vascular cells -- implications in cardiovascular disease.* Braz J Med Biol Res, 2004. **37**(8): p. 1263-73.

155. Bedard, K. and K.H. Krause, *The NOX family of ROS-generating NADPH oxidases: physiology and pathophysiology.* Physiol Rev, 2007. **87**(1): p. 245-313.

156. Lassegue, B. and K.K. Griendling, *Reactive oxygen species in hypertension; An update.* Am J Hypertens, 2004. **17**(9): p. 852-60.

157. Ko, E.A., et al., *Resistance artery remodeling in deoxycorticosterone acetate-salt hypertension is dependent on vascular inflammation: evidence from m-CSF-deficient mice.* Am J Physiol Heart Circ Physiol, 2007. **292**(4): p. H1789-95.

158. De Ciuceis, C., et al., *Reduced vascular remodeling, endothelial dysfunction, and oxidative stress in resistance arteries of angiotensin II-infused macrophage colony-stimulating factor-deficient mice: evidence for a role in inflammation in angiotensin-induced vascular injury.* Arterioscler Thromb Vasc Biol, 2005. **25**(10): p. 2106-13.

159. Bond, M., et al., *Inhibition of transcription factor NF-kappaB reduces matrix metalloproteinase-1, -3 and -9 production by vascular smooth muscle cells.* Cardiovasc Res, 2001. **50**(3): p. 556-65.

160. Ando, H., et al., *Angiotensin II AT1 receptor blockade decreases brain artery inflammation in a stress-prone rat strain.* Ann N Y Acad Sci, 2004. **1018**: p. 345-50.

161. Fleisch, H., *Bisphosphonates: a new class of drugs in diseases of bone and calcium metabolism.* Recent Results Cancer Res, 1989. **116**: p. 1-28.

162. Russell, R.G., *Bisphosphonates: mode of action and pharmacology.* Pediatrics, 2007. **119 Suppl 2**: p. S150-62.

163. Van Rooijen, N. and A. Sanders, *Liposome mediated depletion of macrophages: mechanism of action, preparation of liposomes and applications.* J Immunol Methods, 1994. **174**(1-2): p. 83-93.

164. Van Rooijen, N., *Selective depletion of macrophages by liposome-encapsulated drugs.* 5th ed. Handbook of Experimental Immunology, ed. L. Herzenberg, L. Herzenberg, and D. Weir1996: Blackwell Scientific Publications, Inc. 165.1-165.5.

165. Danenberg, H.D., et al., *Macrophage depletion by clodronate-containing liposomes reduces neointimal formation after balloon injury in rats and rabbits.* Circulation, 2002. **106**(5): p. 599-605.

166. Nuki, Y., et al., *Roles of macrophages in flow-induced outward vascular remodeling.* J Cereb Blood Flow Metab, 2009. **29**(3): p. 495-503.

167. Sandoo, A., et al., *Anti-TNFalpha therapy may lead to blood pressure reductions through improved endothelium-dependent microvascular function in patients with rheumatoid arthritis.* J Hum Hypertens, 2011. **25**(11): p. 699-702.

168. Hurlimann, D., et al., *Anti-tumor necrosis factor-alpha treatment improves endothelial function in patients with rheumatoid arthritis.* Circulation, 2002. **106**(17): p. 2184-7.

169. Elmarakby, A.A., et al., *Tumor necrosis factor alpha blockade increases renal Cyp2c23 expression and slows the progression of renal damage in salt-sensitive hypertension.* Hypertension, 2006. **47**(3): p. 557-62.

170. Sriramula, S., et al., *Involvement of tumor necrosis factor-alpha in angiotensin II-mediated effects on salt appetite, hypertension, and cardiac hypertrophy.* Hypertension, 2008. **51**(5): p. 1345-51.

171. Elmarakby, A.A., et al., *TNF-alpha inhibition reduces renal injury in DOCA-salt hypertensive rats.* Am J Physiol Regul Integr Comp Physiol, 2008. **294**(1): p. R76-83.

172. Bakker, E.N., et al., *Blood flow-dependent arterial remodelling is facilitated by inflammation but directed by vascular tone.* Cardiovasc Res, 2008. **78**(2): p. 341-8.

173. Lin, Y.C., et al., *Simvastatin attenuates the additive effects of TNF-alpha and IL-18 on the connexin 43 up-regulation and over-proliferation of cultured aortic smooth muscle cells.* Cytokine, 2013. **62**(3): p. 341-51.

174. Goetze, S., et al., *TNF-alpha-induced migration of vascular smooth muscle cells is MAPK dependent.* Hypertension, 1999. **33**(1 Pt 2): p. 183-9.

175. Lee, S.J., W.J. Kim, and S.K. Moon, *TNF-alpha regulates vascular smooth muscle cell responses in genetic hypertension.* Int Immunopharmacol, 2009. **9**(7-8): p. 837-43.

176. Li, Y.Y., et al., *Myocardial extracellular matrix remodeling in transgenic mice overexpressing tumor necrosis factor alpha can be modulated by anti-tumor necrosis factor alpha therapy.* Proc Natl Acad Sci U S A, 2000. **97**(23): p. 12746-51.

177. Iademarco, M.F., J.L. Barks, and D.C. Dean, *Regulation of vascular cell adhesion molecule-1 expression by IL-4 and TNF-alpha in cultured endothelial cells.* J Clin Invest, 1995. **95**(1): p. 264-71.

178. Yang, J., et al., *Proximal cerebral arteries develop myogenic responsiveness in heart failure via tumor necrosis factor-alpha-dependent activation of sphingosine-1-phosphate signaling.* Circulation, 2012. **126**(2): p. 196-206.

179. Vecchione, C., et al., *Tumor necrosis factor-alpha mediates hemolysis-induced vasoconstriction and the cerebral vasospasm evoked by subarachnoid hemorrhage.* Hypertension, 2009. **54**(1): p. 150-6.

180. Anderson, H.D., D. Rahmutula, and D.G. Gardner, *Tumor necrosis factor-alpha inhibits endothelial nitric-oxide synthase gene promoter activity in bovine aortic endothelial cells.* J Biol Chem, 2004. **279**(2): p. 963-9.

181. Mohamed, F., et al., *Lack of role for nitric oxide (NO) in the selective destabilization of endothelial NO synthase mRNA by tumor necrosis factor-alpha.* Arterioscler Thromb Vasc Biol, 1995. **15**(1): p. 52-7.

182. Yoshizumi, M., et al., *Tumor necrosis factor downregulates an endothelial nitric oxide synthase mRNA by shortening its half-life.* Circ Res, 1993. **73**(1): p. 205-9.

183. Goodwin, B.L., et al., *Tumor necrosis factor-alpha reduces argininosuccinate synthase expression and nitric oxide production in aortic endothelial cells.* Am J Physiol Heart Circ Physiol, 2007. **293**(2): p. H1115-21.

184. Picchi, A., et al., *Tumor necrosis factor-alpha induces endothelial dysfunction in the prediabetic metabolic syndrome.* Circ Res, 2006. **99**(1): p. 69-77.

185. Manea, A., et al., *Transcriptional regulation of NADPH oxidase isoforms, Nox1 and Nox4, by nuclear factor-kappaB in human aortic smooth muscle cells.* Biochem Biophys Res Commun, 2010. **396**(4): p. 901-7.

186. Raffetto, J.D. and R.A. Khalil, *Matrix metalloproteinases and their inhibitors in vascular remodeling and vascular disease.* Biochem Pharmacol, 2008. **75**(2): p. 346-59.

187. Yan, C. and D.D. Boyd, *Regulation of matrix metalloproteinase gene expression.* J Cell Physiol, 2007. **211**(1): p. 19-26.

188. Overall, C.M. and C. Lopez-Otin, *Strategies for MMP inhibition in cancer: innovations for the post-trial era.* Nat Rev Cancer, 2002. **2**(9): p. 657-72.

189. Moon, S.K., B.Y. Cha, and C.H. Kim, *ERK1/2 mediates TNF-alpha-induced matrix metalloproteinase-9 expression in human vascular smooth muscle cells via the regulation of NF-kappaB and AP-1: Involvement of the ras dependent pathway.* J Cell Physiol, 2004. **198**(3): p. 417-27.

190. Visse, R. and H. Nagase, *Matrix metalloproteinases and tissue inhibitors of metalloproteinases: structure, function, and biochemistry.* Circ Res, 2003. **92**(8): p. 827-39.

191. Brew, K., D. Dinakarpandian, and H. Nagase, *Tissue inhibitors of metalloproteinases: evolution, structure and function.* Biochim Biophys Acta, 2000. **1477**(1-2): p. 267-83.

192. Fernandez-Catalan, C., et al., *Crystal structure of the complex formed by the membrane type 1-matrix metalloproteinase with the tissue inhibitor of metalloproteinases-2, the soluble progelatinase A receptor.* EMBO J, 1998. **17**(17): p. 5238-48.

193. Strongin, A.Y., et al., *Mechanism of cell surface activation of 72-kDa type IV collagenase. Isolation of the activated form of the membrane metalloprotease.* J Biol Chem, 1995. **270**(10): p. 5331-8.

194. Yasmin, et al., *Matrix metalloproteinase-9 (MMP-9), MMP-2, and serum elastase activity are associated with systolic hypertension and arterial stiffness.* Arterioscler Thromb Vasc Biol, 2005. **25**(2): p. 372.

195. Gkaliagkousi, E., et al., *Elevated levels of MMP-9 in untreated patients with stage I essential hypertension.* Clin Exp Hypertens, 2012. **34**(8): p. 561-6.

196. Blankenberg, S., et al., *Plasma concentrations and genetic variation of matrix metalloproteinase 9 and prognosis of patients with cardiovascular disease.* Circulation, 2003. **107**(12): p. 1579-85.

197. Watts, S.W., et al., *Morphological and biochemical characterization of remodeling in aorta and vena cava of DOCA-salt hypertensive rats.* Am J Physiol Heart Circ Physiol, 2007. **292**(5): p. H2438-48.

198. Bouvet, C., et al., *Different involvement of extracellular matrix components in small and large arteries during chronic NO synthase inhibition.* Hypertension, 2005. **45**(3): p. 432-7.

199. Castro, M.M., et al., *Imbalance between matrix metalloproteinases and tissue inhibitor of metalloproteinases in hypertensive vascular remodeling.* Matrix Biol, 2010. **29**(3): p. 194-201.

200. Flamant, M., et al., *Role of matrix metalloproteinases in early hypertensive vascular remodeling.* Hypertension, 2007. **50**(1): p. 212-8.

201. Lee, H.M., et al., *Subantimicrobial dose doxycycline efficacy as a matrix metalloproteinase inhibitor in chronic periodontitis patients is enhanced when combined with a non-steroidal anti-inflammatory drug.* J Periodontol, 2004. **75**(3): p. 453-63.

202. Golub, L.M., et al., *Tetracyclines inhibit connective tissue breakdown by multiple non-antimicrobial mechanisms.* Adv Dent Res, 1998. **12**(2): p. 12-26.

203. Jonat, C., F.Z. Chung, and V.M. Baragi, *Transcriptional downregulation of stromelysin by tetracycline.* J Cell Biochem, 1996. **60**(3): p. 341-7.

204. Castro, M.M., et al., *Metalloproteinase inhibition ameliorates hypertension and prevents vascular dysfunction and remodeling in renovascular hypertensive rats.* Atherosclerosis, 2008. **198**(2): p. 320-31.

205. Castro, M.M., J.E. Tanus-Santos, and R.F. Gerlach, *Matrix metalloproteinases: targets for doxycycline to prevent the vascular alterations of hypertension.* Pharmacol Res, 2011. **64**(6): p. 567-72.

206. Fernandez-Patron, C., M.W. Radomski, and S.T. Davidge, *Vascular matrix metalloproteinase-2 cleaves big endothelin-1 yielding a novel vasoconstrictor.* Circ Res, 1999. **85**(10): p. 906-11.

207. Fernandez-Patron, C., et al., *Vascular matrix metalloproteinase-2-dependent cleavage of calcitonin gene-related peptide promotes vasoconstriction.* Circ Res, 2000. **87**(8): p. 670-6.

208. Martinez, A., et al., *Matrix metalloproteinase-2 cleavage of adrenomedullin produces a vasoconstrictor out of a vasodilator.* Biochem J, 2004. **383**(Pt. 3): p. 413-8.

209. Castro, M.M., et al., *Doxycycline ameliorates 2K-1C hypertension-induced vascular dysfunction in rats by attenuating oxidative stress and improving nitric oxide bioavailability.* Nitric Oxide, 2012. **26**(3): p. 162-8.

210. Su, J., et al., *Mice lacking the gene encoding for MMP-9 and resistance artery reactivity.* Biochem Biophys Res Commun, 2006. **349**(4): p. 1177-81.

211. Bassiouny, H.S., et al., *Flow regulation of 72-kD collagenase IV (MMP-2) after experimental arterial injury.* Circulation, 1998. **98**(2): p. 157-63.

212. Chesler, N.C., D.N. Ku, and Z.S. Galis, *Transmural pressure induces matrix-degrading activity in porcine arteries ex vivo.* Am J Physiol, 1999. **277**(5 Pt 2): p. H2002-9.

213. Browatzki, M., et al., *Angiotensin II stimulates matrix metalloproteinase secretion in human vascular smooth muscle cells via nuclear factor-kappaB and activator protein 1 in a redox-sensitive manner.* J Vasc Res, 2005. **42**(5): p. 415-23.

214. Ruddy, J.M., et al., *Differential effects of mechanical and biological stimuli on matrix metalloproteinase promoter activation in the thoracic aorta.* Circulation, 2009. **120**(11 Suppl): p. S262-8.

215. Rajagopalan, S., et al., *Reactive oxygen species produced by macrophage-derived foam cells regulate the activity of vascular matrix metalloproteinases in vitro. Implications for atherosclerotic plaque stability.* J Clin Invest, 1996. **98**(11): p. 2572-9.

216. Grote, K., et al., *Mechanical stretch enhances mRNA expression and proenzyme release of matrix metalloproteinase-2 (MMP-2) via NAD(P)H oxidase-derived reactive oxygen species.* Circ Res, 2003. **92**(11): p. e80-6.

217. Rude, M.K., et al., *Aldosterone stimulates matrix metalloproteinases and reactive oxygen species in adult rat ventricular cardiomyocytes.* Hypertension, 2005. **46**(3): p. 555-61.

218. Sakurada, M., et al., *Vasculoprotective effect of cilostazol in aldosterone-induced hypertensive rats.* Hypertens Res, 2009.

219. Siwik, D.A., D.L. Chang, and W.S. Colucci, *Interleukin-1beta and tumor necrosis factor-alpha decrease collagen synthesis and increase matrix metalloproteinase activity in cardiac fibroblasts in vitro.* Circ Res, 2000. **86**(12): p. 1259-65.

220. Han, Y.P., et al., *TNF-alpha stimulates activation of pro-MMP2 in human skin through NF-(kappa)B mediated induction of MT1-MMP.* J Cell Sci, 2001. **114**(Pt 1): p. 131-139.

221. Shah, P.K., et al., *Human monocyte-derived macrophages induce collagen breakdown in fibrous caps of atherosclerotic plaques. Potential role of matrix-degrading metalloproteinases and implications for plaque rupture.* Circulation, 1995. **92**(6): p. 1565-9.

222. Galis, Z.S. and J.J. Khatri, *Matrix metalloproteinases in vascular remodeling and atherogenesis: the good, the bad, and the ugly.* Circ Res, 2002. **90**(3): p. 251-62.

CHAPTER 2

Improvement in Middle Cerebral Artery Structure and Endothelial Function in Stroke-Prone Spontaneously Hypertensive Rats after Macrophage Depletion

2.1 - Abstract

Inflammation is involved in the pathogenesis of hypertension. Hypertensive animals have an increased number of perivascular macrophages in cerebral arteries. Macrophages might be involved in remodeling of the cerebral vasculature. We hypothesized that peripheral macrophage depletion would improve middle cerebral artery (MCA) structure and function in hypertensive rats. For macrophage depletion, six-week-old stroke-prone spontaneously hypertensive rats (SHRSP) were treated with liposome-encapsulated clodronate (CLOD, 10ml/kg/every 3 or 4 days, I.P.), or vehicle (PBS lipo). MCA structure and function were analyzed by pressure and wire myography. *Results:* blood pressure was not affected by CLOD. The number of perivascular CD163 positive cells per microscopic field was reduced in the brain of SHRSP+CLOD. CLOD treatment caused an improvement in endothelium-dependent dilation after intralumenal perfusion of ADP and incubation with acetylcholine (Ach). Inhibition of nitric oxide production blunted the Ach response, and endothelium-independent dilation was not altered. At an intralumenal pressure of 80 mmHg, MCA from SHRSP+CLOD showed increased lumen diameter, decreased wall thickness and wall-to-lumen ratio. Cross-sectional area of pial arterioles from SHRSP+CLOD was higher than PBS lipo. These results suggest that macrophage depletion attenuates MCA remodeling and improves MCA endothelial function in SHRSP.

2.2 - Introduction

Hypertension leads to structural changes in the resistance vasculature through the process of vascular remodeling. Remodeling encompasses changes in the vessel wall that reduce the lumen diameter and increase the wall thickness and wall-to-lumen ratio [1] of hypertensive vessels when compared to vessels of normotensive subjects [2, 3]. These changes might impact regional blood flow regulation and lead to increased risk of end-organ damage [4]. In the cerebral circulation, the MCA is an important component of blood flow regulation [5] because cerebral vascular resistance is carried equally between large arteries, like the MCA, and arterioles [6]. Remodeling impairs the MCA's ability to control blood flow by auto-regulation, leading to distal capillary destabilization and organ damage [7]. In addition, it impairs vasodilation [8], which can reduce collateral blood flow following obstruction of an artery. Thus remodeling of the cerebral vasculature might increase the risk of stroke, and the damage caused by cerebral ischemia [8]. Although increased wall stress during hypertension is important to trigger remodeling, studies show that vascular remodeling can be prevented or reversed without reducing blood pressure [9-12], suggesting that perivascular mechanisms might be important modulators of this process. However, the mechanisms underlying hypertensive MCA remodeling are not completely understood.

Essential hypertension is linked with systemic inflammation in humans [13] and rats [14]. Macrophage infiltration is increased in the aorta, mesenteric and intramyocardial arteries [15] and cerebral microvessels [16] of SHRSP when compared to normotensive WKY rats. In the periphery, mice deficient in m-CSF show reduced remodeling of

mesenteric arteries [17, 18]. However, in these studies vascular inflammation was considered a consequence of prolonged exposure to vasoactive agents and not a causative agent of vascular remodeling. Once in the vessel wall, macrophages can release molecules capable of altering the structure and function of blood vessels, thus potentially playing an active role in remodeling of the cerebral vasculature. Therefore, we hypothesized that perivascular macrophages contribute to remodeling of the cerebral and peripheral vasculature in SHRSP. We tested this hypothesis by removing circulating macrophages using CLOD. The MCA was used to study the cerebral vasculature, and third-order branches of the mesenteric arterial arcade, MRA, were used to study the peripheral vasculature.

2.3 - Methods

2.3.1 - Animals and treatments. Six week-old male SHRSP from the colony housed at Michigan State University were randomized into two groups. To remove peripheral macrophages, rats were treated with CLOD. Clodronate was a gift of Roche Diagnostics GmbH and was incorporated into liposomes as described elsewhere [19]. Rats were injected with CLOD (10ml/kg) every 3 or 4 days for 6 weeks, the first dose was administered *via* tail vein; i.p. injections were used thereafter. This treatment regimen causes a prolonged peripheral macrophage depletion [20]. Control rats received PBS lipo (placebo). Rats were treated with CLOD from week 6 to week 12 of age because this is the period during which the blood pressure in SHRSP increases exponentially [21]. We have previously shown that treatments during this period are efficacious in attenuating vascular remodeling [10, 12, 22]. Rats used for the collection of perivascular

adipose tissue (PVAT) from mesenteric arteries were treated as described above with the exception that the treatment was only maintained for two weeks. Rats were maintained on a 12:12hr light: dark cycle, with tap water and regular chow *ad libitum*. At 12 weeks of age, rats were anesthetized with 3% isoflurane and euthanized by decapitation after collection of arterial blood from the abdominal aorta. The experimental protocol was approved by the Institutional Animal Care & Use Committee and was in accordance with the American Physiological Society's "Guiding Principles in the Care and Use of Animals."

2.3.2 - Measurement of blood pressure. Blood pressure was measured by tail-cuff using a RTBP1001 tail-cuff blood pressure system (Kent Scientific, Torrington CT) as described previously [22].

2.3.3 - Flow cytometry. Quantification of circulating and peritoneal phagocytic cells in PBS lipo and CLOD-treated SHRSP was performed using FCM. Blood was collected from the abdominal aorta in heparinized tubes, and the total number of blood leukocytes was quantified using a Z1 Coulter Particle Counter (Beckman Coulter, Fullerton, CA). Aliquots containing $1x10^6$ cells were incubated for 5 min with ACK buffer (in grams/liter: NH_4Cl 8.024, $KHCO_3$ 1.001, EDTA 0.0037) at room temperature for red blood cells lysis. Cells were then washed with FCM buffer (Hank's Balanced Salt Solution with 1% Bovine serum albumin (BSA) and 0.1% sodium azide) three times and incubated with Fc block (BD Biosciences, San Jose, CA) for 20 min on ice. Cells were then incubated with FITC-conjugated anti-CD11b and phycoerythrin-conjugated anti-CD163 (ABD

Serotec, Oxford, UK) for 20 min on ice. Non-specific staining was assessed by first blocking Fc receptors in all cells with an anti-Fc receptor antibody on unstained cells. Cells were washed in FCM buffer twice and fixed with BD Cytofix (BD Biosciences, San Diego, CA), washed twice with FCM buffer and 50,000 events were collected using the BD FACSCanto II coupled to the FACSDiva software (BD Biosciences) and analyzed using FlowJo 8.8.6 (Treestar Software, Ashland, OR). Gating was set using the Fc-blocked non-stained cells. Cells obtained by peritoneal lavage were processed using the same protocol described above.

2.3.4 - Immunofluorescence. Cryosections of the brain (10μm thick) from perfusion-fixed rats were used for IF identification of CD163 (a macrophage marker) and α-SMA. Rats were anesthetized with sodium pentobarbital, the thoracic cavity was exposed and 0.9% NaCl solution (saline) with heparin (1000UI/mL) and papaverin (10 μmol/L) was injected into the left ventricle of the heart to wash the blood and dilate the vasculature. A puncture in the right atria allowed the blood+saline to be washed out. The perfusion pressure was maintained at 80mmHg and 250ml of saline flushed the rat. After, 250 ml of 4% paraformaldehyde was perfused. The brain was then removed and placed in 4% paraformaldehyde for 48 hours, washed in PBS and placed in 20% sucrose-PBS for cryosectioning. Sections were incubated overnight with primary antibodies against CD163 (ABD Serotec, Oxford, UK) and α-SMA (Abcam, Cambridge, MA) and then incubated with fluorescent-tagged secondary antibodies. Sections were then mounted in ProLong Gold antifade reagent with DAPI (Invitrogen, Carlsbad, CA). Images were acquired using an Axioskop 40 (Carl Zeiss Inc., Mexico) coupled to a camera (AxioCam

MRc5, Carl Zeiss Inc.) and the number of perivascular CD163 positive cells in 6 microscopic fields was counted using the AxioVision Rel. 4.6 software. Sections without the primary antibody were negative controls. An investigator blinded to the experimental groups performed the cell counting. Data are expressed as number of perivascular CD163 positive cells per microscopic field.

2.3.5 - Morphometry of pial arterioles. Histological sections of the brain (10μm thick) from perfusion-fixed rats were stained with hematoxilin-eosin for morphometrical analysis of pial arterioles. Images were acquired as described above. Cross-sectional area of pial arterioles was measured using a calibrated AxioVision Rel. 4.6 software by an investigator blinded to the experimental groups. Only the intima and medial layers of arterioles were included in the cross-sectional area measurement. A total of 5 arterioles per animal were measured, and the data was averaged per animal. Data are expressed as mean cross-sectional area.

2.3.6 - Quantitative real-time polymerase chain reaction. mRNA was extracted from cerebral cortex and PVAT using an RNeasy® Lipid Tissue kit (QIAGEN), from CBV using TRIZOL reagent. mRNA was reverse-transcribed (Superscript® VILO, Invitrogen, Carlsbad, CA) and qRT-PCR was performed using Taqman® probes in a 7500 Real Time PCR System (Applied Biosystem). Fold changes from control were calculated using the $2^{-\Delta\Delta CT}$ method [23]. CBV mRNA was normalized to 2-β microglobulin mRNA expression; RP132 was used for cerebral cortex and PVAT mRNA.

2.3.7 - Pressure myography. MCA structure was assessed by pressure myography (Danish Myo Technology, Aarhus, Denmark) as described previously [10]. MCA contractility to 5-HT (0.001 to 10 μmol/L) and endothelium-dependent dilation to intraluminal perfusion of ADP (0.001 to 10 μmol/L) were assessed. MCA's equilibrated in oxygenated physiological salt solution (PSS, in mmol/L: 141.9 NaCl, 4.7 KCl, 1.12 KH_2PO_4, 1.7 $MgSO_4 \cdot 7H_2O$, 2.8 $CaCl_2$, 10 Hepes, 5 Dextrose, 0.5 EDTA, pH 7.4) until development of spontaneous myogenic tone, which was calculated using the following formula: %tone = [1-(active lumen diameter/passive lumen diameter)] x 100. MCA's passive structure was assessed with calcium-free PSS containing 2mmol/L EGTA plus 10 μmol/L of SNP and intralumenal pressure was increased from 3 to 180mmHg in 20mmHg increments. The wall-to-lumen ratio, circumferential wall stress and wall strain were calculated [24]. Passive distensibility was calculated as described previously [25]. The elastic modulus (β-coefficient) was calculated from the stress/strain curves using an exponential model ($y=ae^{\beta x}$) where β is the slope of the curve: the higher the β-coefficient the stiffer the vessel.

2.3.8 - Wire Myography. MCA endothelial function was further assessed using a wire myograph (Danish Myo Technology, Aarhus, Denmark). MCAs were isolated and cleaned, and 2mm rings were mounted into the wire myograph using 40μm-thick stainless steel wires. MCAs were allowed to equilibrate for 30 min in oxygenated PSS at 37°C without tension, which was then increased to 2mN in 0.5mN increments with a 10 minutes equilibration period. After stabilization at 2mN, rings viability was assessed by

exposing them to 1 μmol/L 5-HT, and endothelium integrity was assessed by 1 μmol/L Ach. Rings were washed and pre-constricted with 1 μmol/L 5-HT to build concentration-response curves for Ach (0.0001 to 30 μmol/L) ± the eNOS inhibitor L-NAME, 10 μmol/L, and the NO donor SNP (0.0001 to 30 μmol/L). Rings were washed and constricted with 100 mmol/L KCl to analyze agonist-independent constriction. Data are expressed as percent of KCl constriction.

2.3.9 - Mesenteric resistance artery structure. Third-order branches from the mesenteric vascular bed were isolated and stored on ice-cold PSS for mounting in the pressure myograph after completion of the MCA experiment. Passive structure was assessed as described above with the exception that the intralumenal pressure was increased in 30mmHg increments.

2.3.10 - Statistical analyses. Data are shown as mean ± SEM. Blood pressure, body and organ weights, IF, morphometry, FCM, qRT-PCR and spontaneous tone generation data were analyzed by Student's t-Test. MCA structure, contractility and endothelium-dependent dilation were analyzed by Two-Way ANOVA, with a Bonferroni post-test. A p value of 0.05 or lower was considered significant. Concentration-response curves to 5-HT, ADP, Ach ± L-NAME and SNP were further analyzed by non-linear regression (curve-fit) to calculate logEC50 and changes in pharmacological parameters using the Prism Software (GraphPad, version 5.0a).

2.4 - Results

2.4.1 - Physiological parameters and blood pressure. Data regarding physiological parameters and blood pressure are summarized in Table 2.1. There was no difference in body weights, heart/body weight ratio and kidney/body weight ratio between PBS lipo and CLOD. CLOD treatment caused the expected reduction in spleen/body weight ratio. Systolic and diastolic arterial pressures were not affected by CLOD treatment.

Table 2.1: Physiological variables after CLOD treatment in SHRSP.

	SHRSP+PBS lipo (n=8)	SHRSP+CLOD (n=8)
Final body weight (g)	253 ± 4	247 ± 4
Heart: body weight	0.49 ± 0.02	0.47 ± 0.02
Kidneys: body weight	1.01 ± 0.01	1.03 ± 0.02
Spleen: body weight	0.22 ± 0.01	0.14 ± 0.01*
Systolic blood pressure (mmHg)	202 ± 7	200 ± 5
Diastolic blood pressure (mmHg)	157 ± 7	152 ± 5

Blood pressure measured during the last week of treatment by tail-cuff. Body weight was assessed prior to euthanasia. ****Statistically different from SHRSP+PBS lipo, $p<0.05$, Student's t-test. n.a.: non-applicable.*

2.4.2 - CLOD-treated SHRSP had less circulating and peritoneal macrophages. Peripheral macrophage depletion was assessed by FCM. The number of circulating

macrophages double-positive for CD11b and CD163 was reduced in CLOD-treated rats (0.28±0.03 vs 1.19±0.34% total cells, CLOD (n=3) vs SHRSP (n=4), p=0.04). Similarly, the number of macrophages in the peritoneal lavage was reduced in SHRSP+CLOD (Figure 2.1).

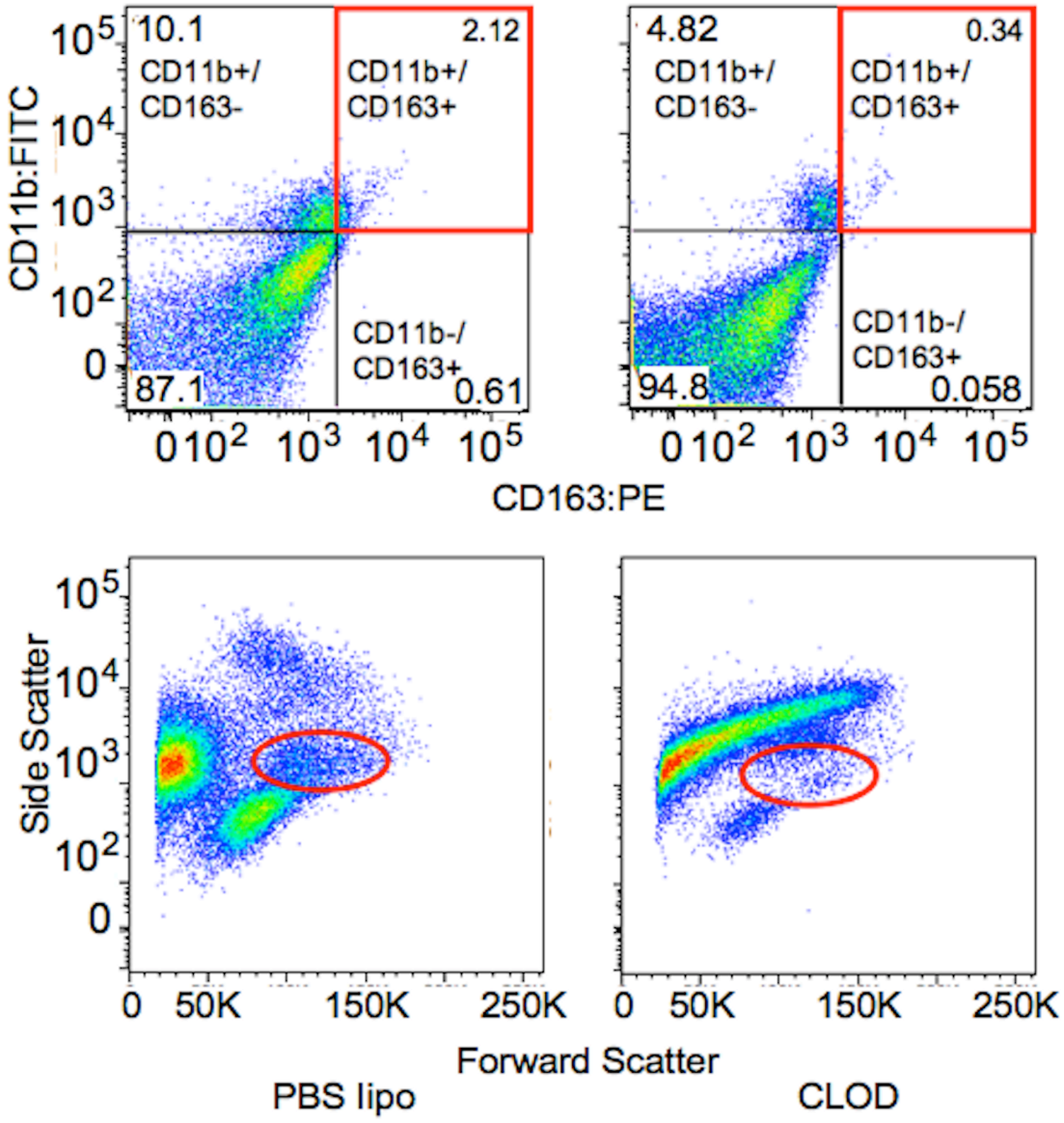

Figure 2.1: Representative FCM analysis for quantification of macrophages in SHRSP treated with PBS lipo or CLOD. Upper panels represent circulating

macrophages in the blood that are double-positive for CD11b and CD163. Note that number of events is higher in in SHRSP treated with CLOD (upper left panel) than SHRSP treated with PBS lipo (upper right panel). The number of macrophages in the peritoneal cavity was quantified by side-scatter and forward-scatter (lower panels). The number of events was smaller in SHRSP+CLOD (lower right panel) than in PBS lipo-treated SHRSP (lower left panel).

2.4.3 - CLOD treatment reduced the number of perivascular CD163 positive cells in the cerebral cortex. To validate that depletion of circulating phagocytes would result in reduction of perivascular phagocytes in the brain, the number of perivascular CD163 positive cells in the cerebral cortex of SHRSP was assessed by IF. CLOD treatment reduced the number of perivascular CD163 positive cells per microscopic field in the cerebral cortex of SHRSP, when compared to SHRSP treated with PBS lipo (Figure 2.2).

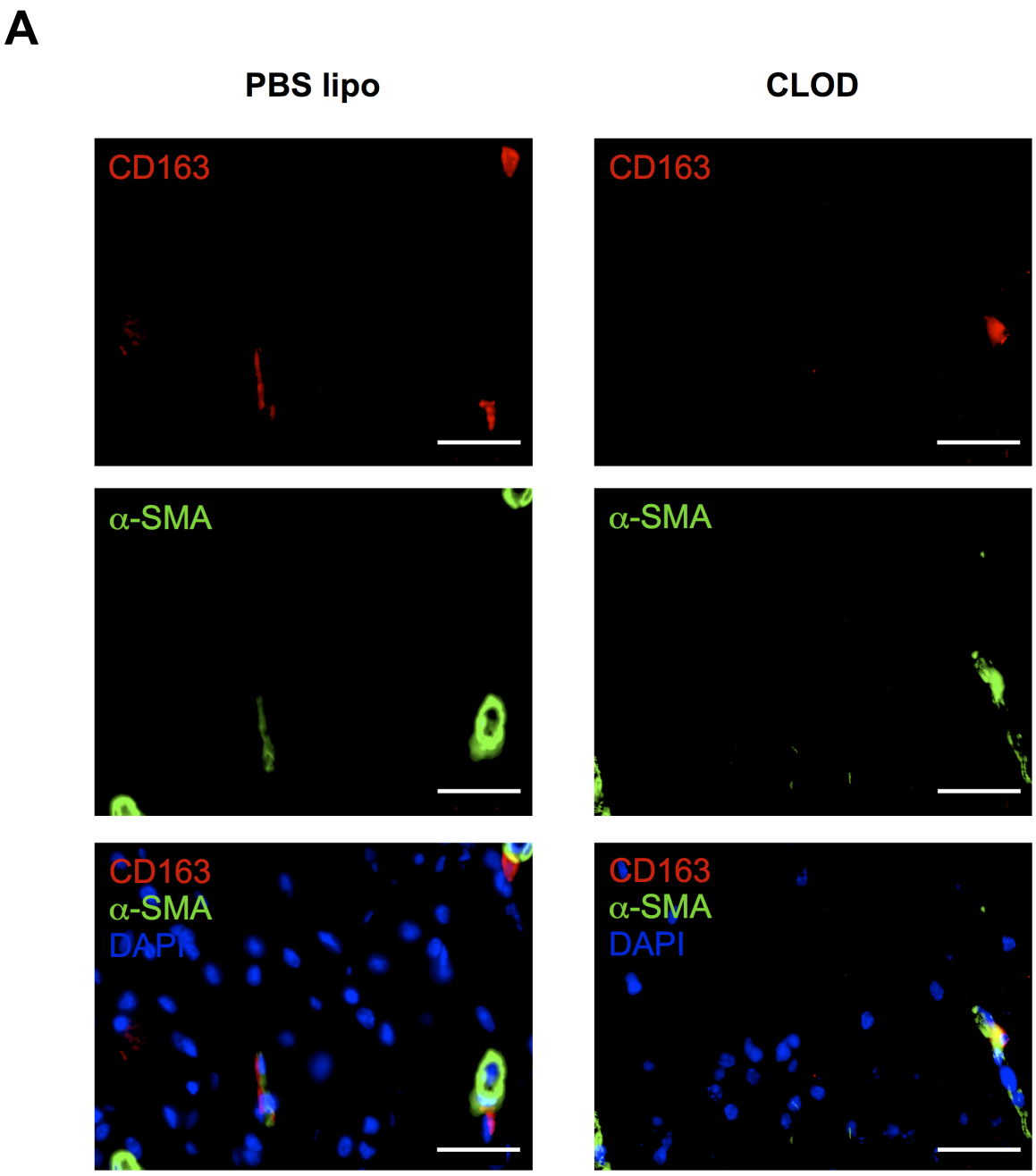

Figure 2.2: CLOD treatment reduced the number of perivascular macrophages in cerebral arteries of SHRSP.

Figure 2.2 (cont'd)

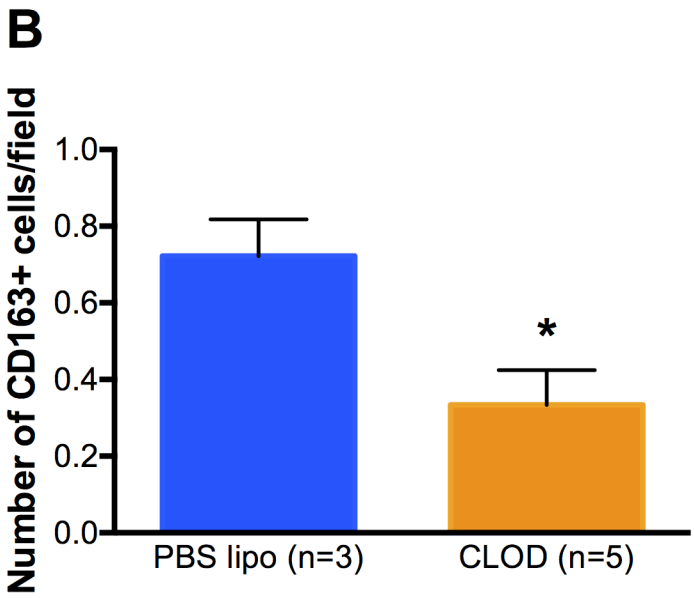

Macrophages were identified as cells with immunoreactivity to CD163 (red), and only CD163+ cells surrounding blood vessels (identified by immunoreactivity for α-SMA, green) were counted. Nuclei were identified by DAPI-staining (blue). Upper panels are representative images from SHRSP treated with PBS lipo, and lower panels are images from CLOD-treated SHRSP. *p<0.05, *Student's* t-test.

2.4.4 - Cross-sectional area of pial arterioles was increased in CLOD-treated SHRSP. Morphometric analysis of pial arterioles showed that CLOD treatment increased their cross-sectional area when compared to SHRSP treated with PBS lipo (Figure 2.3A, p=0.05). A small, although not significant, increase in lumen (Figure 2.3B, p=0.14) and wall cross-sectional were also observed (Figure 2.3C, p=0.12).

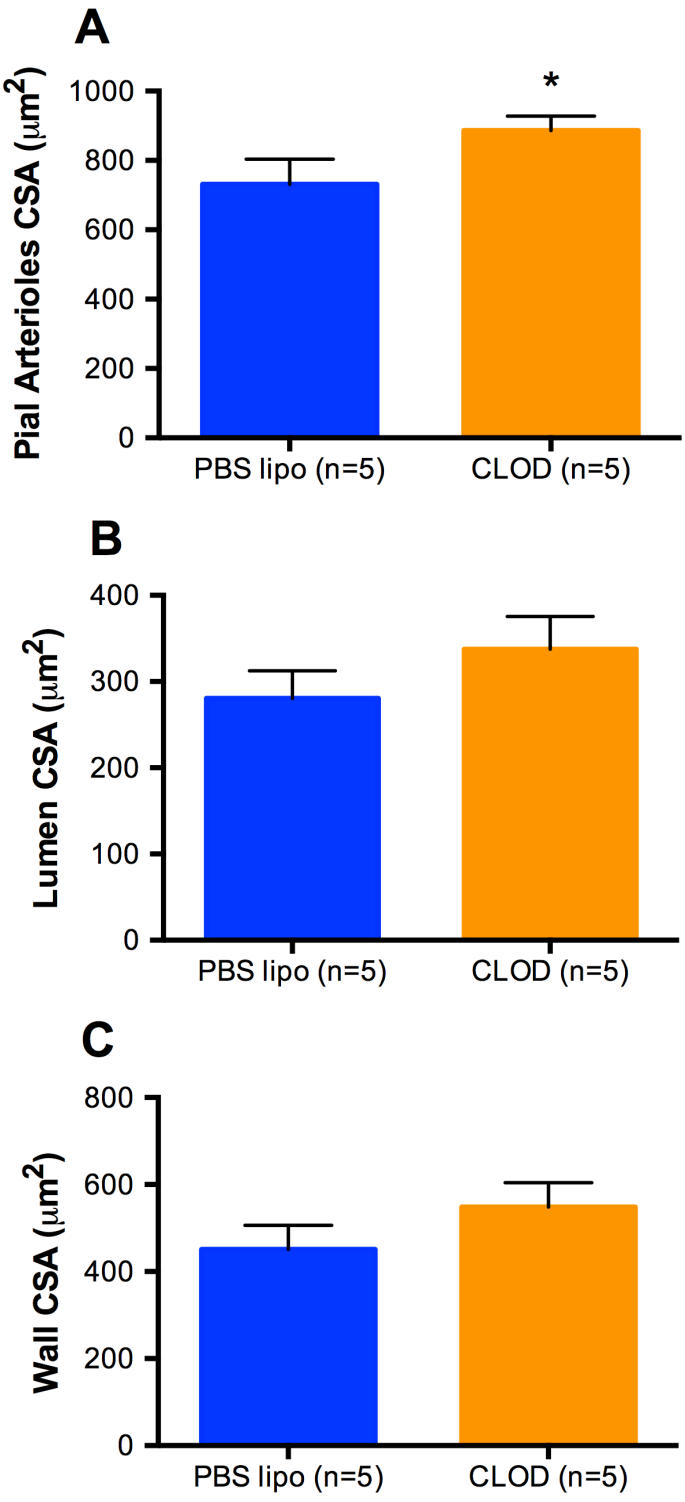

Figure 2.3: Morphometric analyses of pial arterioles.

Figure 2.3 (cont'd)

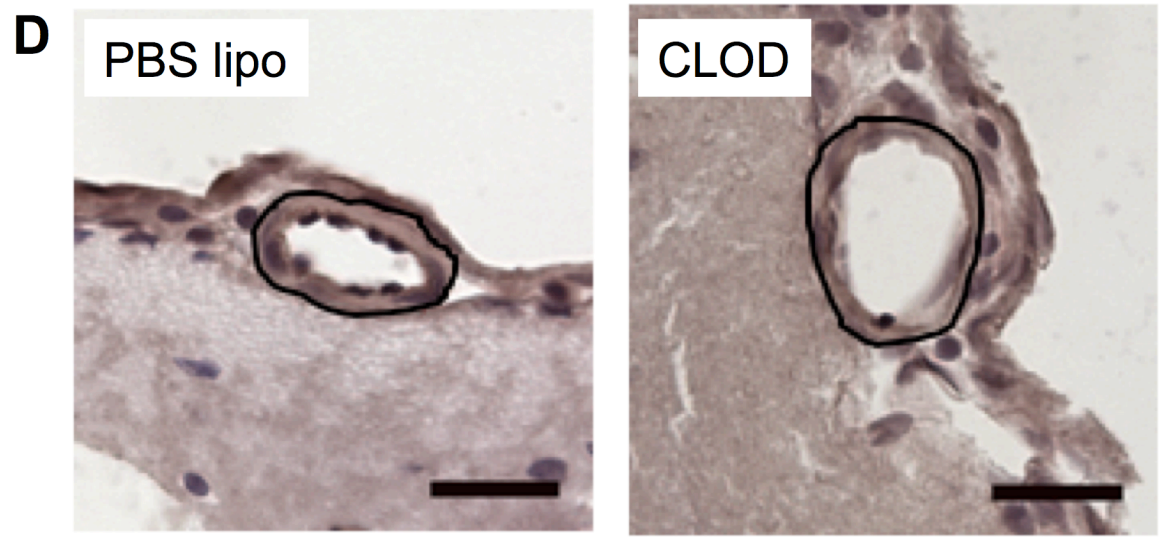

CLOD treatment caused a significant increase in the cross-sectional area (CSA) of pial arterioles in SHRSP, when compared to SHRSP treated with PBS lipo. There was a small, although not-significant, increase in the lumen (B, p=0.14) and wall (C, p=0.12) CSA after 6 weeks of CLOD treatment. D) Representative images of pial arterioles from PBS lipo (left) and CLOD (right)-treated SHRSP. The circled area represents the cross-sectional area of the arteriole. Bar =25μm. Morphometric measurements were performed in 10μm-thick slices of the brain from perfusion-fixed rats. Images were acquired using a 40x objective and CSA measurements performed using the Axioskope Rel. 4.6 software (Carl Zeiss) by an investigator blinded to the experimental groups. Data are means±SEM. *p=0.05, *Student's* t-test.

2.4.5 - CLOD treatment reduced CD68 and TNF-α mRNA expression in the cerebral cortex and CBV. qRT-PCR was used to assess if CLOD treatment reduced the mRNA expression of inflammatory markers and MMP-2. qRT-PCR data are

summarized in Table 2.2. Briefly, CLOD treatment reduced CD68 mRNA expression in the cerebral cortex, but not in CBV. In addition, TNF-α mRNA expression was reduced in the cerebral cortex and CBV.

Table 2.2: Expression of mRNA for markers of inflammation and MMPs in the CBV and cerebral cortex of SHRSP treated with CLOD or PBS lipo.

	PBS lipo (n=8)	CLOD (n=8)
CBV		
CD68	1.004 ± 0.028	1.057 ± 0.095
TNF-α	1.025 ± 0.084	0.818 ± 0.045*
ICAM-1	1.007 ± 0.033	1.029 ± 0.052
MMP-2	1.032 ± 0.090	1.221 ± 0.110$^{\gamma}$
Cerebral cortex		
CD68	1.058 ± 0.120	0.775 ± 0.104*
TNF-α	1.039 ± 0.101	0.760 ± 0.072*

*Fold changes from PBS lipo were calculated using the $2^{-\Delta\Delta CT}$ method [23]. CBV mRNA was normalized to 2-β microglobulin mRNA expression; RP132 was used for cerebral cortex. *Statistically different from SHRSP+PBS lipo, $p<0.05$, Student's t-test. $^{\gamma}p=0.10$, Student's t-test. CBV = cerebral blood vessels.*

2.4.6 - CLOD did not alter MCA's contractility, myogenic tone and myogenic reactivity. Peripheral phagocyte depletion did not change the MCA's spontaneous myogenic tone (Table 2.3) and the response to the contractile agent 5-HT (Figure 2.4).

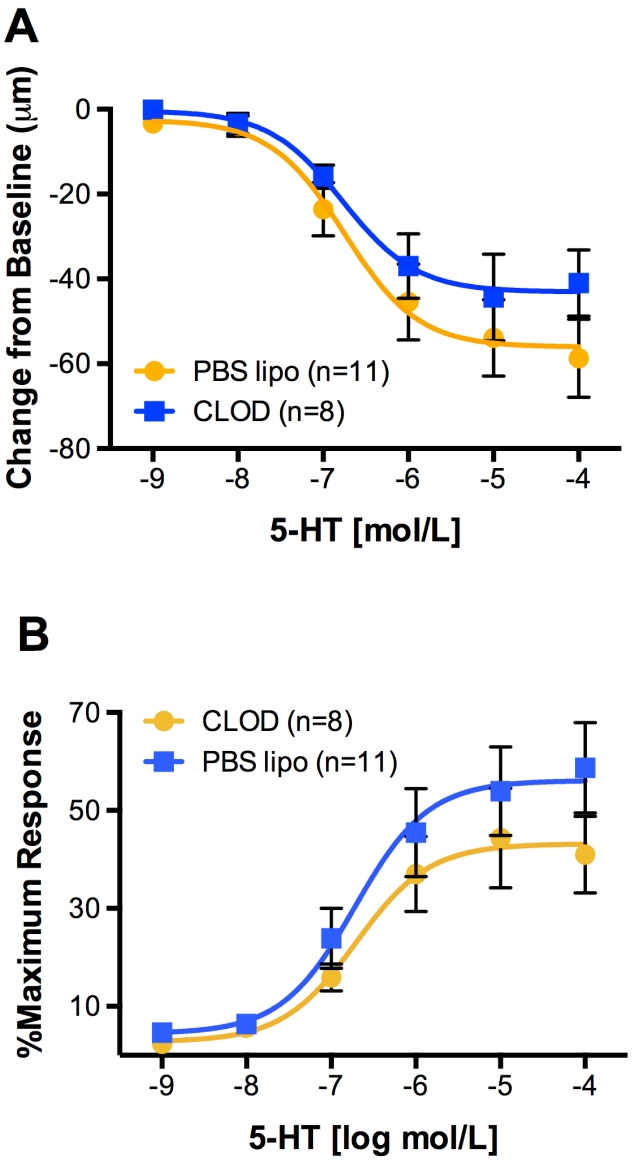

Figure 2.4: CLOD treatment did not alter MCA reactivity to the constricting agent 5-HT. The ability of the MCA to respond to agonist-induced constriction was assessed by adding increasing concentrations of 5-HT in the tissue bath. CLOD treatment did not change the concentration-response curve to 5-HT, as seen by percent of maximum

response (A), or the change in lumen diameter from baseline (B). The MCA was maintained at an intraluminal pressure of 80mmHg and was allowed to equilibrate for 10 min before a measurement was taken. Data are means±SEM.

2.4.7 - CLOD treatment improved MCA's endothelium-dependent dilation. Peripheral phagocyte depletion improved endothelium-dependent dilation of the MCA to intraluminal perfusion of ADP (Figure 2.5). CLOD treatment caused an up and leftward shift in the concentration-response curve of ADP and increased the maximal dilation of the MCA to this agent. However, the logEC50 was not changed by the treatment (-7.02±0.29 vs. -6.54±0.27 mol/L, PBS lipo vs. CLOD). The improvement in endothelium function was further confirmed by incubating MCA rings with Ach in the wire myograph, with or without L-NAME. MCA rings from CLOD-treated SHRSP showed an improvement in Ach-mediated dilation that disappeared after incubation with L-NAME (Figure 2.6A). Endothelium-independent dilation to SNP was not different between treatments (Figure 2.6B). This improvement in Ach dilation was not a consequence of reduced contractility to 5-HT (% KCl constriction: 114±4 vs 111±4, PBS lipo vs CLOD). Despite the improvement in maximum dilation to Ach, its logEC50 was not altered (-9.61±0.18 vs -9.47±0.16 mol/L, PBS lipo vs CLOD).

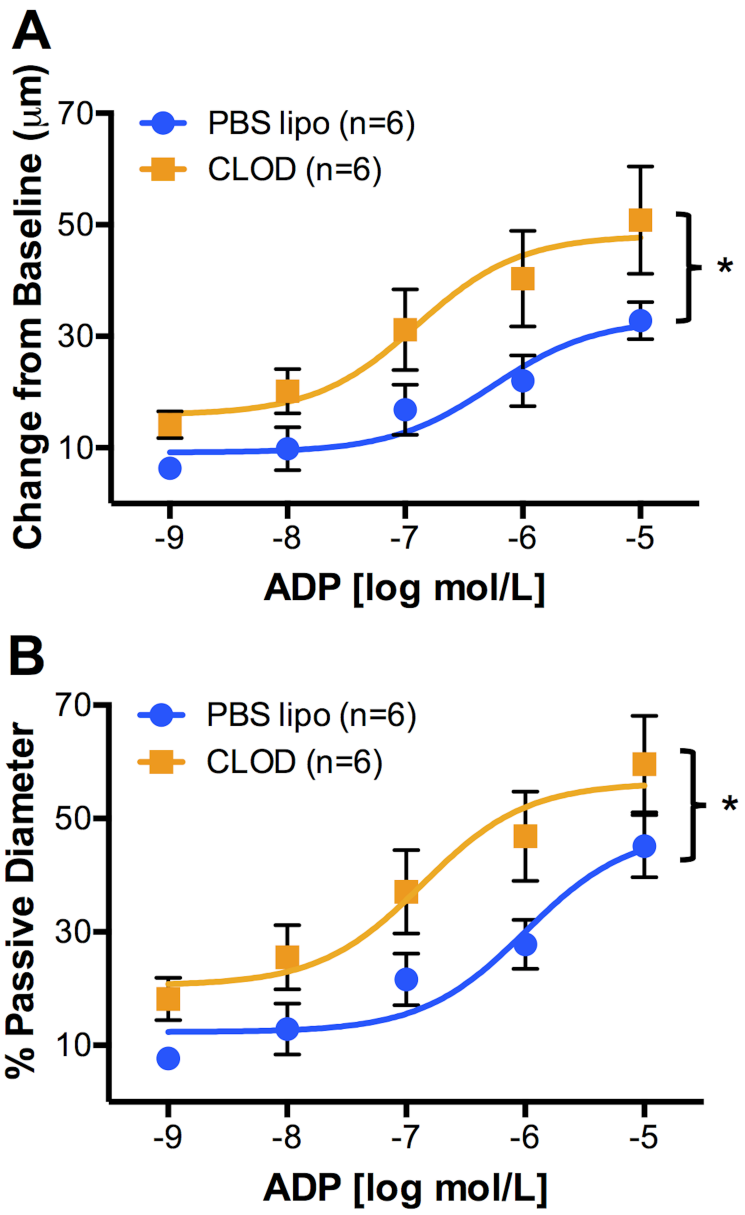

Figure 2.5: CLOD treatment improved endothelium-dependent dilation of the MCA to ADP. CLOD treatment increased both the raw dilation of the MCA, observed as a change in diameter from baseline (A), and the percent of passive diameter (B). *p<0.01, Two-Way ANOVA. Values are means±SEM. The MCA was mounted in a pressure myograph and kept in oxygenated warm PSS under 80mmHg of intraluminal pressure and physiological flow. ADP was added to the intraluminal perfusate.

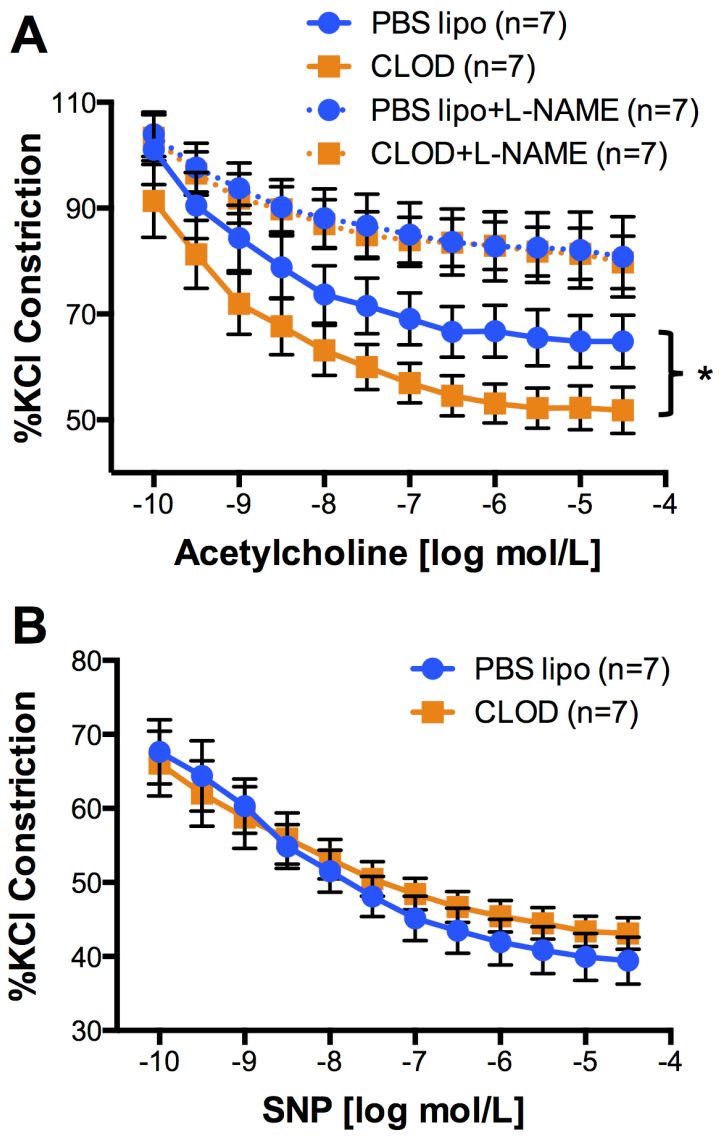

Figure 2.6: CLOD treatment improved MCA dilation to acetylcholine (Ach). MCA rings (2mm) were mounted on a wire myograph and pre-constricted with 1μmol/L 5-hydroxytriptamine. Concentration-response curves to Ach in absence or presence of the eNOS inhibitor L-NAME were constructed. MCA relaxation to Ach was improved in SHRSP after CLOD treatment, and this effect was blunted by pre-incubation of MCA rings with L-NAME (10μmol/L, A). MCA response to the endothelium-independent vasodilator SNP was not different between groups (B). *p<0.05, PBS lipo vs CLOD,

Two-Way ANOVA. Values are means±SEM.

2.4.8 - CLOD treatment improved MCA passive structure. Peripheral macrophage depletion caused an 11% increase in the MCA lumen diameter (Figure 2.7A). The lumen cross-sectional area (CSA) was increased (Table 2.3), without changing the outer diameter (Figure 2.7B) and vessel CSA. Wall thickness (Fig 2.7C), wall CSA (Table 2.3) and the wall-to-lumen ratio (Figure 2.7D) were decreased after CLOD treatment. Vessel stress was increased, without changing strain, stiffness and distensibility. No differences were found in the β-coefficient (Table 2.3). Importantly, PBS lipo had no effect on MCA structure in SHRSP when compared to untreated SHRSP (data not shown).

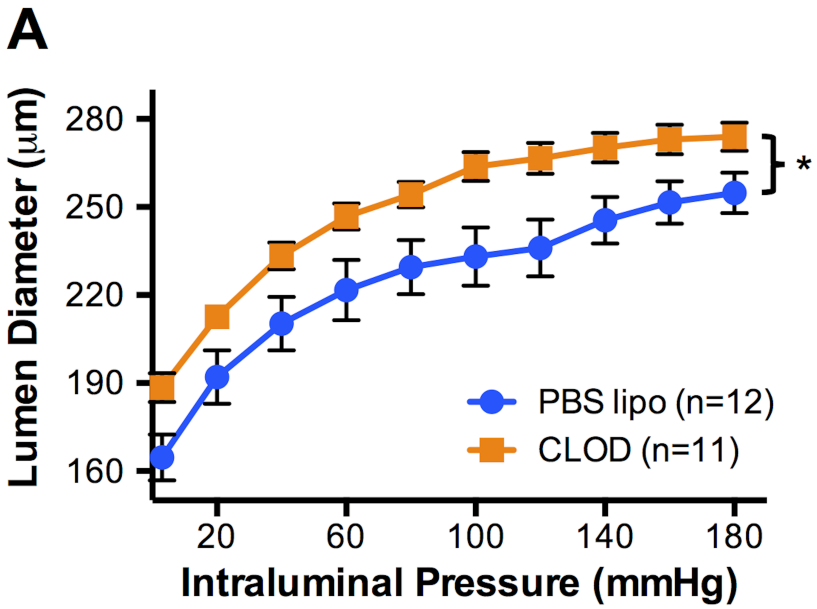

Figure 2.7: Peripheral phagocyte depletion improved MCA passive structure in SHRSP.

Figure 2.7 (cont'd)

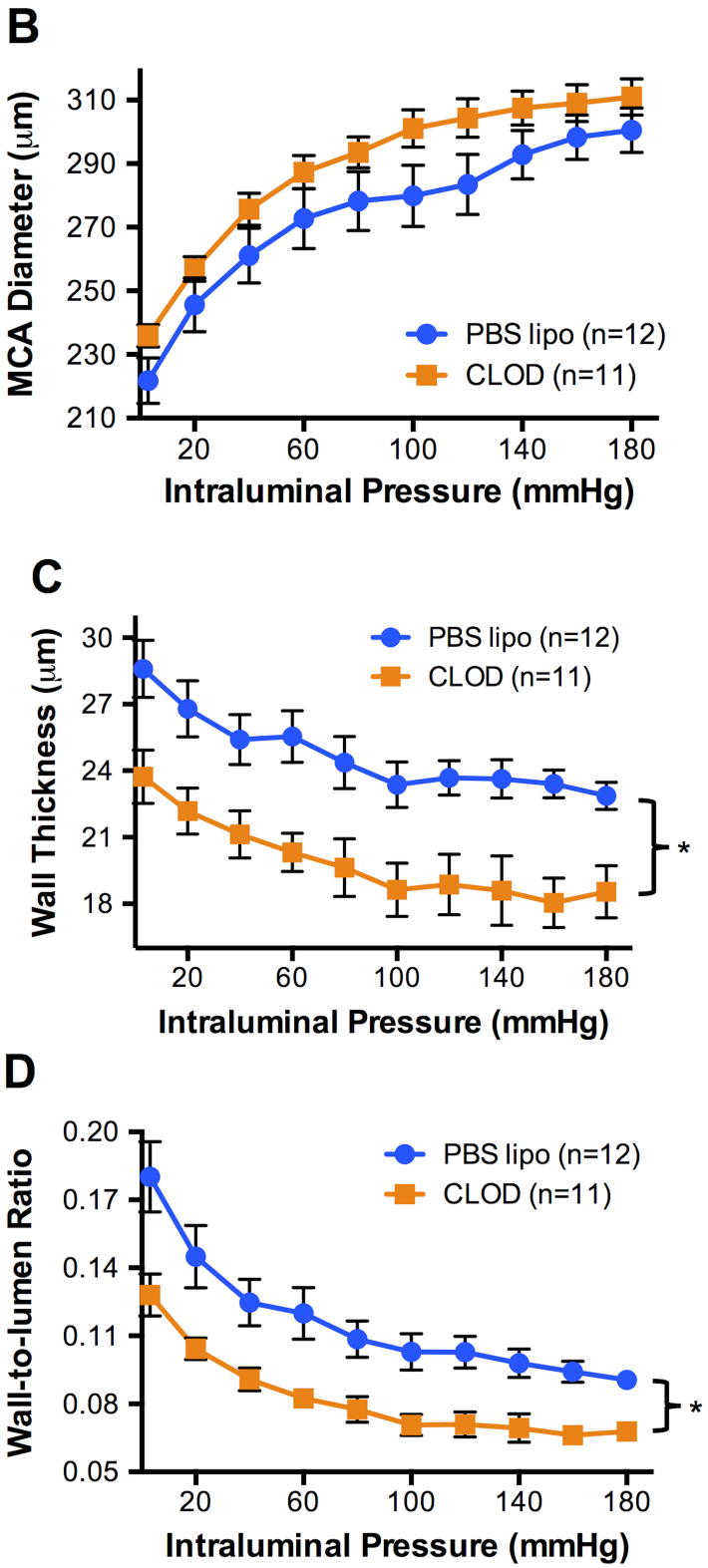

CLOD treatment increased the lumen diameter (A), decreased the wall thickness (C)

and wall-to-lumen ratio (D), without changing outer diameter (B). *p<0.05, PBS lipo vs. CLOD, Two-Way ANOVA. Values are means±SEM. The MCA was mounted in a pressure myograph and kept in oxygenated warm calcium-free PSS supplemented with 2mM EGTA and 10μM under no-flow conditions.

2.4.9 - CLOD treatment did not alter MRA structure. Peripheral phagocyte depletion did not prevent MRA remodeling in SHRSP (Figures 2.8A-D and Table 2.3).

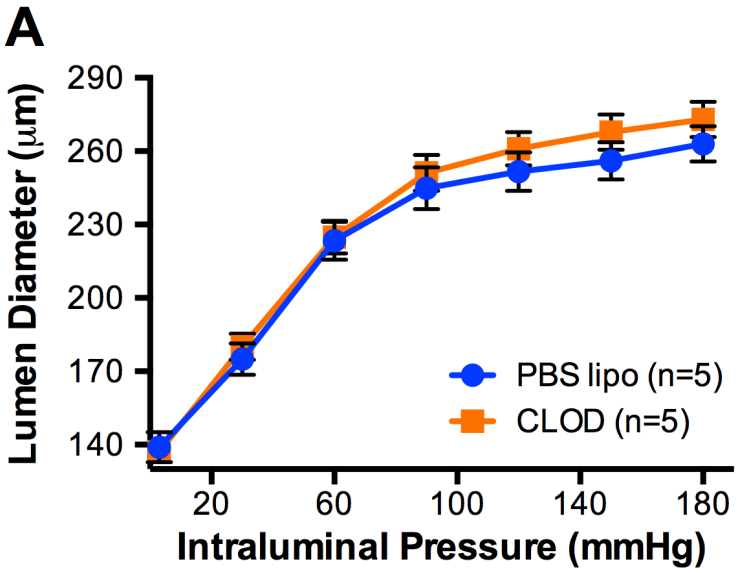

Figure 2.8: Peripheral phagocyte depletion did not improve MRA passive structure in SHRSP.

Figure 2.8 (cont'd)

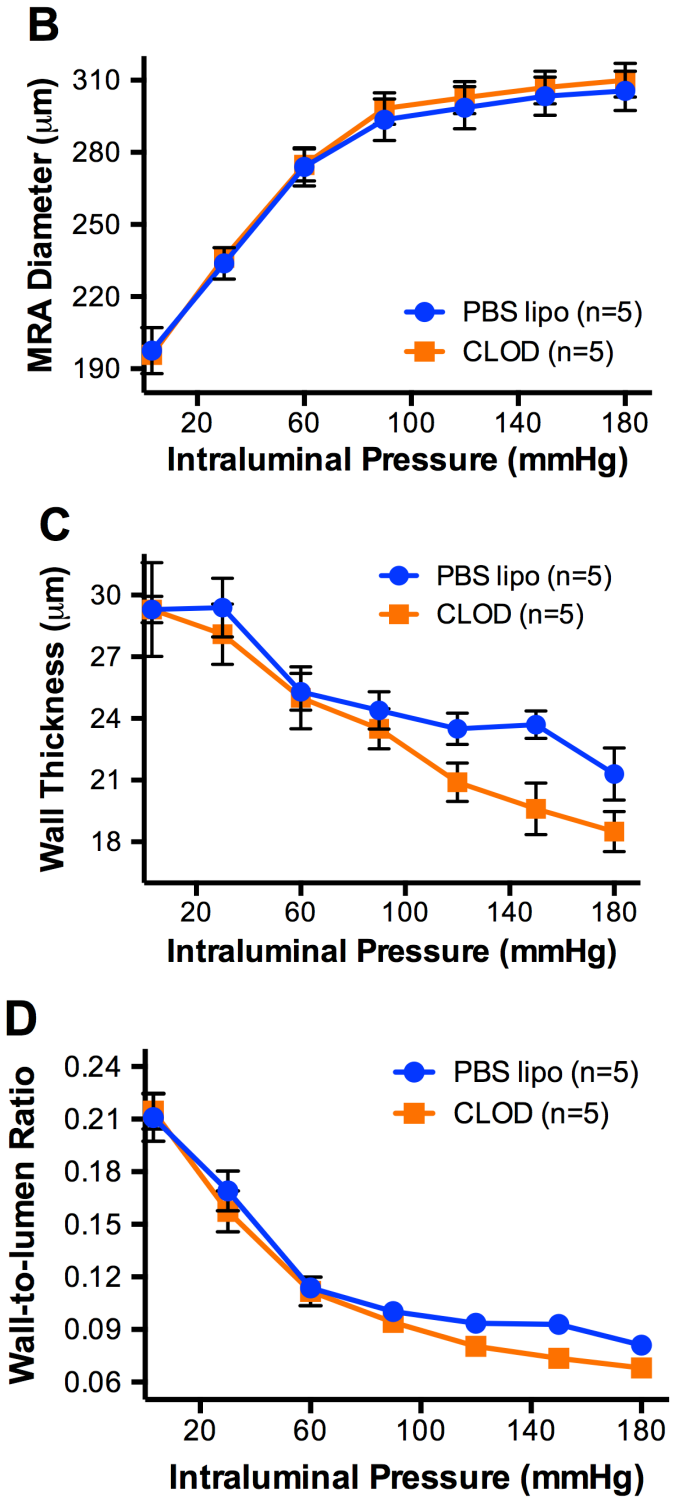

CLOD treatment did not change lumen (A) and outer (B) diameters. There was a small,

but insignificant, reduction in the wall thickness (C) and wall-to-lumen ratio (D) at higher intraluminal pressures. Values are means±SEM. The MRA was mounted in a pressure myograph and kept in oxygenated warm calcium-free PSS supplemented with 2mM EGTA and 10μM of sodium nitroprusside and under no-flow conditions.

Table 2.3: Passive structure of MCA and MRA and MCA spontaneous myogenic tone after 6 weeks of CLOD treatment.

	MCA†			MRA‡		
	PBS lipo (n=12)	CLOD (n=10)	WKY rats (n=4)	PBS lipo (n=5)	CLOD (n=5)	WKY rats (n=4)
Lumen diameter (μm)	230±9	254±4*	286±8	245±7	215±7	280±21
Outer Diameter (μm)	278±9	294±5	314±11	294±7	298±6	311±20
Wall Thickness (μm)	24±1	20±1*	14±1	24±0.8	24±0.9	16±1.4
Wall-to-lumen ratio	0.11±0.008	0.08±0.006*	0.05±0.004	0.10±0.005	0.09±0.005	0.06±0.007
Lumen CSA (μm^2)	42059±3162	50930±1729	64398±3556	47300±2837	49729±2643	62316±8843
Vessel CSA (μm^2)	61496±3933	67864±2185	77452±5011	67935±3433	69975±2812	76675±9850
Wall CSA (μm^2)	19437±1199	16934±1162	13054±1607	20636±866	20246±722	14386±1543
Vessel Strain	0.41±0.06	0.36±0.03	0.45±0.03	0.77±0.03	0.83±0.04	0.74±0.03
Vessel Stress	398±28	543±39*	854±74	454±21	486±28	831±90

Table 2.3 (cont'd).

β-coefficient	7.03±0.9	7.63±0.4	8.61±0.6	3.83±0.08	3.74±0.08	6.23±1.02
%tone generation	34.9±4.1	39.7±6.8	n/a	n/a	n/a	n/a

*Values are means±SEM. †values at an intraluminal pressure of 80mmHg; ‡values at an intraluminal pressure of 90mmHg; *significantly different from PBS lipo ($p<0.05$); n/a: non-applicable. The WKY values contained in this table have been previously published [10], they are included here to provide an indication of the extent of remodeling in SHRSP.*

2.4.10 - CLOD treatment for 2 weeks reduced CD163 and TNF-α in the MRA PVAT. In order to test the hypothesis that macrophage depletion leads to an upregulation in proinflammatory cytokine production by PVAT, we treated SHRSP with CLOD or PBS lipo for 2 weeks and measured mRNA expression of TNF-α and CD163 by qRT-PCR. Our data shows that this treatment regimen reduced mRNA expression of CD163 in PVAT (Figure 2.9A) and caused a trend towards a 2-fold increase in TNF-α mRNA (Figure 2.9B).

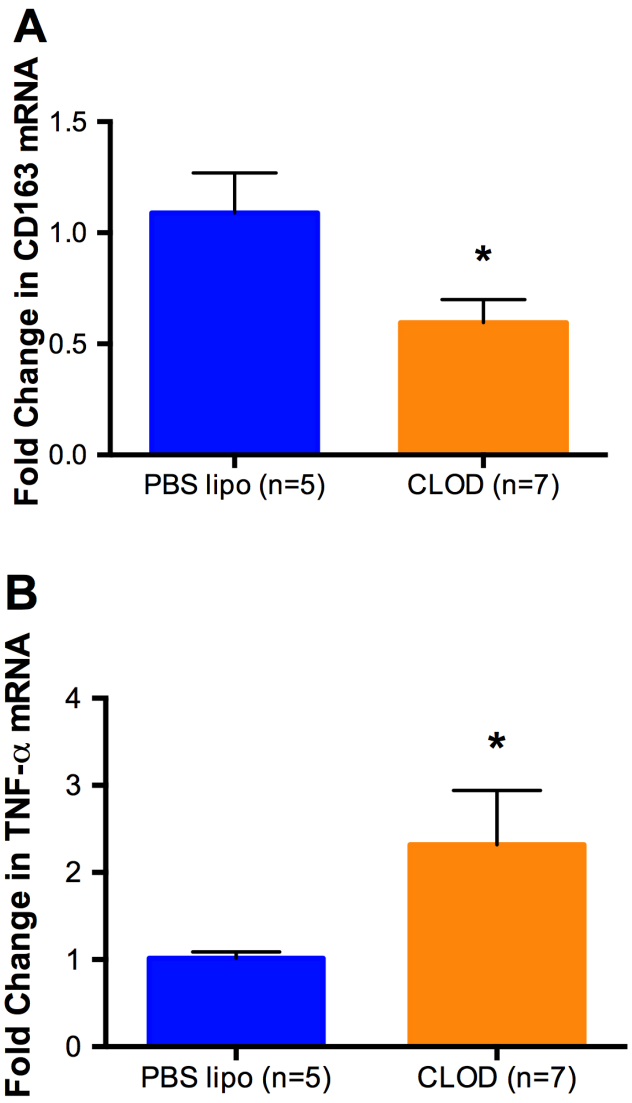

Figure 2.9: Tumor necrosis factor (TNF)-α production by PVAT. Two-weeks

treatment of SHRSP with CLOD resulted in decreased expression of CD163 mRNA (A), suggesting reduction in macrophage number. There was a trend towards an increase in TNF-α mRNA expression in the MRA PVAT (B), suggesting that, in the absence of macrophages, white adipose tissue can produce proinflammatory cytokines that mediate MRA hypertensive remodeling. *p<0.05, *Student's* t-test).

2.5 - Discussion

The novel findings in this study are that peripheral macrophage depletion improves MCA endothelial function and passive structure in SHRSP. An increase in the cross-sectional area of pial arterioles was also observed, suggesting that perivascular macrophages have deleterious effects in the cerebral microcirculation. Interestingly, peripheral and cerebral arteries responded differently to the treatment, suggesting that the mechanisms driving remodeling are different depending on the vascular bed. Importantly, CLOD treatment did not reduce the blood pressure, suggesting the effects of inflammatory cells on the vasculature are blood pressure independent. The increased MCA lumen diameter and endothelium-dependent dilation have the potential to improve cerebral blood flow and prevent, or at least delay the onset of disorders caused by chronic reduction in blood perfusion to the brain, including vascular dementia, Alzheimer's disease and recovery of ischemic stroke. To our knowledge, this is the first study showing a direct link between hypertensive cerebral vascular remodeling and perivascular macrophages in SHRSP.

The link between hypertension and inflammation is clear. In humans, plasma C-reactive protein levels correlate with the development of hypertension [26] and preactivated circulating monocytes are increased in patients with essential hypertension [27]. Inflammatory markers, including interleukin-6, intercellular adhesion molecule-1 and monocyte chemoattractant protein-1 are associated with hypertension [28, 29]. Increased intercellular adhesion molecule-1 and monocyte chemoattractant protein-1 are potentially important because they could increase monocyte/macrophage adhesion and infiltration in the vessel wall. In the spontaneously hypertensive rat, aortic TNF-α mRNA levels are increased [30]. TNF-α is associated with rennin-angiotensin-aldosterone system activation [31], and angiotensin receptor blockade reduces aortic TNF-α expression [30]. Important for the current study, activation of the rennin-angiotensin-aldosterone system is intrinsically involved in hypertensive MCA remodeling [12, 32].

It is unclear whether inflammation is a cause or consequence of hypertension. In SHRSP blood pressure increases gradually over time [12], and CLOD did not prevent this. The lack of an antihypertensive effect of the treatment could be due to, 1) the complexity of hypertension development in the SHRSP, and 2) that inflammation could be a consequence of the hypertension, and exacerbates end-organ damage. The absence of an antihypertensive effect could also be explained by the observation that CLOD did not increase MRA lumen diameter. The mesenteric bed receives 15-20% of the cardiac output [33], thus contributing markedly to total peripheral resistance and, consequently, blood pressure. We speculate that CLOD most likely did not alter the

structure of other vascular beds also involved in the control of blood pressure, including the renal vasculature. SHRSP are known to have increased renal vascular resistance, which is an important factor regulating systemic blood pressure in this model [34]. One caveat of the present study is that blood pressure was measured by tail-cuff. We recognize that telemetry would have been more accurate; however, we have shown that the data obtained with the tail-cuff system used here are very similar to those obtained with telemetry in SHRSP [12]. Therefore, we feel confident that the treatment does not affect blood pressure.

The mechanism of action for CLOD is that macrophages incorporate the liposomes and disrupt them intracellularly. The size and membrane composition of the liposomes causes them to be internalized exclusively by macrophages [19]. Once within the cell, the liposome capsule is digested and clodronate is released. Clodronate is highly polar and does not cross biological membranes, thus accumulating in the cytoplasm to levels that are toxic [35, 36], triggering apoptosis [37]. Thus, these cells are eliminated without damaging adjacent non-phagocytic cells. CLOD have not been widely used in cardiovascular research, but one study showed that CLOD prevented flow-dependent outward carotid artery remodeling [38]. While this is different from hypertension-induced remodeling, this study highlights the usefulness of CLOD in vascular studies. In our study we confirmed the effectiveness of CLOD in reducing the population of circulating phagocytic cells. In addition, we show that the number of perivascular CD163 positive cells in the cerebral cortex was reduced after CLOD treatment, as well as CD68 mRNA expression. We did not observe alteration in CD68 mRNA levels in CBV. The amount of

tissue from CBV is very limited, and it is possible that we are at the limit of resolution for qRT-PCR. TNF-α mRNA is decreased in the cerebral cortex and CBV of CLOD animals. These results suggest that phagocytes might be the primary source of cytokines locally released in the vessel wall. Importantly, CLOD does not cross the blood brain barrier and does not affect microglia [39].

In addition to the structural beneficial effects of CLOD treatment, macrophage depletion caused an improvement in endothelium-dependent dilation to ADP. Phagocytic cells express high levels of NADPH-oxidase, an enzyme involved in production of reactive oxygen species in the vasculature [40]. Reactive oxygen species, particularly the superoxide anion, react with NO and generate peroxinitrite. As a consequence, NO-dependent vasodilation becomes impaired in these vessels. ADP and Ach-mediated dilations are, in part, dependent on NO generation in endothelial cells [41]. Through the removal of an important source of reactive oxygen species, it is possible that the NO bioavailability in the MCA was increased, thus accounting for the increased vasodilatory response to ADP and Ach. This possibility is further supported by the fact that pre-incubation of MCA rings with L-NAME, an eNOS inhibitor, blunted the vasodilatory response to the same level as SHRSP treated with PBS lipo. In addition, there was no difference in response to the NO donor SNP, suggesting that the improvement in relaxation observed in CLOD SHRSP is most likely due to NO production by endothelial cells, and not in the activity of soluble guanylate cyclase in vascular smooth muscle cells. The possible beneficial physiological consequences of improved vasodilation are at least two-fold: 1) improved basal cerebral blood flow and 2) increased vasodilation of

the collateral circulation after blockage of a cerebral artery, thus potentially reducing ischemic damage in the brain of hypertensive subjects.

We found an increase in MCA lumen diameter and decrease in its wall thickness, as well as an increase in the cross-sectional area of pial arterioles after chronic peripheral macrophage depletion. This finding supports our hypothesis that infiltrating phagocytes are causative agents in cerebral vascular remodeling. Once in the vessel wall, these cells have the ability to release many substances that have the potential to alter vascular structure in a paracrine manner, including ROS, proinflammatory cytokines and matrix metalloproteinases. We recently showed that superoxide anion is involved in MCA remodeling in SHRSP, and that superoxide scavenging attenuates remodeling in these animals [22]. Similarly, we showed that inhibition of matrix metalloproteinases with doxycycline prevents hypertensive MCA remodeling [10]. It is possible that by reducing the number of perivascular phagocytes in SHRSP there is a decrease in levels of both these mediators, thus preventing the reduction in lumen diameter of the MCA observed in SHRSP. TNF-α, a major cytokine released by phagocytes, is linked to cerebral vessel weakening and aneurism formation [42], as well as activation of matrix metalloproteinase-2, induction of matrix metalloproteinase-9 expression [43, 44], and, consequently, vascular remodeling. CLOD caused a reduction in TNF-α mRNA expression in CBV and cerebral cortex of SHRSP, suggesting that macrophages might be a major source of TNF-α in the arterial wall. Independently of the mechanism, improvement of the cerebral artery structure after CLOD treatment can have beneficial effects in the ischemic brain. After ischemia/reperfusion injury, the ability of the MCA to

generate tone is diminished [45], and the major determinant of blood flow to the ischemic hemisphere after reperfusion is the lumen diameter of the MCA. In addition, improvement of the endothelial function of the arteries located in the Circle of Willis can increase collateral blood supply in case of MCA occlusion, which will be carried to the ischemic hemisphere by anastomoses in the pial arterioles. The increase in cross-sectional of pial arterioles might add to a global increase in collateral perfusion, thus potentially reducing ischemic insult in the brain.

It is important to recognize that in SHRSP the MCA remodeling is partially an adaptive response to protect the downstream parenchymal arterioles from the elevated blood pressure [46]. Therefore, one could postulate that reducing MCA wall thickness without reducing blood pressure would increase the risk of hemorrhagic stroke due to the increase in wall stress. The SHRSP in this study were not at risk for hemorrhagic stroke because they did not receive a stroke-prone diet. Although the remodeling was attenuated in this study, the MCA's wall was still thicker than in normotensive WKY rats. We have recently showed that in WKY rats the MCA wall thickness is 13.8±1.4μm[10], and in the present study the MCA wall thickness from CLOD-treated SHRSP is 19.6±1.4μm. It is possible that this maintenance in wall thickness is sufficient to protect the cerebral microvasculature in the CLOD-treated SHRSP.

Surprisingly, CLOD treatment did not attenuate MRA remodeling. The finding is in disagreement with the study from Ko *et al* [17] where attenuation of hypertensive MRA remodeling was observed in m-CSF null mice. MRA are surrounded by white adipose

tissue, and adipocytes produce proinflammatory cytokines [47]. mCSF was also shown to be important for adipocyte hyperplasia [48], thus it is possible that mCSF deficiency attenuates MRA remodeling by reducing adipocyte-induced vascular inflammation. In our study, we hypothesized that, in the absence of macrophages, adipocytes would take on a proinflammatory phenotype and this might function as a “backup” mechanism for cytokine release. In fact, we show that TNF-α mRNA expression is increased in the MRA PVAT after a 2-weeks CLOD treatment, supporting our hypothesis. The increase in TNF-α mRNA was accompanied by a reduction in CD163 mRNA expression, showing that even this shorter CLOD treatment depleted macrophages. Thus, despite the reduced macrophage population in the mesenteric PVAT the inflammatory cytokine load on the vessels appears to be increased, and this may be the cause of the continued remodeling in the MRA.

In summary, the present study shows that infiltrating macrophages play an active role in endothelial dysfunction and remodeling of cerebral arteries and arterioles in SHRSP. This study adds to our knowledge of the cerebral vascular dysfunction in chronic hypertersion, a major risk factor for cerebrovascular accidents, vascular dementia and Alzheimer’s disease. Elucidating the mechanisms of hypertensive remodeling of the cerebral arterial tree might lead to new therapies aimed at improving cerebral perfusion, thus reducing acute ischemic damage and preventing the onset of diseases caused by chronic cerebral hypoperfusion.

REFERENCES

REFERENCES

1. Mulvany, M.J., *Vascular remodelling of resistance vessels: can we define this?* Cardiovasc Res, 1999. **41**(1): p. 9-13.

2. Feihl, F., et al., *Hypertension and microvascular remodelling.* Cardiovasc Res, 2008. **78**(2): p. 274-85.

3. Aalkjaer, C., et al., *Evidence for increased media thickness, increased neuronal amine uptake, and depressed excitation--contraction coupling in isolated resistance vessels from essential hypertensives.* Circ Res, 1987. **61**(2): p. 181-6.

4. Intengan, H.D. and E.L. Schiffrin, *Vascular remodeling in hypertension: roles of apoptosis, inflammation, and fibrosis.* Hypertension, 2001. **38**(3 Pt 2): p. 581-7.

5. Harper, S.L., H.G. Bohlen, and M.J. Rubin, *Arterial and microvascular contributions to cerebral cortical autoregulation in rats.* Am J Physiol, 1984. **246**(1 Pt 2): p. H17-24.

6. Faraci, F.M. and D.D. Heistad, *Regulation of large cerebral arteries and cerebral microvascular pressure.* Circ Res, 1990. **66**(1): p. 8-17.

7. Sonoyama, K., et al., *Vascular remodeling: implications for small artery function and target organ damage.* Ther Adv Cardiovasc Dis, 2007. **1**(2): p. 129-37.

8. Heistad, D.D., et al., *Impaired dilatation of cerebral arterioles in chronic hypertension.* Blood Vessels, 1990. **27**(2-5): p. 258-62.

9. Rigsby, C.S., et al., *Effects of Spironolactone on Cerebral Vessel Structure in Rats With Sustained Hypertension.* Am J Hypertens, 2011.

10. Pires, P.W., et al., *Doxycycline, a matrix metalloprotease inhibitor, reduces vascular remodeling and damage after cerebral ischemia in stroke-prone spontaneously hypertensive rats.* Am J Physiol Heart Circ Physiol, 2011. **301**(1): p. H87-97.

11. Kumai, Y., et al., *Protective effects of angiotensin II type 1 receptor blocker on cerebral circulation independent of blood pressure.* Exp Neurol, 2008. **210**(2): p. 441-8.

12. Rigsby, C.S., D.M. Pollock, and A.M. Dorrance, *Spironolactone improves structure and increases tone in the cerebral vasculature of male spontaneously hypertensive stroke-prone rats.* Microvasc Res, 2007. **73**(3): p. 198-205.

13. Peeters, A.C., et al., *Pro-inflammatory cytokines in patients with essential hypertension.* Eur J Clin Invest, 2001. **31**(1): p. 31-6.

14. Chen, C.M. and D. Schachter, *Elevation of plasma immunoglobulin A in the spontaneously hypertensive rat.* Hypertension, 1993. **21**(5): p. 731-8.

15. Pu, Q., et al., *Effects of combined AT1 receptor antagonist/NEP inhibitor on vascular remodeling and cardiac fibrosis in SHRSP.* J Hypertens, 2008. **26**(2): p. 322-33.

16. Nakamura, T., et al., *Pioglitazone exerts protective effects against stroke in stroke-prone spontaneously hypertensive rats, independently of blood pressure.* Stroke, 2007. **38**(11): p. 3016-22.

17. Ko, E.A., et al., *Resistance artery remodeling in deoxycorticosterone acetate-salt hypertension is dependent on vascular inflammation: evidence from m-CSF-deficient mice.* Am J Physiol Heart Circ Physiol, 2007. **292**(4): p. H1789-95.

18. De Ciuceis, C., et al., *Reduced vascular remodeling, endothelial dysfunction, and oxidative stress in resistance arteries of angiotensin II-infused macrophage colony-stimulating factor-deficient mice: evidence for a role in inflammation in angiotensin-induced vascular injury.* Arterioscler Thromb Vasc Biol, 2005. **25**(10): p. 2106-13.

19. Van Rooijen, N. and A. Sanders, *Liposome mediated depletion of macrophages: mechanism of action, preparation of liposomes and applications.* J Immunol Methods, 1994. **174**(1-2): p. 83-93.

20. Ezendam, J., et al., *Macrophages are involved in hexachlorobenzene-induced adverse immune effects.* Toxicol Appl Pharmacol, 2005. **209**(1): p. 19-27.

21. Davidson, A.O., et al., *Blood pressure in genetically hypertensive rats. Influence of the Y chromosome.* Hypertension, 1995. **26**(3): p. 452-9.

22. Pires, P.W., et al., *Tempol, a superoxide dismutase mimetic, prevents cerebral vessel remodeling in hypertensive rats.* Microvasc Res, 2010. **80**(3): p. 445-52.

23. Livak, K.J. and T.D. Schmittgen, *Analysis of relative gene expression data using real-time quantitative PCR and the 2(-Delta Delta C(T)) Method.* Methods, 2001. **25**(4): p. 402-8.

24. Baumbach, G.L. and M.A. Hajdu, *Mechanics and composition of cerebral arterioles in renal and spontaneously hypertensive rats.* Hypertension, 1993. **21**(6 Pt 1): p. 816-26.

25. Chan, S.L., et al., *Effect of PPARgamma inhibition during pregnancy on posterior cerebral artery function and structure.* Front Physiol, 2010. **1**: p. 130.

26. Sesso, H.D., et al., *C-reactive protein and the risk of developing hypertension.* Jama, 2003. **290**(22): p. 2945-51.

27. Dorffel, Y., et al., *Preactivated peripheral blood monocytes in patients with essential hypertension.* Hypertension, 1999. **34**(1): p. 113-7.

28. Chae, C.U., et al., *Blood pressure and inflammation in apparently healthy men.* Hypertension, 2001. **38**(3): p. 399-403.

29. Madej, A., et al., *Plasma concentrations of adhesion molecules and chemokines in patients with essential hypertension.* Pharmacol Rep, 2005. **57**(6): p. 878-81.

30. Sanz-Rosa, D., et al., *Effect of AT1 receptor antagonism on vascular and circulating inflammatory mediators in SHR: role of NF-kappaB/IkappaB system.* Am J Physiol Heart Circ Physiol, 2005. **288**(1): p. H111-5.

31. Marchesi, C., P. Paradis, and E.L. Schiffrin, *Role of the renin-angiotensin system in vascular inflammation.* Trends Pharmacol Sci, 2008. **29**(7): p. 367-74.

32. Dorrance, A.M., N.C. Rupp, and E.F. Nogueira, *Mineralocorticoid receptor activation causes cerebral vessel remodeling and exacerbates the damage caused by cerebral ischemia.* Hypertension, 2006. **47**(3): p. 590-5.

33. Jacobson, E.D., *Physiology of the mesenteric circulation.* Physiologist, 1982. **25**(5): p. 439-43.

34. Nagaoka, A., et al., *Renal hemodynamics and sodium excretion in stroke-prone spontaneously hypertensive rats.* Am J Physiol, 1981. **241**(3): p. F244-9.

35. van Rooijen, N. and A. Sanders, *Elimination, blocking, and activation of macrophages: three of a kind?* J Leukoc Biol, 1997. **62**(6): p. 702-9.

36. Van Rooijen, N., *Selective depletion of macrophages by liposome-encapsulated drugs.* 5th ed. Handbook of Experimental Immunology, ed. L. Herzenberg, L. Herzenberg, and D. Weir1996: Blackwell Scientific Publications, Inc. 165.1-165.5.

37. van Rooijen, N., A. Sanders, and T.K. van den Berg, *Apoptosis of macrophages induced by liposome-mediated intracellular delivery of clodronate and propamidine.* J Immunol Methods, 1996. **193**(1): p. 93-9.

38. Nuki, Y., et al., *Roles of macrophages in flow-induced outward vascular remodeling.* J Cereb Blood Flow Metab, 2009. **29**(3): p. 495-503.

39. Micklus, M.J., et al., *Organ distribution of liposomal formulations following intracarotid infusion in rats.* Biochim Biophys Acta, 1992. **1124**(1): p. 7-12.

40. Touyz, R.M. and E.L. Schiffrin, *Reactive oxygen species in vascular biology: implications in hypertension.* Histochem Cell Biol, 2004. **122**(4): p. 339-52.

41. You, J., et al., *Endothelial-mediated dilations of rat middle cerebral arteries by ATP and ADP.* Am J Physiol, 1997. **273**(3 Pt 2): p. H1472-7.

42. Jayaraman, T., et al., *TNF-alpha-mediated inflammation in cerebral aneurysms: a potential link to growth and rupture.* Vasc Health Risk Manag, 2008. **4**(4): p. 805-17.

43. Han, Y.P., et al., *TNF-alpha stimulates activation of pro-MMP2 in human skin through NF-(kappa)B mediated induction of MT1-MMP.* J Cell Sci, 2001. **114**(Pt 1): p. 131-139.

44. Arenas, I.A., et al., *Angiotensin II-induced MMP-2 release from endothelial cells is mediated by TNF-alpha.* Am J Physiol Cell Physiol, 2004. **286**(4): p. C779-84.

45. Cipolla, M.J., et al., *Reperfusion decreases myogenic reactivity and alters middle cerebral artery function after focal cerebral ischemia in rats.* Stroke, 1997. **28**(1): p. 176-80.

46. Hayashi, K. and T. Naiki, *Adaptation and remodeling of vascular wall; biomechanical response to hypertension.* J Mech Behav Biomed Mater, 2009. **2**(1): p. 3-19.

47. Stern, N. and Y. Marcus, *Perivascular fat: innocent bystander or active player in vascular disease?* J Cardiometab Syndr, 2006. **1**(2): p. 115-20.

48. Levine, J.A., et al., *Adipocyte macrophage colony-stimulating factor is a mediator of adipose tissue growth.* J Clin Invest, 1998. **101**(8): p. 1557-64.

CHAPTER 3

Doxycycline, a matrix metalloproteinase inhibitor, reduces vascular remodeling and damage after cerebral ischemia in stroke-prone spontaneously hypertensive rats.

3.1 - Abstract

Matrix metalloproteinases (MMPs) are a family of zinc-peptidases involved in extracellular matrix turnover. There is evidence that increased MMP activity is involved in remodeling of resistance vessels in chronic hypertension. Thus, we hypothesized that inhibition of MMP activity with Doxycycline (Dox) would attenuate vascular remodeling. Six-week-old male stroke-prone spontaneously hypertensive rats (SHRSP) were treated with Dox (50 mg/kg/day in the drinking water) for six weeks. Untreated SHRSP were controls. Blood pressure was measured by telemetry during the last week. Middle cerebral artery (MCA) and mesenteric resistance artery (MRA) passive structure were assessed by pressure myography. MMP-2 expression in aortas was measured by Western blot. Dox caused a small increase in mean arterial pressure. Active MMP-2 expression was reduced in aorta from SHRSP+Dox. In the MCA, Dox treatment increased the lumen and the outer diameter, as well as reduced MCA's wall/lumen ratio. Damage after transient cerebral ischemia was reduced in SHRSP+Dox when compared to untreated SHRSP. In the MRA, Dox reduced wall thickness and wall-to-lumen ratio, without changing lumen diameter. These results suggest that MMPs are involved in hypertensive vascular remodeling in both the peripheral and cerebral vasculature and that Dox reduced brain damage after cerebral ischemia.

3.2 - Introduction

Primary prevention of ischemic stroke is increasing in importance as a strategy for management of individuals at high-risk. Recently published clinical trials, such as ONTARGET and TRANSCEND, show that therapies aimed at reducing cardiovascular incidents are a valuable tool for prevention of first occurrence of myocardial infarction, heart failure and stroke [1]. In the ONTARGET trial, the beneficial effects observed were not preceded by a reduction in systemic blood pressure. Therefore, it is possible that a major component of the risk for ischemic stroke is not blood pressure itself. The consequences of vascular adaptation to increased intraluminal pressure might provide an additional risk. Hence, prevention of hypertensive vascular remodeling might be a candidate for primary prevention of stroke.

Damage caused by cerebral ischemia is related to the extent of hypertensive remodeling of the middle cerebral artery (MCA) [2-5]. Remodeling of the resistance vasculature encompasses structural changes that lead to a reduction in the lumen diameter and an increase in the wall thickness and wall-to-lumen ratio [6-9]. Together, these alterations may lead to impairment in the ability of vessels to auto-regulate and dilate. In the cerebral vasculature, these impairments might cause a reduction in blood flow and an increase in ischemic damage [4]. When one considers attenuation of vascular remodeling as a primary strategy for stroke prevention, it is important to identify agents that have a maximal effect on the cerebral vasculature and little effect on the periphery, in order to not decrease blood pressure (BP) or impair its control.

Vascular remodeling can be caused by smooth muscle cell hypertrophy or hyperplasia, deposition of extracellular matrix (ECM) elements or a combination of these two factors [9]. ECM turnover in the vessel wall is regulated in part by a family of zinc-dependent proteases known as matrix metalloproteinases (MMPs) [10, 11]. Among them, MMP-2 and -9, also known as gelatinases A and B, are responsible for degradation of basement membrane elements (mainly collagen IV and laminin) and digestion of collagen I fibrils (gelatin) [12, 13]. Increased MMP-2 activity in vessels has been reported in many models of hypertension and is associated with vascular remodeling [11, 14, 15]. Doxycycline (Dox), a tetracycline antibiotic and non-specific MMP inhibitor, was shown to prevent remodeling in aorta of the 2-kidney, 1-clip model of hypertension [16, 17]. However, very little is known about the effects of Dox in the resistance vasculature of hypertensive rats, and how those effects relate to end-organ damage. Therefore, we hypothesized that inhibition of MMPs with Dox would attenuate hypertensive remodeling in the cerebral vasculature of stroke-prone spontaneously hypertensive rats (SHRSP); and that the improvement in cerebrovascular structure would reduce damage induced by cerebral ischemia.

3.3 - Methods

3.3.1 - Animals and treatment: Six-week-old male SHRSP were used for the experiments. Rats were split into 2 groups: one group received Dox in the drinking water for 6 weeks (SHRSP+Dox, 50 mg/kg/day, n=28: 10 were used for pressure myography, 5 for telemetry, 5 for transient MCA occlusion [tMCAO] and 8 for permanent MCA occlusion [pMCAO]). Untreated SHRSP were controls (n=28: 12 were used for

pressure myography, 5 for telemetry, 5 for tMCAO and 6 for pMCAO). Twelve-week-old normotensive Wystar Kyoto (WKY) rats were randomized into 2 groups: untreated WKY (n=4) and WKY+Dox (n=7). They were used for passive vascular structure studies. These were included in the study to validate remodeling in the SHRSP and to evaluate possible blood pressure dependent effects of Dox. Dox dosage was chosen based on the results of a pilot experiment using 3 doses: 25, 50 and 100mg/kg/day. In that study we observed that 50mg/kg/day exerted the best inhibition of MMP-2, thus we performed all further experiments using this dosage. Animals were maintained on a 12:12hr light: dark cycle, with regular chow and water available *ad libitum*. Dox water was prepared fresh daily. The experimental protocols were approved by the Institutional Animal Care & Use Committees in accordance with the American Physiological Society's "Guiding Principles in the Care and Use of Animals".

3.3.2 - Measurement of blood pressure. Blood pressure was measured by telemetry in SHRSP+Dox and untreated SHRSP during the last week of experiment. The catheter of the telemeter (TA11PAC40, Data Sciences International) was inserted into the distal aorta via the femoral artery and the body of the transmitter was placed subcutaneously. Rats were allowed to recover for 1 week prior to the beginning of blood pressure recording. Blood pressure and heart rate were measured every 10 minutes over a 24-hour cycle during the last week of treatment [18]. Averages of the day and night period were used to calculate the daily blood pressure, and the average for the week is reported.

3.3.3 - MCA structure. MCA structure was assessed using pressure myography as described previously [2]. MCAs were isolated and placed in cold physiological salt solution (PSS) (in mmol/L: 141.9 NaCl, 4.7 KCl, 1.7 $MgSO_4$, 0.5 EDTA, 2.8 $CaCl_2$, 10 HEPES, 1.2 KH_2PO_4, and 5 glucose). The first branch-free segment of the MCA most proximal to the circle of Willis was mounted on two glass micropipettes in a pressure myograph (Danish Myo Technology, Aarhus, Denmark). Vessels were bathed with warm oxygenated PSS at an intraluminal pressure of 80 mmHg and the vessels were allowed to equilibrate for 30 minutes. Pressure was then increased to 140 mmHg for 10 minutes then decreased to 80 mmHg to check MCA viability. Vessels that generated less than 20% spontaneous tone were discarded [19]. Tone was calculated using the following formula: %tone = [1-(active lumen diameter/passive lumen diameter)]*100. MCA's vasodilatory ability was assessed using increasing concentrations of bradykinin (0.1nmol/L to 1µmol/L) added to the bath. The MCA was then washed to baseline and the vasoconstrictor 5-hydroxytriptamine (5-HT, 1nmol/L to 10µmol/L) was added to the bath. The MCA was then washed to baseline, and tone generation was assessed by increasing the intraluminal pressures from 3 to 180 mmHg in 20 mmHg increments. MCA was allowed to equilibrate for 5 minutes at each new pressure before the measurement was taken. MCA passive structure was analyzed in calcium-free PSS containing 2mmol/L EGTA following the same pressure increments. Lumen diameter, external diameter and wall thickness at each pressure were measured after a 5-minute equilibration. The wall/lumen ratio, circumferential wall stress and wall strain were calculated using previously described methods [20]. The elastic modulus (β-coefficient) was calculated from the stress/strain curves for the individual vessels, and these curves

were fitted to an exponential model ($y=ae^{\beta x}$) where β is the slope of the curve: the higher the β-coefficient the stiffer the vessel.

3.3.4 - Mesenteric resistance artery (MRA) structure: Passive structure of MRA was analyzed under zero flow and calcium-free conditions as described for the MCA, except that the pressure was raised from 3 to 180 mmHg in 30 mmHg increments.

3.3.5 - Middle cerebral artery occlusion (MCAO): For induction of cerebral ischemia, we used the intraluminal suture model developed by Longa et al. [21] as previously described by our laboratory [5, 22]. All animals subjected to MCAO had Dox withdrawn 48 hours before the procedure in order to avoid any possible acute effects of Dox in the outcome of cerebral ischemia (Dox half-life in rodents is approximately 4 hours [23]). Rats were initially anesthetized with isoflurane in an induction chamber, and anesthesia was maintained with 2% isoflurane in oxygen; body temperature was maintained at 37°C. An incision was made in the top of the head to expose the skull for measurement of pial flow by scanning laser Doppler and attachment of a laser Doppler flow probe to measure blood flow to the region supplied by the MCA (5mm lateral and 1mm posterior to the bregma). A midline incision was made to expose the carotid artery. The lingual and thyroid arteries were cauterized, and the external carotid and pterygopalatine arteries were tied off with suture. A 3-0 nylon monofilament with a rounded end (Doccol, Redland, CA) was inserted into the common carotid artery. This monofilament was then advanced through the internal carotid artery to block blood flow to the MCA where it branches from the circle of Willis. MCA occlusion was verified by a drop in flow

as measured by both scanning laser Doppler and the Doppler flow probe. One set of animals was subject to pMCAO, and after 24 hours, rats were anesthetized and decapitated, and the brain was removed, sliced into 2 mm sections, and stained with 2% 2,3,5-triphenyltetrazolium chloride (TTC) to assess ischemic damage. When using this technique, areas of viable tissue will exhibit a pink color, and areas of non-viable tissue will not develop color. Brains were fixed in 2% paraformaldehyde, and digital images of brain slices were taken. The percentage of infarction was determined by the following equation: %Hemisphere Infarcted = ((VC-VL)/VC)*100 where VC is the volume of normal tissue in the non-ischemic hemisphere and VL is the volume of normal tissue in the ischemic hemisphere [24].

Another set of rats was subjected to transient ischemia (tMCAO). The MCAO was performed as described above, and ischemia was maintained for 1 hour followed by 23 hours of reperfusion. After that, the brain was removed and measurement of ischemic damage was performed as described above.

3.3.6 - Scanning laser Doppler measurement of pial blood flow: Pial blood flow was measured by scanning laser Doppler (PeriScan PIM 3, Perimed, Stockholm, Sweden). Under anesthesia, the rat's skull was exposed and cleaned. The scanning laser Doppler was positioned approximately 18 cm above the skull, and pial blood flow was analyzed in both cerebral hemispheres. The wavelength of the laser light is 670-690 nm with a penetrating depth of 0.5-1 mm. A total of 4 consecutives scans were performed at each time-point. The time-points were: prior to surgery, immediately after MCAO, before and

after reperfusion (on animals subjected to tMCAO) and immediately prior to euthanasia. Mean perfusion in each hemisphere was measured using the LDPIwin 3.1 software (Perimed). Pial blood flows in the ischemic and non-ischemic hemispheres are expressed as a % of pre-ischemic pial blood flow.

3.3.7 - Western Blot. To validate MMP inhibition with Dox, Western blot analysis of MMP-2 expression was performed. Aortas were excised, cleaned of perivascular adipose tissue and blood, and snap-frozen in liquid nitrogen. Tissue was homogenized using a mortar and pestle in RIPA buffer containing a cocktail of protease inhibitors. The protein concentration in the sample was measured using a BCA Protein Assay Kit (Thermo Scientific, Rockford, IL). Aliquots containing approximately 50 µg of protein were resolved in 8% SDS-PAGE under reducing conditions and transferred to a PDVF membrane. The membrane was then blocked for non-specific binding in 4% fat-free dry milk in TBS for 2 hours and incubated with monoclonal mouse anti-rat MMP-2 (Calbiochem/EMD Biosciences, La Jolla, CA) overnight at 4°C. After washing, membranes were incubated with peroxidase-conjugated anti-mouse (Calbiochem/EMD Biosciences, La Jolla, CA) for 1 hour at room temperature and then developed using Amersham ECL Advance Western Blotting Detection Kit (GE Healthcare, Buckinghamshire, UK). The membranes were stripped and re-probed for β-tubulin as loading control. The intensity of the bands was analyzed using ImageJ software and is expressed as a ratio of β-tubulin.

3.3.8 - Gelatin Zymography. Plasma MMP activity was measured by gelatin zymography. Briefly, aliquotes of plasma containing approximately 35 µg of protein were resolved in 8% SDS-PAGE under reducing conditions. The gels were then incubated in 2.5% Triton X-100, three times for 15 minutes each to allow for protein renaturation. The gels were then washed with 50 mmol/L Tris-buffer, pH 7.4 and incubated with Zymogram Development Buffer (Bio-Rad, Hercules, CA) for 20 hours at 37°C. The gels were stained with 0.5% Coomasie blue for 30 minutes and destained (30% methanol, 30% acetic acid, 40% water). Areas of gelatinolytic activity were identified as white bands against a dark background. Gels were scanned using Odyssey Infrared Imaging System (Li-cor Biosciences, Lincoln, NE) for quantification of the area of the bands.

3.3.9 - Thoracic aorta collagen and elastin content: Total collagen content in the vessel wall was measured using Picrosirius red and polarized light as described previously [25, 26]. The data are presented as a ratio between collagen area and wall area. Elastin fibers were identified using an Elastin Stain Kit (Richard-Allan Scientific, Kalamazoo, MI), following the manufacturer's guidelines. Data are presented as a ratio between area of elastin fibers and wall area.

3.3.10 - Statistics. All results are represented as mean ± standard error of the mean (SEM). Vascular structure data were analyzed by Two-Way ANOVA with a Bonferroni *post-hoc* test. All other data was analyzed using *Student's* t-test. A p-value ≤ 0.05 was considered significant.

3.3.11 - Chemicals and Supplies. Unless otherwise stated, all chemicals and supplies were purchased from Sigma Chemical Company (St. Louis, MO).

3.4 - Results

3.4.1 - General findings. Final body weight, heart and kidney weights are summarized in Table 3.1. There were no differences in final body weight in rats from all groups. The heart/body weight ratio, an indicator of cardiac hypertrophy, was increased in SHRSP when compared to WKY rats ± Dox ($p<0.001$), and Dox treatment prevented the cardiac hypertrophy ($p=0.02$) observed in the hypertensive rat. The kidney/body weight ratio was increased in SHRSP when compared to untreated WKY rats; Dox did not attenuate the kidney hypertrophy in SHRSP, but it caused a slight kidney hypertrophy in WKY rats + DOX ($p<0.001$).

3.4.2 - Blood pressure measurements. Heart rate, systolic, diastolic and mean arterial pressures measured by telemetry are shown in Table 3.1. Dox treatment caused a small but significant increase in SHRSP in all the parameters analyzed ($p<0.01$).

Table 3.1: Final body weight, heart: body weight, kidney: body weight and blood pressure values at the end of 6 weeks of treatment.

	SHRSP	SHRSP+Dox	WKY rats	WKY rats+Dox
Final body weight	261±7	266±4	265±5	270±6
Heart: body weight	0.50±0.02*	0.44±0.01*,†	0.32±0.01	0.31±0.01
Kidney: body weight	0.97±0.02*	1.00±0.02*	0.67±0.01	0.73±0.01†,‡
Systolic Arterial Pressure	184±3	193±3†	n.a.	n.a.
Diastolic Arterial Pressure	128±2	135±2†	n.a.	n.a.
Mean Arterial Pressure	156±3	164±2†	n.a.	n.a.
Heart Rate	311±5	321±1†	n.a.	n.a.

*Values are means±SEM. Data were analyzed by one-way ANOVA. *statistically different from normotensive WKY rats, p<0.05; †statistically different from untreated SHRSP, p<0.05; ‡statistically different from untreated WKY rats, p<0.05.*

3.4.3 - Western blot. To validate MMP inhibition after Dox treatment, we performed western blots using an antibody specific to MMP-2 in homogenates of SHRSP aorta. As expected, Dox treatment decreased the concentration of active-MMP-2 (p=0.03) without changing the concentration of pre-MMP-2 (Figure 3.1).

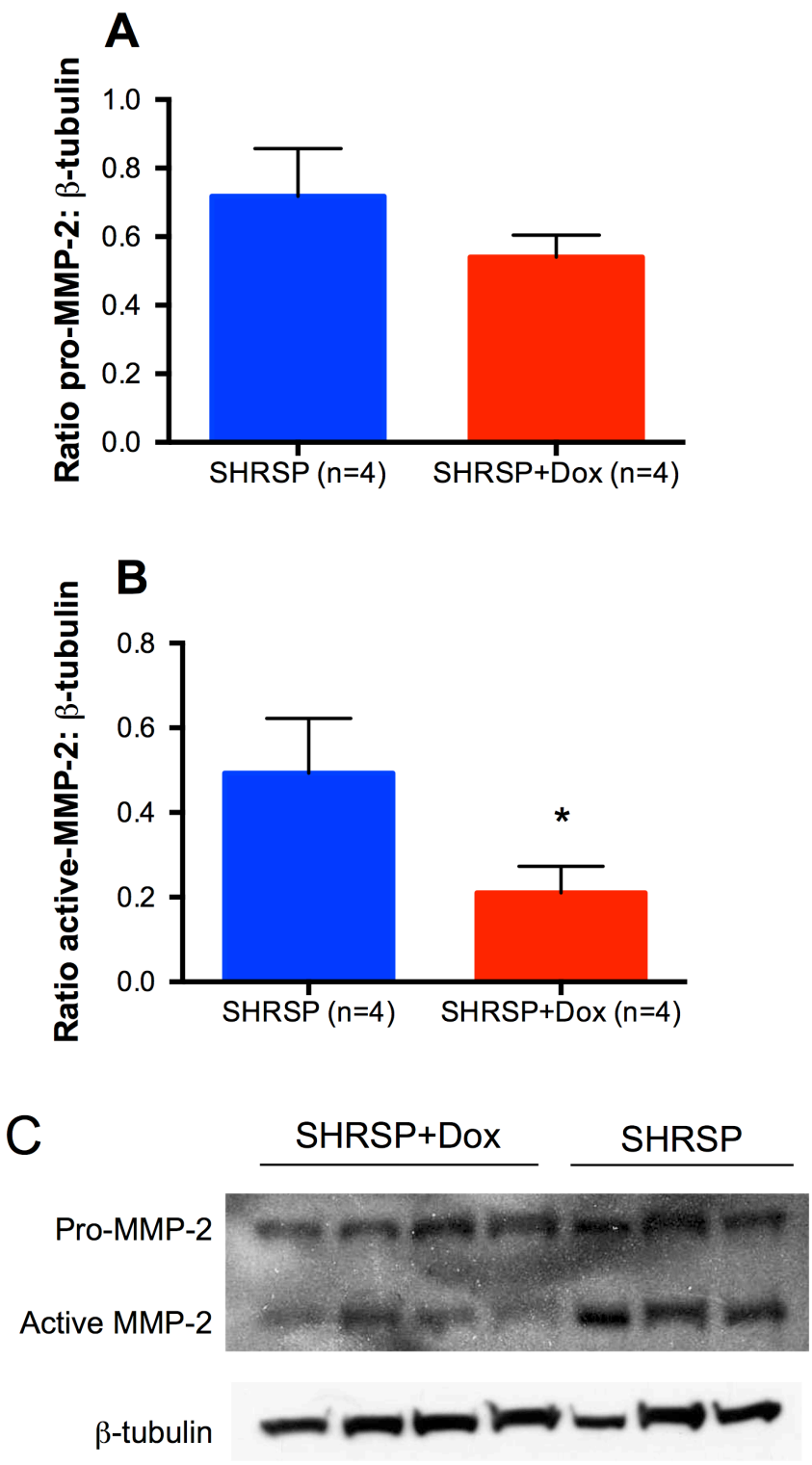

Figure 3.1: Dox treatment reduced the expression of active-MMP-2 in the aorta of SHRSP. Aliquots of aorta supernatants containing 50μg of protein were resolved by

SDS-PAGE and transferred to a PVDF membrane for Western blot analysis. Dox treatment reduced the expression of active-MMP-2 (B), but not pro-MMP-2 (A), in the aorta of SHRSP. Data are shown as a ratio of MMP-2 expression: β-tubulin expression (loading control). Representative images of blots are shown in B. *p<0.05, *Student's* t-test.

3.4.4 - MCA reactivity and tone generation. Constriction of MCA to 5-HT and dilation to BK was not changed by Dox treatment in SHRSP (Figure 3.2A and 3.2B). No changes in myogenic tone generation over a range of intraluminal pressures were observed (Fig 3.2C).

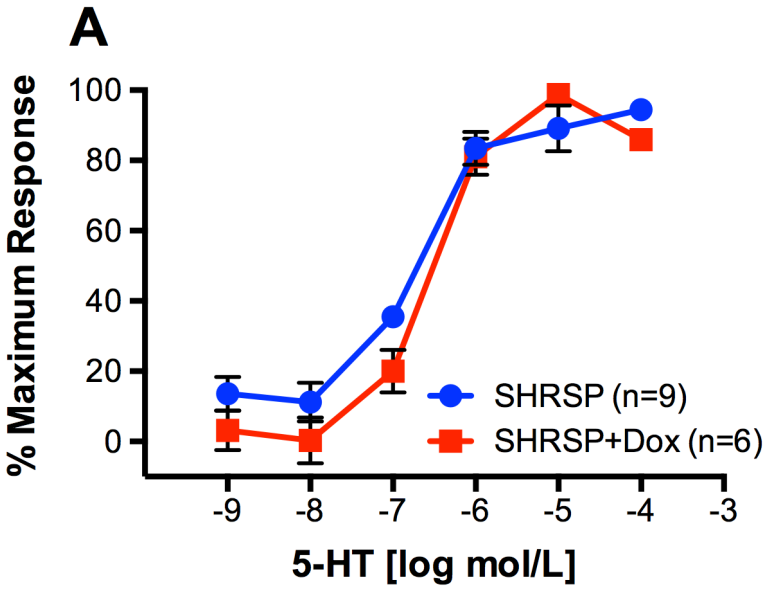

Figure 3.2: Dox treatment did not alter MCA reactivity to 5-HT (A) and BK (B) and did not alter MCA myogenic response to increases in intraluminal pressure (C).

Figure 3.2 (cont'd)

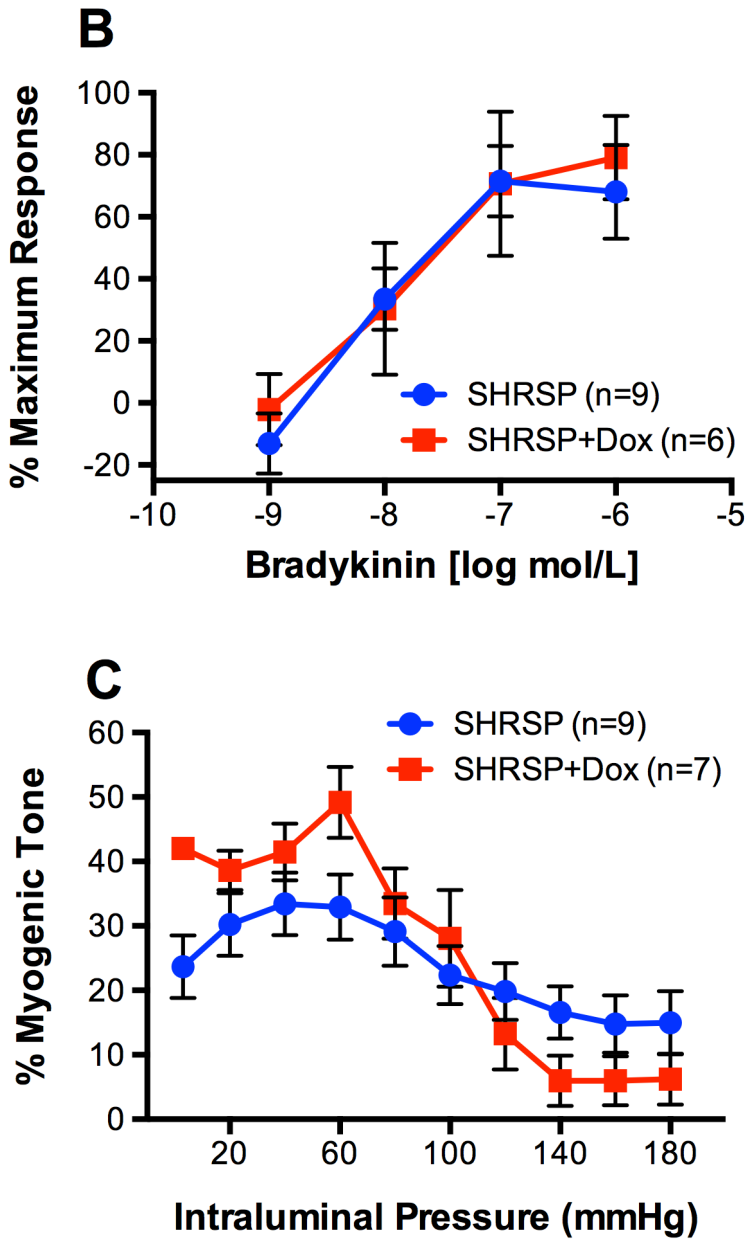

MCAs were maintained at 80mmHg intraluminal pressure and drugs were added to the bath in a cumulative fashion. The vessel was allowed to equilibrate for 10 minutes at every dose to reach steady-state. To assess myogenic tone (C), intraluminal pressure was increased from 3 to 180mmHg in 20mmHg increments, and the vessel was allowed

to equilibrate for 5 minutes at each pressure before measurement was taken. Values are means±SEM. Data were analyzed by two-way ANOVA.

3.4.5 - MCA passive structure. Passive structure of MCA was measured under calcium-free and zero flow conditions. Remodeling was observed in the MCA of SHRSP as a reduction in outer and lumen diameter and an increase in wall thickness and wall-to-lumen ratio when compared to normotensive WKY rats, treated or not with Dox. Dox treatment attenuated MCA remodeling in SHRSP, as shown by an increase in the outer and lumen diameter (Figures 3.3A and 3.3B), and the outer and lumen cross-sectional area (CSA, Figures 4.4A and 4.4B). Dox treatment also decreased the wall-to-lumen ratio (Figure 4.3D) over the range of intraluminal pressures analyzed. The MCA stress was higher in SHRSP+Dox and WKY rats±Dox at intraluminal pressures higher than 60 mmHg, without any statistical differences in vessel strain (Figures 4.4C and 4.4D). Interestingly, no differences were observed in vessel distensibility (Figure 5.5A) and stiffness (β-coeficient: 8.8±1.6 vs 8.01±0.5, SHRSP vs SHRSP+Dox, Figure 5.5B). Dox did not alter MCA passive structure in WKY rats.

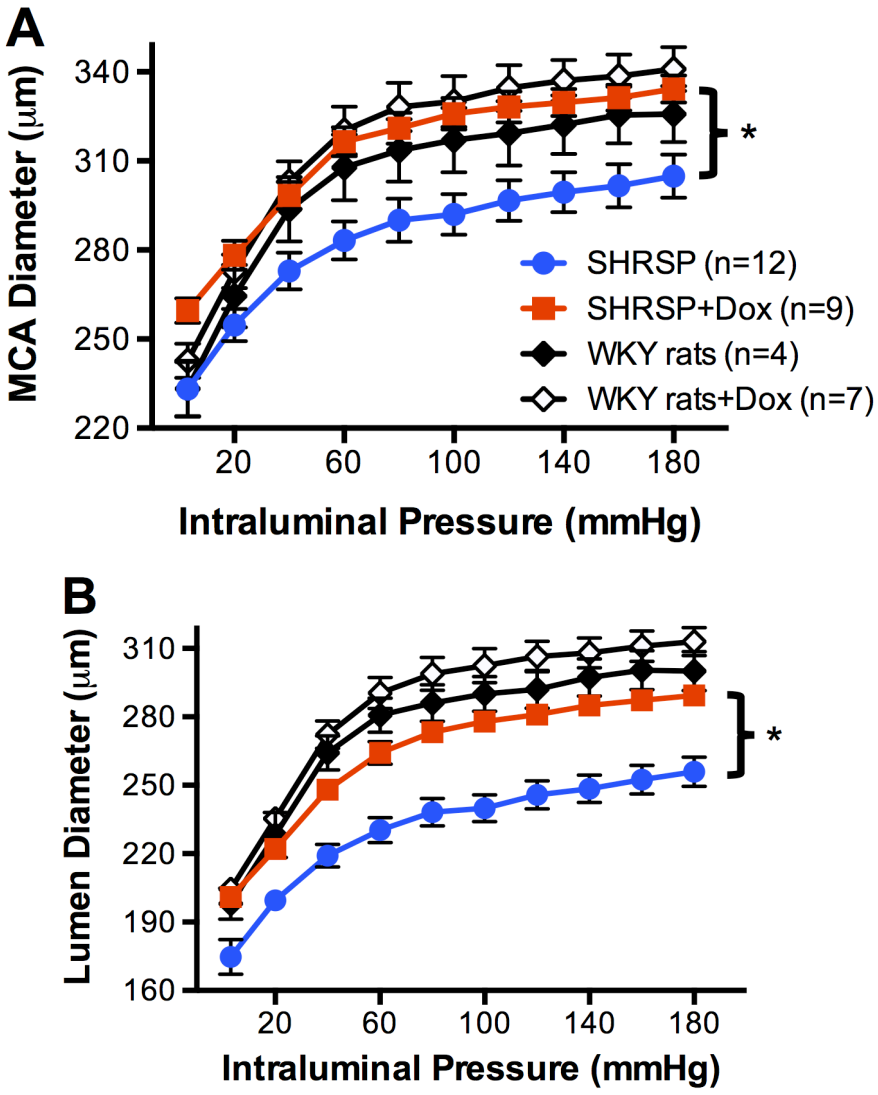

Figure 3.3: Dox treatment attenuated hypertensive remodeling of the MCA in SHRSP.

Figure 3.3 (cont'd)

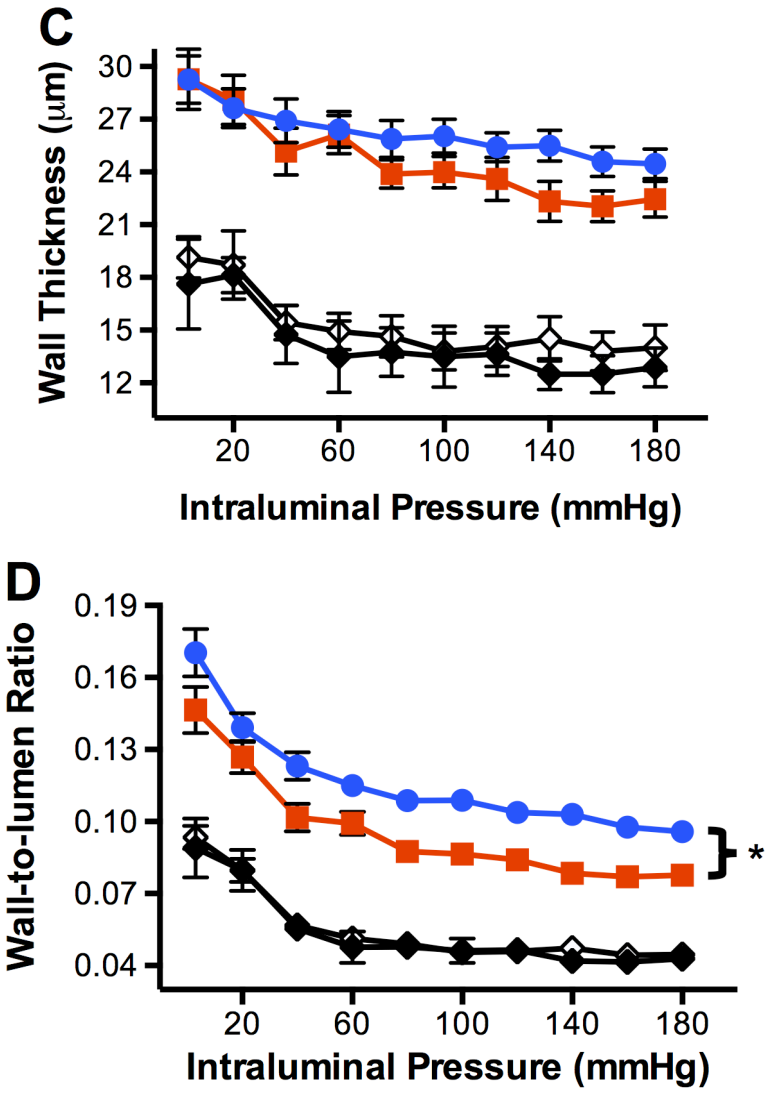

Outer (A) and lumen diameter (B) were increased in SHRSP+Dox and were not different from WKY rats±Dox. Wall thickness was increased in SHRSP±Dox when compared to WKY rats±Dox (C). The wall-to-lumen ratio was improved by Dox treatment, even without decrease in wall thickness (D). Measurements were obtained from cannulated MCAs using pressure myography under zero flow and calcium-free conditions. Values are means±SEM. Data were analyzed by two-way ANOVA. *$p<0.001$.

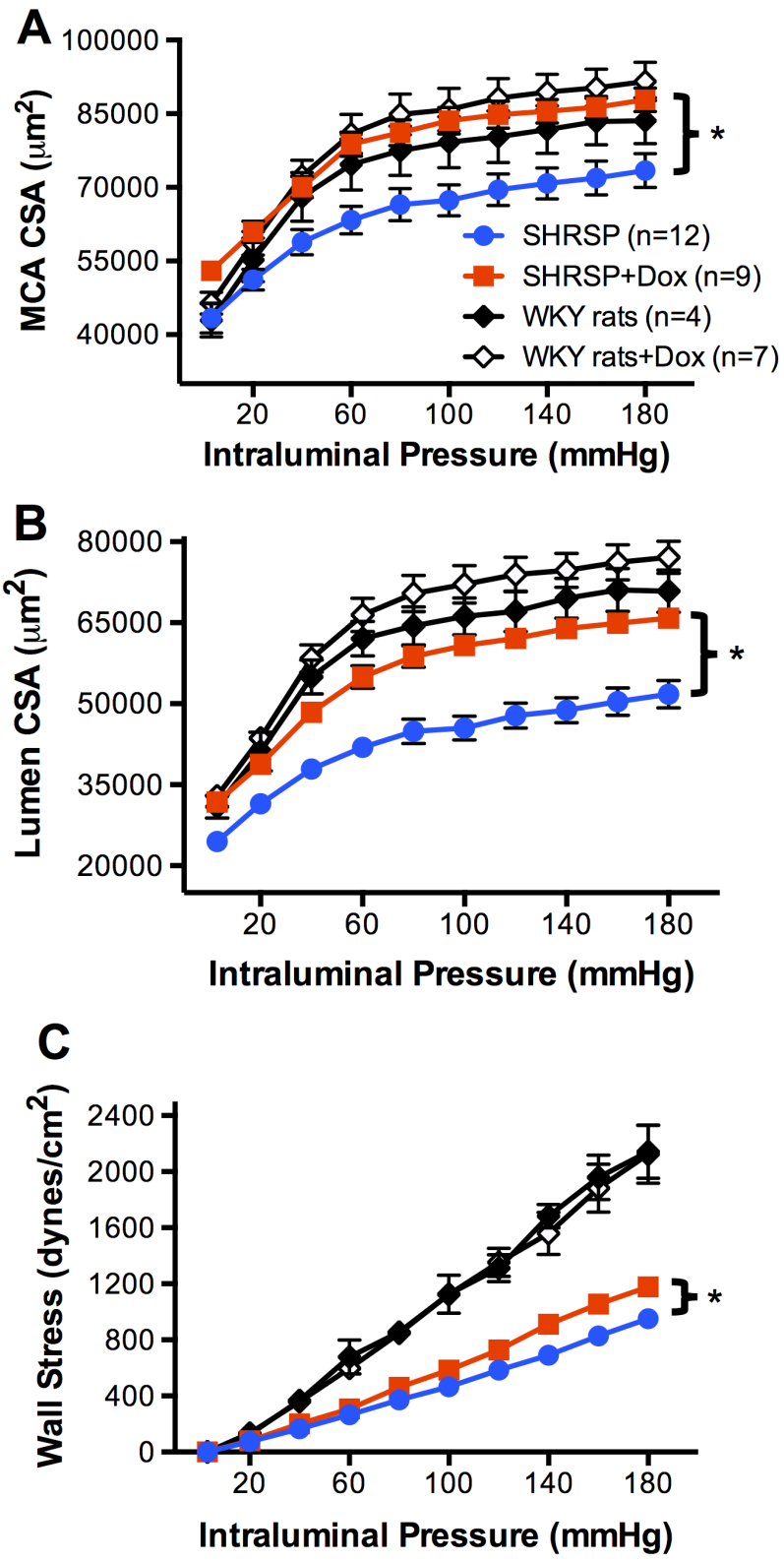

Figure 3.4: Dox treatment attenuated hypertensive remodeling of the MCA.

Figure 3.4 (cont'd)

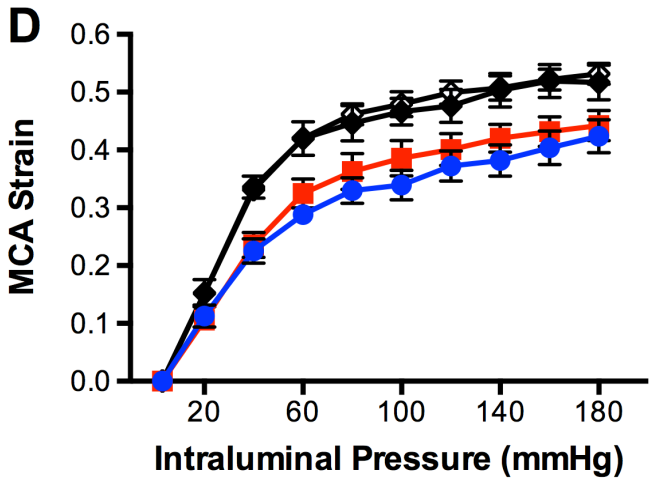

Outer (A) and lumen (B) CSA were significantly increased in the MCA from SHRSP+Dox when compared to untreated SHRSP, and not different from WKY rats±Dox. Intraluminal stress was higher in WKY rats±Dox than SHRSP+Dox and untreated SHRSP at intraluminal pressures above 60mmHg (C). SHRSP+Dox showed higher intraluminal stress than untreated SHRSP (C). Strain was not different between the experimental groups (D). Measurements were obtained from MCAs using pressure myography under no-flow and zero calcium conditions. Values are mean±SEM. *$p<0.001$, two-way ANOVA.

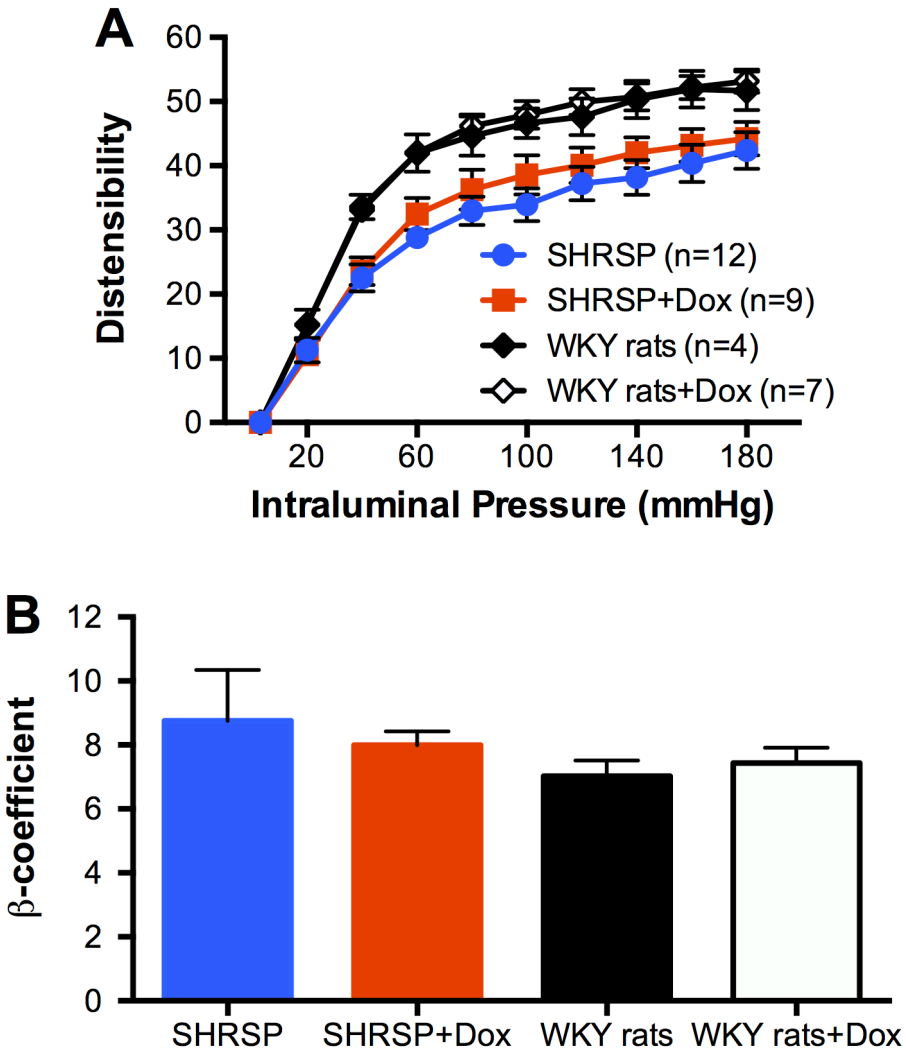

Figure 3.5: MCA distensibility and stiffness were not changed by Dox treatment. MCA from SHRSP had less distensibility than MCA from WKY rats, and Dox treatment did not change distensibility in either strain (A). The elastic modulus of the MCA (β-coefficient) was not increased in hypertensive animals when compared to normotensive WKY rats (B, number of animals: SHRSP=12, SHRSP+Dox=9, WKY rats=4, WKY rats+Dox=7).

3.4.6 - MRA passive structure. In the SHRSP, MRA remodeling was observed as an increase in wall thickness, wall CSA and wall-to-lumen ratio when compared to normotensive WKY rats±Dox (Figures 3.6A, 3.6B and 3.6C, respectively), without changes in outer (at 90mmHg: 320±10 vs 311±20μm, SHRSP vs WKY rats) and lumen diameter (at 90mmHg: 263±10 vs 280±20μm, SHRSP vs WKY rats). Dox treatment prevented the increase in wall thickness and wall CSA, thus leading to a decrease in wall-to-lumen ratio in SHRSP (Figures 3.6A, 3.6B and 3.6C, respectively). However, as with the MCA, no differences were observed in vessel distensibility (at 90mmHg: 73±5 vs 83±7, SHRSP vs SHRSP+Dox) or stiffness (β-coefficient: 5.53±0.46 vs 5.62±0.44, SHRSP vs SHRSP+Dox). Dox did not change MRA structure in normotensive WKY rats.

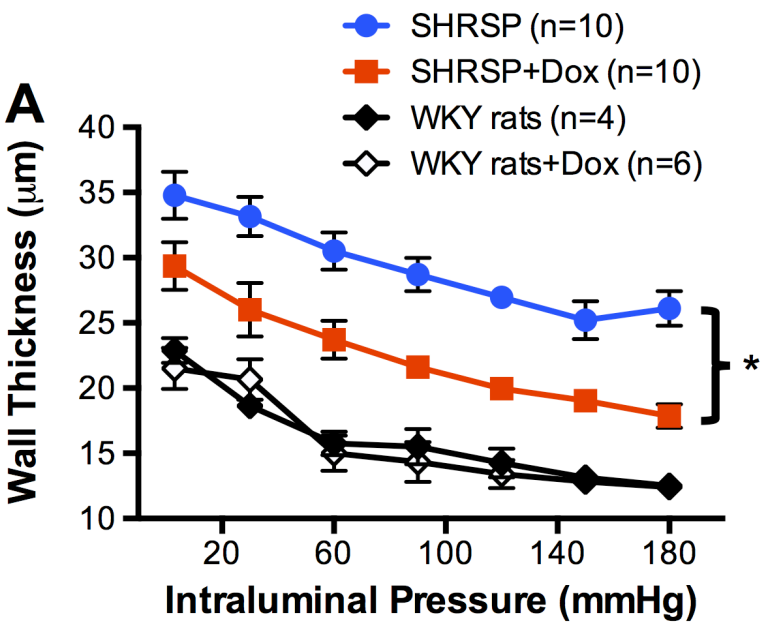

Figure 3.6: Chronic hypertension induces wall hypertrophy in MRA, and this was prevented by Dox treatment.

Figure 3.6 (cont'd)

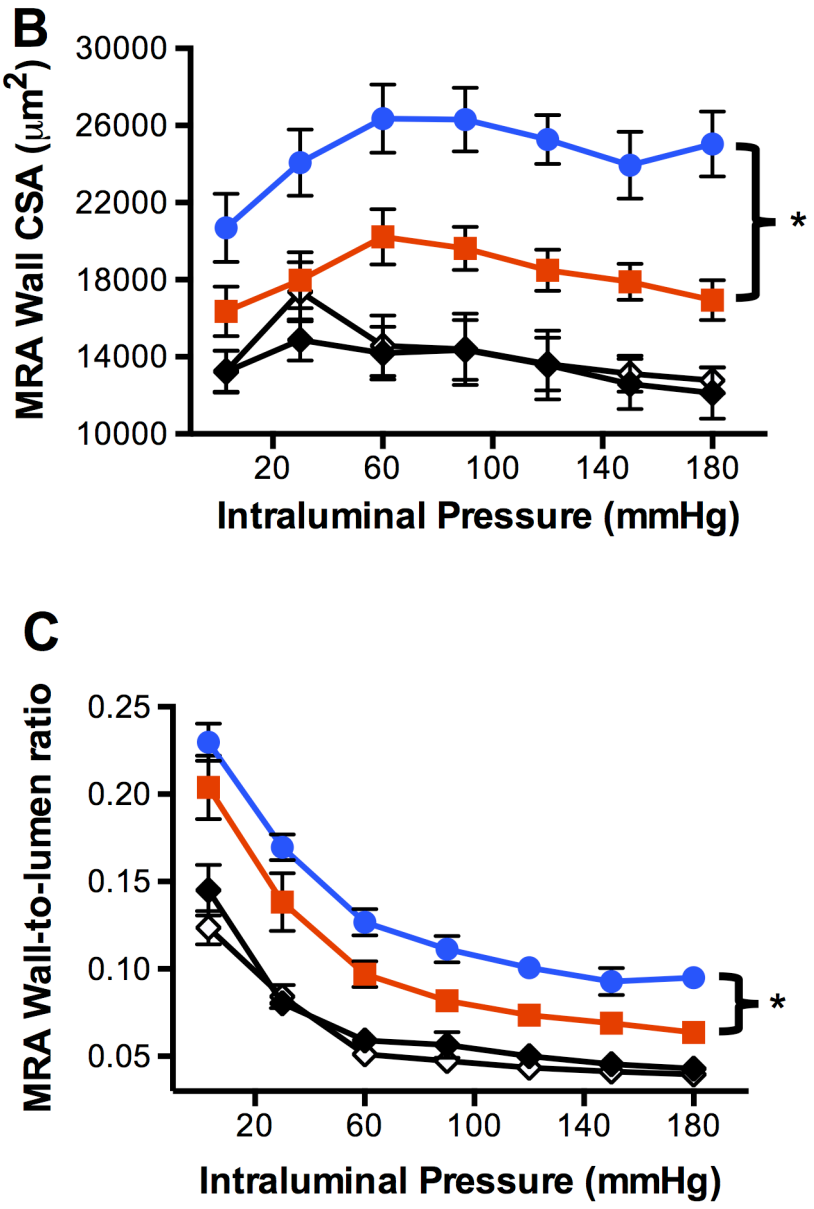

MRA wall thickness (A), wall CSA (B) and wall-to-lumen ratio (C) were increased in untreated SHRSP when compared to WKY rats±Dox. Dox treatment attenuated this increase in wall mass in SHRSP, although wall thickness and wall CSA were higher in SHRSP+Dox than WKY rats±Dox. Measurements were obtained from cannulated

MCAs using pressure myography under zero flow and calcium-free conditions. Values are mean±SEM. *p<0.001, two-way ANOVA.

3.4.7 - Cerebral ischemia. Dox treatment in SHRSP did not change infarct size after pMCAO (57.6±4.1 vs 57.4±3.7%HI, SHRSP vs SHRSP+Dox, Figure 3.7A). In addition, post-ischemic and 24 hours post-ischemic mean pial blood flow was not altered by Dox treatment in both the ischemic (Figure 3.7B) and non-ischemic (Figure 3.7C) hemispheres. Interestingly, Dox treatment reduced the brain damage caused by tMCAO in SHRSP. As shown in Figure 3.8A, SHRSP+Dox had a 50% reduction in the infarcted area in the brain (45.5±4.7 vs 20.7±3.8%HI, SHRSP vs SHRSP+Dox, p<0.05, Figure 3.8A). The reduction in infarct was accompanied by an increase in the pial blood flow 23 hours after reperfusion in the ischemic hemisphere (Figure 3.8B). Pial blood flow was not altered by Dox treatment at any other time point analyzed in the ischemic hemisphere (Figure 3.8B). In addition, blood flow was not different between SHRSP and SHRSP+Dox in the non-ischemic hemisphere at any time points analyzed (Figure 3.8C).

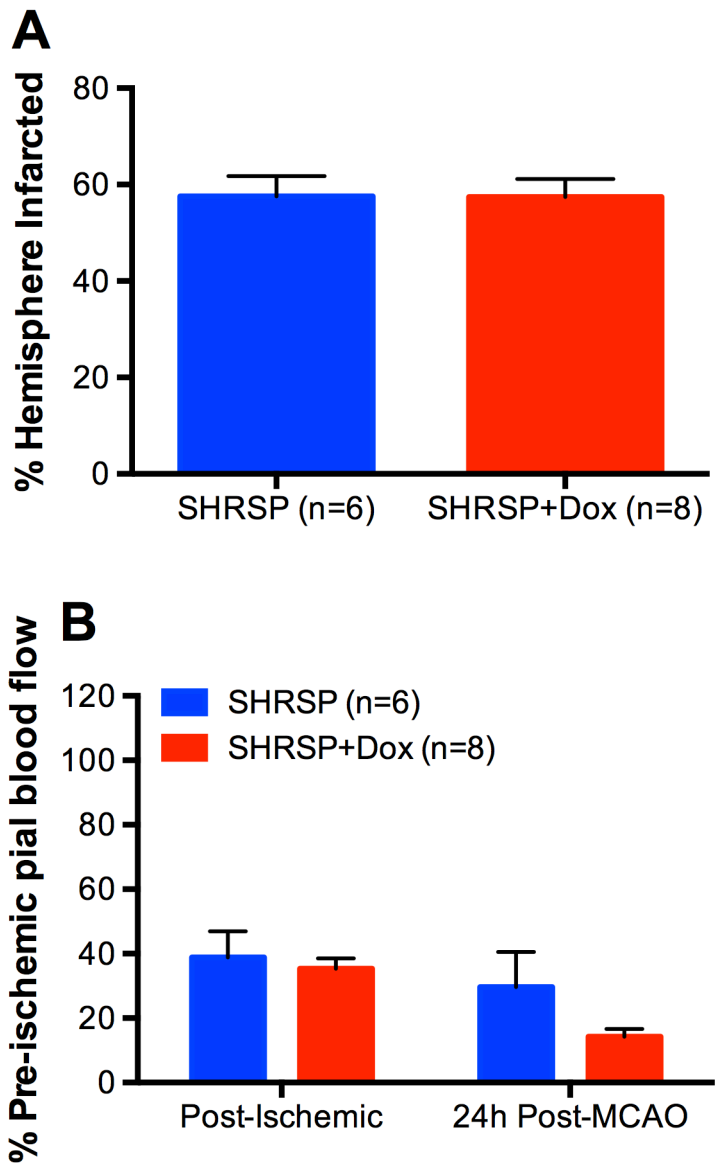

Figure 3.7: Dox treatment did not reduce cerebral damage after pMCAO.

Figure 3.7 (cont'd)

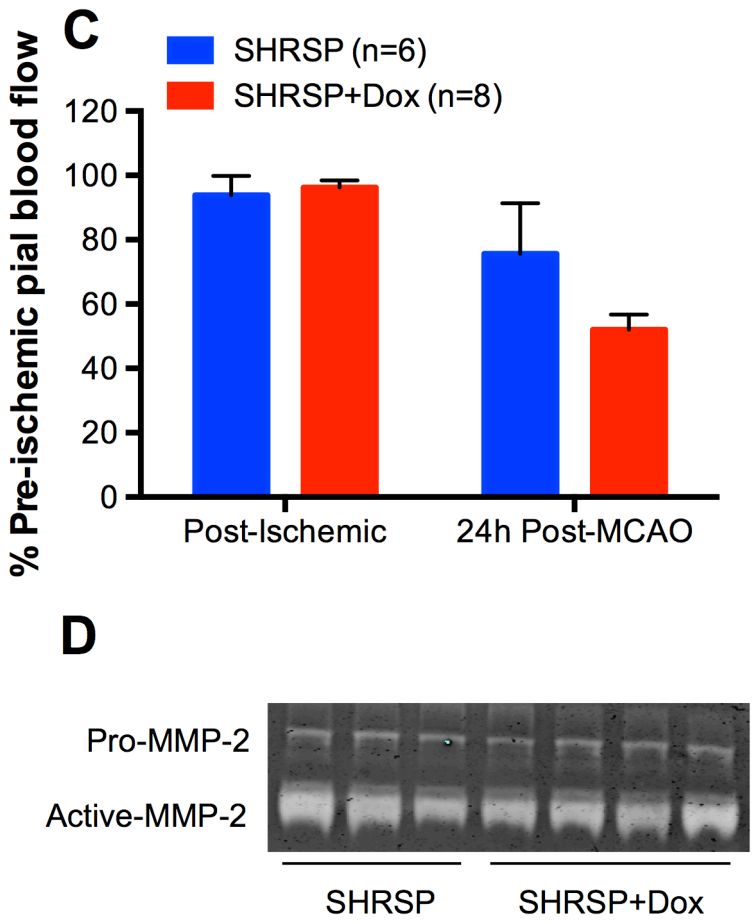

TTC staining of the brain of SHRSP that underwent pMCAO showed no differences in infarct size after Dox treatment (A). Data is expressed as %hemisphere infarcted (%HI). Pial blood flow, as measured by scanning laser Doppler, was also not altered by Dox treatment in the ischemic (B) and non-ischemic (C) hemispheres. Pial blood flow data is shown as %pre-ischemic blood flow. Values are mean±SEM. In panel D is a representative gelatin zymography of plasma samples 24 hours after cerebral ischemia. No difference was observed in activity of pro-MMP-2 and active MMP-2 between SHRSP and SHRSP+DOX. MMP-9 activity was not observed in the plasma of these animals.

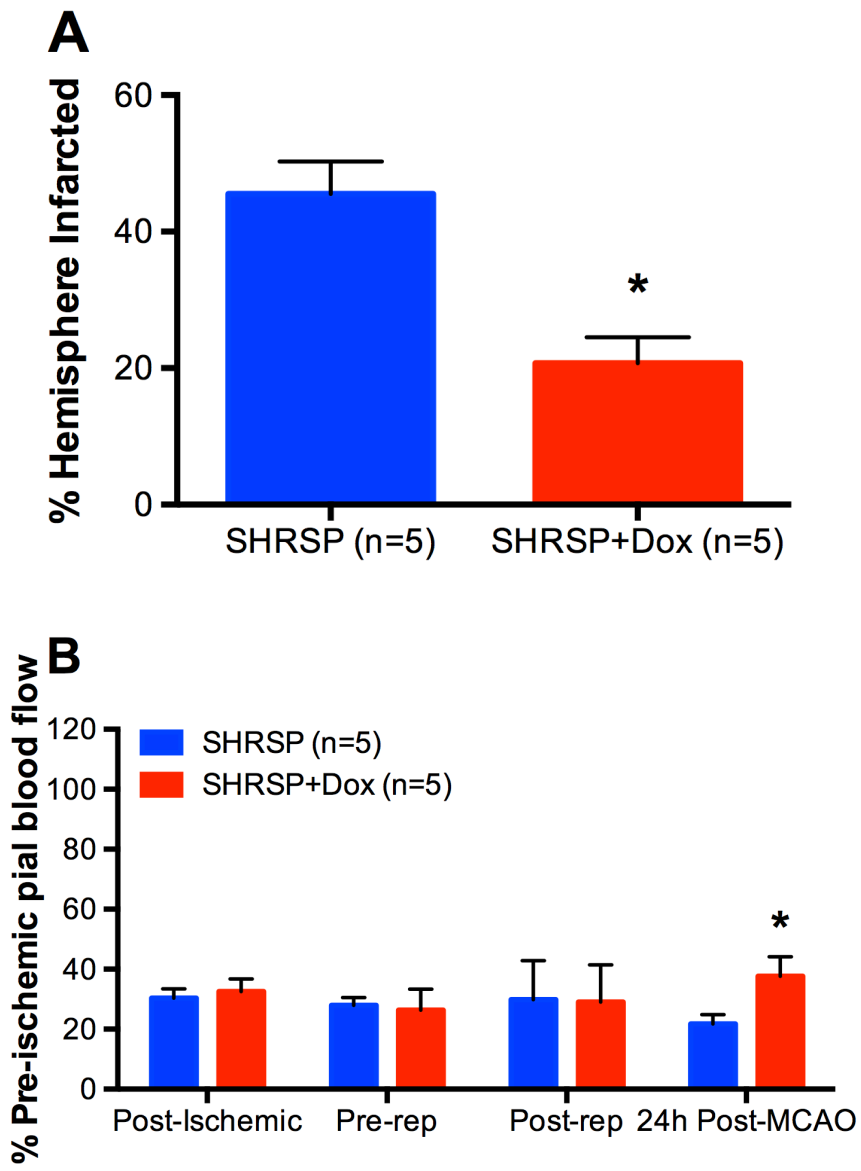

Figure 3.8: Dox treatment reduced cerebral damage after tMCAO and improved pial blood flow in SHRSP.

Figure 3.8 (cont'd)

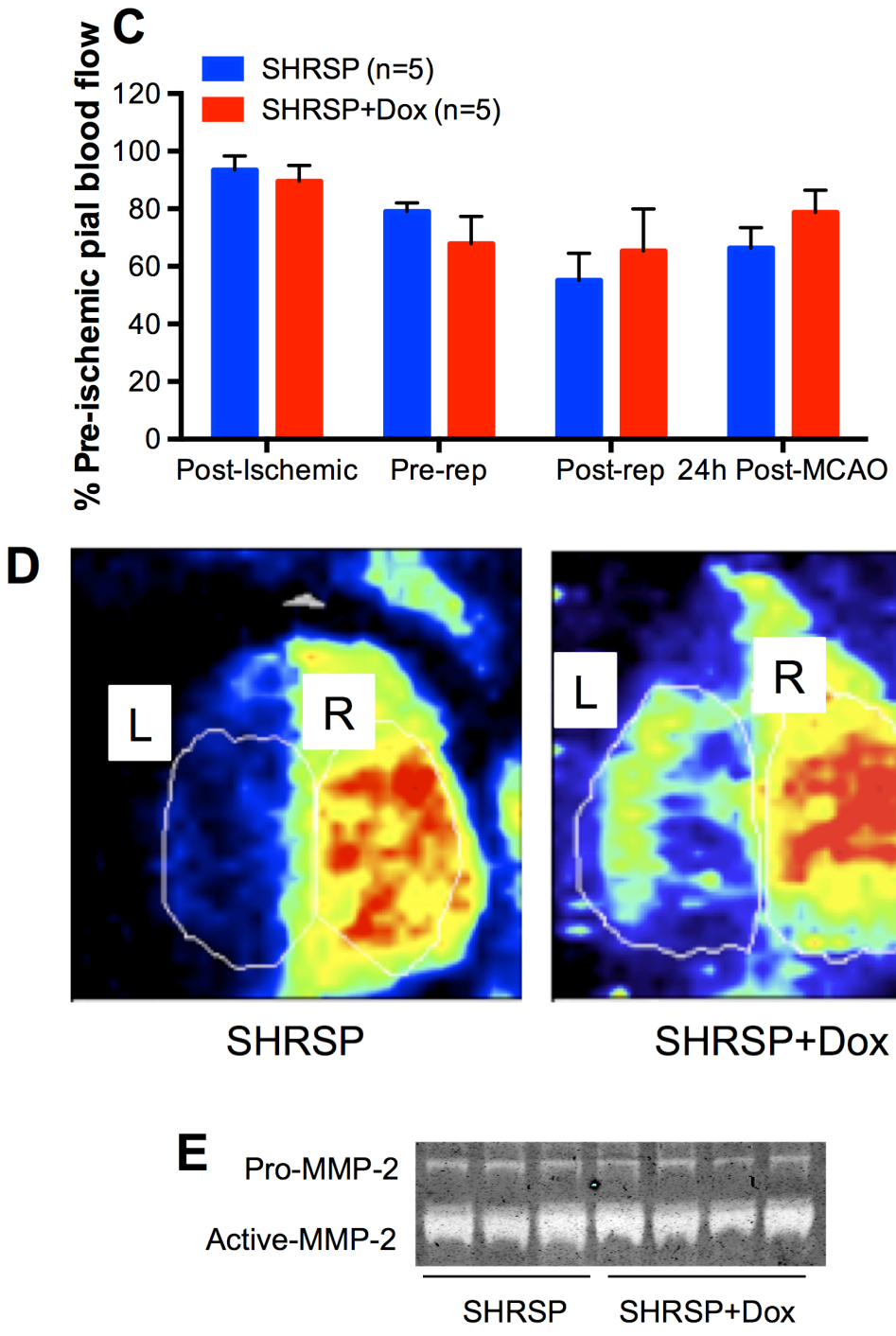

TTC staining of the brain of SHRSP that underwent tMCAO showed a reduction in infarct size in SHRSP+Dox (A, number of animals: SHRSP=5, SHRSP+Dox=5). The upper panels are representative images of infarcts from untreated SHRSP and

SHRSP+Dox. The white area is tissue damaged by ischemia, and the dark area is viable tissue. The lower panel shows cerebral infarct expressed as %hemisphere infarcted (%HI). The reduction in infarct was accompanied by an increase in pial blood flow in the ischemic hemisphere 23 hours after reperfusion, as measured by scanning laser Doppler (B). Pial blood flow in the non-ischemic hemisphere was not altered by Dox treatment (C). Pial blood flow data is shown as %pre-ischemic pial blood flow. Values are means±SEM. *p<0.05, *Student's* t-test. Panel D shows representative images of scanning laser Doppler 23 hours after reperfusion in untreated SHRSP (left image) and SHRSP+Dox (right image). In both images the left hemisphere is the ischemic hemisphere and the drawn line corresponds to the ROI (R: non-ischemic hemisphere; L: ischemic hemisphere). The color gradient in the images relates to perfusion: darker colors (black, blue) represent lower perfusion, and brighter colors (yellow, red) represent higher perfusion. Panel E is a representative gelatin zymography of plasma samples 24 hours after cerebral ischemia. No difference was observed in activity of pro-MMP-2 and active MMP-2 between SHRSP and SHRSP+Dox. MMP-9 activity was not observed in the plasma of these animals.

3.4.8 - Gelatin zymography. Activity of both the pre- and active- forms of MMP-2 in the plasma of the animals subjected to pMCAO (Figure 7D) or tMCAO (Figure 8E) was not altered by Dox. MMP-9 activity was not detected in the plasma of these animals.

3.4.9 - Thoracic aorta collagen and elastin content. Collagen content in the thoracic aorta was not changed by Dox treatment (0.064±0.008 vs 0.060±0.008 area collagen/wall area, SHRSP vs SHRSP+Dox). Similarly, Dox treatment did not alter elastin content (0.21±0.01 vs 0.22±0.1, area elastin/wall area, SHRSP vs SHRSP+Dox). As a consequence, the collagen/elastin ratio was not affected by Dox treatment (0.31±0.05 vs 0.29±0.10, SHRSP vs SHRSP+Dox).

3.5 - Discussion

Ischemic stroke is the major cause of adult disability in the United States. The only FDA-approved pharmacotherapy for ischemic stroke can be administered to only 4.5% of stroke patients. With very few available options for the treatment of stroke, to reduce stroke risk it seems prudent to identify therapies aimed at primary prevention. We have shown previously that improving MCA structure reduces the damage caused by cerebral ischemia [2, 4, 22]. In the present report we show that chronic Dox treatment attenuates the hypertensive vascular remodeling observed in SHRSP. This was associated with an increase in pial blood flow in the infarcted hemisphere 23 hours after reperfusion and decreased damage after tMCAO. Although tetracycline antibiotics are in clinical trials as acute therapies for stroke treatment [27], this is the first study showing beneficial protective effects to the brain and vasculature after chronic Dox treatment. Importantly, the beneficial effects on stroke outcome are not caused by an acute effect of Dox, since it was withdrawn 48 hours prior to the induction of cerebral ischemia.

MMP activity is triggered in the vessel wall by multiple stimuli. Alterations in flow [28] and increases in transmural pressure [29] stimulate MMP-2 and -9 activity in blood vessels. In addition, vasoactive compounds, particularly the components of the renin-angiotensin-aldosterone system (RAAS), are linked to increased MMP activity. Angiotensin (Ang) II stimulates MMP-2 and -9 expression in the rat thoracic aorta, independently of pressure [30], and MMP-2 gene expression is increased in aldosterone-induced hypertensive rats [31]. We have shown that the RAAS is an important factor involved in the MCA remodeling observed in SHRSP [2, 3]. It is possible that one of the mechanisms underlying aldosterone-dependent remodeling in the SHRSP is an up-regulation of MMP activity.

Many studies show that the MCA from hypertensive animals undergoes inward remodeling, which includes a reduction in lumen diameter [3, 4, 22, 32, 33]. This process begins in hypertensive rats early in the development of the disease [34]. These changes in MCA structure can be an adaptive mechanism to protect the vessel from increased stress [35] and prolonged vasoconstriction [36] observed during the rise in blood pressure. Independently of the etiology, the re-arrangement of the wall components will ultimately lead to a reduction in lumen CSA that may or may not be accompanied by wall hypertrophy. In this scenario, MMPs might play an important role, since they are the primary enzymes involved in ECM turnover within the vessel wall [13]. In the SHRSP, the blood pressure rises exponentially between 6 and 12 weeks of age [2]. During this time the remodeling process is highly active making this period attractive for interventions aimed to reduce vascular remodeling.

In the present study, we show that treatment of SHRSP with Dox attenuates MCA remodeling, observed as an increase in the MCA outer and lumen diameters, outer and lumen CSA and a reduction in wall-to-lumen ratio. Interestingly, vessel stiffness and distensibility were not changed by Dox treatment, suggesting that the alterations in structure observed are not due to changes in ECM composition. This is corroborated by the observation that the collagen and elastic fiber content in the aorta were not changed by Dox treatment despite the reduction in active-MMP-2 expression. We recognize that aortas are neither a resistance nor a cerebral blood vessel. However, they were used in this study to provide a measurement of MMP activity in the same animals used for vascular structure studies. MCA wall thickness was not reduced by Dox treatment. This is in agreement with our previous findings using the MR antagonist spironolactone [2] and potassium supplementation [22]. The increase in MCA wall thickness in SHRSP is an adaptive response to the increase in shear stress due to elevated intraluminal pressure. Thus, in Dox-treated SHRSP, the MCA remains protected against increased intraluminal shear stress as result of the slight increase in blood pressure. Importantly, none of the Dox-treated animals showed any evidence of intracerebral hemorrhage, an important consequence of elevation in blood pressure in SHRSP. Dox did not cause any alteration in MCA passive structure in normotensive WKY rats, suggesting that it attenuates vascular remodeling when a stimulus such as increased intraluminal pressure is present.

Interestingly, the remodeling process seems to be different in the MRA when compared to the MCA, since Dox had no effect on MRA lumen diameter. The reasons underlying these differences in remodeling behavior are not clear, but structural differences between these vessels might account for the disparity, at least in part. The MCA does not have an external elastic lamina [37], whereas MRA do. Moreover, MRA are surrounded by perivascular adipose tissue (PVAT), and the MCA is not. PVAT is associated with vascular inflammation and ROS generation in the vasculature [38], and both processes are linked to remodeling [39, 40]. Lastly, the physiological role of the vascular bed in regulation of systemic BP might also account for the differences. The mesenteric bed receives 15-20% of the cardiac output, thus contributing largely to total peripheral resistance (TPR) and BP regulation. Since lumen diameter is a major determinant of TPR [8], it is possible that the lack of increase in lumen diameter is a consequence of the maintenance of TPR to prevent drops in blood pressure. However, to evaluate this we would need to study tone generation and reactivity of these vessels, and this was not possible in the current study. Despite that, the results observed in the MRA are still positive, since we did not observe reduction in BP in SHRSP+Dox.

We [2-4] and others [41] have shown that MCA passive structure is associated with the extent of damage following cerebral ischemia. During occlusion of the MCA, collateral vessels dilate in order to supply blood to the ischemic hemisphere in an attempt to reduce tissue hypoxia. In the SHRSP, the ability of the collateral vessels to dilate in response to ischemia is impaired [42]. In animals subjected to pMCAO, this vasodilator mechanism is one of the major factors that modulate the extent of cerebral damage. In our experiment, Dox treatment had no effect on pial blow flow after pMCAO.

Importantly, tone generation and BK-induced vasodilation in the MCA were not changed by Dox treatment despite the improvement in MCA structure. Thus, it is possible that when facing hypoxia, the collateral vessels still exhibited impaired vasodilation, resulting in no reduction in infarct size.

Interestingly, Dox treatment reduced brain damage after tMCAO and improved pial blood flow in the ischemic hemisphere 23 hours after reperfusion. This improvement could be explained by the fact that the MCA lumen diameter in DOX-treated SHRSP was greatly increased. In this model of cerebral ischemia, the blockage of the MCA was removed after 60 minutes, allowing reperfusion of the vessel. During reperfusion, the ability of the MCA to generate tone is diminished [43, 44] and vasodilation is augmented [45]. Together, these responses might lead to a maximal dilation of the MCA. Blood flow under these conditions might be determined mainly by the lumen diameter of the cerebral vasculature. In fact, pial blood flow in the ischemic hemisphere was greater in SHRSP+Dox 23 hours after reperfusion than in untreated SHRSP. Interestingly, in SHRSP with or without Dox, pial blood flow 23 hours post-reperfusion was less than pre-ischemic blood flow. This could be a direct consequence of impaired vasodilation of the collateral circulation. Other factors such as hypotension and microvascular obstructions could also reduce blood flow. The current study does not discard these possibilities. Importantly, the occlusion of the MCA was similar in both groups, since the pial blood flow immediately after MCAO was not different between groups and we observed a similar drop in blood flow in the MCA territory by laser Doppler. In addition,

plasma MMP-2 activity was not different between the groups, suggesting that MMP inhibition was not present 24 hours after ischemia.

One caveat to our measurement of blood flow is that it was measured through an intact skull. Therefore the perfusion units reported are a combination of skull, pial and cortical blood flow. We opted not to perform a craniotomy in order to produce as physiologically relevant a stroke as possible. The rats used were 12-weeks-old and have relatively thin skulls, hence thinning of their skulls was not necessary. In addition, the raw perfusion in the ischemic core is almost undetectable when analyzed by scanning laser Doppler, suggesting that the contribution of flow from the skull and dura is minimal.

Other mechanisms might account for the reduction in infarct after tMCAO in SHRSP+Dox. Tetracycline antibiotics such as Dox have important anti-inflammatory activities, and this could potentially reduce the damage after ischemia [46]. Even though Dox was not present in the animals at the time of ischemia, it is possible that the anti-inflammatory effects are longer lasting. Another important effect is protection of the blood-brain-barrier (BBB). MMPs have been implicated in BBB disruption following transient ischemia [47, 48] and hemorrhagic transformation after reperfusion [49]. The potential that BBB breakdown is reduced in SHRSP+Dox warrants further investigation.

In summary, the present study shows that Dox treatment attenuates hypertensive vascular remodeling despite the small increase in blood pressure associated with Dox

treatment. Moreover, it reduces the damage caused by tMCAO. Further studies need to be performed to elucidate the underlying mechanisms of these effects.

3.6 - Conclusion

Ischemic stroke is the major cause of adult disability in the United States, and the third leading cause of death. Therapeutic options for patients with cerebral ischemia are few. All the treatments consist of removal of the clot, either pharmacologically or mechanically, and they have intrinsic risks. Hence, therapies aimed at primary prevention of cerebral ischemia might become an important tool for management of patients at high risk, such as in the case of hypertensive patients with uncontrolled blood pressure. To this end, development of strategies to attenuate cerebrovascular remodeling would be valuable. In this context, Dox might be useful, since it is a well-tolerated and inexpensive tetracycline antibiotic that could be administered chronically.

REFERENCES

REFERENCES

1. Fitchett, D., *Results of the ONTARGET and TRANSCEND studies: an update and discussion.* Vasc Health Risk Manag, 2009. **5**(1): p. 21-9.

2. Rigsby, C.S., D.M. Pollock, and A.M. Dorrance, *Spironolactone improves structure and increases tone in the cerebral vasculature of male spontaneously hypertensive stroke-prone rats.* Microvasc Res, 2007. **73**(3): p. 198-205.

3. Dorrance, A.M., N.C. Rupp, and E.F. Nogueira, *Mineralocorticoid receptor activation causes cerebral vessel remodeling and exacerbates the damage caused by cerebral ischemia.* Hypertension, 2006. **47**(3): p. 590-5.

4. Dorrance, A.M., et al., *A high-potassium diet reduces infarct size and improves vascular structure in hypertensive rats.* Am J Physiol Regul Integr Comp Physiol, 2007. **292**(1): p. R415-22.

5. Osmond, J.M. and A.M. Dorrance, *11beta-hydroxysteroid dehydrogenase type II inhibition causes cerebrovascular remodeling and increases infarct size after cerebral ischemia.* Endocrinology, 2009. **150**(2): p. 713-9.

6. Heagerty, A.M., et al., *Small artery structure in hypertension. Dual processes of remodeling and growth.* Hypertension, 1993. **21**(4): p. 391-7.

7. Baumbach, G.L. and S. Ghoneim, *Vascular remodeling in hypertension.* Scanning Microsc, 1993. **7**(1): p. 137-42; discussion 143.

8. Mulvany, M.J., *Vascular remodelling of resistance vessels: can we define this?* Cardiovasc Res, 1999. **41**(1): p. 9-13.

9. Feihl, F., et al., *Hypertension and microvascular remodelling.* Cardiovasc Res, 2008. **78**(2): p. 274-85.

10. Raffetto, J.D. and R.A. Khalil, *Matrix metalloproteinases and their inhibitors in vascular remodeling and vascular disease.* Biochem Pharmacol, 2008. **75**(2): p. 346-59.

11. Flamant, M., et al., *Role of matrix metalloproteinases in early hypertensive vascular remodeling.* Hypertension, 2007. **50**(1): p. 212-8.

12. Nagase, H., R. Visse, and G. Murphy, *Structure and function of matrix metalloproteinases and TIMPs.* Cardiovasc Res, 2006. **69**(3): p. 562-73.

13. Galis, Z.S. and J.J. Khatri, *Matrix metalloproteinases in vascular remodeling and atherogenesis: the good, the bad, and the ugly.* Circ Res, 2002. **90**(3): p. 251-62.

14. Deutsch, C., et al., *Diet-induced obesity causes cerebral vessel remodeling and increases the damage caused by ischemic stroke.* Microvasc Res, 2009. **78**(1): p. 100-6.

15. Castro, M.M., et al., *Antioxidant Treatment Reduces Matrix Metalloproteinase-2-Induced Vascular Changes in Renovascular Hypertension.* Free Radic Biol Med, 2009.

16. Castro, M.M., et al., *Metalloproteinase inhibition ameliorates hypertension and prevents vascular dysfunction and remodeling in renovascular hypertensive rats.* Atherosclerosis, 2008. **198**(2): p. 320-31.

17. Castro, M.M., et al., *Imbalance between matrix metalloproteinases and tissue inhibitor of metalloproteinases in hypertensive vascular remodeling.* Matrix Biol, 2010. **29**(3): p. 194-201.

18. King, A.J., J.W. Osborn, and G.D. Fink, *Splanchnic circulation is a critical neural target in angiotensin II salt hypertension in rats.* Hypertension, 2007. **50**(3): p. 547-56.

19. Cipolla, M.J., et al., *Threshold duration of ischemia for myogenic tone in middle cerebral arteries: effect on vascular smooth muscle actin.* Stroke, 2001. **32**(7): p. 1658-64.

20. Baumbach, G.L. and M.A. Hajdu, *Mechanics and composition of cerebral arterioles in renal and spontaneously hypertensive rats.* Hypertension, 1993. **21**(6 Pt 1): p. 816-26.

21. Longa, E.Z., et al., *Reversible middle cerebral artery occlusion without craniectomy in rats.* Stroke, 1989. **20**(1): p. 84-91.

22. Rigsby, C.S., D.M. Pollock, and A.M. Dorrance, *Dietary potassium supplementation improves vascular structure and ameliorates the damage caused by cerebral ischemia in normotensive rats.* Nutr Metab (Lond), 2008. **5**: p. 3.

23. English, A.R., *Apha-6-deoxyocytetracycline. 3. Total and unbound antibiotic serum concentrations after oral administration to mice.* Proc Soc Exp Biol Med, 1967. **126**(2): p. 487-91.

24. Swanson, R.A., et al., *A semiautomated method for measuring brain infarct volume.* J Cereb Blood Flow Metab, 1990. **10**(2): p. 290-3.

25. Junquiera, L.C., L.C. Junqueira, and R.R. Brentani, *A simple and sensitive method for the quantitative estimation of collagen.* Anal Biochem, 1979. **94**(1): p. 96-9.

26. Junqueira, L.C., G. Bignolas, and R.R. Brentani, *Picrosirius staining plus polarization microscopy, a specific method for collagen detection in tissue sections.* Histochem J, 1979. **11**(4): p. 447-55.

27. Fagan, S.C., et al., *Minocycline to Improve Neurologic Outcome in Stroke (MINOS). A Dose-Finding Study.* Stroke, 2010.

28. Bassiouny, H.S., et al., *Flow regulation of 72-kD collagenase IV (MMP-2) after experimental arterial injury.* Circulation, 1998. **98**(2): p. 157-63.

29. Chesler, N.C., D.N. Ku, and Z.S. Galis, *Transmural pressure induces matrix-degrading activity in porcine arteries ex vivo.* Am J Physiol, 1999. **277**(5 Pt 2): p. H2002-9.

30. Ruddy, J.M., et al., *Differential effects of mechanical and biological stimuli on matrix metalloproteinase promoter activation in the thoracic aorta.* Circulation, 2009. **120**(11 Suppl): p. S262-8.

31. Sakurada, M., et al., *Vasculoprotective effect of cilostazol in aldosterone-induced hypertensive rats.* Hypertens Res, 2009.

32. Hajdu, M.A. and G.L. Baumbach, *Mechanics of large and small cerebral arteries in chronic hypertension.* Am J Physiol, 1994. **266**(3 Pt 2): p. H1027-33.

33. Izzard, A.S., et al., *Myogenic and structural properties of cerebral arteries from the stroke-prone spontaneously hypertensive rat.* Am J Physiol Heart Circ Physiol, 2003. **285**(4): p. H1489-94.

34. Izzard, A.S., et al., *Small artery structure and hypertension: adaptive changes and target organ damage.* J Hypertens, 2005. **23**(2): p. 247-50.

35. Folkow, B., G. Grimby, and O. Thulesius, *Adaptive structural changes of the vascular walls in hypertension and their relation to the control of the peripheral resistance.* Acta Physiol Scand, 1958. **44**(3-4): p. 255-72.

36. Short, D., *Morphology of the intestinal arterioles in chronic human hypertension.* Br Heart J, 1966. **28**(2): p. 184-92.

37. Lee, R.M., *Morphology of cerebral arteries.* Pharmacol Ther, 1995. **66**(1): p. 149-73.

38. Marchesi, C., et al., *Endothelial nitric oxide synthase uncoupling and perivascular adipose oxidative stress and inflammation contribute to vascular dysfunction in a rodent model of metabolic syndrome.* Hypertension, 2009. **54**(6): p. 1384-92.

39. Touyz, R.M., *Reactive oxygen species and angiotensin II signaling in vascular cells -- implications in cardiovascular disease.* Braz J Med Biol Res, 2004. **37**(8): p. 1263-73.

40. Intengan, H.D. and E.L. Schiffrin, *Vascular remodeling in hypertension: roles of apoptosis, inflammation, and fibrosis.* Hypertension, 2001. **38**(3 Pt 2): p. 581-7.

41. Osmond, J.M., et al., *Obesity increases blood pressure, cerebral vascular remodeling, and severity of stroke in the Zucker rat.* Hypertension, 2009. **53**(2): p. 381-6.

42. Coyle, P. and D.D. Heistad, *Blood flow through cerebral collateral vessels in hypertensive and normotensive rats.* Hypertension, 1986. **8**(6 Pt 2): p. II67-71.

43. Cipolla, M.J., et al., *Reperfusion decreases myogenic reactivity and alters middle cerebral artery function after focal cerebral ischemia in rats.* Stroke, 1997. **28**(1): p. 176-80.

44. Cipolla, M.J. and A.B. Curry, *Middle cerebral artery function after stroke: the threshold duration of reperfusion for myogenic activity.* Stroke, 2002. **33**(8): p. 2094-9.

45. Marrelli, S.P., et al., *P2 purinoceptor-mediated dilations in the rat middle cerebral artery after ischemia-reperfusion.* Am J Physiol, 1999. **276**(1 Pt 2): p. H33-41.

46. Jin, R., G. Yang, and G. Li, *Inflammatory mechanisms in ischemic stroke: role of inflammatory cells.* J Leukoc Biol, 2010. **87**(5): p. 779-89.

47. Rosenberg, G.A., E.Y. Estrada, and J.E. Dencoff, *Matrix metalloproteinases and TIMPs are associated with blood-brain barrier opening after reperfusion in rat brain.* Stroke, 1998. **29**(10): p. 2189-95.

48. Lee, C.Z., et al., *Matrix metalloproteinase-9 inhibition attenuates vascular endothelial growth factor-induced intracerebral hemorrhage.* Stroke, 2007. **38**(9): p. 2563-8.

49. Rosenberg, G.A. and Y. Yang, *Vasogenic edema due to tight junction disruption by matrix metalloproteinases in cerebral ischemia.* Neurosurg Focus, 2007. **22**(5): p. E4.

CHAPTER 4

Tumor necrosis factor-alpha inhibition attenuates middle cerebral artery remodeling but increases infarct size after cerebral ischemia in stroke-prone spontaneously hypertensive rats.

4.1 - Abstract

Hypertension leads to vascular inflammation evidenced by an increase in perivascular macrophages and proinflammatory cytokines in the arterial wall. Removal of perivascular macrophages reduced tumor necrosis factor (TNF)-α expression in cerebral arteries and attenuates inward remodeling, suggesting that this cytokine might be a mediator of inflammation-induced changes in the hypertensive vasculature. Thus, we hypothesized that TNF-α inhibition would improve the structure of the middle cerebral artery (MCA) and reduce damage after cerebral ischemia in hypertensive rats. Six-week-old male stroke-prone spontaneously hypertensive rats (SHRSP) were treated with the TNF-α inhibitor etanercept (ETN, 1.25mg/kg/day i.p. daily) or PBS (equivolume) for 6 weeks. MCAs were cannulated in a pressure myograph to study myogenic tone generation, constriction and passive structure. Cerebral ischemia was induced by MCA occlusion (MCAO). Basal pial artery flow was higher in SHRSP+ETN than SHRSP+PBS. There was no difference in myogenic tone generation, but MCAs from SHRSP+ETN showed increased constriction to serotonin. ETN treatment increased the lumen diameter and reduced the wall thickness and wall-to-lumen ratio of the MCA in SHRSP. Cerebral infarct size was increased in SHRSP+ETN after transient MCAO, despite an improvement in dilation of non-ischemic MCA. There was no difference in infarct size after permanent MCAO. Our data suggests that TNF-α inhibition attenuates

hypertensive MCA remodeling but exacerbates cerebral damage following ischemia/ reperfusion injury.

4.2 - Introduction

Cerebrovascular accidents are a major cause of adult disability in developed countries [1]. In recent years much effort has been directed to developing neuroprotective strategies to improve the outcome of cerebral ischemia, with few translational achievements. Primary prevention remains an important strategy to manage individuals at risk of having a stroke. Hypertension is a primary risk factor for stroke, and hypertension-induced remodeling of cerebral arteries has been linked to larger infarcts following experimentally-induced cerebral ischemia [2, 3]. The mechanisms underlying hypertensive cerebral artery remodeling have not been fully elucidated, but we recently showed that macrophage-mediated vascular inflammation is involved in this process [4].

Inflammatory mediators play a role in the pathophysiology of hypertension and end-organ damage. Many circulating factors known to be important in hypertension induce vascular inflammation, including angiotensin II [5], aldosterone [6] and endothelin-I [7]. These factors are also associated with hypertensive vascular remodeling [8-10]. Thus, it is possible that vascular inflammation is in part responsible for the remodeling and vascular damage induced by these vasoactive mediators, particularly through proinflammatory cytokines, including tumor necrosis factor (TNF)-α. We recently proposed that TNF-α might be involved in hypertensive remodeling of both the cerebral and mesenteric vasculatures [4]. Further, other studies showed that TNF-α is involved

in the renal damage observed in hypertensive salt-sensitive rats [11, 12], and TNF-α inhibition reduces infarct following cerebral ischemia in normotensive rats [13]. Thus, we hypothesized that TNF-α inhibition with etanercept (ETN) would attenuate remodeling of the middle cerebral artery (MCA) and mesenteric resistance arteries (MRA) in hypertensive rats, as well as reduce infarct after cerebral ischemia in stroke-prone spontaneously hypertensive rats (SHRSP). The structure of the MCA and third order MRA was assessed by pressure myography. Pial blood flow was measured by scanning laser Doppler flowmetry and ischemic stroke was achieved by the intraluminal suture model for MCA occlusion.

4.3 - Methods

4.3.1 - Animals and treatment. Six week-old male SHRSP from the colony housed at Michigan State University were randomized into two groups: one group was treated with the TNF-α inhibitor ETN (1.25mg/kg i.p. daily) or an equal volume of PBS (vehicle) i.p. daily . Rats were treated with ETN or PBS 6 to 12 weeks of age. We have previously shown that treatments during this period are efficacious in attenuating vascular remodeling [4, 14, 15]. Rats were maintained on a 12:12hr light: dark cycle, with tap water and regular chow *ad libitum*. At 12 weeks of age, rats were anesthetized with 3% isoflurane, weighed and euthanized by decapitation after exsanguination. All organs used in this study were harvested after decapitation. The experimental protocol was approved by the Institutional Animal Care & Use Committee and was in accordance with the American Physiological Society's "Guiding Principles in the Care and Use of Animals."

A separate group of 12-weeks-old male SHRSP was used to assess the effects of acute ETN treatment. Rats were subjected to transient middle cerebral artery occlusion (protocol described below) and received ETN (1.25mg/kg, i.p.) or equivolume PBS at reperfusion and 24 hours after ischemia.

4.3.2 - Measurement of arterial pressure. Blood pressure during the last week of treatment was measured by tail-cuff using a RTBP1001 tail-cuff blood pressure system (Kent Scientific, Torrington CT) as described previously [14].

4.3.3 - Pressure myography studies. MCA function and structure were assessed by pressure myography (Danish Myo Technology, Aarhus, Denmark) as described previously [15]. Briefly, we analyzed MCA spontaneous myogenic tone generation, contractility to 5-hydroxytriptamine (5-HT), and structural and mechanical properties. MCAs were equilibrated in oxygenated (95%O_2, 5% CO_2) physiological salt solution (PSS, in mmol: 141.9 NaCl, 4.7 KCl, 1.12 KH_2PO_4, 1.7 $MgSO_4 \bullet 7H_2O$, 2.8 $CaCl_2$, 10 Hepes, 5 Dextrose, 0.5 EDTA, pH 7.4) until development of spontaneous myogenic tone, which was calculated using the following formula: %tone = [1-(active lumen diameter/passive lumen diameter)] x 100. MCA contractility to 5-HT was assessed by a cumulative concentration-response curve (1nmol/L to 100μmol/L). The MCA was incubated for 10 minutes at each concentration until a steady state of contraction was achieved before the measurement of diameter was performed. Passive structure was assessed with calcium-free PSS containing 2mmol/L EGTA plus 10μmol/L sodium

nitroprusside and intraluminal pressure was increased from 3 to 180mmHg in 20mmHg increments. The wall-to-lumen ratio and circumferential wall stress and were calculated [16]. Passive distensibility was calculated as described previously [17]. The elastic modulus (β-coefficient) was calculated from the stress/strain curves using an exponential model ($y=ae^{\beta x}$) where β is the slope of the curve and is directly correlated to vascular stiffness.

MRA passive structure was assessed with calcium-free PSS containing 2mmol/L EGTA plus 10µmol/L sodium nitroprusside and intraluminal pressure was increased from 3 to 180mmHg with 30mmHg increments. All structural parameters analyzed in the MCA were analyzed in the MRA.

4.3.4 - MCA occlusion. Cerebral ischemia was induced using the intraluminal suture model of MCA occlusion [18]. Rats were initially anesthetized with isoflurane in an induction chamber, and anesthesia was maintained with 2% isoflurane in oxygen; body temperature was maintained at 37°C. An incision was made in the top of the head to expose the skull for measurement of pial blood flow by scanning laser Doppler flowmetry and attachment of a laser Doppler flow probe to measure blood flow to the region supplied by the MCA (5mm lateral and 1mm posterior to the bregma). A midline incision was made to expose the carotid artery. The lingual and thyroid arteries were cauterized, and the external carotid was tied off with suture. A 3-0 nylon monofilament with a rounded end (Doccol, Redland, CA) was inserted into the common carotid artery. This monofilament was then advanced through the internal carotid artery to block blood

flow to the MCA where it branches from the circle of Willis. MCA occlusion was verified by a drop in blood flow as measured by both scanning laser Doppler flowmetry and the Doppler flow probe. One set of rats was subjected to transient ischemia (tMCAO). The MCAO was performed as described above, and ischemia was maintained for 1 hour followed by 47 hours of reperfusion. Rats were then anesthetized and decapitated, the brain was removed and sliced into 2 mm sections for subsequent staining with 2% 2,3,5-triphenyltetrazolium chloride (TTC) for 20 minutes to assess ischemic damage. With this staining the area of viable tissue will stain pink and areas of infarcted tissue will remain white. Brain slices were fixed in 4% paraformaldehyde, and digital images were taken. The percentage of infarction was determined by the following equation: %Hemisphere Infarcted = ((VC-VL)/VC)*100 where VC is the volume of normal tissue in the non-ischemic hemisphere and VL is the volume of normal tissue in the ischemic hemisphere [19].

Another set of rats was subject to permanent MCAO (pMCAO) with the ischemia duration of 24 hours, after which the rats were anesthetized and decapitated, the brain was removed and measurement of ischemic damage was performed as described above.

4.3.5 - Scanning laser Doppler flowmetry. Pial blood flow was measured as described previously by our laboratory [15]. Briefly, under anesthesia, the rat's skull was exposed and cleaned and pial blood flow was analyzed in both cerebral hemispheres. The time-points were analyzed were: prior to surgery, immediately after MCAO, before

and after reperfusion (in animals subjected to tMCAO) and immediately prior to euthanasia. Mean perfusion in each hemisphere was measured using the LDPIwin 3.1 software (Perimed). Pial blood flow data are expressed a % of pre-ischemic blood flow in each hemisphere (for MCAO studies) or perfusion units (for basal pial blood flow).

4.3.6 - Endothelium-dependent dilation of the non-ischemic MCA after tMCAO. Endothelial function of the non-ischemic MCA was assessed by intraluminal perfusion of ADP in a pressure myograph. A branch-free segment of the MCA from the non-ischemic hemisphere (contralateral) was isolated and mounted between two glass cannulas in a pressure myograph chamber, which was then placed in an inverted microscope (Nikon) coupled to a camera. The MCA was then bathed in PSS, pressurized at 80mmHg and maintained under physiological flow rate (20dynes/cm^2) in order to generate spontaneous myogenic tone. Increasing concentrations of ADP (0.1nmol/L to 10µmol/L) were then added to the intraluminal perfusate, and changes in MCA diameter were recorded by the MyoView software (Danish Myo Technology, Aarhus, Denmark).

4.3.7 - Statistical analyses. Body weight, heart/ body weight, kidney/ body weight, blood pressure, spontaneous myogenic tone generation, basal pial blood flow and infarct size (%HI) data were analyzed by Student's t-test or a non-parametric alternative when the data did not fit a normal distribution model. Data regarding MCA contractility to 5-HT and dilation to ADP, MCA and MRA passive structure and post-ischemic pial blood flow were analyzed by Two-Way Analysis of Variance (ANOVA) or a non-parametric test. Bonferroni's correction for multiple comparisons was performed as a

post-test. All statistical analyses were carried out using the GraphPad Prism 6.0 software (GraphPad, San Diego, CA, USA). Difference between means was considered statistically significant when $p < 0.05$.

4.4 - Results

4.4.1 - Physiological variables. Data describing blood pressure, body weight and organs weight are summarized in Table 4.1. Briefly, ETN treatment did not alter blood pressure, body weight, heart/body weight and kidney/body weight in SHRSP.

Table 4.1: Physiological variables after ETN treatment in SHRSP.

	SHRSP+PBS (n=8)	SHRSP=ETN (n=8)
Body weight (g)	253 ± 7	246 ± 5
Heart/ body weight ratio	0.534 ± 0.01	0.539 ± 0.01
Kidney/ body weight ratio	0.986 ± 0.03	0.981 ± 0.01
Systolic blood pressure (mmHg)	208 ± 7	198 ± 3*
Diastolic blood pressure (mmHg)	161 ± 7	152 ± 2$^{\Psi}$

*Values are means±SEM. Body weight was assessed prior to euthanasia; blood pressure was measure by tail-cuff as described in the Methods. *p=0.10, Mann-Whitney test; $^{\Psi}$p=0.08, Mann-Whitney test.*

4.4.2 - MCA myogenic tone and contractility. To assess if TNF-α inhibition alters the function of the MCA in SHRSP, we studied spontaneous myogenic generation and

constriction to 5-HT. There was no change in MCA spontaneous myogenic tone generation (Table 4.2). Contractility to 5-HT was increased in pressurized MCA from SHRSP+ETN, although the post-test did not identify the individual points in the curve that were different (Fig 4.1A). Normalization of the constriction data by the passive diameter of the MCA confirmed the increase in constriction, suggesting that the increased contractility was not due to changes in MCA passive structure (Fig 4.1B).

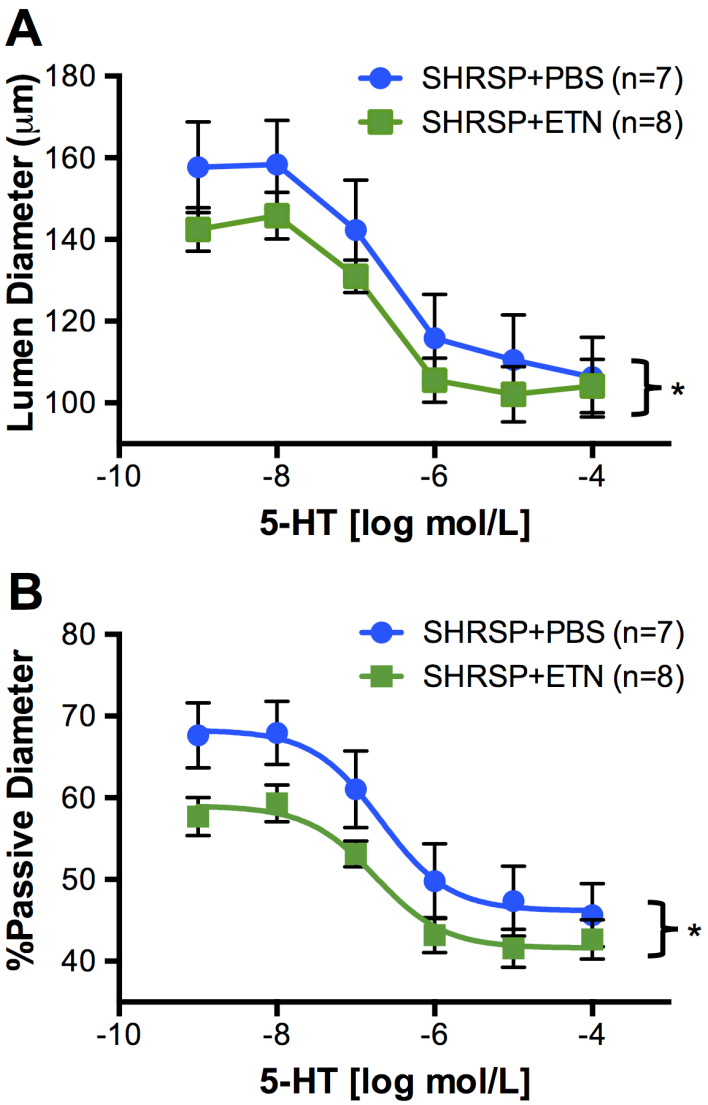

Figure 4.1: ETN treatment increased MCA contractility to 5-hydroxytriptamine (5-HT). (A) The lumen diameter of the MCA from SHRSP+ETN at each concentration of 5-

HT was smaller than that from SHRSP+PBS. When the data was normalized by the passive diameter of the MCA the differences were more pronounced (B). *p=0.04, Two-way ANOVA. The pressurized MCA was allowed to equilibrate for 10 min before a measurement was taken and the next dose of 5-HT was added. Data are means±SEM.

4.4.3 - MCA passive structure. To test the hypothesis that TNF-α is involved in MCA remodeling in SHRSP, we assessed MCA structure and mechanical properties by pressure myography. Treatment of SHRSP with ETN caused a small increase in the outer diameter of the MCA (Fig 4.2A). Lumen diameter was significantly increased in SHRSP+ETN when compared to SHRSP+PBS at intraluminal pressures above 40mmHg (Fig 4.2B). MCA wall thickness (Fig 4.2C) and wall-to-lumen ratio (Fig 4.2D) were reduced by ETN treatment in SHRSP. Although no changes were observed in the MCA cross-sectional area (CSA), the lumen CSA was increased after ETN treatment, and the wall CSA was decreased (Table 4.2). Wall stress was higher in the MCA from SHRSP+ETN (Fig 4.3A); there were no differences in distensibility (Fig 4.3B) and in the β-coefficient (Fig 4.3C).

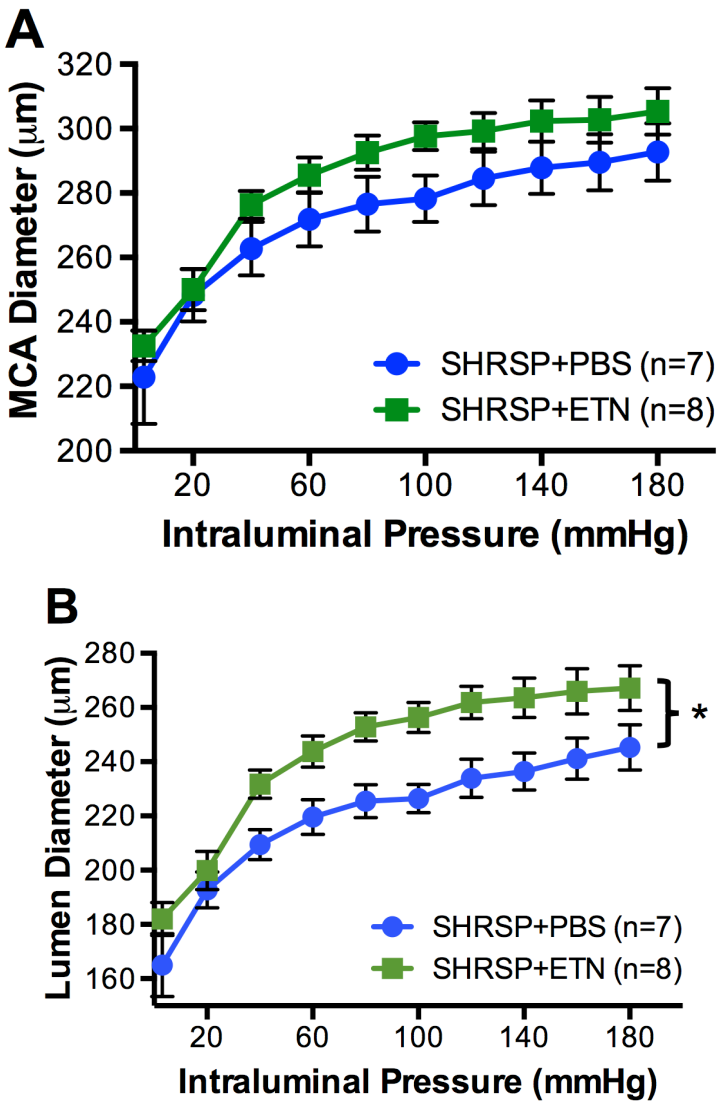

Figure 4.2: TNF-α inhibition with ETN improved the structure of the MCA in SHRSP.

Figure 4.2 (cont'd)

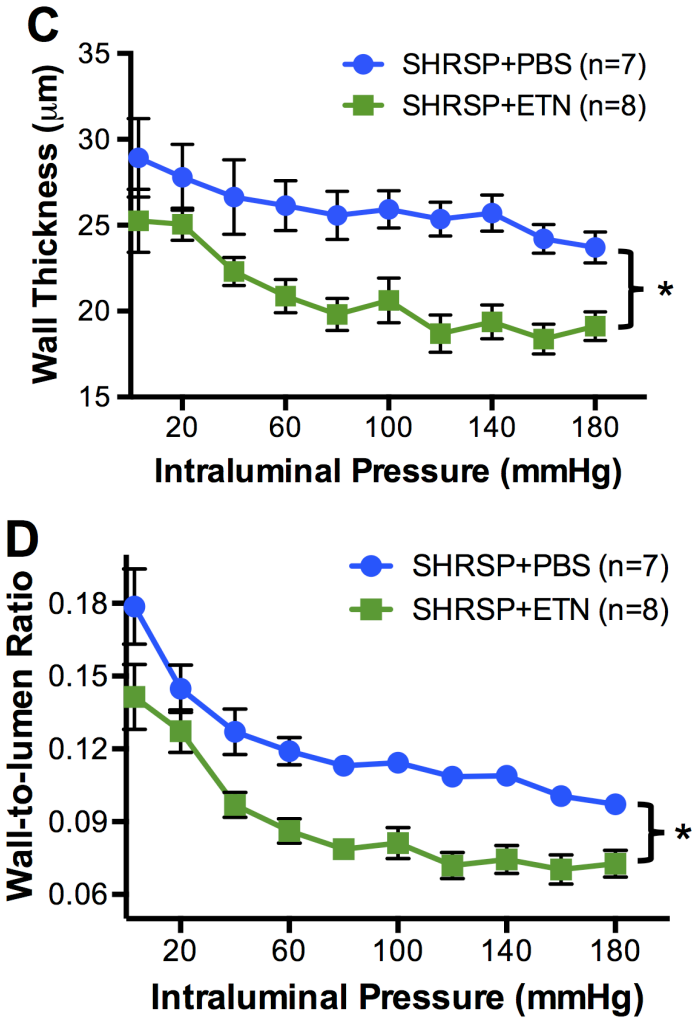

Although there were no differences in the outer diameter of the MCA (A), ETN treatment for 6 weeks caused an increase in the lumen diameter (B). The wall thickness was reduced (C), as well as the wall-to-lumen ratio (D) of the MCA in SHRSP+ETN. *$p<0.01$, SHRSP+PBS vs. SHRSP+ETN, Two-Way ANOVA. Data are means±SEM.

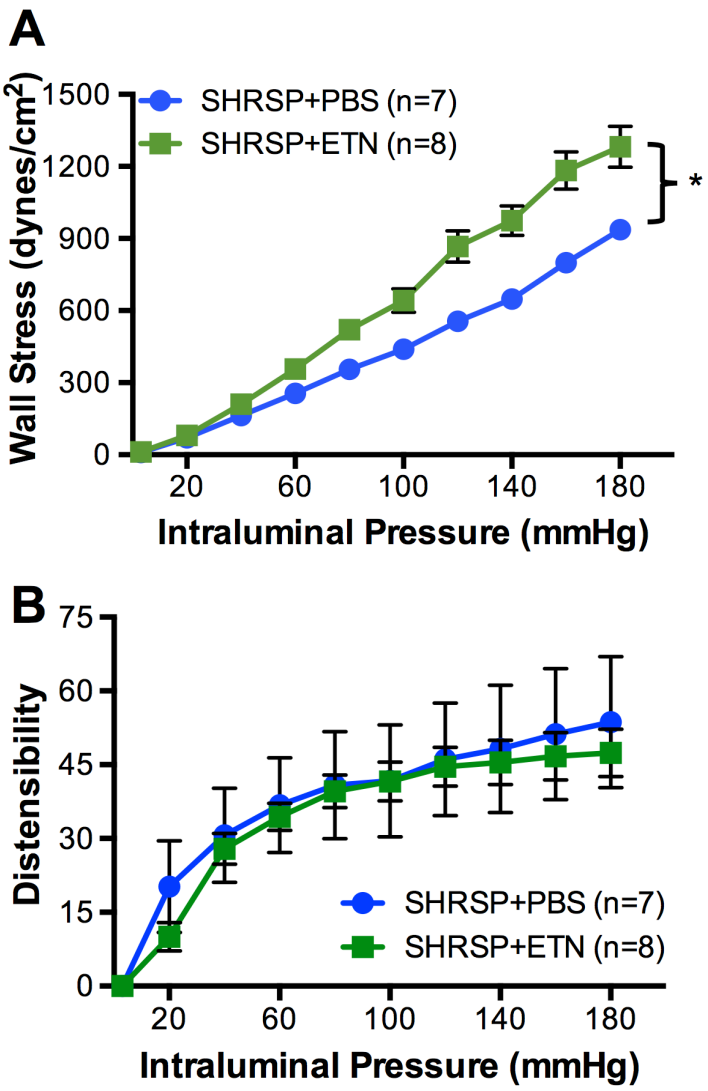

Figure 4.3: Mechanical properties of the MCA from SHRSP after 6 weeks of treatment with ETN or placebo.

Figure 4.3 (cont'd)

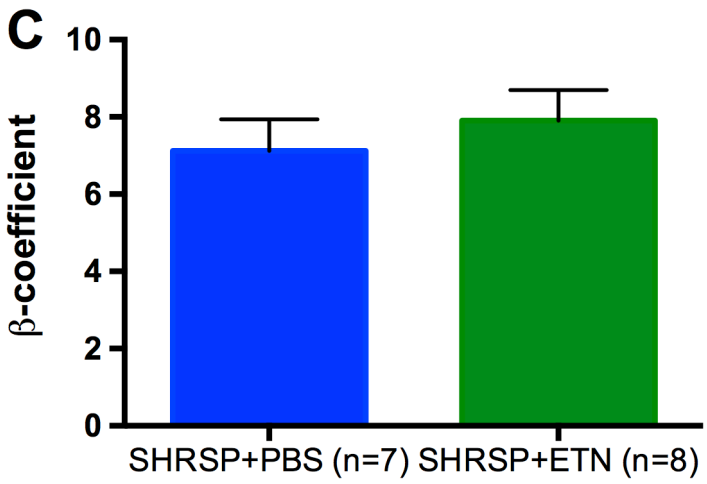

As a consequence of the increase in lumen diameter and decrease in wall thickness, wall stress (A) was higher in the MCA from SHRSP+ETN than in SHRSP+PBS (*p<0.001, Two-way ANOVA). No differences were observed in distensilibity (B), measured as percent increase in diameter from 3mmHg, or stiffness (C), calculated by the β-coefficient from individual stress-strain curves. Data are means±SEM.

Table 4.2: ETN attenuated MCA remodeling in SHRSP.

	SHRSP+PBS (n=7)	SHRSP+ETN (n=8)	WKY rats (n=4)
Lumen diameter (μm)	225±6	253±5*	286±8
Outer Diameter (μm)	278±9	293±5	314±11
Wall Thickness (μm)	26±1	20±1*	14±1

Table 4.2 (cont'd)

	SHRSP+PBS (n=7)	SHRSP+ETN (n=8)	WKY rats (n=4)
Wall-to-lumen ratio	0.113±0.01	0.079±0.01*	0.05±0.004
Lumen CSA (μm^2)	40086±2175	50374±2062*	64398±3556
Vessel CSA (μm^2)	60422±3771	67351±2426	77452±5011
Wall CSA (μm^2)	20337±1683	16976±857*	13054±1607
Distensibility	41±11	40±3	45±3
Vessel Stress (dynes/ cm^2)	356±11	520±31*	854±74
β-coefficient	7.12±0.7	7.91±0.7	8.61±0.6
Myogenic tone (%)	28±7	33±2	N.A

*Values are mean±SEM at an intraluminal pressure of 80mmHg; *significantly different from SHRSP+PBS ($p<0.05$); N.A.: non-applicable. The WKY values contained in this table have been previously published [15], they are included here to provide an indication of the extent of the remodeling in SHRSP.*

4.4.4 - Basal pial blood flow. To analyze if the improvement in MCA structure caused a change in basal cerebral perfusion, we assessed pial blood flow in anesthetized rats using scanning laser Doppler flowmetry. We observed a small but significant increase in basal pial blood flow in ETN-treated rats (Fig 4.4A).

4.4.5 - Transient MCAO. To test the hypothesis that improvement in MCA structure would reduce the cerebral infarct in SHRSP, cerebral ischemia/ reperfusion was experimentally induced by tMCAO, with 1 hour of ischemia and 47 hours of reperfusion. Our data shows that SHRSP treated with ETN for 6 weeks had significantly larger infarcts when compared to rats treated with PBS (Fig 4.4B), despite the observation that pial blood flow was not different between groups at any of the time points observed (Figs 4.4C and 4.4D).

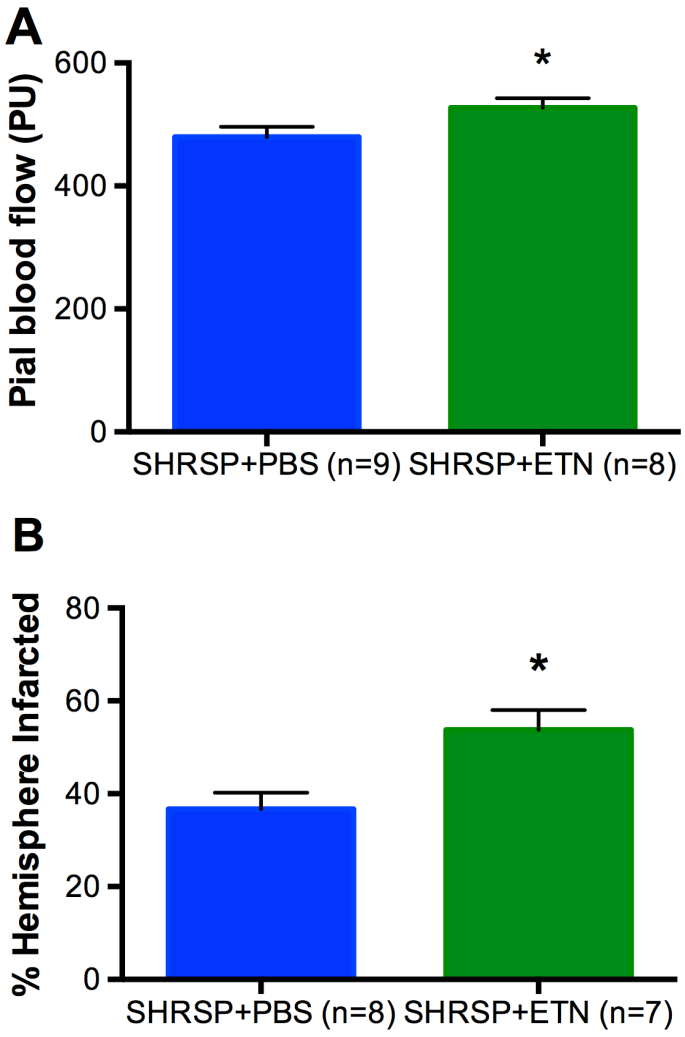

Figure 4.4: Pial blood flow and cerebral infarct after transient MCAO in SHRSP treated with PBS or ETN.

Figure 4.4 (cont'd)

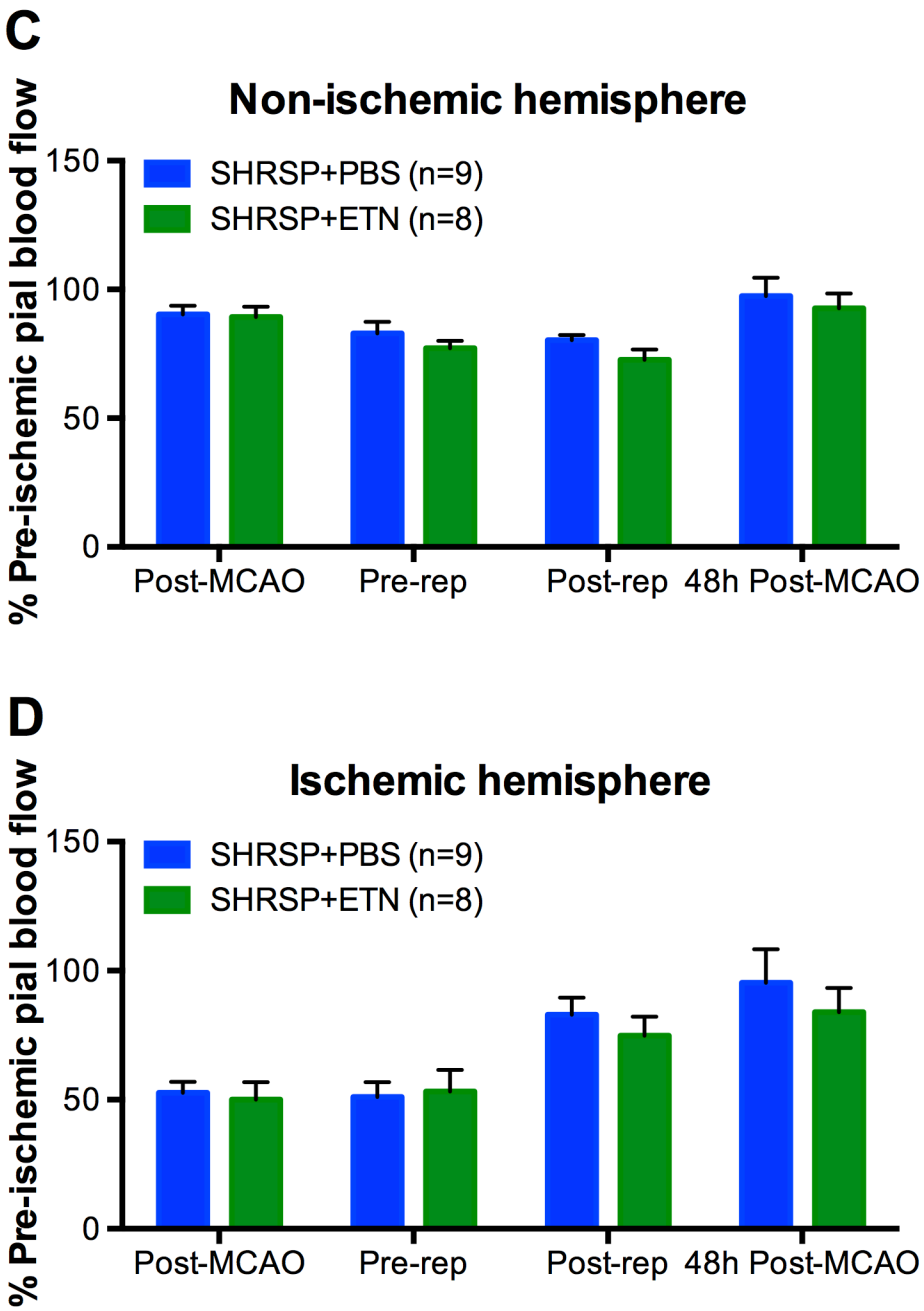

Basal pial blood flow measured by scanning laser Doppler flowmetry was increased in SHRSP+ETN when compared to SHRSP+PBS (A, *p<0.05, *Student's* t-test). Cerebral infarct after transient MCAO (1 hour of ischemia, 47 hours of reperfusion) was larger in ETN-treated SHRSP than in PBS-treated controls (*p<0.01, Student's t-test). Pial blood

flow in both the non-ischemic (C) and ischemic (D) hemispheres was not different between groups. Data are means±SEM.

4.4.6 - Post-ischemic endothelium-dependent dilation of the contralateral MCA. In order to evaluate if the increased infarct size observed in SHRSP+ETN was due to impaired endothelial function of cerebral arteries, we studied the dilatory response of the non-ischemic MCA to ADP. Post-ischemic dilation of the non-ischemic MCA ADP was reduced in SHRSP+PBS when compared to rats that underwent sham surgery, and ETN treatment recovered ADP-induced dilation of the MCA (Fig 4.5A and 4.5B).

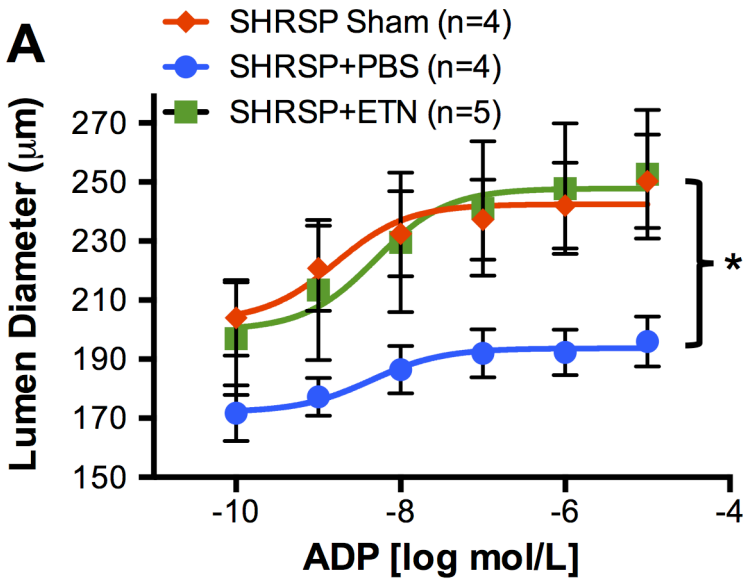

Figure 4.5: Endothelial function of the non-ischemic MCA is impaired in SHRSP+PBS.

Figure 4.5 (cont'd)

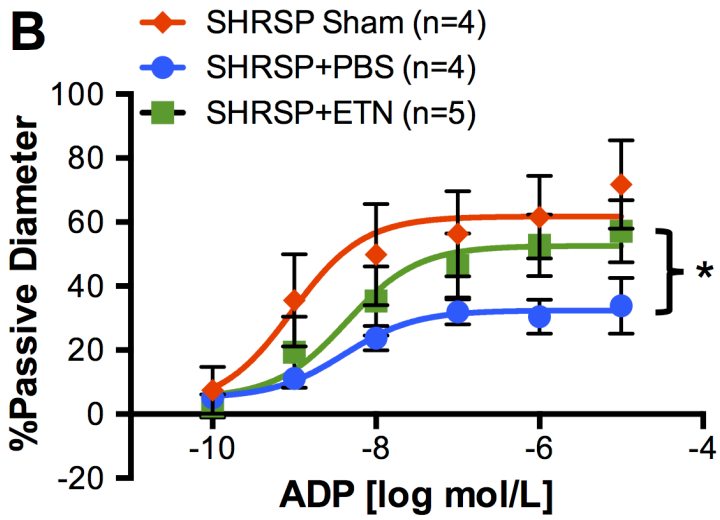

In order to evaluate if the increased infarct size observed in SHRSP+ETN after transient MCAO was a consequence of impaired vasodilation of cerebral arteries, MCA from the non-ischemic hemisphere were cannulated and exposed to increasing concentrations of ADP. As observed in (A), transient MCAO caused an impairment in endothelium-dependent dilation in SHRSP+PBS when compared with the MCA from sham-operated rats (open diamonds). The impairment seems to be mediated in part by TNF-α, because ETN treatment prevented the loss in response to intraluminal perfusion of ADP. Normalization of the data by the passive diameter of the MCA maintained the difference (B). *$p<0.01$, Two-way ANOVA. Data are means±SEM **.**

4.4.7 - ETN at the time of reperfusion. In order to assess if the increased infarct observed after TNF-α inhibition was a consequence of the chronic ETN treatment, a group of untreated SHRSP with 12 weeks of age were subject to tMCAO and received either ETN or PBS (1.25mg/kg, i.p.) at reperfusion and 24 hours after reperfusion. Using this experimental protocol we observed that there was no difference in infarct size

between SHRSP that received PBS or ETN (%HI: 37.7±4.6 vs 42.7±9.6, SHRSP+PBS vs SHRSP+ETN, p=0.33).

4.4.8 - Permanent MCAO. To evaluate if the larger cerebral infarct observed in SHRSP+ETN after tMCAO were a consequence of reperfusion injury, a different group of rats underwent pMCAO with 24 hours of ischemia. There were no differences between SHRSP+PBS and SHRSP+ETN in infarct size (Fig 4.6A) and pial blood flow to the non-ischemic (Fig 4.6B) and ischemic hemispheres (Fig 4.6C) after pMCAO.

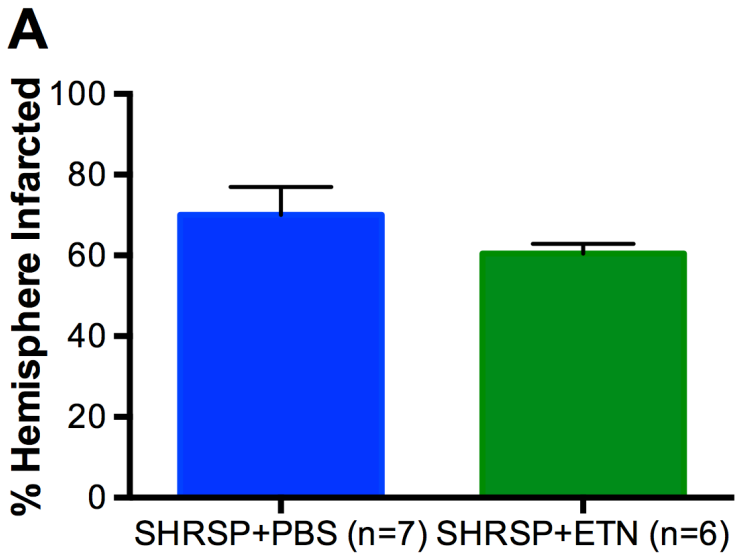

Figure 4.6: ETN treatment did not increase cerebral infarct after permanent MCAO.

Figure 4.6 (cont'd)

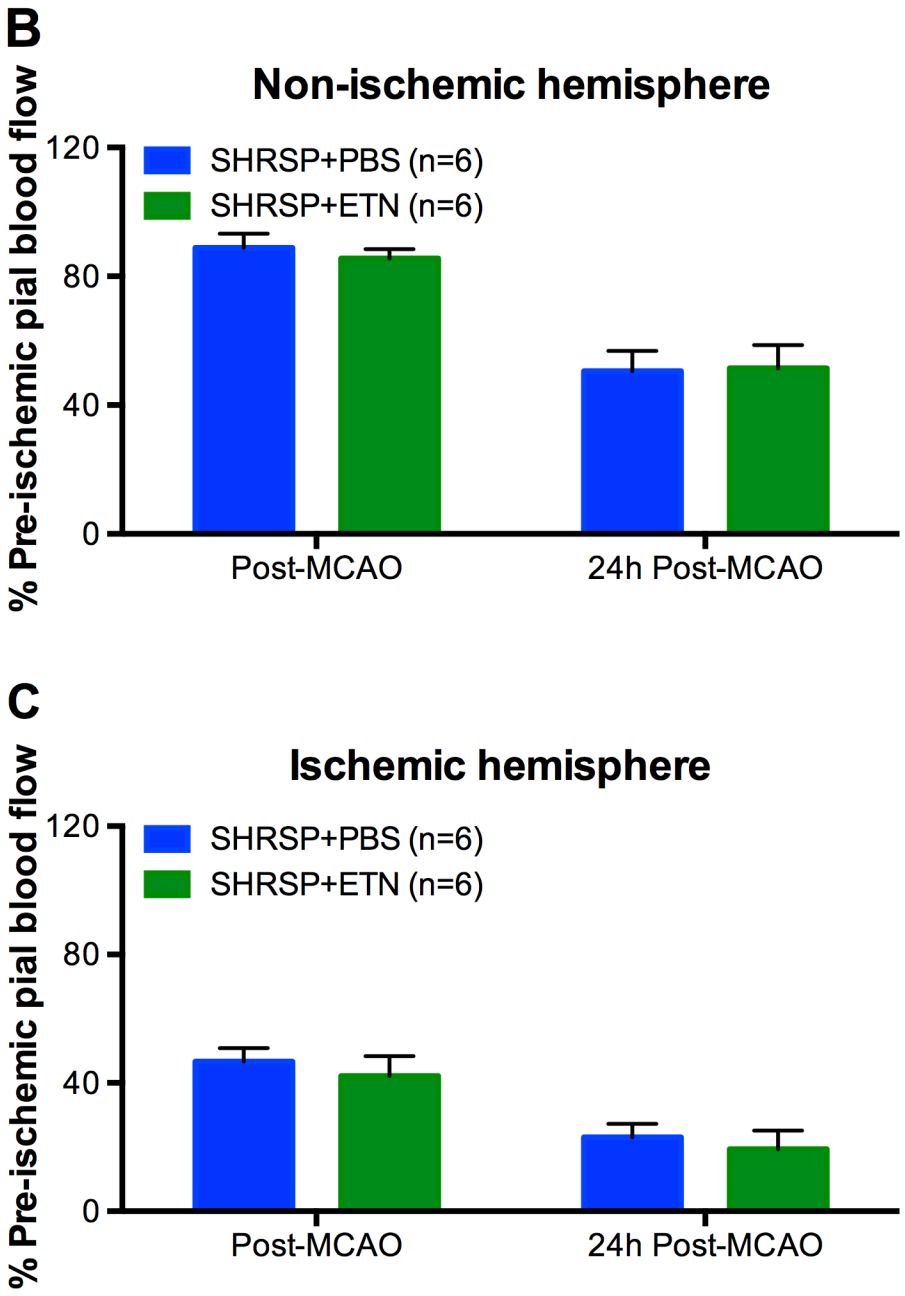

To assess if the increase in cerebral infarct size after transient MCAO in SHRSP was linked to reperfusion injury, SHRSP treated with ETN or PBS for 6 weeks were subjected to permanent MCAO. After 24 hours of ischemia, we observed that there was no difference in infarct size between groups (A), as well as no changes in pial blood flow

in the non-ischemic (B) and ischemic (C) hemispheres. Data are means±SEM.

4.4.9 - Post-MCAO survival. All rats subjected to transient MCAO survived for 48 hours post-ischemia. However, 5 out of 11 SHRSP+PBS subjected to permanent MCAO did not survive for the 24 hours post-stroke (45% mortality), whereas 6 out of 6 SHRSP+ETN subjected to permanent MCAO survived for 24 hours (0% mortality).

4.4.10 - MRA passive structure. To assess if the improvement in vascular structure observed in the MCA after chronic ETN treatment also occurred in peripheral vascular beds, we studied the MRA. ETN treatment attenuated MRA remodeling by a trend towards increase in MRA lumen diameter (Fig 7A, p=0.065). The wall thickness was decreased after ETN treatment (Fig 7B), as was the wall-to-lumen ratio (Fig 7C). Wall stress was increased in SHRSP+ETN (Table 2), as was the MRA distensibility (Fig 7D). MRA stiffness was reduced in SHRSP+ETN, as observed by a reduction in the β-coefficient value (Table 4.3).

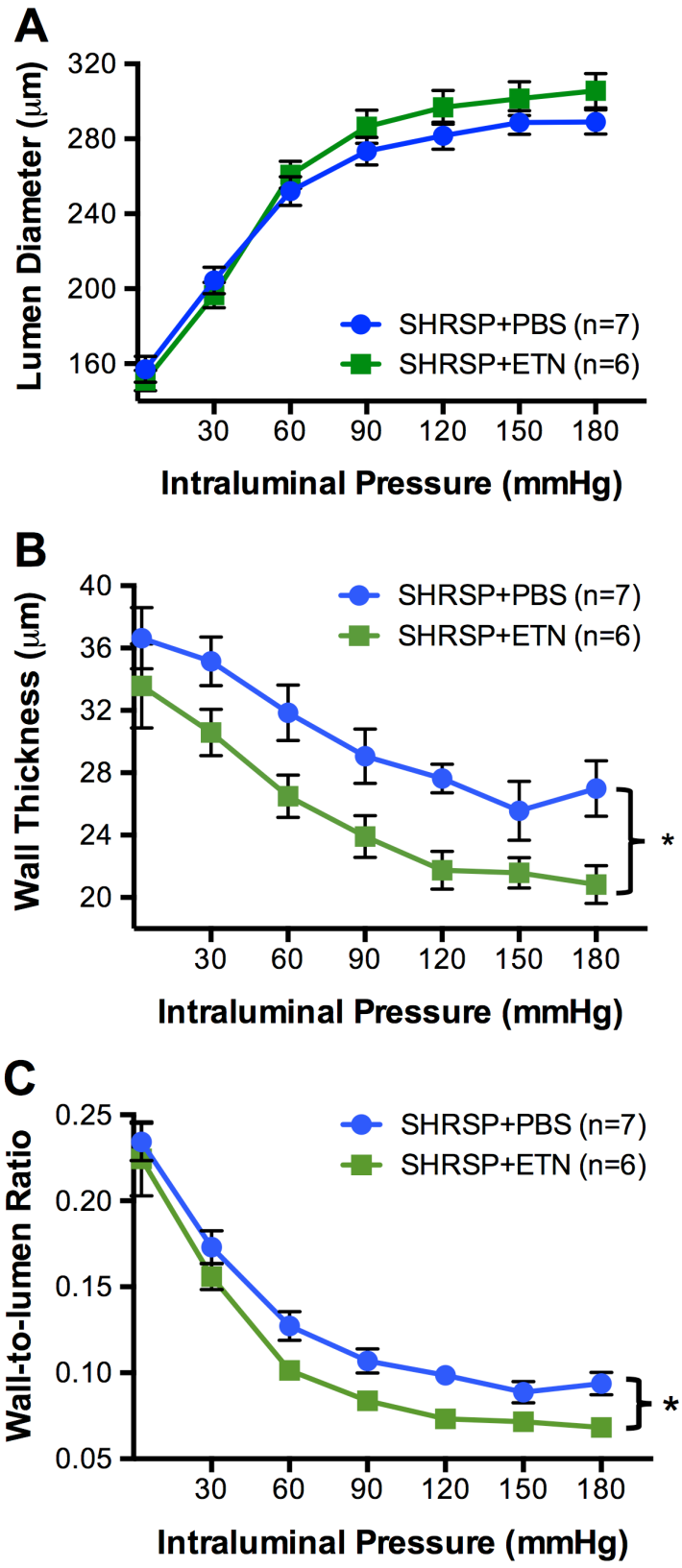

Figure 4.7: ETN treatment reduced wall hypertrophy in MRA of SHRSP.

Figure 4.7 (cont'd)

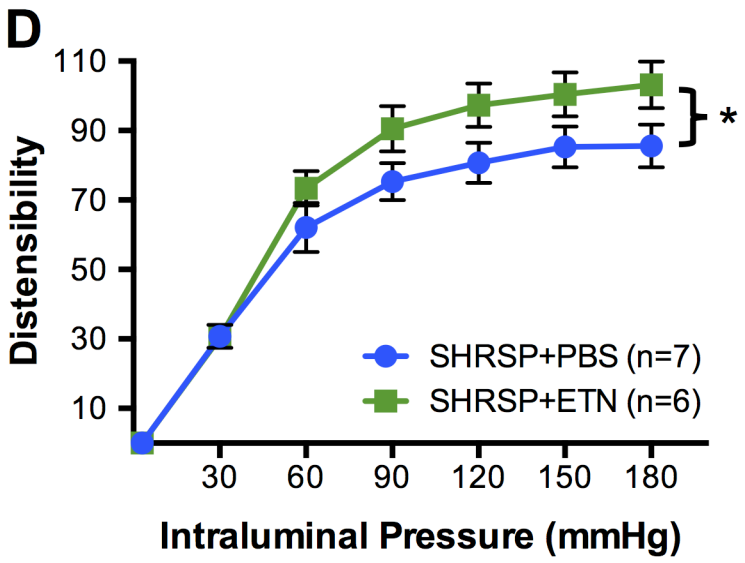

Although inward remodeling was not prevented (A), wall thickness (B) and the wall-to-lumen ratio (C) of third-order MRA were reduced in SHRSP+ETN when compared to SHRSP+PBS. Further, ETN treatment caused an increase in distensibility (D). *p<0.01, Two-way ANOVA. Data are means±SEM.

Table 4.3: ETN attenuated remodeling of the MRA in SHRSP.

	SHRSP+PBS (n=6)	SHRSP+ETN (n=6)	WKY rats (n=4)
Lumen diameter (μm)	273±7	287±9	280±21
Outer Diameter (μm)	332±8	334±10	311±20
Wall Thickness (μm)	29±2	24±1*	16±1.4
Wall-to-lumen ratio	0.11±0.007	0.08±0.005*	0.06±0.007
Lumen CSA (μm^2)	58969±3052	64776±3945	62316±8843

Table 4.3 (cont'd)

Vessel CSA (μm^2)	86643±4179	88167±5157	76675±9850
Wall CSA (μm^2)	27674±2014	23391±1777	14386±1543
Distensibility	75±5	91±7*	74±3
Vessel Stress (dynes/ cm^2)	433±31	546±41*	831±90
β-coefficient	4.16±0.3	3.34±0.1*	6.23±1.02

*Values are mean±SEM at an intraluminal pressure of 90mmHg; *significantly different from SHRSP+PBS ($p<0.05$). The WKY values contained in this table have been previously published [15], they are included here to provide an indication of the extent of the remodeling in SHRSP.*

4.5 - Discussion

The main findings of the present study are: (i) chronic TNF-α inhibition improved the structure of the MCA, as evidenced by an increase in lumen diameter and a decrease in wall thickness and wall-to-lumen ratio; this was associated with an increase in basal pial blood flow; (ii) similar to the MCA, passive structure of the MRA was also improved, with ETN treatment causing a reduction in wall thickness and wall-to-lumen ratio; (iii) despite the improvement in the MCA structure, cerebral infarct after tMCAO was increased in SHRSP+ETN. To the best of our knowledge this is the first report to show that chronic TNF-α inhibition affects structural parameters of the vasculature independently of a reduction in systemic blood pressure. It is also the first study to assess the effects of chronic TNF-α inhibition in the outcome of cerebral ischemia in hypertensive subjects.

The involvement of TNF-α in the development of hypertension has been elucidated in the recent years. Anti- TNF-α therapy caused a modest reduction in both systolic and diastolic blood pressures in humans with rheumatoid arthritis [20]. In the angiotensin II-salt model of hypertension in rodents, ETN treatment delayed the development of hypertension [11], although after the delay the blood pressure was similar between control and ETN-treated groups. Deletion of TNF-α in mice prevented the rise in mean arterial pressure after angiotensin II infusion, and this effect was lost after administration of exogenous TNF-α, suggesting a direct link between TNF-α and angiotensin II - induced hypertension [21]. In our study we observed a small but insignificant ($p=0.10$) reduction in systolic blood pressure in the genetically hypertensive SHRSP. One caveat of the present study is that blood pressure was assessed by tail cuff instead of radiotelemetry. However, we showed previously that blood pressure measurements in rats using tail cuff are similar to those obtained by radiotelemetry [3]. Independently of the method used, it is unlikely that a 10mmHg reduction in blood pressure will be physiologically relevant in SHRSP.

The main finding of this study is that ETN treatment during the exponential rise in blood pressure in SHRSP attenuates MCA remodeling. We observed an increase in lumen diameter and a reduction in wall thickness and wall-to-lumen ratio in the MCA of SHRSP after 6 weeks of ETN treatment. This finding is not without precedence, since TNF-α is a known proliferative stimulus for vascular smooth muscle cells [22-24]. TNF-α also induces the expression and activity of matrix metalloproteinases [23]. Vascular smooth muscle cell proliferation and matrix metalloproteinases activity are involved in

hypertensive remodeling [15]. The source of TNF-α in cerebral arteries seems to be perivascular macrophages, since we recently showed that reducing the number of these cells in the cerebral vasculature reduces TNF-α mRNA expression and attenuates MCA remodeling [4]. We also observed a small increase in basal pial blood flow in SHRSP after ETN treatment. This increase could be due to (i) increased flow through the large arteries of the Circle of Willis that feed the pial circulation, (ii) an increase in the lumen diameter of pial arteries and arterioles, or (iii) a reduction in basal myogenic tone of cerebral arteries. Although we did not observe reduced myogenic tone in the MCA of SHRSP, a recent study showed that TNF-α mediates increased myogenic tone in the posterior cerebral artery in gerbils with heart failure [25].

Despite the improvement in the structure of the MCA, SHRSP treated with ETN for 6 weeks had larger infarcts after transient MCAO. This observation is in disagreement with the reports for normotensive animals [13]. We hypothesized that the increased infarct could be a consequence of: (i) reduced blood flow due to impaired post-reperfusion dilation of cerebral arteries or (ii) an exacerbation of the reperfusion injury due to the chronic immunosuppression. We will discuss these two hypotheses separately.

To assess if ETN impairs post-reperfusion vasodilation, SHRSP were treated with ETN or PBS for 6 weeks prior to transient MCAO and isolation of the MCA from the non-ischemic hemisphere to study endothelium-dependent dilation. We observed that MCA from SHRSP subjected to transient MCAO showed reduced dilation to intraluminal

perfusion of ADP when compared to MCA from SHAM rats, and that ETN treatment restored endothelium-dependent dilation to levels similar to sham rats. Impairment in endothelium-dependent dilation of cerebral arteries post-cerebral ischemia was shown to occur in the basilar artery [26] and in peripheral vascular beds, including the mesenteric circulation [27]. Our data presents the possibility that part of this dysfunction is mediated by TNF-α. In fact, patients with rheumatoid arthritis treated with anti-TNF-α therapies show improved endothelium-dependent dilation of brachial arteries [28, 29]. In the MCA, ADP elicits dilation by endothelial production of nitric oxide and endothelium-derived hyperpolarizing factor [30]. TNF-α was shown to impair dilations mediated by nitric oxide in coronary arteries [31] and endothelium-derived hyperpolarizing factor in human omental arteries [32]. Importantly, dilation through endothelium-derived hyperpolarizing factor is prevalent in the post-ischemia MCA [33]. It is possible that the prolonged ETN treatment either enhanced the EDHF-mediated dilation or preserved nitric oxide-dependent dilation, leading to a dilatory response similar to that observed in sham-operated SHRSP.

To test the hypothesis that the increased damage is a consequence of exacerbated reperfusion injury due to chronic immunosuppression, we designed two studies. In the first we subjected SHRSP treated with ETN for 6 weeks to permanent MCAO (study 1); in the second we subjected untreated SHRSP to tMCAO and administered ETN at the time of reperfusion (study 2). In both studies we observed that there were no differences in infarct size or pial blood flow. Together, these data suggest that the increase in infarct following tMCAO is likely due to a deleterious effect of the prolonged

immunosuppression after 6 weeks of ETN treatment. This effect could be directly linked to a reduction in macrophage infiltration to the ischemic hemisphere. Macrophage infiltration peaks at 2 days after ischemia/reperfusion injury in rodents [34], and this event is dependent on the expression of adhesion molecules by endothelial cells [35]. TNF-α is a potent inducer of adhesion molecules [36, 37], thus it is possible that the prolonged inhibition reduced the levels of adhesion molecules, consequently reducing leukocyte infiltration and exacerbating the damage.

The effects of TNF-α and its inhibition on the outcome of cerebral ischemia are controversial. Some studies show that acute TNF-α generation is involved in neuronal death and infarct development following MCAO in SHR [38], and that TNF-α inhibition reduces infarct development after cerebral ischemia/reperfusion [13]. However, others show that knock-out of TNF-α receptors increases damage after MCAO [39, 40]. It seems that TNF-α has a dual role in the evolution of the infarct following cerebral ischemia/reperfusion injury: on the one hand TNF-α induces neuronal apoptosis [41], thus leading to increased neuronal death and larger infarcts; conversely, TNF-α stimulates activation of microglia [39], which are important for neuronal survival in the early stages following ischemia, particularly alternatively polarized microglia [42]. It is possible that in our study the chronic administration of ETN acted *via* the later mechanism, preventing microglia activation, which, associated with a possible loss of leukocyte infiltration, could potentially lead to an accumulation of cytotoxic molecules in the ischemic hemisphere. It is still unknown if this is the mechanism responsible for the increase in infarct size observed in our study.

Finally, the lack of a protective effect of ETN in the outcome of pMCAO could be explained by *survival bias*. In SHRSP treated with vehicle there was a 45% mortality (5 out of 11), whereas in the SHRSP+ETN group there was no mortality. It is possible that the rats treated with vehicle that survived for 24 hours had smaller infarcts; and the rats with larger infarcts did not survive until the time point established for euthanasia and analysis of infarct size. Since we did not evaluate infarct size in the rats that died before 24 hours post-pMCAO, we might have skewed our results towards smaller infarcts in vehicle-treated SHRSP subjected to pMCAO.

Macrophage depletion did not alter MRA remodeling in SHRSP [4], but treatment of SHRSP with ETN attenuated remodeling in this peripheral vascular bed. Macrophage depletion in SHRSP caused an increase in TNF-α mRNA expression in perivascular adipose tissue, suggesting that these cells might produce TNF-α, which appears to be an important mediator of hypertensive remodeling in the mesenteric vasculature The findings in this study support that hypothesis, since ETN improved MRA structure in the SHRSP. Interestingly, MRA showed an improvement in mechanical properties, including reduced stiffness and increased distensibility, which was not observed in the MCA. TNF-α was shown to increase collagen deposition in the rodent heart [43], thus it is possible that ETN decreased collagen deposition in the MRA, increasing distensibility. Moreover, TNF-α was shown to increase expression and activity of matrix metalloproteases -2 and -9 in cultured human aortic smooth muscle cells [44]. We [15] and others [45] have shown that matrix metalloproteases are important mediators of

hypertensive artery remodeling. It is possible that TNF-α acts upstream of matrix metalloproteases, inducing their expression and activity, thus worsening remodeling in the peripheral vasculature.

In summary, we show that TNF-α inhibition with ETN improves the structure of resistance arteries in both the cerebral and mesenteric vasculature in chronic hypertension. Despite the improvement in cerebral vascular structure, infarct size following cerebral ischemia/reperfusion injury was larger in SHRSP+ETN. This effect seems to be a consequence of a possible deleterious impact of prolonged immunosuppression on the reperfusion injury.

REFERENCES

REFERENCES

1. Go, A.S., et al., *Heart disease and stroke statistics--2013 update: a report from the American Heart Association.* Circulation, 2013. **127**(1): p. e6-e245.

2. Dorrance, A.M., et al., *Spironolactone reduces cerebral infarct size and EGF-receptor mRNA in stroke-prone rats.* Am J Physiol Regul Integr Comp Physiol, 2001. **281**(3): p. R944-50.

3. Rigsby, C.S., D.M. Pollock, and A.M. Dorrance, *Spironolactone improves structure and increases tone in the cerebral vasculature of male spontaneously hypertensive stroke-prone rats.* Microvasc Res, 2007. **73**(3): p. 198-205.

4. Pires, P.W., et al., *Improvement in Middle Cerebral Artery Structure and Endothelial Function in Stroke-Prone Spontaneously Hypertensive Rats after Macrophage Depletion.* Microcirculation, 2013.

5. Marchesi, C., P. Paradis, and E.L. Schiffrin, *Role of the renin-angiotensin system in vascular inflammation.* Trends Pharmacol Sci, 2008. **29**(7): p. 367-74.

6. Briet, M. and E.L. Schiffrin, *Vascular actions of aldosterone.* J Vasc Res, 2013. **50**(2): p. 89-99.

7. Schiffrin, E.L., *Vascular endothelin in hypertension.* Vascul Pharmacol, 2005. **43**(1): p. 19-29.

8. Rigsby, C.S., et al., *Effects of Spironolactone on Cerebral Vessel Structure in Rats With Sustained Hypertension.* Am J Hypertens, 2011.

9. Li, J.S., R. Lariviere, and E.L. Schiffrin, *Effect of a nonselective endothelin antagonist on vascular remodeling in deoxycorticosterone acetate-salt hypertensive rats. Evidence for a role of endothelin in vascular hypertrophy.* Hypertension, 1994. **24**(2): p. 183-8.

10. Touyz, R.M., *Intracellular mechanisms involved in vascular remodelling of resistance arteries in hypertension: role of angiotensin II.* Exp Physiol, 2005. **90**(4): p. 449-55.

11. Elmarakby, A.A., et al., *Tumor necrosis factor alpha blockade increases renal Cyp2c23 expression and slows the progression of renal damage in salt-sensitive hypertension.* Hypertension, 2006. **47**(3): p. 557-62.

12. Elmarakby, A.A., et al., *TNF-alpha inhibition reduces renal injury in DOCA-salt hypertensive rats.* Am J Physiol Regul Integr Comp Physiol, 2008. **294**(1): p. R76-83.

13. Sumbria, R.K., R.J. Boado, and W.M. Pardridge, *Brain protection from stroke with intravenous TNFalpha decoy receptor-Trojan horse fusion protein.* J Cereb Blood Flow Metab, 2012. **32**(10): p. 1933-8.

14. Pires, P.W., et al., *Tempol, a superoxide dismutase mimetic, prevents cerebral vessel remodeling in hypertensive rats.* Microvasc Res, 2010. **80**(3): p. 445-52.

15. Pires, P.W., et al., *Doxycycline, a matrix metalloprotease inhibitor, reduces vascular remodeling and damage after cerebral ischemia in stroke-prone spontaneously hypertensive rats.* Am J Physiol Heart Circ Physiol, 2011. **301**(1): p. H87-97.

16. Baumbach, G.L. and M.A. Hajdu, *Mechanics and composition of cerebral arterioles in renal and spontaneously hypertensive rats.* Hypertension, 1993. **21**(6 Pt 1): p. 816-26.

17. Chan, S.L., et al., *Effect of PPARgamma inhibition during pregnancy on posterior cerebral artery function and structure.* Front Physiol, 2010. **1**: p. 130.

18. Longa, E.Z., et al., *Reversible middle cerebral artery occlusion without craniectomy in rats.* Stroke, 1989. **20**(1): p. 84-91.

19. Swanson, R.A., et al., *A semiautomated method for measuring brain infarct volume.* J Cereb Blood Flow Metab, 1990. **10**(2): p. 290-3.

20. Sandoo, A., et al., *Anti-TNFalpha therapy may lead to blood pressure reductions through improved endothelium-dependent microvascular function in patients with rheumatoid arthritis.* J Hum Hypertens, 2011. **25**(11): p. 699-702.

21. Sriramula, S., et al., *Involvement of tumor necrosis factor-alpha in angiotensin II-mediated effects on salt appetite, hypertension, and cardiac hypertrophy.* Hypertension, 2008. **51**(5): p. 1345-51.

22. Lin, Y.C., et al., *Simvastatin attenuates the additive effects of TNF-alpha and IL-18 on the connexin 43 up-regulation and over-proliferation of cultured aortic smooth muscle cells.* Cytokine, 2013. **62**(3): p. 341-51.

23. Lee, S.J., W.J. Kim, and S.K. Moon, *TNF-alpha regulates vascular smooth muscle cell responses in genetic hypertension.* Int Immunopharmacol, 2009. **9**(7-8): p. 837-43.

24. Rajesh, M., et al., *CB2 cannabinoid receptor agonists attenuate TNF-alpha-induced human vascular smooth muscle cell proliferation and migration.* Br J Pharmacol, 2008. **153**(2): p. 347-57.

25. Yang, J., et al., *Proximal cerebral arteries develop myogenic responsiveness in heart failure via tumor necrosis factor-alpha-dependent activation of sphingosine-1-phosphate signaling.* Circulation, 2012. **126**(2): p. 196-206.

26. Coucha, M., W. Li, and A. Ergul, *The effect of endothelin receptor A antagonism on basilar artery endothelium-dependent relaxation after ischemic stroke.* Life Sci, 2012. **91**(13-14): p. 676-80.

27. Martinez-Revelles, S., et al., *Endothelial dysfunction in rat mesenteric resistance artery after transient middle cerebral artery occlusion.* J Pharmacol Exp Ther, 2008. **325**(2): p. 363-9.

28. Capria, A., et al., *Long-term anti-TNF-alpha treatments reverse the endothelial dysfunction in rheumatoid arthritis: the biological coherence between synovial and endothelial inflammation.* Int J Immunopathol Pharmacol, 2010. **23**(1): p. 255-62.

29. Galarraga, B., et al., *Clinical improvement in rheumatoid arthritis is associated with healthier microvascular function in patients who respond to antirheumatic therapy.* J Rheumatol, 2010. **37**(3): p. 521-8.

30. You, J., et al., *Endothelial-mediated dilations of rat middle cerebral arteries by ATP and ADP.* Am J Physiol, 1997. **273**(3 Pt 2): p. H1472-7.

31. Picchi, A., et al., *Tumor necrosis factor-alpha induces endothelial dysfunction in the prediabetic metabolic syndrome.* Circ Res, 2006. **99**(1): p. 69-77.

32. Gillham, J.C., et al., *TNF-alpha alters nitric oxide- and endothelium-derived hyperpolarizing factor-mediated vasodilatation in human omental arteries.* Hypertens Pregnancy, 2008. **27**(1): p. 29-38.

33. Marrelli, S.P., et al., *P2 purinoceptor-mediated dilations in the rat middle cerebral artery after ischemia-reperfusion.* Am J Physiol, 1999. **276**(1 Pt 2): p. H33-41.

34. Jin, R., G. Yang, and G. Li, *Inflammatory mechanisms in ischemic stroke: role of inflammatory cells.* J Leukoc Biol, 2010. **87**(5): p. 779-89.

35. Yilmaz, G. and D.N. Granger, *Cell adhesion molecules and ischemic stroke.* Neurol Res, 2008. **30**(8): p. 783-93.

36. Springer, T.A., *Traffic signals for lymphocyte recirculation and leukocyte emigration: the multistep paradigm.* Cell, 1994. **76**(2): p. 301-14.

37. Iademarco, M.F., J.L. Barks, and D.C. Dean, *Regulation of vascular cell adhesion molecule-1 expression by IL-4 and TNF-alpha in cultured endothelial cells.* J Clin Invest, 1995. **95**(1): p. 264-71.

38. Barone, F.C., et al., *Tumor necrosis factor-alpha. A mediator of focal ischemic brain injury.* Stroke, 1997. **28**(6): p. 1233-44.

39. Bruce, A.J., et al., *Altered neuronal and microglial responses to excitotoxic and ischemic brain injury in mice lacking TNF receptors.* Nat Med, 1996. **2**(7): p. 788-94.

40. Gary, D.S., et al., *Ischemic and excitotoxic brain injury is enhanced in mice lacking the p55 tumor necrosis factor receptor.* J Cereb Blood Flow Metab, 1998. **18**(12): p. 1283-7.

41. McCoy, M.K. and M.G. Tansey, *TNF signaling inhibition in the CNS: implications for normal brain function and neurodegenerative disease.* J Neuroinflammation, 2008. **5**: p. 45.

42. Hu, X., et al., *Microglia/macrophage polarization dynamics reveal novel mechanism of injury expansion after focal cerebral ischemia.* Stroke, 2012. **43**(11): p. 3063-70.

43. Li, Y.Y., et al., *Myocardial extracellular matrix remodeling in transgenic mice overexpressing tumor necrosis factor alpha can be modulated by anti-tumor necrosis factor alpha therapy.* Proc Natl Acad Sci U S A, 2000. **97**(23): p. 12746-51.

44. Lin, C.P., et al., *Monascus purpureus-fermented rice inhibits tumor necrosis factor-alpha-induced upregulation of matrix metalloproteinase 2 and 9 in human aortic smooth muscle cells.* J Pharm Pharmacol, 2011. **63**(12): p. 1587-94.

45. Castro, M.M., et al., *Imbalance between matrix metalloproteinases and tissue inhibitor of metalloproteinases in hypertensive vascular remodeling.* Matrix Biol, 2010. **29**(3): p. 194-201.

CHAPTER 5

5.1 – General conclusions

The data presented in this dissertation shows a definitive link between vascular inflammation and hypertensive artery remodeling in SHRSP. The studies described here proved the overall hypothesis that vascular inflammation is associated with hypertensive inward remodeling of the MCA. This hypothesis was tested through three specific aims: removal of perivascular macrophages with CLOD, inhibition of MMPs with Dox and TNF-α antagonism with ETN.

The first aim was designed to assess the role played by perivascular macrophages in hypertensive remodeling and dysfunction of the MCA. Treatment of SHRSP with CLOD for 6 weeks caused a 50% reduction in the number of perivascular macrophages surrounding cerebral microvessels. Even though CLOD did not reduce blood pressure, it caused an improvement in endothelium-dependent, NO-mediated dilation of the MCA. CLOD also attenuated inward remodeling in both the MCA and pial arterioles. TNF-α mRNA was down regulated in CBV and in the cerebral cortex from CLOD-treated SHRSP, but no changes in MMP-2 mRNA were observed. The structural changes in the MCA were not observed in the MRA, most likely due to a overproduction of TNF-α by perivascular adipose tissue after CLOD treatment. The second and third aims of this project attempted to identify molecular mediators of macrophage-induced inward remodeling of the MCA in SHRSP.

The second aim was designed to study the effects of chronic Dox treatment on MCA remodeling in SHRSP, and link them to the outcome of MCA occlusion. Dox treatment for 6 weeks caused a down regulation of active MMP-2 in aortas from SHRSP, suggesting that the treatment was effective in inhibiting vascular MMP-2

activity. Dox treatment attenuated inward hypertrophic remodeling of both the MCA and MRA in SHRSP, although bradykinin-mediated dilation of the MCA was not changed. The improvement in MCA structure caused a reduction in cerebral infarct size after ischemia/ reperfusion injury, which was linked to increased post-ischemic cerebral blood flow. Interestingly, Dox did not reduce cerebral infarct or improve post-ischemic blood flow after pMCAO.

The third aim assessed the role of TNF-α in inward remodeling of the MCA in SHRSP, and the outcome of cerebral ischemia. SHRSP were treated with ETN for 6 weeks, and this regimen resulted in a trend towards a reduction in blood pressure in these rats ($p=0.10$). The inward remodeling and wall hypertrophy normally observed in the MCA and MRA from SHRSP. The increase in the MCA lumen diameter was linked to an increase in basal pial blood flow. Contrary to the hypothesis, the improvement in MCA structure and basal pial blood flow did not reduce cerebral infarct in SHRSP. In fact, ischemic damage after ischemia/ reperfusion injury was higher in SHRSP+ETN than in placebo-treated rats. No differences were found in the cerebral infarct size after permanent MCA occlusion or ischemia/ reperfusion injury in SHRSP that received acute ETN treatment at reperfusion. This suggests that chronic TNF-α inhibition might exacerbate reperfusion injury in the post-ischemic brain of SHRSP.

Taken together, these data show that MMPs and TNF-α are important mediators of inward hypertrophic remodeling of the MCA in SHRSP, although their cellular sources might differ. The overarching hypothesis predicted that macrophages were the main source for both MMPs and TNF-α in CBV from SHRSP. However, macrophage depletion with CLOD did not reduce mRNA expression of MMP-2, suggesting that other

cell types might be the source of this protease in the arterial wall. However, a few considerations should be made: 1) even though MMP-2 mRNA was unchanged after CLOD, protein levels and activity could be reduced; 2) it is possible that the increase in MMP-2 occurs earlier than the time-point studied; 3) perivascular macrophages release other MMPs, such as MMP-12, which are important for MCA inward remodeling. These possibilities need to be investigated.

The studies described here suggest that the mechanisms regulating hypertensive remodeling differ between cerebral arteries and mesenteric resistance arteries. CLOD did not attenuate hypertrophic remodeling of the MRA, even though it did so in the MCA. I hypothesized that in vascular beds rich in perivascular adipose tissue, such as the mesenteric arcade, adipocytes act as “backup” cells to produce remodeling mediators. The hypothesis was tested by a short-term treatment (2 weeks) of SHRSP with CLOD. CD68 mRNA, a marker of macrophages, was reduced in perivascular adipose tissue of SHRSP, and TNF-α mRNA was increased. This finding has a few implications: 1) adipocytes have the ability to produce proinflammatory cytokines in the absence of macrophages; 2) factors released by macrophages, such as TNF-α, are important mediators of remodeling.

The data presented in this dissertation show that infarct size after cerebral ischemia/ reperfusion injury is not determined only by the MCA’s lumen diameter and dilatory capacity. MMPs inhibition with Dox reduced infarct size after tMCAO, an effect associated with higher post-ischemic pial blood flow and increased MCA lumen diameter. Since Dox was removed two days prior to tMCAO induction and its half-life is approximately 4 hours in rodents, this effect was not a consequence of Dox itself.

Therefore, it can be argued that the increase in the MCA diameter is the key factor determining ischemic damage in this situation. However, SHRSP treated with ETN had bigger infarcts after tMCAO, even though MCA diameter and post-ischemic dilation were increased. In addition, pial blood flow was not increased after tMCAO in ETN-treated SHRSP. These data suggests that there is an important inflammatory component determining the outcome of tMCAO, which may be protective in the stroke acute phase. They also highlight the importance of blood flow recovery to prevent ischemic damage in the acute phase of ischemia/ reperfusion injury.

MMP inhibition with Dox and TNF-α inhibition with ETN did not reduce the damage after permanent MCAO. In this model of ischemic stroke, infarct size is mainly determined by the ability of collateral arteries and arterioles to dilate in order to supply blood to the blocked artery's territory. Neither Dox nor ETN increased post-pMCAO pial blood flow in SHRSP, suggesting a lack of compensation by collaterals. This was not surprising after Dox treatment, since bradykinin dilation was not improved in SHRSP+Dox. On the other hand, MCAs from SHRSP+ETN showed increased constriction to 5-HT, which could have reduced the ability of collaterals to dilate. In addition, myogenic tone of cerebral arteries was not reduced by Dox or ETN, which could further impair collateralization and contribute to ischemic damage.

In summary, the studies described in this dissertation show the association between hypertensive inward remodeling of cerebral arteries and vascular inflammation. Perivascular macrophages likely regulate remodeling of the MCA through release of TNF-α, but not MMP-2, in the vascular wall. Although not released by perivascular macrophages, MMPs are involved in MCA remodeling. The improvement in MCA

structure after Dox treatment translated into reduced infarct size after ischemia/ reperfusion injury. On the other hand, TNF-α inhibition improved MCA structure, but increased ischemic damage after ischemia/ reperfusion injury. It is possible that MMP inhibition may be a safer alternative to manage hypertensive patients at risk for cerebrovascular accidents.

5.2 – Considerations of the model and treatment regimens used

The SHRSP used in the studies described here are a well-accepted model of cerebrovascular disease and malignant essential hypertension. It could be argued that the studies were conducted with young rats, and that the prevalence of hypertension and cardiovascular diseases in young humans is low. However, the National Health and Nutrition Examination Survey (NHANHES) show that approximately 10% of the population is hypertensive at 20 years of age (reviewed in [1]).

It is important to note that the studies in this dissertation aimed at elucidating the role played by inflammatory mediators in the development of MCA remodeling. As described in the General Introduction (section 1.3.7), blood pressure in SHRSP increases exponentially between 6 and 12 weeks of age. Hemodynamic effects, such as increased circumferential stress in the wall, are triggers for the remodeling process, and they are elevated when blood pressure starts to rise. Previous studies from our laboratory propose that the remodeling process is more active when blood pressure is increasing, thus therapies aimed at prevention should be given during this time. The results presented here further corroborate this hypothesis, and expand it suggesting that vascular inflammation is a key component for hypertensive remodeling of the MCA.

5.3 – Novel findings

My studies are the first to show an association between vascular inflammation during the exponential rise in blood pressure in SHRSP and remodeling of the MCA. Further, we proposed some molecular links between inflammatory cells and hypertensive remodeling, as follows:

- Perivascular macrophages present in cerebral arteries are likely originated in the periphery and infiltrate into the vascular wall. This conclusion is supported by the observation that CLOD reduced the number of perivascular macrophages, even though liposomes with the same composition as those used here have been shown to not cross the blood-brain-barrier [2];
- Once in the vessel wall, macrophages release substances that modulate MCA remodeling and endothelial function. It is likely that TNF-α is important in this situation, since CLOD reduced TNF-α mRNA expression in cerebral arteries;
- Macrophage depletion improved endothelium-dependent, NO-mediated dilation of the MCA. This suggests that macrophages also release molecules capable of reducing NO bioavailability;
- CLOD treatment attenuated inward remodeling of the MCA and pial arteries, but had no protective effect against remodeling of MRA. We showed that, in the absence of macrophages, perivascular adipose tissue produces TNF-α, thus maintaining the hypertrophic remodeling of MRA;
- MMPs are actively involved in remodeling of the MCA and MRA in SHRSP, even though macrophages may not be the major source of MMP-2 in the vascular wall;

- MMPs inhibition with Dox reduced infarct size after tMCAO, but not pMCAO, in SHRSP. This effect was independent on acute effects of Dox and linked to increases post-ischemic pial blood flow in the ischemic hemisphere;
- TNF-α inhibition with ETN attenuated inward remodeling of the MCA and hypertrophic remodeling of the MRA. This further suggest that TNF-α may be the link between perivascular macrophages and hypertensive vascular remodeling;
- ETN treatment caused a modest, yet significant, increase in basal pial blood flow in SHRSP;
- tMCAO leads to impaired endothelium-dependent dilation of the non-ischemic MCA, through a mechanism dependent on TNF-α, since ETN improved post-ischemic dilation;
- Chronic TNF-α inhibition did not increase post-ischemic pial blood flow and resulted in larger infarcts after tMCAO in SHRSP. This was not an acute effect of TNF-α inhibition because administration of ETN at reperfusion did not increase infarct size in SHRSP;
- The increase in infarct size observed after chronic ETN treatment is possibly associated with the reperfusion injury, and not ischemia itself. Support for this possibility comes from the observation that ETN did not change infarct size after pMCAO in SHRSP.

5.4 – Limitations

- Blood pressure in the CLOD and ETN studies was assessed by tail-cuff, which is not the state-of-the-art in the field. Tail-cuff blood pressure measurements are

performed in restrained rats, which could add a stress factor to blood pressure measurements. However, we reported that when tail-cuff blood pressure measurements are performed in a quiet room, and the rats are previously trained, the data is similar to that obtained by radiotelemetry [3];

- Pressure myography is a powerful technique to study *ex vivo* vascular structure and function, but it has its limitations. Measurements of vascular diameter and wall thickness are precise, but all other variables, such as cross-sectional areas, are derived. The mathematical derivation itself adds imprecisions, which makes statistical significance of the data difficult to achieve.
- Pressurized arteries are filled with and immersed in PSS, and with that the effects of blood viscosity are lost. Additionally, all arterial branches are blocked to fully pressurize the artery, thus it is not possible to assess segmental vascular resistance;
- Blood flow measurement by scanning laser Doppler flowmetry is a relatively new technique and has limited depth of penetration in the tissue (approximately 1 to 2mm depth). Since the skull was not thinned or removed prior to the measurement, we only assessed blood flow in the pial circulation and most superficial layers of the cerebrum. However, the studies described here show that the technique can be sensitive to even small changes in blood flow. Moreover, the drop in blood flow observed after MCAO further validates the sensitivity of this technique. Additionally, since blood flow measurement is not terminal, this technique allows for data collection at different time points.

5.5 – Perspectives

Ischemic stroke is the major cause of adult disability in the United States and the second leading cause of death from cardiovascular diseases. Therapeutic options for patients with cerebral ischemia are few and can only be given to a small percentage of patients. Thus, management of risk factors might be a better option. Hypertension is the major modifiable risk factor for ischemic stroke occurrences. This dissertation proposes that part of the risk is through inward remodeling and dysfunction of the cerebral vasculature induced by vascular inflammation and MMPs. Thus, development of strategies to attenuate cerebrovascular remodeling would be valuable. In fact, we show that Dox might be a viable treatment option since it is a well-tolerated and inexpensive tetracycline antibiotic that could be administered chronically. Additionally, the findings with ETN treatment warrant further assessment of cardiovascular risk in patients that receive anti-TNF-α therapy chronically. It is possible that the risk of having an ischemic stroke in these patients is reduced, but the morbidity and mortality followed by cerebral ischemia may be higher.

REFERENCES

REFERENCES

1. Go, A.S., et al., *Heart disease and stroke statistics--2013 update: a report from the American Heart Association.* Circulation, 2013. **127**(1): p. e6-e245.

2. Micklus, M.J., et al., *Organ distribution of liposomal formulations following intracarotid infusion in rats.* Biochim Biophys Acta, 1992. **1124**(1): p. 7-12.

3. Rigsby, C.S., D.M. Pollock, and A.M. Dorrance, *Spironolactone improves structure and increases tone in the cerebral vasculature of male spontaneously hypertensive stroke-prone rats.* Microvasc Res, 2007. **73**(3): p. 198-205.